PHOTOCATALYTIC SINGLE-ELECTRON REDUCTION OF ELECTRON-DEFICIENT Π-SYSTEMS FOR REGIOSELECTIVE CARBON-CARBON BOND FORMATION

Igor Dmitriev

UNIVERSITAT ROVIRA i VIRGILI

Photocatalytic single-electron reduction of electron-deficient π-systems for regioselective carbon-carbon bond formation

Igor A. Dmitriev

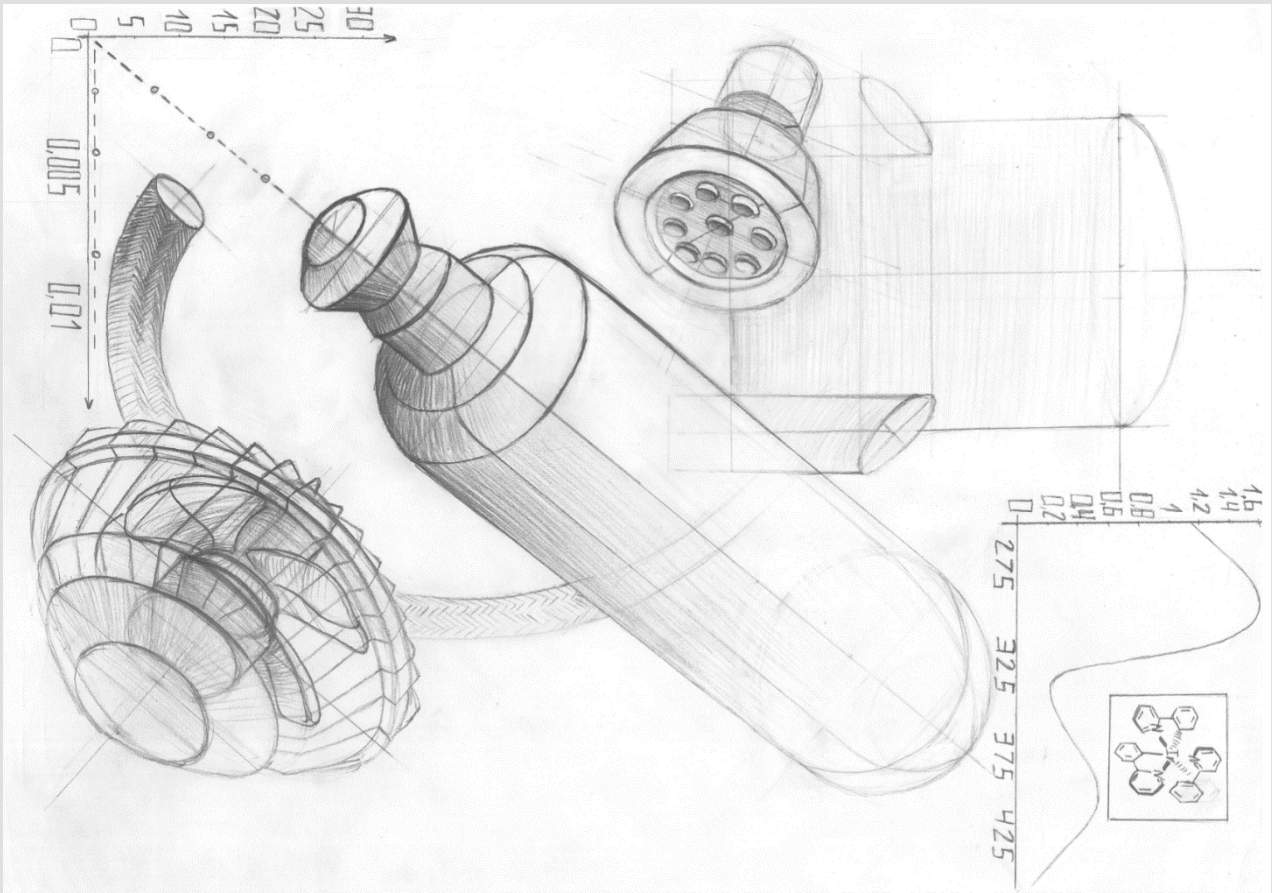

Doctoral Thesis
2024

UNIVERSITAT ROVIRA I VIRGILI
PHOTOCATALYTIC SINGLE-ELECTRON REDUCTION OF ELECTRON-DEFICIENT Π-SYSTEMS FOR REGIOSELECTIVE CARBON-CARBON BOND FORMATION
Igor Dmitriev

Igor A. Dmitriev

Photocatalytic single-electron reduction of electron-deficient π-systems for regioselective carbon-carbon bond formation

Doctoral Thesis

Supervised by Prof. Paolo Melchiorre

ICIQ – Institut Català d'Investigació Química

Tarragona

2024

UNIVERSITAT ROVIRA I VIRGILI
PHOTOCATALYTIC SINGLE-ELECTRON REDUCTION OF ELECTRON-DEFICIENT Π-SYSTEMS FOR REGIOSELECTIVE CARBON-CARBON BOND FORMATION
Igor Dmitriev

UNIVERSITAT ROVIRA i VIRGILI

ICIQ Institut Català d'Investigació Química

Prof. Paolo Melchiorre, Full Professor at the University of Bologna, previously ICIQ Group Leader

I STATE that the present study, entitled "Photocatalytic single-electron reduction of electron-deficient π-systems for regioselective carbon-carbon bond formation", presented by IGOR A. DMITRIEV for the award of the degree of Doctor, has been carried out under my supervision at the Institut Català d'Investigació Química (ICIQ).

Tarragona, June 26th 2024

Doctoral Thesis Supervisor

Prof. Paolo Melchiorre

UNIVERSITAT ROVIRA I VIRGILI
PHOTOCATALYTIC SINGLE-ELECTRON REDUCTION OF ELECTRON-DEFICIENT Π-SYSTEMS FOR REGIOSELECTIVE CARBON-CARBON BOND FORMATION
Igor Dmitriev

Acknowledgements

First of all, I express my gratitude to my supervisor, Professor Paolo Melchiorre, for giving me the opportunity to embark on this PhD journey, for his support and guidance, and for always providing growth and learning opportunities, even in difficult times.

Then, I ascertain that I have only been in the position to start this journey due to the efforts and passion of the educators and mentors from my school and university, to whom I am deeply grateful. Special thanks to *Boris V. Missyul*, who enkindled my passion for chemistry, and to my mentors *Vyacheslav I. Supranovich*, *Vitalij V. Levin*, and former supervisor *Alexander D. Dilman* for their time and efforts.

I would also like to thank all members of the group who have been great colleagues and friends. I am grateful to *Florian* and *Shuo* for being the best box mates throughout this journey. Special thanks to *Davide* for all the time we spent together in Tarragona and Mülheim, and for introducing me to the world of classical music. Thank you *Wei* for being a great partner in the olefin project, *Laura* for the support during difficult times of writing the thesis, *Thomas* for chemical discussions and important help with the thesis, *Matteo* for always being amusingly flabbergasted by my choices of words, and former visiting students *Tommy* and *Antonio* for good times in the lab and in Berlin/Abruzzo. Thanks also to ICIQ colleagues who I shared many lunches and chemical discussions with: *Dmitry*, *Filip*, *Alvaro*, and *Daniel*.

Thank you *Nuria* for the administrative support, *Sonia* for helping with fellowship management, and *Miguel* for making sure the GC instruments functioned the most amount of time physically possible.

Друзья, спасибо всем вам за поддержку в эти не самые лёгкие для всех нас времена. Надеюсь, несмотря на все текущие события, мы будем продолжать держаться друг за друга через границы и километры. Спасибо также моим родителям, сделавшим всё возможное и невозможное для того, чтобы я мог писать сейчас эти строки.

Finally, I am grateful for the predoctoral fellowship from “la Caixa” Foundation (ID 100010434, LCF/BQ/DI21/11860027) and financial support provided by Agencia Estatal de Investigación (PID2019-106278GB-I00) and MCIN/AEI/10.13039/501100011033 (CEX2019-000925-S).

”la Caixa” Foundation

UNIVERSITAT ROVIRA I VIRGILI
PHOTOCATALYTIC SINGLE-ELECTRON REDUCTION OF ELECTRON-DEFICIENT Π-SYSTEMS FOR REGIOSELECTIVE CARBON-CARBON BOND FORMATION
Igor Dmitriev

List of Publications

The results presented in this thesis have been published:

- Le Saux, E.; Georgiou, E.; Dmitriev, I. A.; Hartley, W. C.; Melchiorre, P. "Photochemical Organocatalytic Functionalization of Pyridines via Pyridinyl Radicals" *J. Am. Chem. Soc*. **2023**, *145*, 47
- Zhou, W.[§]; Dmitriev, I. A.[§]; Melchiorre, P. "Reductive Cross-Coupling of Olefins via a Radical Pathway" *J. Am. Chem. Soc.* **2023**, *145*, 25098; §: equal contribution.

UNIVERSITAT ROVIRA I VIRGILI
PHOTOCATALYTIC SINGLE-ELECTRON REDUCTION OF ELECTRON-DEFICIENT Π-SYSTEMS FOR REGIOSELECTIVE CARBON-CARBON BOND FORMATION
Igor Dmitriev

To my sister Valentina

UNIVERSITAT ROVIRA I VIRGILI
PHOTOCATALYTIC SINGLE-ELECTRON REDUCTION OF ELECTRON-DEFICIENT Π-SYSTEMS FOR REGIOSELECTIVE CARBON-CARBON BOND FORMATION
Igor Dmitriev

Table of Contents

Chapter I

General Overview

The research work described in this thesis focuses on the development of new photocatalytic methods for the selective construction of carbon-carbon bonds. Specifically, the photocatalytic reduction of electron-deficient π-systems was studied as a means of achieving unconventional reactivity. In this chapter, the concept of photochemistry and the different mechanisms of photochemical activation of organic molecules are introduced, outlining the synthetic tools utilized in the development of this doctoral thesis.

1.1 Photochemistry

Photochemistry is the branch of chemistry focusing on the understanding of the chemical effects caused by interactions between photons and matter.[1] The first systematic investigation of light-induced chemical transformations was made by Carl W. Scheele in 1777, when he noted that silver chloride degrades fastest under irradiation by violet light. It was not until the beginnings of the 19th and 20th centuries that the theoretical basis of photochemistry were formulated:[2]

- *Grotthus-Draper law*: "only the light absorbed is effective in producing photochemical change"
- *Stark–Einstein law*: "for each photon of light absorbed by a chemical system, only one molecule is activated"

The photochemical theory as we know it today was made possible by Planck's theoretical proposal that electromagnetic radiation could only be emitted or absorbed in discrete packages.[3] Einstein provided a solid physical explanation for this theory, stating that the electromagnetic radiation itself is granular, with each package being discrete and localized, and called "light quantum".[4] With this theoretical advance, it became possible to quantitatively assess the interactions between light and matter.[1]

---

[1] Balzani, V., Ceroni, P., Juris, A. "Photochemistry and Photophysics: Concept, Research and Applications" Weinheim, Wiley-VCH, **2014**.

[2] Rennie, R.; Law J. "A Dictionary of Chemistry" **2016**, *Oxford University Press.*

[3] Planck, M. "On the Theory of the Energy Distribution Law of the Normal Spectrum" *Verhandl. Dtsch. phys. Ges.* **1900**, *2*, 237

[4] Einstein, A. "Über einen die Erzeugung und Verwandlung des Lichtes betreffenden heuristischen Gesichtspunkt" **1905**, Annalen der Physik.

The interaction between a molecule in its *ground state* (the initial state, *i*) and a photon possessing suitable energy triggers an electronic transition from the highest occupied molecular orbital (HOMO, Figure 1.1a) to the lowest unoccupied molecular orbital (LUMO, Figure 1.1a) of the absorbing compound.[1] This light-promoted transition brings the molecule in an electronically excited state (the final state, *f*). The electronic distribution of the ground and excited states are described by wave functions Ψ (Ψ_i and Ψ_f), while E_i and E_f correspond to their relative energies (Figure 1.1b).

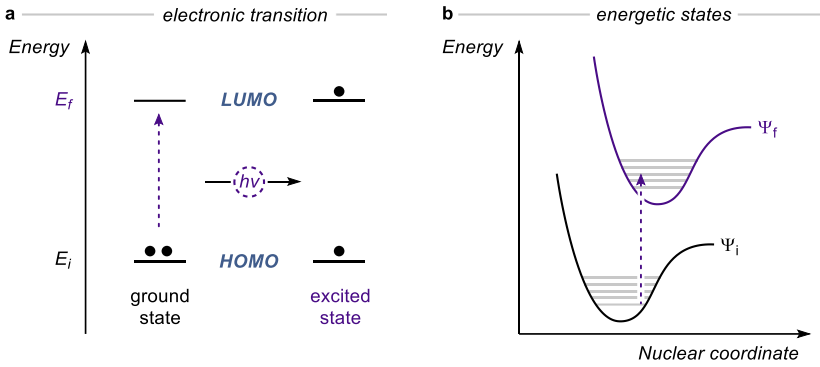

Figure 1.1. (**a**) Energy of the absorbed photon promotes the transition of an electron from the highest occupied molecular orbital (HOMO) to the lowest unoccupied molecular orbital (LUMO). (**b**) Electronic transition from the ground state Ψ_i to the excited state Ψ_f.

In order to have a productive transition, the photon must possess an energy equal to the energy difference between the ground and the excited state, according to Planck's equation (Eq. 1.1; *h* is Planck's constant and *v* is the frequency of the light):

$$h\nu = E_f - E_i \qquad \textbf{(1.1)}$$

This electronic transition changes the physical and chemical properties of the molecule, considerably broadening the spectrum of the available reactions.[5]

The first example of application of synthetic photochemistry was described by Giacomo Ciamician and Paul Silber, who, in their pioneering studies, used Italian sunlight to perform transformations of organic molecules.[6] For a long time, direct excitation of organic molecules was the dominant approach in synthetic photochemistry. One example is the Paterno-Buchi reaction, a thermally forbidden [2+2] cycloaddition between an aldehyde **1** and an olefin **2**

[5] Hoffmann. "Photochemical Reactions as Key Steps in Organic Synthesis" *Chem. Rev.* **2008**, *108*, 1052

[6] (a) Ciamician, G.; Silber, P. "Chemische Lichtwirkungen" *Ber. Dtsch. Chem. Ges.* **1900**, *33*, 2911; (b) Ciamician, G. "The Photochemistry of the Future", *Science*, **1912**, *926*, 385.

(Figure 1.2).[7] The irradiation by UV light promotes the electronic transition ($\Psi_i \rightarrow \Psi_f$), bringing the aldehyde **1** into the excited state, allowing the [2+2] cycloaddition to proceed.

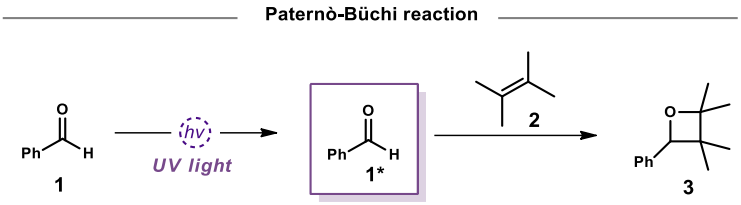

Figure 1.2. The Paterno-Buchi reaction.

1.2 Photoredox and hydrogen atom transfer catalysis

The major issue of the unimolecular *direct excitation* approach is that organic molecules tend to absorb mainly in the UV region, due to their large HOMO-LUMO gap. Additionally, organic molecules generally possess low molar attenuation coefficient, and their excited-state lifetime tends to be short. In order to overcome these limitations, a bimolecular approach was developed, which removed the requirement for the substrate to interact with light, thus widening the applicability of light-promoted reactions. Specifically, a substoichiometric amount of *photomediator* or *photocatalyst* can be utilized, which upon photoexcitation can activate the substrate via *single electron transfer*[8] (SET) or *energy transfer*[9] (EnT). Such photocatalysts are generally metal complexes or organic dyes with suitable photophysical properties, such as long excited-state lifetimes and high molar attenuation coefficients in the visible region of light, allowing lower energy irradiation to be used instead of harsh UV light.[10]

[7] (a) Paternò, E.; Cheffi, G. "Sintesi in chimica organica per mezzo della luce. Nota II. Composti degli idrocarburi non saturi con aldeidi e chetoni" *Gazz. Chim. Ital.* **1909**, *39*, 341; (b) Büchi, G.; Inman, C. G.; Lipinsky, E. S. "Light-catalyzed Organic Reactions. I. The Reaction of Carbonyl Compounds with 2-Methyl-2-butene in the Presence of Ultraviolet Light" *J. Am. Chem. Soc.* **1954**, *76*, 4327.

[8] Kavarnos, G. J. "Fundamentals of Photoinduced Electron Transfer" **1993**, *VCH*.

[9] Strieth-Kalthoff, F.; James, M. J.; Teders, M.; Pitzer, L.; Glorius, F. "Energy transfer catalysis mediated by visible light: principles, applications, directions" *Chem. Soc. Rev.* **2018**, *47*, 7190

[10] Yoon, T. P.; Ischay, M. A.; Du, J. "Visible Light Photocatalysis as a Greener Approach to Photochemical Synthesis" *Nat. Chem.* **2010**, *2*, 527

While the first uses of photocatalysts in basic organic transformations were reported in the late 1970s and early 1980's,[11] it was not until the seminal works by MacMillan,[12] Yoon,[13] and Stephenson[14] in 2008 and 2009 that the use of these photocatalysts initiated a renaissance in the field of synthetic photochemistry. These three reports employed the Ru^{II} complex $[Ru(bpy)_3]^{2+}$ as a photocatalyst mediating SET or EnT processes, which were utilized in fully developed synthetic procedures.[15]

As their pioneering example,[12] MacMillan and co-workers in 2008 combined organo- and photocatalysis to achieve stereoselective α-alkylation of aldehydes (Figure 1.3). The proposed mechanism consists of two closed catalytic cycles. In the organocatalytic cycle, condensation of aldehyde **4** with chiral aminocatalyst delivers enamine **I**. Visible light irradiation promotes the excitation of Ru^{II} photocatalyst **PC**, which can perform sacrificial SET oxidation of enamine **I**, delivering the reduced-state Ru^{I}. A favorable SET between the reduced photocatalyst Ru^{I} and alkyl bromide **5** generates radical **II**, which is subsequently trapped by the chiral enamine **I** in a stereoselective fashion. Yoon and coworkers later proposed that a radical chain propagation mechanism was responsible for product formation. Thus, the photoexcited ruthenium catalyst acted as an initiator, and the chain process was propagated by the reductive properties of the α-amino radical **III**.[16]

[11] (a) Hedstrand, D. M.; Kruizinga, W. M.; Kellogg, R. M. "Light induced and dye accelerated reductions of phenacyl onium salts by 1,4-dihydropyridines" *Tetrahedron Lett.* **1978**, 19, 1255; (b) Cano-Yelo, H.; Deronzier, A. "Photocatalysis of the Pschorr reaction by tris-(2,2′-bipyridyl)ruthenium(II) in the phenanthrene series" *J. Chem. Soc. Perkin Trans. 2*, **1984**, 1093 (c) Hironaka, K.; Fukuzumi, S.; Tanaka, T. "Tris(bipyridyl)ruthenium(II)-photosensitized reaction of 1-benzyl-1,4-dihydronicotinamide with benzyl bromide" *J. Chem. Soc., Perkin Trans. 2* **1984**, 1705.

[12] Nicewicz, D. A.; MacMillan, D. W. C. "Merging Photoredox Catalysis with Organocatalysis: The Direct Asymmetric Alkylation of Aldehydes" *Science* **2008**, *322*, 77.

[13] Ischay, M. A.; Anzovino, M. E.; Du, J.; Yoon, T. P. "Efficient Visible Light Photocatalysis of [2+2] Enone Cycloadditions" *J. Am. Chem. Soc.* **2008**, *130*, 12886.

[14] Narayanam, J. M. R.; Tucker, J. W.; Stephenson, C. R. J. "Electron-Transfer Photoredox Catalysis: Development of a Tin-Free Reductive Dehalogenation Reaction" *J. Am. Chem. Soc.* **2009**, *131*, 8756.

[15] Paris, J. P.; Brandt, W. W. "Charge Transfer Luminescence of a Ruthenium(II) Chelate" *J. Am. Chem. Soc.* **1959**, *81*, 5001.

[16] Cismesia, M. A.; Yoon, T. P. "Characterizing Chain Processes in Visible Light Photoredox Catalysis" *Chem. Sci.* **2015**, *6*, 5426.

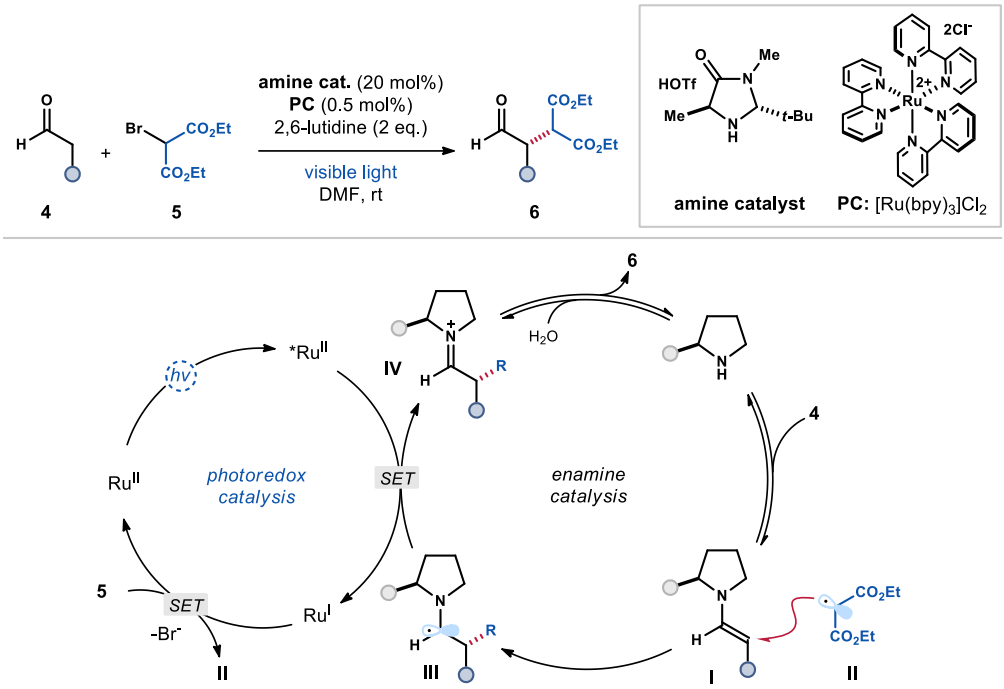

Figure 1.3. The beginning of photoredox catalysis: combining photoredox and organocatalysis for the enantioselective α-alkylation of aldehydes.

Due to the renewed interest in radical reactivity, other strategies were developed to form radicals. One such effective strategy is *hydrogen atom transfer* (HAT), which is based on different physical properties compared to the SET strategy, allowing for the activation of previously unavailable substrates within the realm of photocatalysis. HAT is a chemical process consisting of the concerted movement of two elementary particles – a proton and an electron – between two substrates in a single step.[17] While the movement of electron in SET is governed by the redox potentials of the reactants, the thermodynamic viability of a HAT process is dependent on the *bond dissociation energy* (BDE) of *C-H* bond of the substrate (Figure 1.4.a). The kinetic parameters of the HAT process largely depend on the *polarity*, or *philicity*, of the radicals involved in the reaction. Radicals possessing high energy of *singly occupied molecular orbital* (SOMO) are called *nucleophilic*, while low SOMO energy radicals are called *electrophilic*.[18] A *C-H* bond that after a HAT process would yield a

[17] (a) Capaldo, L.; Ravelli, D. "Hydrogen Atom Transfer (HAT): A Versatile Strategy for Substrate Activation in Photocatalyzed Organic Synthesis" *Eur. J. Org. Chem.* **2017**, 2056 (b) Capaldo, L.; Ravelli, D.; Fagnoni, M. "Direct Photocatalyzed Hydrogen Atom Transfer (HAT) for Aliphatic C–H Bonds Elaboration" *Chem. Rev.* **2022**, *122*, 1875

[18] (a) De Vleeschouwer, F.; Van Speybroeck, V.; Waroquier, M.; Geerlings, P.; De Proft, F. "Electrophilicity and Nucleophilicity Index for Radicals" *Org. Lett.* **2007**, *9*, 2721; (b) Fischer, H.; Random, L. "Factors Controlling the Addition of Carbon-Centered Radicals to Alkenes–An Experimental and Theoretical

nucleophilic radical is called *hydridic*, or *protic* if an electrophilic radical is formed. The rate of *polarity matched* HAT processes in which a hydridic atom is abstracted by an electrophilic radical, or a protic atom by a nucleophilic radical, is expected to be increased compared to *polarity mismatched* reactions (Figure 1.4.b).[19]

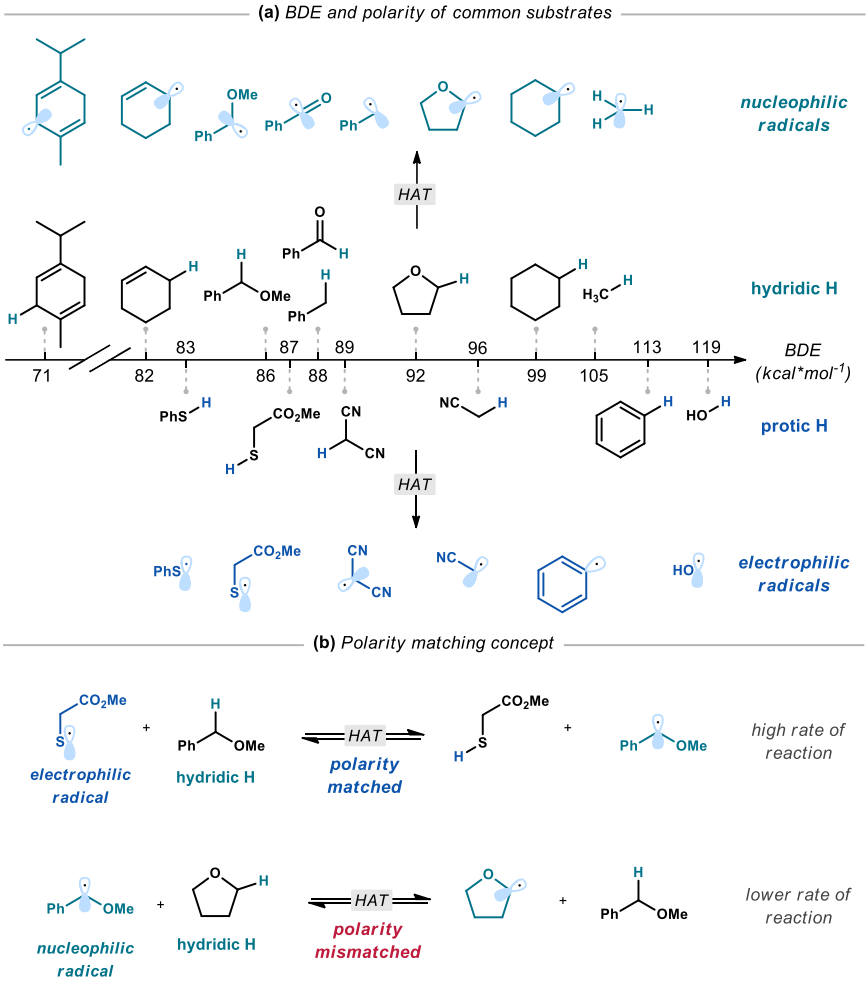

Figure 1.4. (a) BDE and polarity of some common substrates; (b) Polarity matching and its effect on rate of HAT reaction.

Perspective" *Angew. Chem. Int. Ed.* **2001**, *40*, 1340; (c) Héberger, K.; Lopata, A. "Assessment of nucleophilicity and electrophilicity of radicals, and of polar and enthalpy effects on radical addition reactions." *J. Org. Chem.* **1998**, *63*, 8646; (d) Giese, B. "Formation of C-C Bonds by Addition of Free Radicals to Alkenes." *Angew. Chem., Int. Ed.* **1983**, *22*, 753; (e) J. M. Tedder, "Which Factors Determine the Reactivity and Regioselectivity of Free Radical Substitution and Addition Reactions?" *Angew. Chem. Int. Ed. Engl.* **1982**, *21*, 401.

[19] Roberts, B.P. "Polarity-reversal catalysis of hydrogen-atom abstraction reactions: concepts and applications in organic chemistry" *Chem. Soc. Rev.*, **1999**, *28*, 25

In a pioneering report from 2014, the group of MacMillan demonstrated the possibility of merging the photoredox catalysis with a HAT-mediated catalytic cycle, which enabled generation of radicals from weak *C-H* bonds. Specifically, the *C-H* arylation of benzylic ethers **8** was achieved using the thiol **9** (BDE(*S-H*) = 87 kcal/mol) as HAT mediator in combination with iridium-based photoredox catalyst *fac*-Ir(ppy)$_3$ (Figure 1.5).[20] In this transformation, a long-lived cyanoaryl radical-anion **IV** is generated *via* SET reduction of cyanoarene **7** by the excited state *Ir^{III} of the iridium photocatalyst **PC**. This resulted in the formation of oxidized form Ir^{IV} that underwent SET oxidation with the deprotonated thiol catalyst **9**, generating thiyl radical **V**. This electrophilic radical abstracted a hydridic hydrogen atom from the weak *C-H* bond (BDE = 86 kcal/mol) of benzyl ether **8** in a polarity-matched HAT process, forming a stabilized radical **VI** which subsequently coupled with the persistent cyanoaryl radical anion **IV**, furnishing product **10**. This protocol highlights the utility of thiols as HAT catalysts for activation of weak hydridic *C-H* bonds, as thiols are easily deprotonated and oxidized to form electrophilic thiyl radicals **V** which are favorably poised to abstract the target C-H bonds of substrates such as **8**.

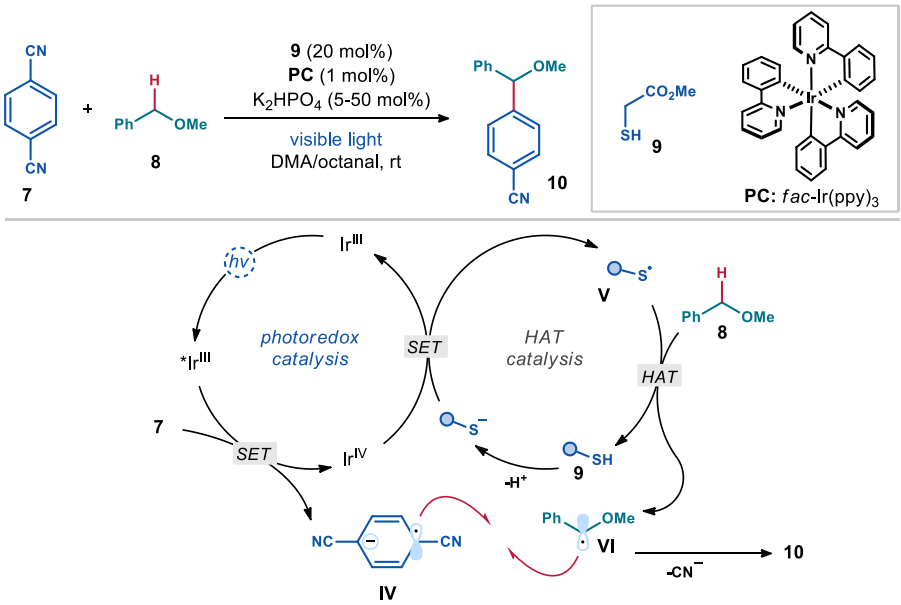

Figure 1.5. Combining photoredox catalysis with HAT catalysis for *C-H* arylation of benzyl ethers.

[20] Qvortrup, K.; Rankic, D. A.; MacMillan, D. W. C. "A General Strategy for Organocatalytic Activation of C−H Bonds via Photoredox Catalysis: Direct Arylation of Benzylic Ethers" *J. Am. Chem. Soc*. **2014**, *136*, 626.

The efficiency of radical cross-coupling in this transformation is assured by the so called *persistent radical effect*,[21] which outlines two conditions for an effective radical cross-coupling to occur: (*i*) the radicals involved should be produced at a similar rate; (*ii*) one of the radicals should have a longer lifetime (lower self-coupling rate constant). The first condition is ensured by the coupling of fast photoredox and HAT catalytic cycles, while the cyanoaryl radical anion **IV** is persistent and thus qualifies for the second condition.

1.3 Excitation of organic intermediates

The use of a photoredox catalyst is not the only way to exploit the power of visible light in photocatalytic processes. For example, our research group has shown that some organocatalytic intermediates (e.g. chiral enamines) with an established reactivity in polar pathways can engage in photoinduced SET processes upon light excitation. In fact, upon reaching their excited state, these organocatalytic intermediates can promote the formation of radicals via SET pathways, which are subsequently trapped in a stereoselective fashion. Combining the photo-activity and the ground-state activity of organocatalytic intermediates allowed the development of asymmetric radical transformations unachievable in the thermal domain.[22]

For instance, our group found that, when an electron-poor benzylic bromide **11** was mixed with chiral enamines **I**, the colorless reaction mixture changed color to become bright yellow (Figure 1.6).[23] This empirical observation was rationalized on the basis of the electron donor-acceptor (EDA) theory. According to Mulliken quantum mechanical rationalization,[24] the association of an electron-rich species, the donor, and an electron-poor species, the acceptor, can promote the formation of a new ground-state complex.[25] This new chemical entity, called an EDA complex, possesses a red-shifted absorption profile compared to ground states of both donor and acceptor, meaning that this EDA complex can usually be excited by visible light. Irradiation of the EDA complex promotes an intra-complex SET from the donor to the acceptor, which eventually leads to radical generation.[22] This property was exploited for the α-alkylation of aldehydes, where the electron-rich enamine **I** acted as the donor, whereas the electron-poor bromide **11** was the acceptor partner (Figure 1.6, orange box). Light-mediated

---

[21] Leifert, D.; Studer, A. "The Persistent Radical Effect in Organic Synthesis" *Angew. Chem. Int. Ed*. **2020**, *59*, 74.

[22] Silvi, M.; Melchiorre, P. "Enhancing the potential of enantioselective organocatalysis with light" *Nature*, **2018**, *554*, 41

[23] Arceo, E.; Jurberg, I. D.; Álvarez-Fernández, A.; Melchiorre, P. "Photochemical Activity of a Key Donor–Acceptor Complex Can Drive Stereoselective Catalytic α-alkylation of Aldehydes" *Nat. Chem.* **2013**, *5*, 750

[24] Mulliken, R. S. "Molecular Compounds and their Spectra. III. The Interaction of Electron Donors and Acceptors*" J. Phys. Chem.* **1952**, *56*, 801.

[25] Crisenza, G. E. M.; Mazzarella, D.; Melchiorre, P. "Synthetic Methods Driven by the Photoactivity of Electron Donor–Acceptor Complexes" *J. Am. Chem. Soc.* **2020**, *142*, 5461

intra-complex SET reduced the benzyl bromide, forming the reactive benzyl radical **VII** upon fragmentation of the bromide, which served as a leaving group. Stereoselective trapping of the ensuing carbon-centered radical **VII** by the enamine **I** afforded the chiral product **12**.

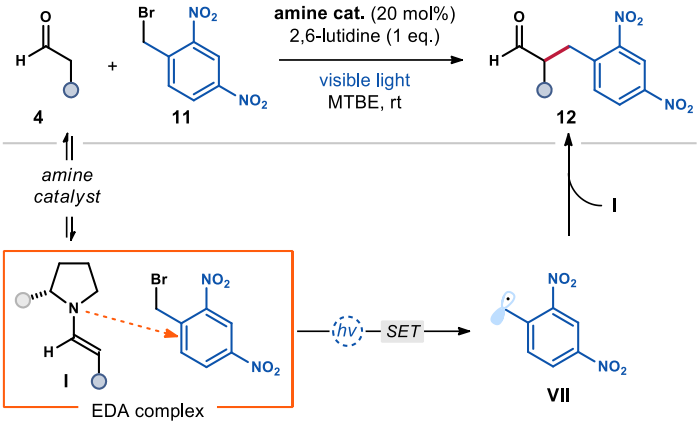

Figure 1.6. EDA strategy for the enantioselective α-benzylation of aldehydes.

Our group later found that organic intermediates such as enamines can also directly absorb visible light without the need for EDA complex formation. For example, while enamines behave as nucleophiles in the ground state,[26] they act as strong SET reductants upon excitation by 390 nm light (Figure 1.7).[27] Their significant reducing power (E^*_{red} = -2.5 V vs Ag/AgCl) was exploited to generate malonyl radicals **II** from bromomalonates **2** which otherwise would not engage in EDA complex formation with enamines. The chiral enamine **I** subsequently intercepted radical **II** in a stereoselective fashion to afford the α-amino radical **III**. This species then reduced another molecule of substrate **2** in a radical chain propagation step. The resulting iminium **IV** was eventually hydrolyzed to product **3**, releasing the aminocatalyst. These works highlighted how a well-established intermediate in ground-state polar chemistry could be repurposed using light to trigger new radical processes by employing its excited state reactivity.[28]

[26] Mukherjee, S.; Yang, J. W.; Hoffmann, S.; List, B. "Asymmetric Enamine Catalysis" *Chem. Rev.* **2007**, *107*, 5471.

[27] Silvi, M.; Arceo, E.; Jurberg, I. D.; Cassani, C.; Melchiorre, P. "Enantioselective Organocatalytic Alkylation of Aldehydes and Enals Driven by the Direct Photoexcitation of Enamines" *J. Am. Chem. Soc.* **2015**, *137*, 6120.

[28] Silvi, M.; Melchiorre, P. "Enhancing the Potential of Enantioselective Organocatalysis with Light" *Nature* **2018**, *554*, 41.

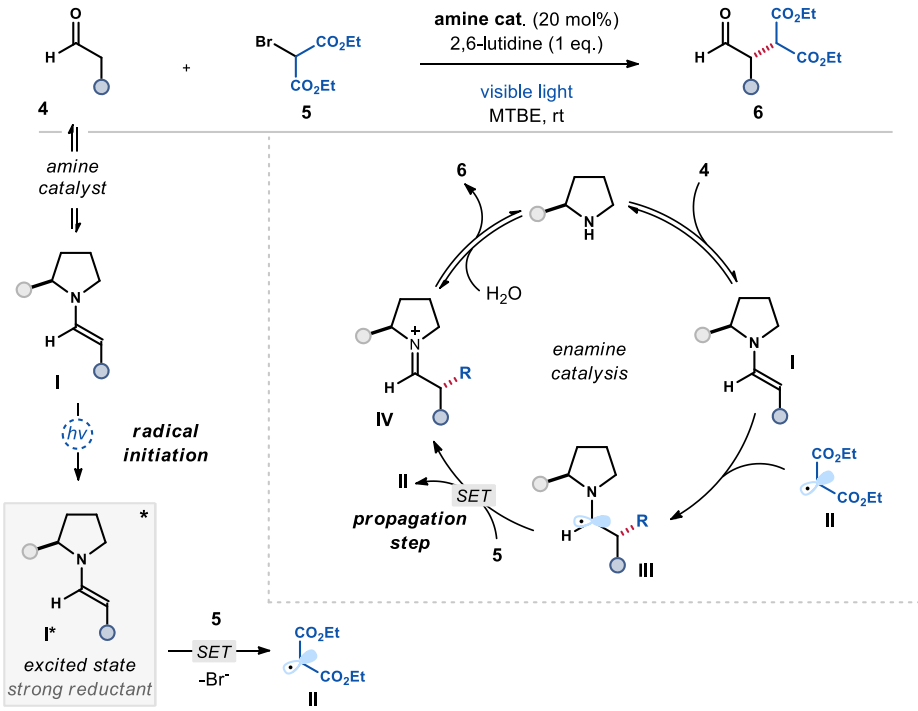

Figure 1.7. Direct photoexcitation of enamines **I** for the stereoselective α-alkylation of aldehydes.

In 2022, our group utilized the EDA complex formation to enable HAT-mediated cross-coupling between stabilized allylic and benzylic radicals.[29] Specifically, a deprotonated dithiophosphoric acid HAT catalyst **DTPA** first served as a donor to activate redox-active esters **13** *via* formation of an EDA complex (Figure 1.8). Light excitation of the EDA complex triggered an SET event, furnishing benzylic radicals **VII** and the thiyl radical **V** (path *i*). This electrophilic thiyl radical **V** then performed polarity-matched HAT with a hydridic *C-H* bond of cyclic allylic substrate **14**, producing an allylic radical **VIII** and regenerating the **DTPA** catalyst. The allylic and benzylic radicals then coupled with each other, furnishing products **15a**. However, when redox-active esters **13b** were used, non-stabilized radicals **IX** were furnished upon light-triggered intracomplex SET (path *ii*), which resulted in low yield of radical cross-coupling due to high rate of homo-coupling process for these radicals. To satisfy the persistent radical effect criteria, a three-component protocol was designed, adding a styrene derivative **16** to trap radical **IX** and produce kinetically stabilized benzylic radical **X** that was involved in an efficient radical cross-coupling with the allylic radical, furnishing the products **15b** .

[29] Le Saux, E.; Zanini, M.; Melchiorre, P., "Photochemical Organocatalytic Benzylation of Allylic C-H Bonds." *J. Am. Chem. Soc.* **2022**, *144*, 1113

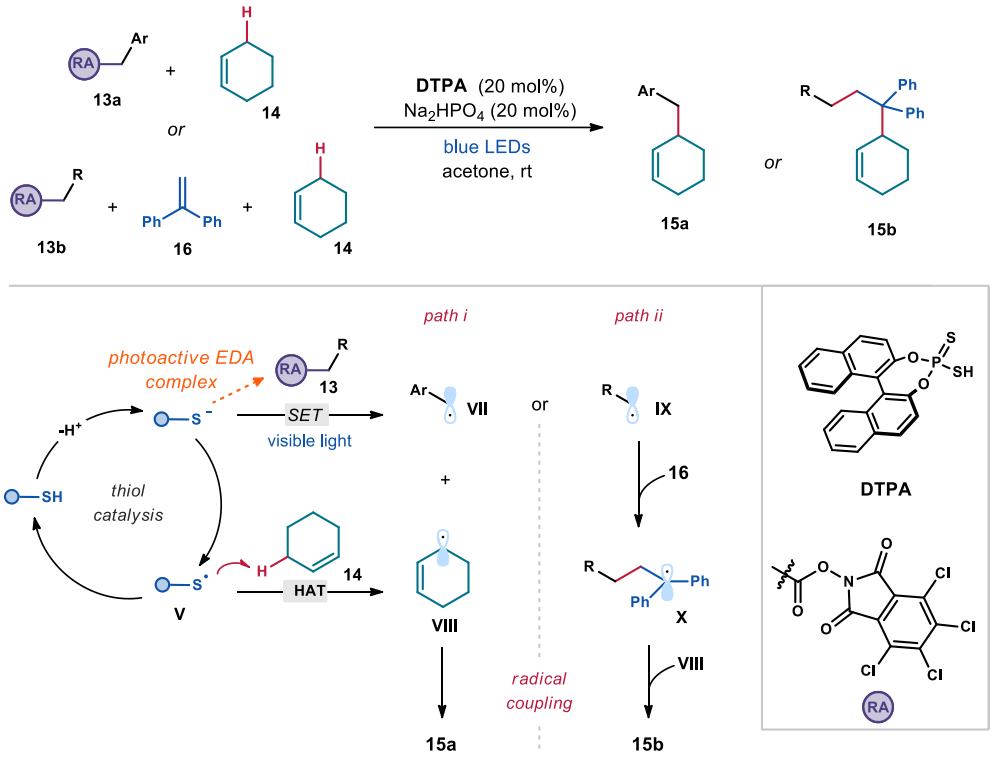

Figure 1.8. Merging EDA strategy with HAT catalysis for benzylic allylation.

The examples discussed in this chapter illustrate the versatility of photocatalytic methods developed over the past decade and a half. The photochemical strategies and the concepts of radical reactivity outlined in this introduction were instrumental in the design and execution of the scientific projects developed during this doctoral thesis. The following section will provide a general overview of targets pursued in these projects.

1.4 General objectives and summary

The principal objective of this doctoral thesis was to develop new photo-induced radical carbon-carbon bond-forming reactions. The three reactivity concepts discussed previously, namely photoredox catalysis, the direct excitation of organic intermediates, and HAT catalysis, were used to generate radicals under mild reaction conditions and design new processes (Figure 1.9).

In Chapter II, I used a dithiophosphoric acid (**DTPA**) catalyst that, upon deprotonation and direct UV light excitation, was capable of reducing pyridinium ions, providing a novel method for the regioselective allylation of pyridines. Here both the SET and the HAT properties of this catalyst were essential to successfully develop the system. In Chapter III, a novel

reductive olefin cross-coupling protocol was developed by combining photoredox catalysis and HAT catalysis. The protocol allowed the SET reduction of electron-poor olefins, which subsequently coupled with electron-neutral olefins, furnishing sp^3-rich products with unusual connectivity from easily available substrates.

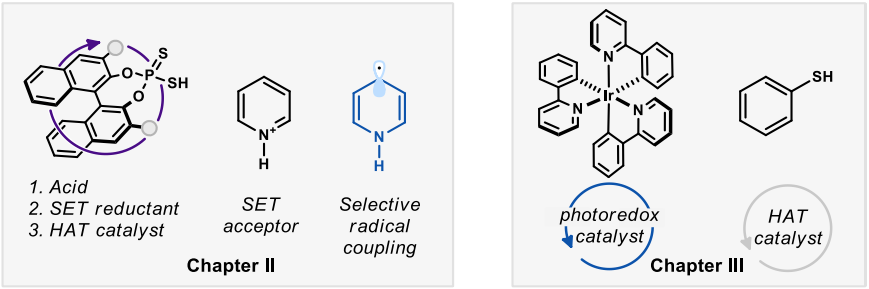

Figure 1.9. Schematic representation of the main tools employed in the following chapters.

1.4.1 Photochemical functionalization of pyridines via pyridinyl radicals

Chapter II details a new photochemical method for the functionalization of pyridines in a process mediated by catalyst **DTPA** (Figure 1.10). First, this catalyst acts as Brønsted acid for pyridine protonation. The SET reduction of the electron-deficient π-system of the resulting pyridinium ion is then accomplished by the deprotonated catalyst, which underwent direct excitation by UV light irradiation to become a strong reductant in the excited state. Finally, the oxidized catalyst (a thiyl radical) acts as a HAT abstractor for the activation of allylic *C-H* bonds. Through this catalytic sequence, in which the catalyst performs three distinct catalytic activities, pyridinyl and allylic radicals are formed. These radicals can then participate in a coupling process with high regioselectivity, ultimately yielding C4-functionalized pyridines.

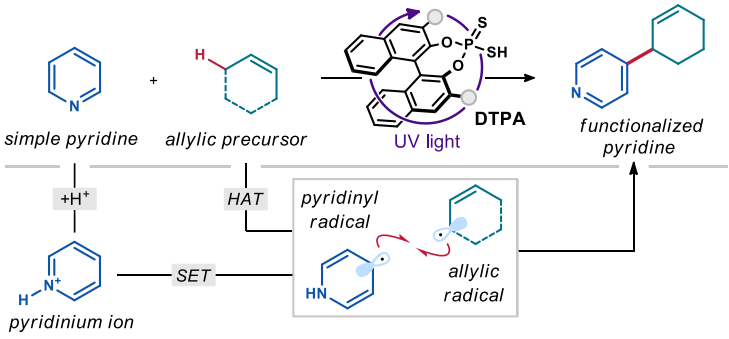

Figure 1.10. C4-selective allylation of pyridines enabled by pyridinyl radical formation.

This work was developed as a collaboration with Dr. Emilien Le Saux, who discovered the reaction, contributed to the optimization and scope survey, and performed photophysical studies. Dr. Eleni Georgiou took part in the exploration of the reaction's scope and mechanistic elucidations, and Dr. Will Hartley performed computational experiments to support our mechanistic rationale. I contributed to the initial optimization, the investigations of the process generality, and the mechanistic understanding of this transformation.

1.4.2 Reductive cross-coupling of olefins via a radical pathway

A new light-driven strategy for the reductive olefin cross-coupling is detailed in chapter III. Central to this strategy, which combined SET and HAT chemistry, was the exploitation of the electronic differences between two olefin substrates. This enabled the selective generation of radicals via photoredox-mediated SET reduction of the electron-deficient olefins. After subsequent protonation, radical addition to readily available neutral olefins, followed by HAT reduction mediated by a thiol catalyst, sp^3-rich products with distinct connectivity are formed.

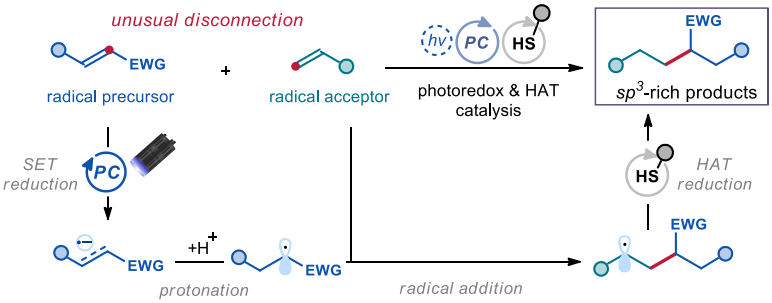

Figure 1.11. Reductive olefin cross-coupling enabled by the combination of photoredox and HAT catalysis.

This work was developed in collaboration with Dr. Wei Zhou, who discovered the reaction and contributed to its optimization, scope survey, and mechanistic understanding. I contributed to the discovery process, the reaction optimization, the investigations of the process generality, and the mechanistic investigation.

Chapter II

Photochemical Functionalization of Pyridines via Pyridinyl Radicals

Target

To develop a new strategy for pyridine functionalization using catalytically generated pyridinyl radicals as key intermediates in a radical coupling process.

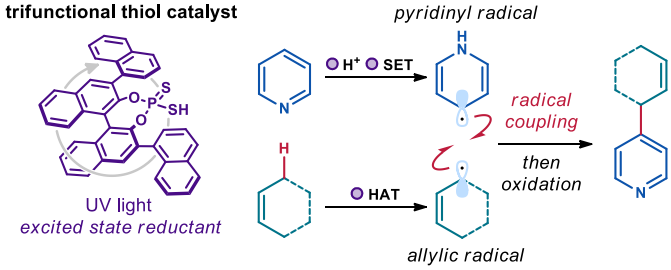

Tools

A novel photocatalytic strategy based on a dithiophosphoric acid (DTPA) catalyst that enables pyridinyl radical generation via successive protonation of pyridine and single electron reduction of the pyridinium cation. The resulting pyridinyl radical is then involved in a radical coupling with an allylic radical generated via hydrogen atom transfer (HAT) process.[1]

2.1 Introduction

Pyridines and related nitrogen heterocycles are ubiquitous in biologically active molecules, with pyridine being the most abundant heteroaromatic ring in FDA-approved drugs.[2] A simple substitution of a phenyl ring for a pyridine in a structure of a drug candidate can improve its activity, metabolic stability, membrane permeability and many other pharmacokinetic

[1]The project discussed in this chapter has been conducted in collaboration with Dr. Emilien Le Saux, Dr. Eleni Georgiou, and Dr. Will C. Hartley. I performed the initial optimization of the reaction conditions and was involved with the investigation of the scope of the reaction and its mechanistic elucidation. This study has been published: Le Saux, E.; Georgiou, E.; Dmitriev, I. A.; Hartley, W. C.; Melchiorre, P. "Photochemical Organocatalytic Functionalization of Pyridines via Pyridinyl Radicals" *J. Am. Chem. Soc.* **2023**, *145*, 47.

[2] (a) Vitaku, E.; Smith, D. T.; Njadarson, J. T. "Analysis of the Structural Diversity, Substitution Patterns, and Frequency of Nitrogen Heterocycles among U.S. FDA Approved Pharmaceuticals" *J. Med. Chem.* **2014**, *57*, 10257; (b) Bhutani, P.; Joshi, G.; Raja, N.; Bachhav, N.; Rajanna, P. K.; Bhutani, H.; Paul, A. T.; Kumar, R. "U.S. FDA Approved Drugs from 2015−June 2020: A Perspective" *J. Med. Chem.* **2021**, *64*, 2339.

properties, highlighting the privileged status of this moiety.[3] Pyridine-derived ligands are also common as ligands of transition metal catalysts, enabling a multitude of industrial processes (Figure 2.1).

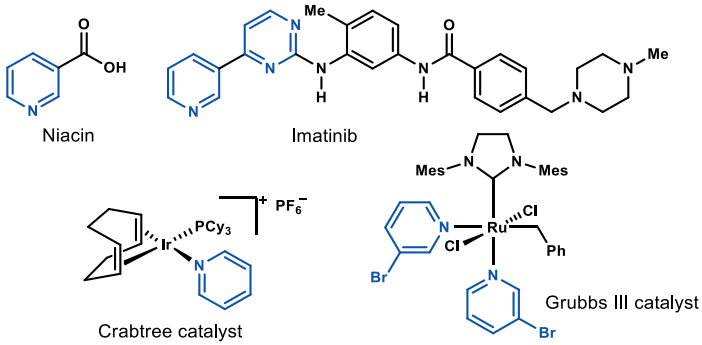

Figure 2.1. Examples of bio-relevant compounds and organometallic catalysts containing pyridine and diazine units. Cy: Cyclohexyl; Mes: mesityl.

The importance of pyridines has been a long-standing incentive for the development of new methods of their construction and site-selective modification. Historically, multicomponent condensation reactions, pioneered by Knoevenagel and Hantzsch and further developed by Chichibabin, have been the most common way for the *de novo* synthesis of pyridine rings.[4] The robustness of such strategies and harsh conditions required (>100°C) are well-suited for industrial production of simple pyridines. However, in the context of academic research and drug development flexible approaches with high functional group tolerance are desirable. One such approach, the *direct* functionalization of pyridines, offers rapid and direct modification of pre-formed scaffolds and is particularly useful for the late-stage modification of complex intermediates.[5]

In this framework, *Minisci reaction* – the addition of a carbon-centered radical to a heteroaromatic substrate – is a prime example.[6] As depicted in Figure 2.2, the key step of Minisci reaction is the formation of pyridinium ion **I** via protonation of pyridine **1a** (the

[3] Ling, Y.; Hao, Z-Y.; Liang, D.; Zhang, C-L.; Liu, Y-F.; Wang, Y. "The Expanding Role of Pyridine and Dihydropyridine Scaffolds in Drug Design" *Drug. Des. Devel. Ther*. **2021**, *15*, 4289.

[4] Allais, C.; Grassot, J-M.; Rodriguez, J.; Constantieux, T. "Metal-Free Multicomponent Syntheses of Pyridines" *Chem. Rev*. **2014**, *114*, 10829.

[5] (a) Murakami, K.; Yamada, S.; Kaneda, T.; Itami, K. "C-H Functionalization of Azines" *Chem. Rev*. **2017**, *117*, 9302. (b) Failla, M.; Lombardo, G. W.; Orlando, P.; Fiorito, D.; Bombonato, E.; Ronchi, P.; Passarella, D.; Fasano, V. "Late-Stage Functionalisation of Pyridine-Containing Bioactive Molecules: Recent Strategies and Perspectives" *Eur. J. Org. Chem.*, **2023**, *26*, e202300074

[6] (a) Minisci, F.; Bernardi, R.; Bertini, F.; Galli, R.; Perchinummo, M. "Nucleophilic Character of Alkyl Radicals – VI A New Convenient Selective Alkylation of Heteroaromatic Bases" *Tetrahedron* **1971**, *27*, 3575; (b) Proctor, R. S. J.; Phipps, R. J. "Recent Advances in Minisci-Type Reactions" *Angew. Chem. Int. Ed*. **2019**, *58*, 13666; (c) Zhang, X.; Li, S.; Qiu, F.; Wu, J; Jia, P. "Photocatalyzed Minisci-Type Reactions for Late-Stage Functionalization of Pharmaceutically Relevant Compounds" *Green Chem.*, **2024**, *26*, 3595.

detailed mechanism is described in the next section). This intermediate is more susceptible to attack by nucleophilic carbon radical **II** due to the lowering of the energy of the lowest unoccupied molecular orbital (LUMO) by the positive charge. Additionally, due to charge localization on the nitrogen atom, a certain degree of regioselectivity is achieved: formation of *C3*-substituted products is mostly avoided, while *C2*- and *C4*-alkylation products form in varied ratios, with *C2*-products usually being favored. Altogether, this reactivity provides a convenient tool for rapid structural diversification at the late stages of synthetic routes, finding numerous applications in medicinal chemistry.[6b] In the industrial setting, however, the separation of the regioisomers proves challenging, hampering a more widespread adoption of this strategy.[7]

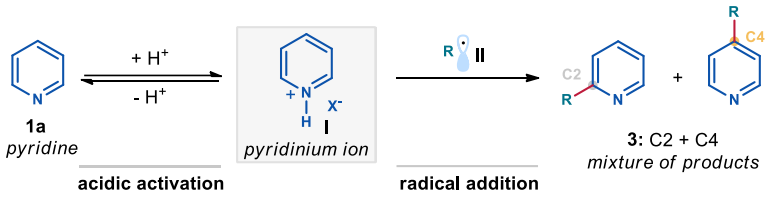

Figure 2.2. The key steps of Minisci reaction and the associated challenge of regioselectivity.

In the radical domain, the Minisci reaction is the only strategy available for the direct functionalization of pyridines. This prompted us to investigate a mechanistically divergent radical-based method for pyridine functionalization that could potentially provide products with distinct positional selectivity. Specifically, we focused on the pyridinyl radical **III** (Figure 2.3.a) as a possible intermediate *en route* to pyridine functionalization. The dimerization of pyridinyl radicals formed by electrolysis of *N*-alkylpyridinium salts was studied in 1998, concluding that *C4*-*C4* coupled dimers are favored possibly due to electron spin density distribution across the pyridinyl core, with *C6*-*C6* or *C4*-*C6* dimers forming in cases of steric hindrance around the *C4* position (Figure 2.3.b).[8]

[7] Duncton, M. A. J. "Minisci Reactions: Versatile CH-Functionalizations for Medicinal Chemists" *Med. Chem. Commun.* **2011**, *2*, 1135.

[8] Carelli, V.; Liberatore, F.; Casini, A.; Tortorella, S.; Scipione, L.; Di Rienzo, B. "On the Regio- and Stereoselectivity of Pyridinyl Radical Dimerization" *New J. Chem.* **1998**, *22*, 999.

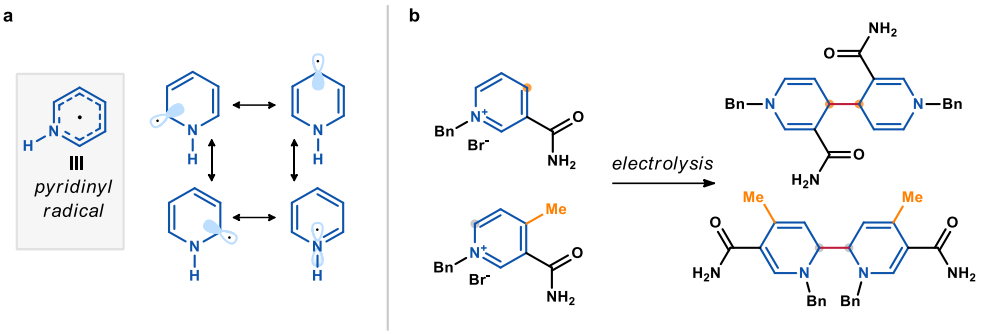

Figure 2.3. (**a**) Pyridinyl radical **III** and its resonance structures. (**b**) Effect of substitution on dimerization of pyridinyl radicals. Bn: benzyl.

The radical **III** has also been used as a one-electron shuttle for the catalytic electroreduction of carbon dioxide[9], but otherwise has been neglected in synthetic chemistry thus far. We hypothesized that the uncharted reactivity of pyridinyl radical **III** could give rise to novel opportunities for the site-selective functionalization of pyridines, especially given that some indications towards potential regioselectivity can be distilled out from previous studies in Figure 2.3.

This chapter details how this opportunity has been exploited, describing a new method for regioselective radical functionalization of pyridines **1** (Figure 2.4). The process has utilized the acidic activation of pyridines to form pyridinium ions **I** that are readily susceptible to SET reduction, furnishing pyridinyl radicals **III**. These radicals were coupled with stabilized allylic radicals **IV** with high degree of regioselectivity, furnishing *C4*-functionalized products.

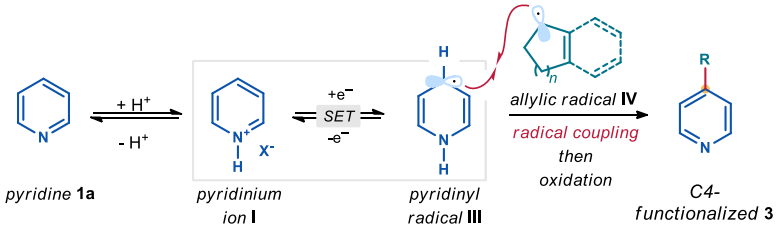

Figure 2.4. Regioselective functionalization of pyridines via pyridinyl radical formation.

In the following sections, the important literature precedents on the methods of radical functionalization of pyridines are discussed, as well as literature data that served as inspiration for this project.

[9] (a) Seshadri, G.; Lin, C.; Bocarsly, A. B. "A New Homogeneous Electrocatalyst for the Reduction of Carbon Dioxide to Methanol at Low Overpotential" *J. Electroanal. Chem.* **1994**, *372*, 145; (b) Barton Cole, E.; Lakkaraju, P. S.; Rampulla, D. M.; Morris, A. J.; Abelev, E.; Bocarsly, A. B. "Using a One-Electron Shuttle for the Multielectron Reduction of CO_2 to Methanol: Kinetic, Mechanistic, and Structural Insights" *J. Am. Chem. Soc.* **2010**, *132*, 11539.

2.2 Background

2.2.1 Radical addition to pyridines: the Minisci reaction

The venerable Minisci reaction is a broadly used and versatile method for the functionalization of pyridines and related heterocycles using radical pathway. In contemporary chemical literature, the term "Minisci reaction" is often used as a general descriptor for all processes involving addition of a carbon-centered radical **II** to a heterocycle **1** followed by a formal loss of a hydrogen atom by intermediate **V** (Figure 2.5.a). Although radical addition to aromatic systems was known since 1924,[10] the first protocol for the radical attack on a heterocyclic core was reported in 1964, when it was found that aryl radicals **VI**, generated from aryldiazonium salts upon heating, could undergo addition to pyridines at the *C2*-, *C3*-, and *C4*-positions (Figure 2.5.b).[11] Lynch and coworkers discovered that increasing the concentration of aryldiazonium salts increased the proportion of the *C2*-substituted product, attributing it to *N*-activation of pyridine in form of pyridinium ion **VII** upon addition of pyridine to the diazonium salt. This interpretation was in agreement with previous theoretical work predicting higher reactivity at the *C2*-position of pyridinium ions in radical substitution reactions.[12] In a subsequent study, the group of Lynch used acetic acid as a solvent to protonate pyridine, further demonstrating the participation of pyridinium ions in the reaction.[13] In 1968, Minisci described the addition of redox-generated alkyl radicals to protonated heteroaromatics,[14] a protocol that was further developed into what is now known as Minisci reaction.[15] This reaction involves generation of alkyl radicals **II** via oxidation of carboxylic acids **4** utilizing persulfate as an oxidant and mediated by silver salts (Figure 2.5.c).

---

[10] Gomberg, M.; Bachmann, W. E. "The synthesis of biaryl compounds by means of the diazo reaction" *J. Am. Chem. Soc.* **1924**, *46*, 2339.

[11] (a) Abramovitch, R. A.; Saha, J. G. "Reaction of Pyridine with *ortho*-Substituted Phenyl Radicals, and the Influence of Oxygen upon Isomer Ratios in the Gomberg-Hey Reaction" *J. Chem. Soc*. **1964**, 2175; (b) Lynch, B. M.; Chang, H. S. "Concentration-Dependent Orientations in Free-Radical Phenylations of Heteroaromatic Compounds" *Tetrahedron Lett.* **1964**, *5*, 2965.

[12] Brown, R. D.; Heffernan, L. N. "The Chemistry of Pyridine, Pyrimidine, and Pyrazine" *Austral. J. Chem.* **1956**, *9*, 83.

[13] Dou, H. J. M.; Lynch, B. M. "Selective Free-Radical Phenylations: nitrogen-Heteroatomic Compounds in Acidic Media" *Tetrahedron Lett.* **1965**, *6*, 897.

[14] (a) Minisci, F.; Galli, R.; Cecere, M.; Malatesta, V.; Caronna, T. "Nucleophilic Character of Alkyl Radicals: New Syntheses by Alkyl Radicals Generated in Redox Processes" *Tetrahedron Lett.* **1968**, *9*, 5609; (b) Minisci, F.; Galli, R.; Malatesta, V.; Caronna, T. "Nucleophilic Character of Alkyl Radicals – II: Selective Alkylation of Pyridine, Quinoline and Acridine by Hydroperoxides and Oxaziranes" *Tetrahedron*, **1970**, *26*, 4083.

[15] Minisci, F.; Bernardi, R.; Bertini, F.; Galli, R.; Perchinummo, M. "Nucleophilic Character of Alkyl Radicals – VI A New Convenient Selective Alkylation of Heteroaromatic Bases" *Tetrahedron* **1971**, *27*, 3575.

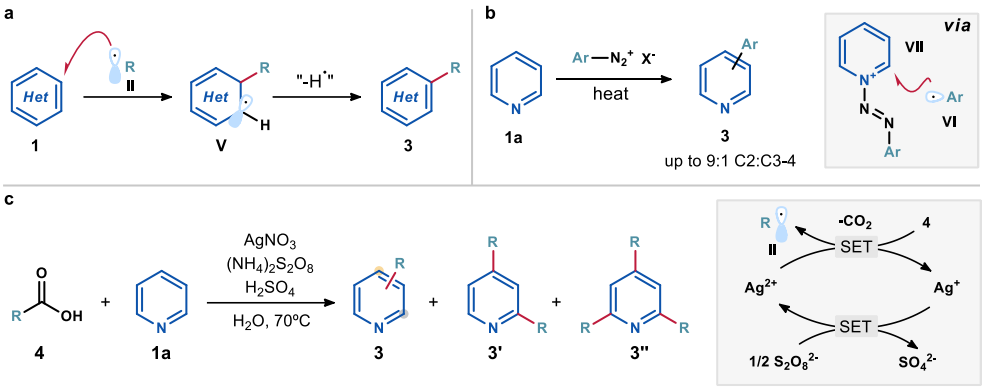

Figure 2.5. (**a**) General concept of the Minisci reaction. (**b**) Initial reports on the radical arylation of pyridine. (**c**) The original Minisci protocol.

These seminal reports highlight the fundamental chemical aspects of the Minisci reaction: (*i*) nucleophilic radicals are required; (*ii*) acidic activation improves the regioselectivity but mixtures of *C2/C4* alkylated products are generally formed; and (*iii*) overalkylation is difficult to prevent and control.

The mechanistic model of the reaction rationalizing the regioselectivity outcomes was proposed by Minisci in 1987 and is illustrated in Figure 2.6.[16]

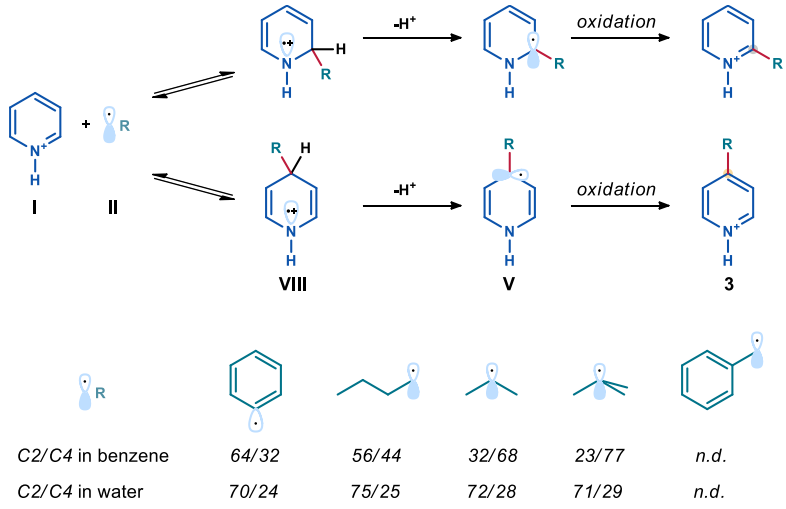

Figure 2.6. Mechanistic model of Minisci reactions.

[16] Minisci, F.; Vismara, E.; Fontana, F.; Morini, G.; Serravalle, M. "Polar effects in free-radical reactions. Solvent and isotope effects and effects of base catalysis on the regio- and chemoselectivity of the substitution of protonated heteroaromatic bases by nucleophilic carbon-centered radicals" *J. Org. Chem.* **1987**, *52*, 730.

The reaction starts from an attack by a nucleophilic radical **II** on the pyridinium ion **I** at either *C2* or *C4* position, furnishing an intermediate radical-cation **VIII**. This intermediate undergoes subsequent deprotonation to form radical **V**, which is finally oxidized to furnish the functionalized product **3**. Both reaction medium and the nature of the radical **II** affect the reaction outcome. For less stabilized radicals such as Ph$^{\bullet}$, the initial radical attack is irreversible and the regioselectivity is determined by the initial position of attack (*C2/C4 ca.* 2/1, in line with the statistical outcome). For more stabilized radicals, such as *t*Bu$^{\bullet}$, the reversibility of addition is significant and therefore the regioselectivity is determined by comparative rate of deprotonation of intermediates **VIII**, influenced by the polarity of the media (*C2/C4* = 23/77 in benzene vs 71/29 in water). Other parameters, including temperature and *pH*, also affect the outcome of the reaction, depending on the nature of the radical **II** and following the outlined principles. Altogether, this highlights the multivariable nature and difficulty of predicting and influencing the regioselectivity of a given Minisci reaction, while maintaining the fact that even in the most optimal conditions the regioselectivity is not perfect. Additionally, stabilized radicals such as benzylic radical proved challenging for classical Minisci conditions, as high degree of addition reversibility provides an avenue for homocoupling of these radicals, producing bibenzyl as sole product. Moreover, elevated temperatures and stoichiometric oxidants are required, somewhat limiting the attractiveness of this protocol.

Recently, the development of photoredox catalysis has allowed for the generation of radicals under milder conditions, leading to a renaissance in the field of radical chemistry.[17] An initial application of photoredox conditions for Minisci reaction was reported by DiRocco and co-workers at Merck in 2014.[18] A late-stage functionalization campaign was undertaken on biologically active heterocycles, *e.g.* Voriconazole **5**, but classical Minisci conditions (Figure 2.5.c) proved to be too harsh for these fragile compounds. Instead, an iridium photocatalyst $[Ir\{dF(CF_3)ppy\}_2(dtbpy)]PF_6$ and visible light irradiation offered suitable conditions (Figure 2.7). The excited state of the photocatalyst Ir^{III*} reduced the protonated *tert*-butyl peracetate **IX** to produce a *tert*-butoxyl radical **X**. This radical underwent spontaneous *β*-scission, producing acetone along with a methyl radical **II**, which then added to the protonated heterocycle **I**. After deprotonation, the resulting α-amino radical **V** was oxidized by Ir^{IV} to the methylated product **7**, turning over the catalytic cycle by regenerating the ground-state Ir^{III} catalyst. The use of mild reagents and ambient temperature allowed the methylation of a

[17] Shaw, M. H.; Twilton, J.; MacMillan, D. W. C. "Photoredox Catalysis in Organic Chemistry" *J. Org. Chem.* **2016**, *81*, 6898.

[18] DiRocco, D. A.; Dykstra, K.; Krska, S.; Vachal, P.; Conway, D. V.; Tudge, M. "Late-Stage Functionalization of Biologically Active Heterocycles Through Photoredox Catalysis" *Angew. Chem. Int. Ed*. **2014**, *53*, 4802.

variety of complex heterocycles in moderate to good yields, though the challenges of regioselectivity and overalkylation persisted.[19]

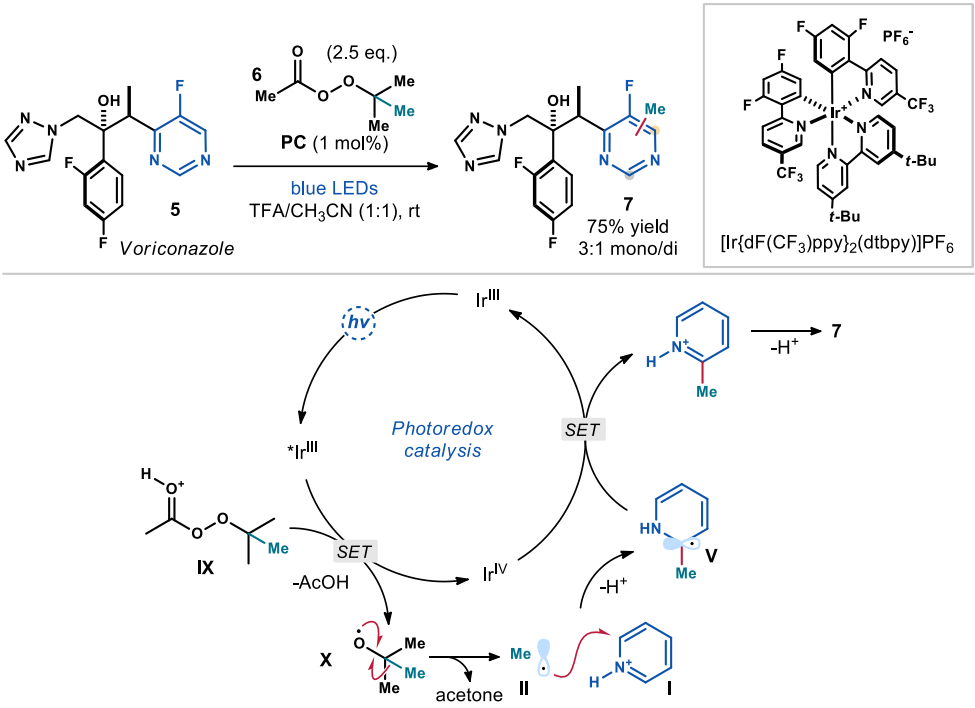

Figure 2.7. Photocatalytic Minisci-type methylation.

One way of alleviating the regioselectivity issue has been discovered recently. In the polar domain, bulky *N*-activating groups are utilized to direct complete *C4*-selectivity in pyridine functionalization processes, as they hinder *C2*- and *C6*-positions.[20] This strategy has recently been translated into the radical domain by involving such sterically hindered *N*-activated pyridines **8** in Minisci reactions (Figure 2.8). In one example reported by the group of Hong, *N*-aminopyridinium salts **8a** served as excellent substrates for *C4*-selective radical

[19] O'Hara, F.; Blackmond, D. G.; Baran, P. S. "Radical-Based Regioselective C−H Functionalization of Electron-Deficient Heteroarenes: Scope, Tunability, and Predictability" *J. Am. Chem. Soc*. **2013**, *135*, 12122.

[20] (a) Nakao, Y.; Yamada, Y.; Kashihara, N.; Hiyama, T. "Selective C-4 Alkylation of Pyridine by Nickel/Lewis Acid Catalysis" *J. Am. Chem. Soc*. **2010,** *132*, 13666; (b) Tsai, C.-C.; Shih, W.-C.; Fang, C.-H.; Li, C.-Y.; Ong, T.-G.; Yap, G. P. A. "Bimetallic Nickel Aluminum Mediated Para-Selective Alkenylation of Pyridine: Direct Observation of η^2,η^1-Pyridine Ni(0)− Al(III) Intermediates Prior to C−H Bond Activation" *J. Am. Chem. Soc*. **2010**, *132*, 11887; (c) Obradors, C.; List, B. "Azine Activation via Silylium Catalysis" *J. Am. Chem. Soc*. **2021**, *143*, 6817.

functionalization.[21] In another effort, the Baran group used *N*-alkylated pyridinium salts **8b**.[22] These substrates underwent Minisci reaction with complete *C4*-selectivity, though initial installation of this group was difficult for *C2/C6* substituted pyridines. The synthesis of activated substrates **8a** and **8b** starting from pyridine is a two- to three-step process involving harsh electrophiles and/or elevated reaction temperatures, which could limit the usefulness of such protocols for late-stage functionalization campaigns.

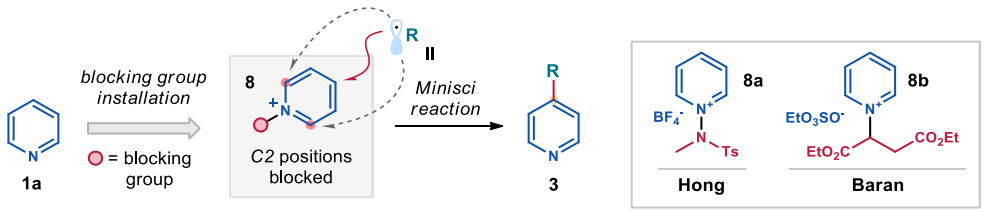

Figure 2.8. General concept of blocking group strategies for regioselective addition of radicals to pyridines.

Another challenge persisting to this day is the involvement of stabilized radicals (benzylic, allylic) and electrophilic radicals in a Minisci reaction (Figure 2.9). Only three Minisci protocols for azine *C-H* benzylation have been reported, though they are limited to the functionalization of isoquinolines,[23] benzothiazole,[24] and 4-cyanopyridines.[25]

[21] (a) Moon, Y.; Park, B.; Kim, I.; Kang, G.; Shin, S.; Kang, D.; Baik, M. H.; Hong, S. "Visible Light Induced Alkene Aminopyridylation using N-aminopyridinium Salts as Bifunctional Reagents" *Nat. Commun*. **2019**, *10*, 4117; (b) Jung, S.; Shin, S.; Park, S.; Hong, S. "Visible-Light-Driven C4-Selective Alkylation of Pyridinium Derivatives with Alkyl Bromides" *J. Am. Chem. Soc*. **2020**, *142*, 11370; (c) Lee, W.; Jung, S.; Kim, M.; Hong, S. "Site Selective Direct C-H Pyridylation of Unactivated Alkanes by Triplet Excited Anthraquinone" *J. Am. Chem. Soc*. **2021**, *143*, 3003.

[22] Choi, J.; Laudadio, G.; Godineau, E.; Baran, P. S. "Practical and Regioselective Synthesis of C-4-Alkylated Pyridines" *J. Am. Chem. Soc*. **2021**, *143*, 11927.

[23] Wan, M.; Lou, H.; Liu, L. "C1-Benzyl and Benzoyl Isoquinoline Synthesis Through Direct Oxidative Cross-Dehydrogenative Coupling with Methyl Arenes" *Chem. Commun*. **2015**, *51*, 13953.

[24] Li, Z.-E.; Jin, L.-K.; Cai, C. "Efficient Synthesis of 2-Substituted Azoles: Radical C–H Alkylation of Azoles with Dicumyl Peroxide, Methylarenes and Cycloalkanes Under Metal-Free Condition" *Org. Chem. Front*. **2017**, *4*, 2039.

[25] Georgiou, E.; Spinnato, D.; Chen, K.; Melchiorre, P. "Switchable Photocatalysis for the Chemodivergent Benzylation of 4-Cyanopyridines" *Chem. Sci*. **2022**, *13*, 806.

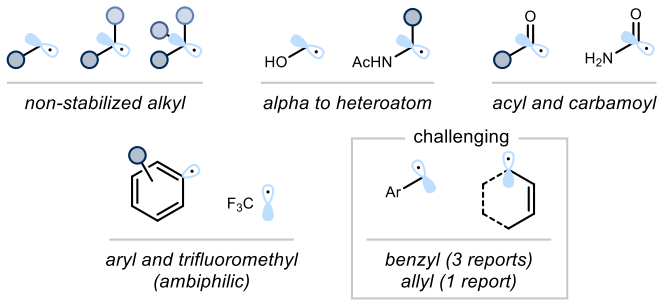

Figure 2.9. Radicals amenable to Minisci reactions, and the challenging ones (grey inset).

For the radical *C-H* allylation of pyridines, only one protocol has been reported so far.[26] It utilized semiconductor quantum dots (**QD**) in a visible light-mediated process, generating allylic radicals **IV** from alkenes **2** and involving them in a reaction with heteroarenes **1** (Figure 2.10). The precise mechanism of interaction between the allylic radical **IV** and heteroarene **1** was not detailed by the authors. The products were obtained in good yields, with the scope mostly limited to isoquinolines.

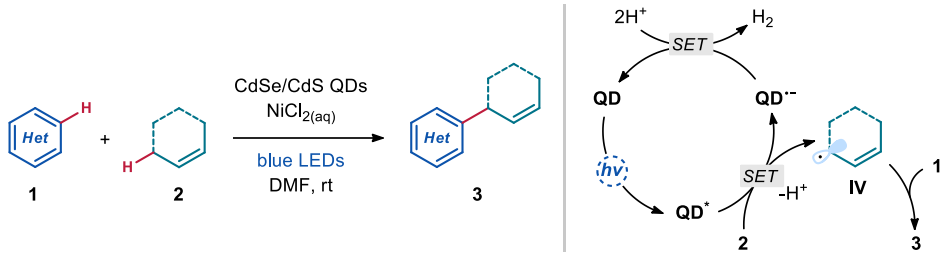

Figure 2.10. Quantum dot-enabled allylation of heteroarenes.

Overall, the addition of radicals to pyridines is a powerful tool for rapid late-stage functionalization campaigns. However, the issues of regioselectivity, overalkylation, and incompatibility with stabilized radicals have not yet been completely resolved.

2.2.2 Radical *ipso*-substitutions

An alternative strategy for site-selective radical functionalization of azines is the *ipso*-substitution reaction. Historically, pyridines **9** bearing a cyano group at the *C2*- or *C4*-position

[26] Huang, C.; Qiao, J.; Ci, R.-N.; Wang, X.-Z.; Wang, Y.; Wang, J.H.; Chen, B.; Tung, C.-H.; Wu, L.-Z. "Quantum Dots Enable Direct Alkylation and Arylation of Allylic C(sp^3)-H Bonds with Hydrogen Evolution by Solar Energy" *Chem* **2021**, *7*, 1244.

were used (Figure 2.11).[27] This moiety is strongly electron-withdrawing, enabling facile single-electron transfer (SET) reduction processes due to aforementioned LUMO-lowering effect. SET reduction of the pyridine **9a** affords a persistent pyridinyl radical-anion **XI**, stabilized by the electron-withdrawing nature of the substituent.[28] This radical-anion **XI** can couple efficiently with another radical **II** to generate intermediate **XII**, furnishing functionalized pyridine **3** after elimination of the cyanide leaving group.

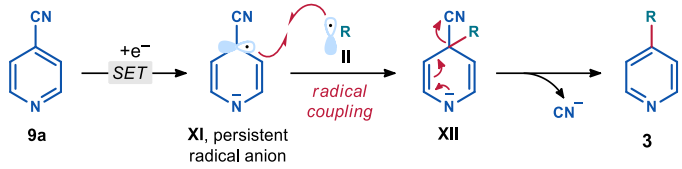

Figure 2.11. General mechanism for radical *ipso*-substitution reactions.

This strategy has now become widely utilized, especially in combination with photoredox catalysis. The first photoredox implementation was described by the MacMillan group in 2011 (Figure 2.12).[29] The strongly reducing excited state of $Ir(ppy)_3$ photocatalyst ($E(Ir^{IV}/Ir^{III*})$ = -1.73 V vs SCE) reduced cyanopyridine **9a** (E(**9a**/**XI**) = -2.1 V vs SCE)[30] to produce the persistent radical anion **XI** and the oxidized form of the photocatalyst Ir^{IV}. Then, anilines **13** were oxidized by Ir^{IV} to radical cations **XIV**, which subsequently underwent deprotonation to α-amino radicals **XV**. Finally, radicals **XI** and **XV** coupled to furnish the product **14** in good yield.

[27] a) Vittimberga B. M., Minisci F., Morrocchi S., "Photoinitiated electron transfer-substitution reaction of diphenyl ketyl with protonated 4-cyanopyridine" *J. Am. Chem. Soc*. **1975**, *97*, 4397; b) Bernardi R., Caronna T., Morrocchi S., Ursini M., "Photochemically induced reactions of selected ketones with 4-cyanopyridine in neutral and acidic medium" *J. Heterocycl. Chem.* **1996**, *33*, 1137; c) T. Hoshikawa, M. Inoue, "Photoinduced direct 4-pyridination of C(sp^3)–H Bonds" *Chem. Sci.* **2013**, *4*, 3118; d) Tong, S.; Li, K.; Ouyang, X.; Song, R.; Li, J. "Recent Advances in the Radical-Mediated Decyanative Alkylation of Cyano(hetero)arene" *Green Synth. Catal*. **2021**, *2*, 145.

[28] Leifert D.; Studer A. "The Persistent Radical Effect in Organic Synthesis" *Angew. Chem. Int. Ed*. **2020**, *59*, 74.

[29] McNally, A.; Prier, C. K.; MacMillan, D. W. C. "Discovery of an α-Amino C-H Arylation Reaction using the Strategy of Accelerated Serendipity" *Science* **2011**, *334*, 1114.

[30] Petersen R. A.; Evans H. D. "Heterogeneous electron transfer kinetics for a variety of organic electrode reactions at the mercury-acetonitrile interface using either tetraethylammonium perchlorate or tetraheptylammonium perchlorate electrolyte" *J. Electroanal. Chem.*, **1987**, *222*, 129.

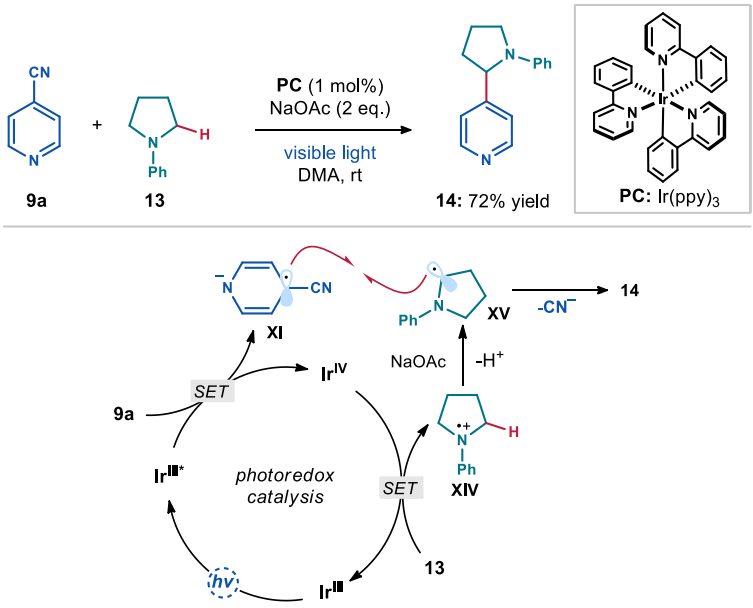

Figure 2.12. Radical *ipso*-substitution of cyanopyridines with α-amino radicals.

Since then, the scope of radicals capable of coupling with cyanopyridines has been expanding. Stabilized radicals such as α-amino, benzylic, allylic radicals have been widely employed for this chemistry. However, the use of non-stabilized alkyl radicals has remained rare.[31]

The major drawback of this *ipso*-substitution strategy is the use of cyanopyridines, as their synthesis is not straightforward. Cyanation of pyridines tends to be poorly regioselective, and the protocols are generally not suitable for complex pharmaceutical and agrochemical candidates.[32] An alternative solution was introduced by McNally and coworkers in the form of pyridine phosphonium salts **9b** (Figure 2.13.a). These salts could be prepared from pyridines **1** with complete *C4*-regioselectivity in a single step and were initially developed as substrates for nucleophilic cross-coupling reactions.[33] Later, their reasonable reduction potential (E_{red} = -1.5 V vs SCE) was noticed and utilized in radical processes upon activation through SET reduction. The resulting α-phosphonium radicals **XVI** had a similar reactivity profile to cyanopyridine radical anions **XI**, undergoing facile *ipso*-substitution reactions with

[31] Lipp, B.; Nauth, A. M.; Opatz, T. "Transition-Metal-Free Decarboxylative Photoredox Coupling of Carboxylic Acids and Alcohols with Aromatic Nitriles" *J. Org. Chem.* **2016**, *81*, 6875.

[32] (a) Yu, X.; Tang, J.; Jin, X.; Yamamoto, Y.; Bao, M. "Manganese-Catalyzed C-H Cyanation of Arenes with N-Cyano-N-(4-methoxy)phenyl-p-toluenesulfonamide" *Asian J. Org. Chem*. **2018**, *7*, 550; (b) Zhao, D.; Xu, P.; Ritter, T. "Palladium-Catalyzed Late-Stage Direct Arene Cyanation" *Chem* **2019**, *5*, 97.

[33] (a) Anderson, R. G.; Jett, B. M.; McNally, A. "A Unified Approach to Couple Aromatic Heteronucleophiles to Azines and Pharmaceuticals" *Angew. Chem. Int. Ed*. **2018**, 57, 12514; (b) Patel, C.; Mohnike, M.; Hilton, M. C.; McNally, A. "A Strategy to Aminate Pyridines, Diazines, and Pharmaceuticals via Heterocyclic Phosphonium Salts" *Org. Lett*. **2018**, *20*, 2607.

stabilized radicals, such as cyanopyridinyl radicals (Figure 2.13.a, path *i*) or benzylic radicals (Figure 2.13.a, path *ii*). In the first protocol (path *i*), B_2pin_2 was used as an electron transfer reagent to furnish pyridinyl radicals from both cyanopyridine **9a** and triphenylphosphonium salt **9b**, leading to pyridine-pyridine cross-coupling.[34] In the second protocol (path *ii*), photoredox catalysis was used to produce benzylic radicals from potassium trifluoroborate salts **15** for the subsequent *ipso*-substitution reaction.[35] The synthetic utility of these protocols was demonstrated by functionalizing several complex pyridines in good yields (selected examples on Figure 2.13.b).

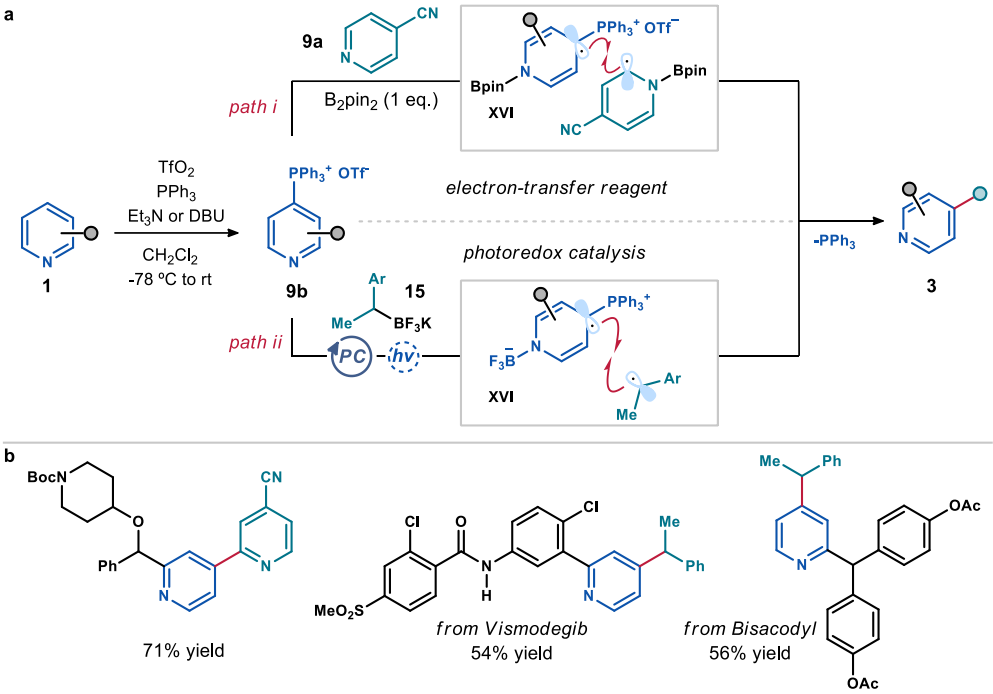

Figure 2.13. (**a**) Pyridine triphenylphosphonium salts **9b** as an alternative to cyanopyridines. (**b**) Selected examples from the scope of both transformations.

Overall, radical *ipso*-substitution is a potent alternative to Minisci-type reactions, as both the regioselectivity issue is alleviated and the pools of radicals amenable to these transformations

[34] Koniarczyk, J. L.; Greenwood, J. W.; Alegre-Requena, J. V.; Paton, R. S.; McNally, A. "A Pyridine−Pyridine Cross-Coupling Reaction via Dearomatized Radical Intermediates" *Angew. Chem. Int. Ed*. **2019**, *58*, 14882.

[35] Greenwood, J. W.; Boyle, B. T.; McNally, A. "Pyridylphosphonium Salts as Alternatives to Cyanopyridines in Radical−Radical Coupling Reactions" *Chem. Sci*. **2021**, *12*, 10538.

are complementary to each other. However, the necessity of pre-functionalization of pyridines is a limiting factor for the usefulness in broad-scope functionalization campaigns.

2.2.3 Pyridyl radicals

Another possible approach to functionalization of pyridines is the use of pyridyl radicals as intermediates. Pyridyl radicals are similar in reactivity to aryl radicals and could be obtained in a similar manner, *e.g.* via SET reduction of halopyridines **16** to pyridyl radicals **XVII** (Figure 2.14).[36] Pyridines have high bond-dissociation energy (BDE) of aromatic *C-H* bonds (110 kcal·mol^{-1} for *C4-H* in pyridine), making pyridyl radicals potent hydrogen atom abstractors.[37] Consequently, these intermediates are difficult to engage in *C-C* bond-forming events due to HAT competition leading to hydrogenated byproduct. Nevertheless, limited examples of pyridine functionalization via pyridyl radicals have been reported.

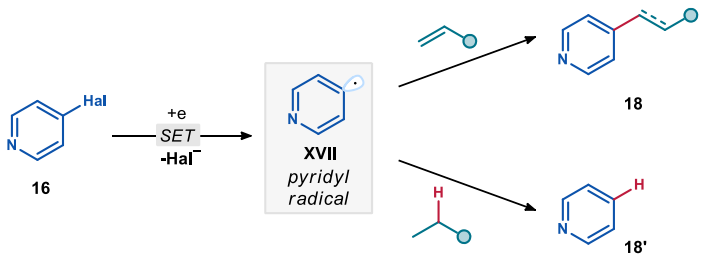

Figure 2.14. Reductive generation of pyridyl radicals **XVII** and competition between addition to π-systems and HAT.

In 2015, a photocatalytic method for the alkylation of perfluoropyridines **16a** with alkenes **17** was reported by Weaver (Figure 2.15).[38] The authors proposed that the excited state of the photoredox catalyst ($E^*(Ir^{IV}/Ir^{III*})$ = -2.01 V vs SCE) was capable of reducing **16a** to a radical anion (E_{red} = -2.17 V vs SCE) with the help of irreversible fluoride extrusion to form the pyridyl radical **XVII**. This radical subsequently attacked alkene **17**, forming an alkyl radical **XVIII** which delivered the final product **18** upon HAT. The turnover of the photocatalyst was achieved via SET oxidation of DIPEA by Ir^{IV}. Functionalized pyridines **18** were obtained in good yields, but as mixtures with the hydrodefluorination product **18'** due to aforementioned

[36] (a) Kvasovs, N.; Gevorgyan, V. "Contemporary Methods for Generation of Aryl Radicals" *Chem. Soc. Rev.* **2021**, *50*, 2244; (b) Andrieux, C. P.; Blocman, C.; Dumas-Bouchiat J. M.; Saveant, J. M. "Heterogeneous and homogeneous electron transfers to aromatic halides. An electrochemical redox catalysis study in the halobenzene and halopyridine series" *J. Am. Chem. Soc.*, **1979**, *101*, 3431.

[37] Wren, W.S.; Vogelhuber, K.M.; Garver, J.M.; Kato, S.; Sheps, L.; Bierbaum, V. M.; Lineberger, W.C. "C–H Bond Strengths and Acidities in Aromatic Systems: Effects of Nitrogen Incorporation in Mono-, Di-, and Triazines" *J. Am. Chem. Soc.* **2012**, *134*, 6584.

[38] Sing, A.; Kubik, J. J.; Weaver, J. D. "Photocatalytic C–F Alkylation; Facile Access to Multifluorinated Arenes" *Chem. Sci*. **2015**, *6*, 7206.

HAT competition issue. To mitigate this issue, an excess of alkene **17** was used to push the process towards radical addition. Subsequently, pyridine arylation was achieved in a similar manner by utilizing arenes instead of alkenes as radical traps.[39]

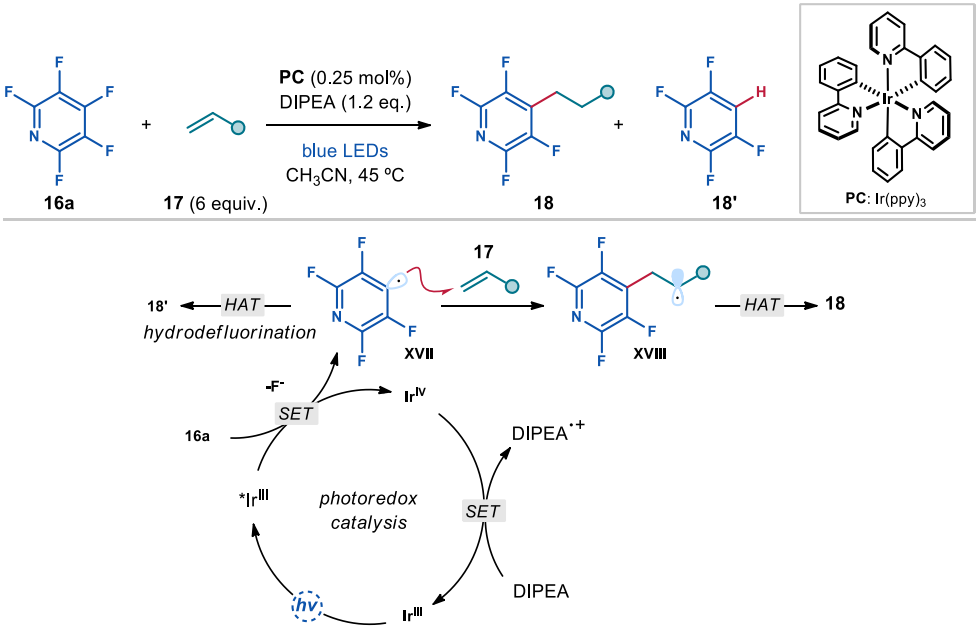

Figure 2.15. Photocatalytic alkylation of perfluoropyridine.

The addition of pyridyl radicals to olefins was also extensively studied by Jui and co-workers, employing bromo- and iodo-pyridines **16** as radical precursors. The first report described the alkylation of pyridines with Michael acceptors **17a** (Figure 2.16), a process that operated in a similar mechanistic manifold to that proposed by Weaver.[40] This time only 3 equivalents of the radical trap were required, producing azines **18** in good to excellent yield. Authors discovered that inclusion of water as a cosolvent decreased the solubility of the hydrogen atom source (Hantzsch ester, **HEH**), inhibiting the formation of the hydrodehalogenation side-product. In a subsequent report, the scope was expanded to include unactivated olefins as alkylating reagents.[41]

[39] Senaweera, S.; Weaver, J. D. "Dual C−F, C−H Functionalization via Photocatalysis: Access to Multifluorinated Biaryls" *J. Am. Chem. Soc*. **2016**, *138*, 2520.

[40] Aycock, R. A.; Wang, H.; Jui, N. T. "A Mild Catalytic System for Radical Conjugate Addition of Nitrogen Heterocycles" *Chem. Sci*. **2017**, *8*, 3121.

[41] Byington, A. J.; Riu, M.-L. Y.; Jui, N. T. "Anti-Markovnikov Hydroarylation of Unactivated Olefins via Pyridyl Radical Intermediates" *J. Am. Chem. Soc*. **2017**, *139*, 6582.

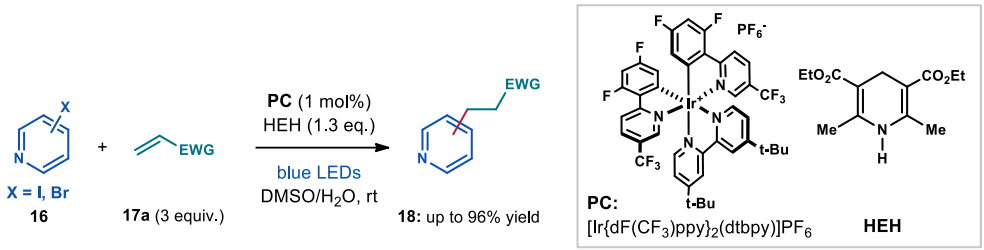

Figure 2.16. Photocatalytic alkylation of halopyridines.

Once again, the main drawback of these protocols is the necessity of pre-functionalization of pyridines before the main reaction could take place. Moreover, the HAT activity of pyridyl radicals has to be accounted for when designing the procedures, limiting synthetic viability.

Overall, each contemporary radical strategy for the functionalization of pyridines suffers from some limitations. Minisci reactions are convenient and enable late-stage diversification campaigns, but are prone to regioselectivity issues, overalkylation and are rarely productive with stabilized radicals. To achieve regioselectivity and/or reactivity, other approaches require pre-installation of certain functionalities (*N*-blocking groups, cyano/triarylphosphonium/halogen groups on the ring), limiting the convenience of these protocols.

2.2.4 Pyridinyl radicals

Pyridinyl radicals (not to be confused with pyridyl radicals) are neutral open-shell species in which the radical is delocalized across the π-system of the pyridine ring. One well-known example is the radical cation of methyl viologen, the species that is detrimental for the potency and toxicity of the herbicide Paraquat, as it is capable of generating "activated oxygen" species, *e.g.* superoxide radical anion and hydrogen peroxide, upon redox cycling *in vivo* (Figure 2.17).[42]

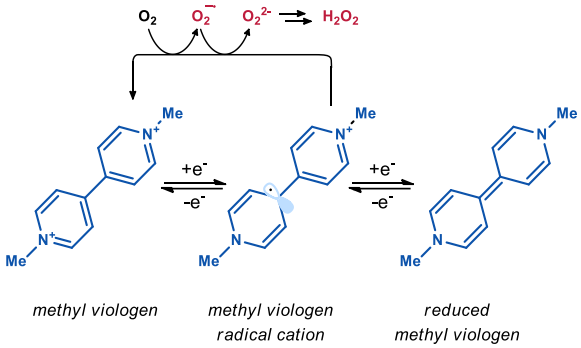

Figure 2.17. Redox forms of methyl viologen and generation of "activated oxygen".

There are two main pathways to synthesize a pyridinyl radical: SET reduction of pyridinium π-system, or oxidation of 1,4-dihydropyridine. Due to the importance of NAD(P)H/NAD(P)$^+$ cofactors in biological redox processes, this system has been extensively studied and will serve as an illustrative example.[43] Land and Swallow demonstrated that pyridinyl radical NAD$^\bullet$ could be formed both via oxidation of the 1,4-dihydropyridine ring of the coenzyme NADH, and through reduction of the pyridinium NAD$^+$ (Figure 2.18.a).[44]

Some pyridinyl radicals are stable: for example, upon reduction of *N*-alkyl pyridinium **19** with sodium amalgam, the resultant pyridinyl radical **20** could be isolated by distillation as a stable green liquid (Figure 2.18.b).[45] A simple pyridinyl radical **III** was characterized by electron paramagnetic resonance (EPR) spectroscopy in 1973 by the group of Fessenden (Figure 2.18.

[42] Bus J.S.; Gibson J.E. "Paraquat: Model for Oxidant-Initiated Toxicity" *Environmental Health Perspectives* **1984**, *55*, 37.

[43] (a) Carillo N.; Ceccarelli E. A. "Open questions in ferredoxin-NADP+ reductase catalytic mechanism" *Eur. J. Biochem.* **2003**, *270*, 1900; (b) Zhu, X.-Q.; Li, H.-R.; Li, Q.; Ai, T.; Lu, J.-Y.; Yang, Y.; Cheng, J.-P. "Determination of the C4-H Bond Dissociation Energies of NADH Models and Their Radical Cations in Acetonitrile" *Chem. Eur. J.* **2003**, *9*, 871.

[44] E. J. Land; A. J. Swallow "One-electron reactions in biochemical systems as studied by pulse radiolysis. I. Nicotinamide-adenine dinucleotide and related compounds" *Biochim. Biophys. Acta* **1968**, *162*, 327.

[45] Kosower, E. M. "Stable Pyridinyl Radicals" *Top. Curr. Chem.* **1983**, *112*, 117.

c).[46] The spin distribution was calculated from the measured hyperfine splitting constants, demonstrating a stark variance between different positions, with maximum on the *C4* carbon.

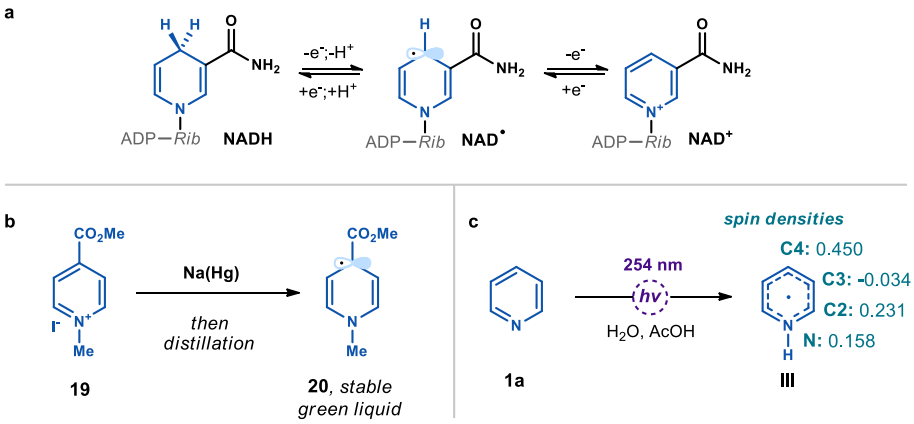

Figure 2.18. Early studies on pyridinyl radicals. (**a**) NADH/NAD•/NAD$^+$ transformations. (**b**) Example of a stable pyridinyl radical. (**c**) EPR studies and experimental spin density values for the pyridinyl radical **III**.

Pyridinyl radical dimerization has been known since 1881,[47] and the regio- and stereoselectivity outcomes of this process have been rationalized in 1998, as discussed in section 2.1 (Figure 2.3.b).[8] Radical **III** has also been used as a one-electron shuttle for the catalytic electroreduction of carbon dioxide,[9] but otherwise has not been used in synthetic chemistry thus far. Overall, the diverse chemistry seemingly available within the pyridinium/pyridinyl radical redox system motivated us to investigate how to direct these properties for the design of a robust synthetic protocol for pyridine site-selective functionalization.

[46] Fessenden, R. W.; Neta, P. "ESR Spectra of Radicals Produced by Reduction of Pyridine and Pyrazine" *Chem. Phys. Lett.* **1973**, *18*, 14.
[47] Hofmann A. W. "Zur Geschichte der Pyridinbasen" *Ber. Dtsch. Chem. Ges.* **1881**, *14*, 1497.

2.3 Design and target of the project

The project discussed in this chapter was inspired by the idea to direct the LUMO-lowering effect of protonation of pyridines towards exploiting the SET reduction pathway instead of radical attack for the functionalization of pyridines. This idea provides a complementary strategy to both Minisci reaction and *ipso*-substitution of cyanopyridines (Figure 2.19).

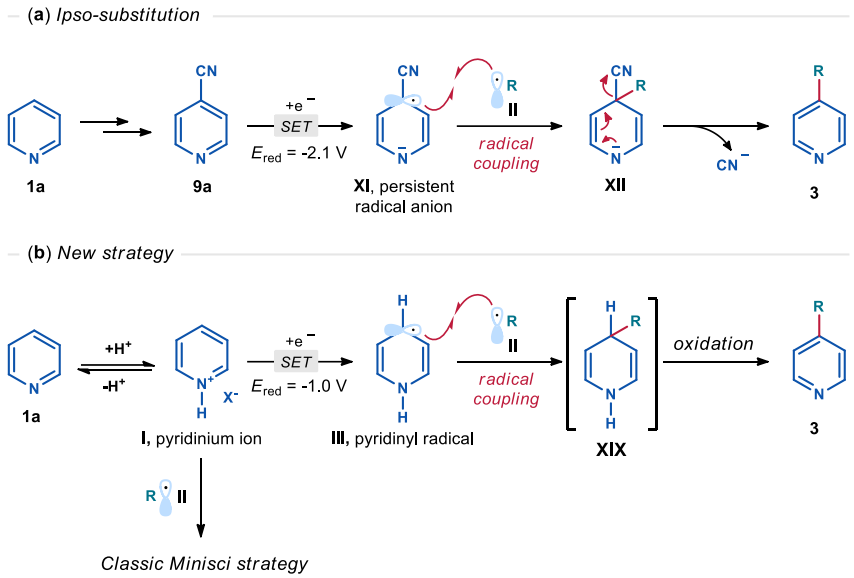

Figure 2.19. (a) Established ipso-substitution strategy for pyridine functionalization (b) Proposed strategy for direct pyridine functionalization and its relationship to the classic Minisci protocol.

Specifically, we noted that in the *ipso*-substitution protocol (Figure 2.19.a), the first role of the electron withdrawing substituent is to enable efficient SET by lowering the reduction potential (E(**9a**/**XI**)= -2.1 V vs Ag/AgCl).[30] The same could be achieved by simple protonation of the pyridine (Figure 2.19.b), removing the requirement of pre-functionalization (E(**I**/**III**)= -1.0 V vs Ag/AgCl).[48] While the resulting radical-anion **XI** in the ipso-substitution protocol is persistent, we theorized that the unsubstituted pyridinyl radical **III** could also be capable of radical-radical cross-coupling with stabilized radicals **II**, e.g. allylic or benzylic.

This pyridinyl radical **III** could be generated in a catalytic process through SET reduction of pyridinium ions **I**. We recognized that dithiophosphoric acid **A1**, previously studied by our research group for allylic *C-H* benzylation (detailed transformation discussed in Section

[48] Lucio, A. J.; Shaw, S. K. "Pyridine and Pyridinium Electrochemistry on Polycrystalline Gold Electrodes and Implications for CO2 Reduction." *J. Phys. Chem. C* **2015**, *119*, 12523.

1.3),[49] could be a suitable candidate to promote this pathway (Figure 2.20). It is both strongly acidic[50] and upon deprotonation, the electron-rich thiolate could drive the formation of photoactive electron donor-acceptor (EDA) complexes. [51] We hypothesized that the catalyst **A1** can thus form EDA complexes with pyridines **1** after proton exchange and formation of pyridinium ions **I**, enabling subsequent reduction of **I** to pyridinyl radical **III** via light-triggered intracomplex SET. The catalyst turnover could be achieved via hydrogen atom transfer (HAT) from a cyclic alkene **2** to form an allylic radical **IV**,[49] which upon radical coupling with **III** and subsequent oxidation would afford the *C-H* allylated pyridine **3**. We anticipated the radical coupling to occur preferentially at the *C4* position in accordance with the previously discussed effects of spin density distribution in pyridinyl radical coupling reactions (sections 2.1 and 2.2.4).[9,46]

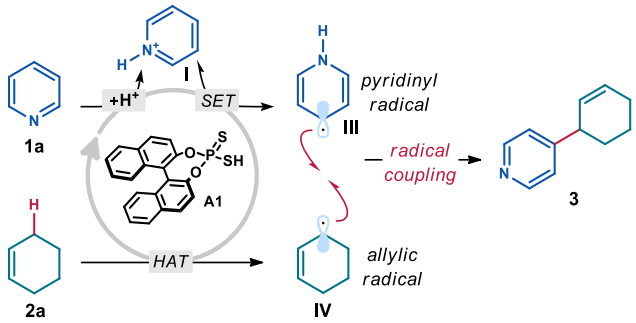

Figure 2.20. Our proposed protocol for pyridinyl radical-mediated C-H allylation of pyridines.

[49] Le Saux, E.; Zanini, M.; Melchiorre, P., "Photochemical Organocatalytic Benzylation of Allylic C-H Bonds." *J. Am. Chem. Soc.* **2022**, *144*, 1113.

[50] Yang, C.; Xue, X.-S.; Jin, J.-L.; Li, X.; Cheng, J.-P. "Theoretical Study on the Acidities of Chiral Phosphoric Acids in Dimethyl Sulfoxide: Hints for Organocatalysis" *J. Org. Chem*. **2013**, *78*, 7076.

[51] Crisenza, G. E. M.; Mazzarella, D.; Melchiorre, P. "Synthetic Methods Driven by the Photoactivity of Electron Donor–Acceptor Complexes" *J. Am. Chem. Soc*. **2020**, *142*, 5461.

2.4 Results and discussion

2.4.1 Preliminary studies

Our research group exhibits a profound interest in employing light to elucidate new excited-state reactivity in catalytic intermediates with well-established polar characteristics. For instance, electron-rich enamines are nucleophilic in their ground state, yet they can function as both donors in photoactive electron donor-acceptor (EDA) complexes[52] and as potent reductants upon photoexcitation (detailed transformations discussed in Section 1.3).[53] A significant distinction between these photochemical activation pathways is the irradiation wavelength required: for enamines, blue light (455 nm) was sufficient to excite the EDA complex, whereas direct excitation demanded higher energy light (405 nm).

With this in mind, we decided to test which photoactivation path would be suitable for the catalyst **A1** in a known model reaction similar to our desired transformation. We replicated a radical *ipso*-substitution protocol between and cyclohexene **2a** and 1,4-dicyanobenzene **21** (Figure 2.21), originally documented by the MacMillan group, which employed an external photoredox catalyst to reduce **21** and a thiol catalyst to mediate the HAT path from **2a** (similar transformation is discussed in Section 1.2).[54] As electron-deficient **21** is known to engage in EDA formation,[55] we first tested this reaction under irradiation by visible light, utilizing acid **A1** as the sole catalyst, replacing both catalysts from the original procedure. However, no arylated product **22** was formed. Given that the anion of **A1** absorbs light in the near-UV region, a wavelength of 365 nm was selected to test the direct excitation pathway. Upon irradiation, the desired *C-H* arylation product **22** was produced almost quantitatively.

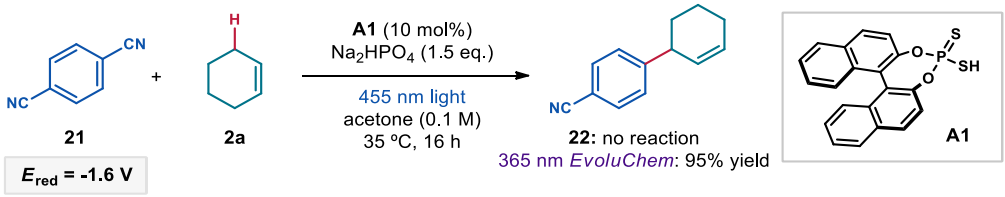

Figure 2.21. Initial discovery of the direct excitation of dithiophosphoric acid **A1**.

---

[52] (a) Arceo, E.; Jurberg, I. D.; Álvarez-Fernández, A.; Melchiorre, P. "Photochemical Activity of a Key Donor-Acceptor Complex Can Drive Stereoselective Catalytic α-Alkylation of Aldehydes" *Nat. Chem.* **2013**, *5*, 750.

[53] Silvi, M.; Arceo, E.; Jurberg, I. D.; Cassani, C.; Melchiorre, P. "Enantioselective Organocatalytic Alkylation of Aldehydes and Enals Driven by the Direct Photoexcitation of Enamines" *J. Am. Chem. Soc.* **2015**, *137*, 6120.

[54] Cuthbertson, J. D.; MacMillan, D. W. C. "The Direct Arylation of Allylic sp^3 C-H Bonds via Organic and Photoredox Catalysis." *Nature* **2015**, *519*, 74.

[55] Anunziata, J.D.; Galaverna, N.S.; Singh, J.O.; Silber, J.J "n-π Electron donor–acceptor complexes. III. Aliphatic amines with dicyanobenzenes. Electric and steric effects of the N-substituents on complex formation" *Canadian Journal of Chemistry* **1986**, *64*, 1491

This preliminary result indicated that the deprotonated catalyst **A1** is capable of functioning as a strong SET reductant under UV light irradiation. As the substrate is pyridine **1a**, which is known to engage in EDA formation,[56] we performed preliminary UV-visible absorption studies to probe which mode of activation could be operative (Figure 2.22). The following spectra were recorded between 330 nm and 450 nm: pyridine **1a**, which did not show absorption in this region (blue line); catalyst **A1** (grey line), which absorbed up to 350 nm; deprotonated catalyst **A1**, prepared as equimolar mixture with Na_2HPO_4 as Brønsted base (purple line), which absorbed up to 370 nm; equimolar mixture of **A1** and **1a** (green line), which had the same absorption profile as the deprotonated catalyst **A1**, overall dismissing the formation of a photoactive EDA complex.

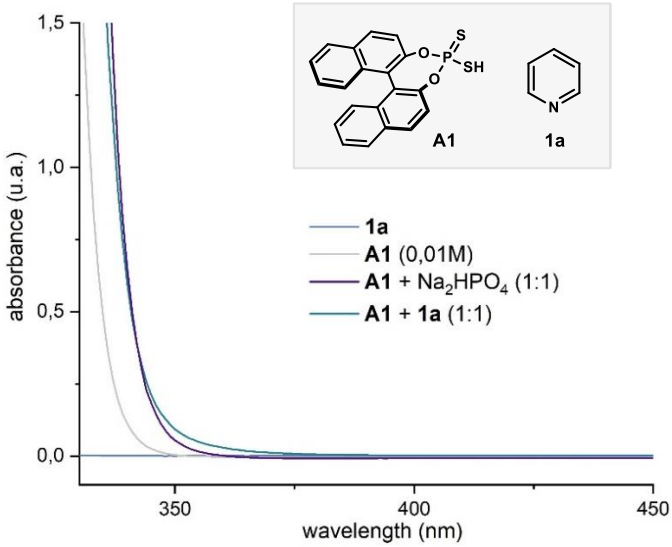

Figure 2.22. Preliminary UV-vis absorption studies.

We then evaluated the redox properties of pyridine **1a** and protonated pyridine **I** to form the target pyridinyl radical **III** via SET to gauge the effect of protonation on the possible SET reduction of the substrates. To achieve this, we performed cyclic voltammetry experiments (Figure 2.23). While no reduction of pyridine **1a** was observed at potentials as low as -2.5 V, pyridinium ion **I** displayed a reversible reduction wave at approximately -0.6 V.[57] Given that the photocatalyst **A1** was capable of reducing the 1,4-dicyanobenzene **21** in our initial studies (E_{red}(**21**) = -1.6 V vs SCE)[54], we felt confident to proceed with our planned studies.

[56] Lasky, M. R.; Salvador, T. K.; Mukhopadhyay, S.; Remy, M. S.; Vaid, T. P.; Sanford, M. S. "Photochemical C(sp^2)-H Pyridination via Arene-Pyridinium Electron Donor-Acceptor Complexes" *Angew. Chem., Int. Ed.* **2022**, *61*, e202208741.

[57] Elgrishi, N.; Rountree, K. J.; McCarthy, B. D.; Rountree, E. S.; Eisenhart, T. T.; Dempsey, J. L. "A Practical Beginner's Guide to Cyclic Voltammetry" *J. Chem. Educ.* **2018**, *95*, 197.

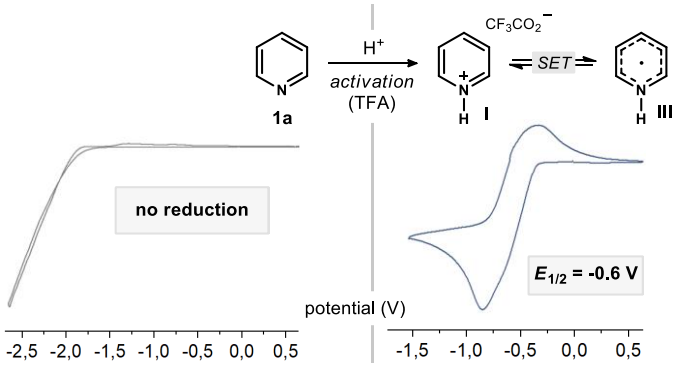

Figure 2.23. Electrochemical studies of pyridine **1a** and pre-formed pyridinium ion **I**. Ag/AgCl (3.0M NaCl) reference electrode in CH_3CN.

2.4.2 Optimization

We selected the simple pyridine **1a** as the model substrate, cyclohexene **2a** as the allylic radical precursor, and dithiophosphoric acid **A1** as the catalyst. After irradiation under 365 nm light for 16 hours, the formation of product **3a** was observed in 17% yield with an 8:1 regioisomeric ratio in favor of the *C4*-adduct over the *C2* allylation product (Table 2.1, entry 1). Adjusting the wavelength to less energetic 390 nm or 455 nm completely inhibited the reactivity (entries 2 and 3). As demonstrated by cyclic voltammetry studies (Figure 2.23), protonation of pyridine **1a** (pK_{aH} = 5.3) by the catalyst **A1** (calc. pK_a = -4.21)[50] to form the pyridinium **I** enables a thermodynamically feasible SET reduction. Therefore, the effect of acids and bases was next evaluated. Benzoic acid (pK_a = 4.2) had a weak negative effect on the reaction (entry 4), while a much stronger TFA (pK_a = 0.2) completely shut down reactivity (entry 5). A weak inorganic base (pK_{aH} = 7.2) slightly increased the overall yield (entry 6), while a tertiary amine base (pK_{aH} = 10.7) inhibited the reaction completely (entry 7). We found that inclusion of 2,4,6-collidine (pK_{aH} = 7.4) significantly increased the yield of the reaction (entry 8), albeit with a decreased regioselectivity.[58] A substoichiometric amount of collidine was sufficient for the reaction to proceed (entry 9). Control experiments under air and without catalyst **A1** afforded no product **3a** (entries 10 and 11). Finally, we found that reactivity under blue light could be enabled by using an external photoredox catalyst **4CzIPN** (entry 12), with product **3a** formed in 47% yield.

[58] A possible role of 2,4,6-collidine is discussed in section 2.5.4.

Table 2.1. Preliminary optimization campaign.

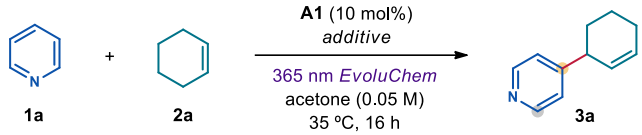

entry	additive	other variations	yield **3a** (%)[a]	C4:C2[a]
1	-	-	17	8:1
2	-	455 nm	*n.d.*	*n.d.*
3	-	390 nm	traces	-
4	benzoic acid (1.5 eq)	-	14	6:1
5	TFA (80 mol%)	-	*n.d.*	-
6	Na_2HPO_4 (1.5 eq.)	-	23	4:1
7	DIPEA (1.5 eq.)	-	*n.d.*	-
8	2,4,6-collidine (1.5 eq.)	-	41	4:1
9	**2,4,6-collidine (50 mol%)**	**-**	**40**	**4:1**
10	-	under air	*n.d.*	-
11	-	no catalyst	*n.d.*	-
12	**4CzIPN (5 mol%)**	**455 nm**	**47**	**4:1**

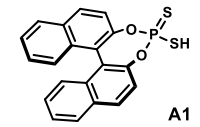

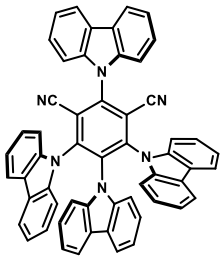

Reaction performed on a 0.2 mmol scale using 10 equiv. of **2a** under irradiation with a 365 nm EvoluChem LED lamp. [a]Yields and regioisomeric ratios of **3a** determined by ^{1}H NMR analysis of the crude reaction mixtures using trichloroethylene as the internal standard. *n.d.:* not detected.

The results from entries 9 and 12 prompted us to continue the optimization using two distinct sets of conditions: (*i*) under UV light irradiation, and (*ii*) under blue light irradiation using an external photocatalyst. We undertook a campaign aimed at the structural evaluation and optimization of the dithiophosphoric acid catalyst (Figure 2.24). A series of 3,3'-substituted derivatives of **A1** were synthesized and tested in the model reaction in the absence of the external photoredox catalyst. The 1-naphtyl-substituted catalyst **A2** performed the best, furnishing **3a** in 67% yield with a 6:1 regioisomeric ratio in favor of the *C4* selectivity.[59] Importantly, purification by column chromatography afforded product **3a** as a single regioisomer. Other dithiophosphoric acids **A3-7** were also competent, though less effective catalysts for the reaction. Thiophosphoric acid (**A8**) and imide (**A9**) were ineffective.

[59] A possible rationale for the higher reactivity offered by **A2** in comparison to **A1** is given in section 2.5.2.

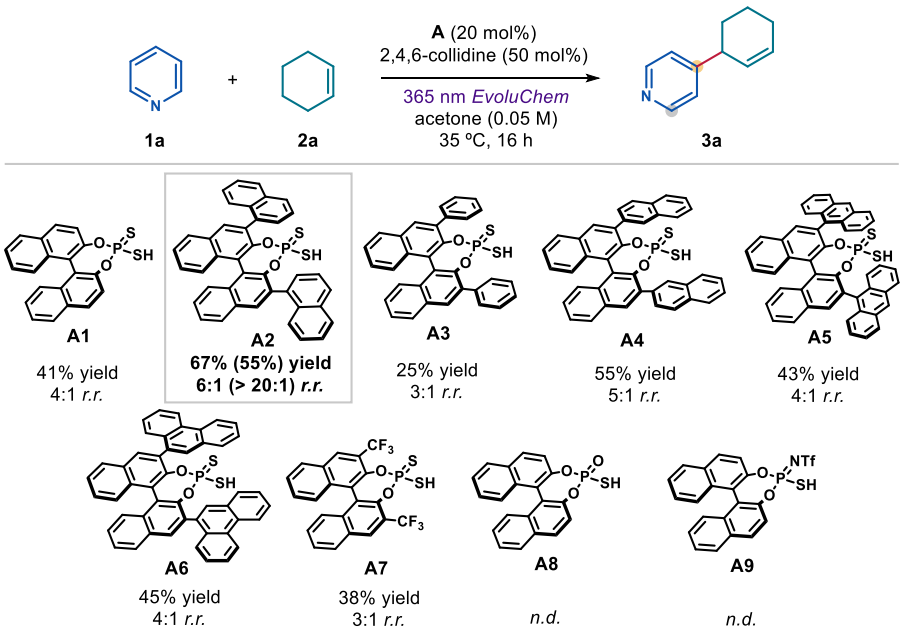

Figure 2.24. Screening of substituted dithiophosphoric acids in the UV light-mediated allylation of pyridine and control experiments with thiophosphoric acid and imide. Reaction performed on a 0.2 mmol scale using 10 equiv. of **2a** under irradiation with a 365 nm EvoluChem LED light. Yields and regioisomeric ratios of **3a** were determined by ^{1}H NMR analysis of the crude reaction mixtures using trichloroethylene as the internal standard. Yields and regioisomeric ratios of the isolated **3a** are reported in parentheses. *n.d.:* not detected.

With the optimized catalyst **A2** (20 mol%), a number of photoredox catalysts was screened next under blue light irradiation (Table 2.2). Cationic iridium complexes were effective (entries 4 and 5), with [Ir(dtbbpy)(ppy)$_2$]PF$_6$ forming **3a** in 79% yield and 4:1 regioselectivity. While inclusion of a photoredox catalyst secured a higher chemical yield, the approach based on the direct excitation of the dithiophosphoric acid catalyst **A2** with UV light was taken forward for investigating the reaction scope, as it avoided the use of precious metals in the reaction protocol and afforded product with higher regioselectivity. For both sets of conditions, acetone was the solvent of choice, with acetonitrile and DCE delivering the product in low yield (<20%).

Table 2.2. Screening of photoredox catalysts.

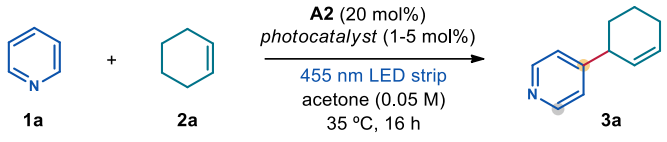

entry	photocatalyst	yield **3a** (%)[a]	C4:C2[a]
1	4CzIPN	51	2:1
2	$Ir(ppy)_3$	*n.d.*	-
3	Mes-Acr$^+BF_4^-$	*n.d.*	-
4	$[Ir\{dF(CF_3)ppy\}_2(dtbbpy)]PF_6$	23	4:1
5	**$[Ir(dtbbpy)(ppy)_2]PF_6$**	**79 (65)**	**4:1 (> 20:1)**
6[b]	$[Ir(dtbbpy)(ppy)_2]PF_6$	*n.d.*	-

Reaction performed on a 0.2 mmol scale using 10 equiv. of **2a** under irradiation with a 455 nm 14 W LEDs strip. [a]Yields and ratios of regioisomers of **3a** were determined by ^{1}H NMR analysis of the crude reaction mixtures using trichloroethylene as the internal standard. Yields and regioisomeric ratios of isolated **3a** are reported in parentheses. [b]Without **A2**. *n.d.:* not detected.

2.4.3 Mechanistic proposal

Based on these preliminary experiments, a mechanistic hypothesis for the desired transformation is depicted in Figure 2.25. The photophysical and other mechanistic experiments described in Section 2.5 will provide data to support this hypothesis. We propose that the dithiophosphoric acid catalyst **A** protonates pyridine **1a**, yielding pyridinium **I** and the photoactive anion $\mathbf{A}^-$. Upon absorption of UV light, $\mathbf{A}^-$ reaches a highly reducing excited state $\mathbf{[A^-]^*}$. SET reduction of pyridinium ion **I** by $\mathbf{[A^-]^*}$ generates the key pyridinyl radical **III** and a sulfur-centered electrophilic radical $\mathbf{A^\bullet}$. The latter is known to undergo a *C–H* abstraction from cyclohexene derivative **2** (HAT properties of thiyl radicals are discussed in Sections 1.2 and 1.3),[49] delivering an allylic radical **IV** and catalyst **A**, thus turning over the catalytic cycle. Finally, radical cross-coupling between **III** and **IV** results in the formation of the functionalized pyridine **3** after subsequent oxidation.[60]

[60] A possible mechanistic explanation of the oxidation pathway is discussed in section 2.5.5.

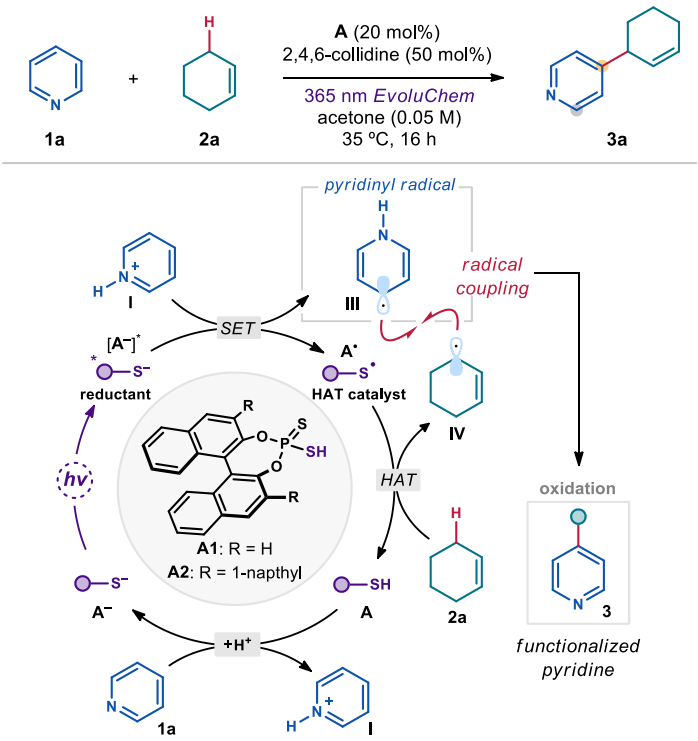

Figure 2.25. Proposed reaction mechanism.

2.4.4 Generality of the system

Using the optimized conditions described in Figure 2.24, the scope of the pyridine allylation process was evaluated (Figure 2.26). When regioisomeric mixture was detected in the crude product, the ratio was determined and reported in the figure. The *r.r.* reported in brackets and the chemical yields refer to the material after chromatographic isolation, which usually furnished the product with >20/1 *r.r. Ortho*-substituted pyridines reacted in good yields and were isolated exclusively as *C4*-allylated products **3b** and **3c**. The introduction of *m*-halogen substituents led to the formation of *C4*-functionalized pyridines **3d** and **3e** with high regioselectivity. Electron-withdrawing CF_3 and CN substituents at the *meta* position were also tolerated, affording the C4 products **3f** and **3g** in fair yields. An alkyl substituent was also accepted (**3h**). The introduction of a bulkier aryl substituent at *meta* position caused a switch of regioselectivity in favor of the *C6* position (**3i**). Considering the importance of nicotinic acid and its derivatives as lipid-controlling drugs,[61] we tested the reactivity of niacin (vitamin B3) and nicotinate esters, nicotinamides, and halogenated derivatives. These substrates

[61] Carlson, L. A. "Nicotinic Acid: The Broad-Spectrum Lipid Drug. A 50th Anniversary Review." *J. Intern. Med.* **2005**, *258*, 94

afforded products **3j**–**s** in fair yields with a positional preference for *C6* functionalization. A series of amino acid nicotinates proved to be suitable substrates, showcasing the potential of this method for the functionalization of complex pyridines (entries **3t-w**). Other azines, including isoquinolines (**3x** and **3y**), pyrimidines (**3z-bb**), and pyridazine (**3cc**), also delivered the allylated products with high regioselectivity and synthetically useful yields.

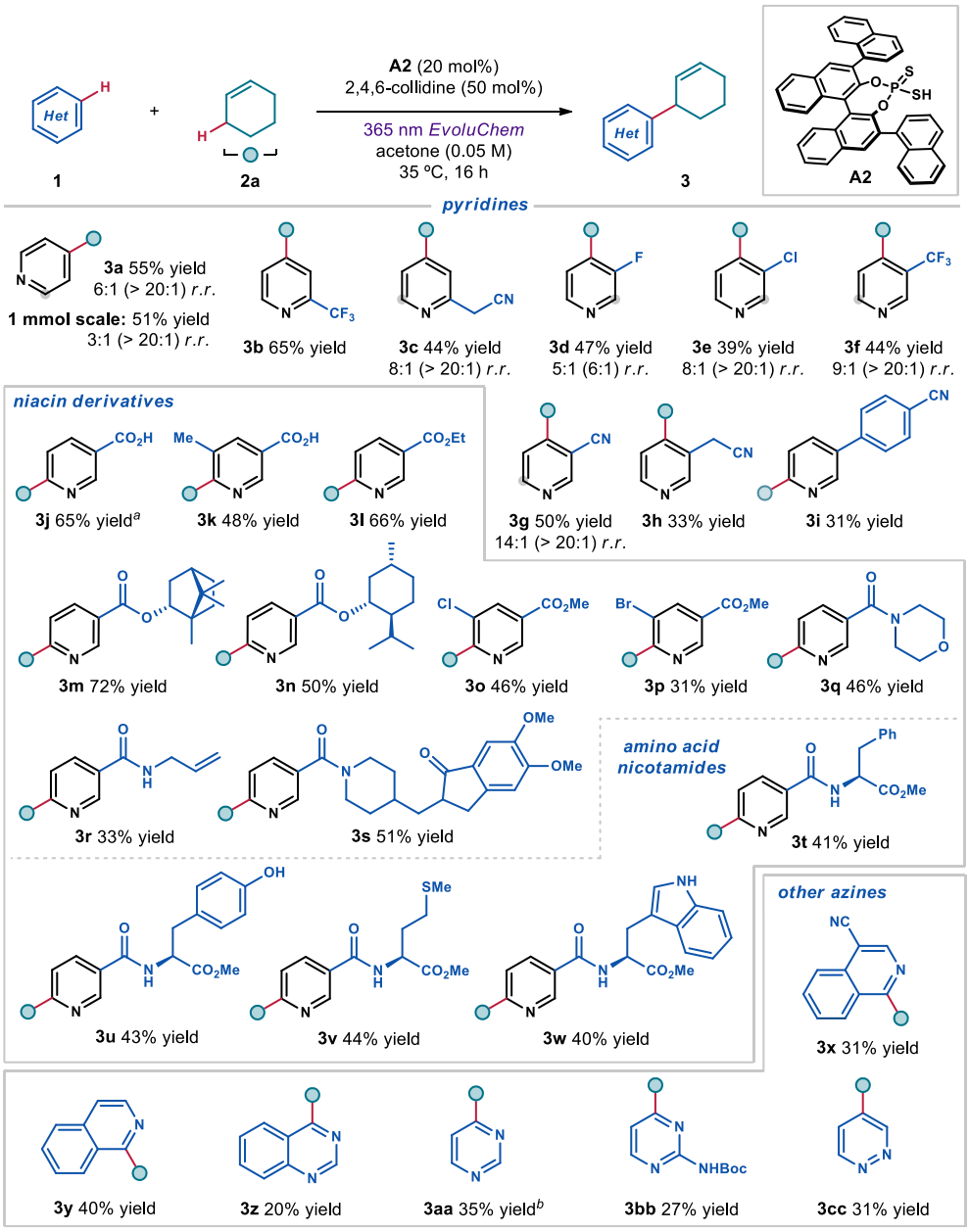

Figure 2.26. Scope of azines. Reactions performed on a 0.2 mmol scale using 10 equiv. of **2a**. Yields refer to isolated products **3** after purification. Products **3** were isolated as single regioisomers (>20:1 r.r.) upon chromatography, unless otherwise stated. When more than one regioisomer was observed, the minor site of functionalization is highlighted by a gray circle. In these cases, the regioisomeric ratio (*r.r.*) of the crude mixture is specified, and the *r.r.* after isolation is reported in parentheses. When applicable, *d.r.* was ~1:1. [a]Yield determined by ^{1}H NMR analysis using trichloroethylene as internal standard. [b]The conditions described in Table 2.2 entry 5 were used. Boc: *tert*-butyloxycarbonyl.

Next, we turned our attention to the direct functionalization of pharmaceuticals (Figure 2.27). The *C2*-substituted pyridine *Bisacodyl* (laxative) afforded the *C4*-allylated product in 33% yield (product **3dd**). Three niacin derivatives, *Nicoboxil* (rubefacient), *Picamilon* (dietary supplement), and *Etofibrate* (hypolipidemic agent) were successfully functionalized in moderate to good yields with exclusive *C6* regioselectivity (products **3ee-gg**). Finally, the pyrimidine-based *Voriconazole* (antifungal) afforded the *C4*-allylated adduct in 44% yield (product **3hh**).

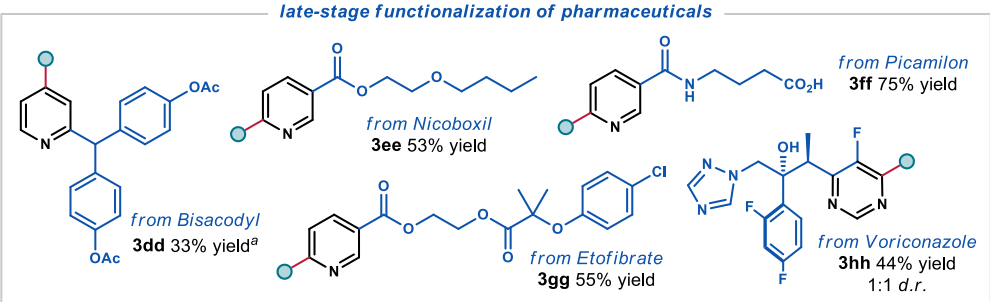

Figure 2.27. Allylation of pharmaceuticals. Reactions performed on a 0.2 mmol scale using 10 equiv. of **2a**. Yields refer to isolated products **3** after purification. Products **3** were obtained as single regioisomers (>20:1 r.r.). [a]Using the visible light conditions described in Table 2.2 entry 5.

We then explored the scope of other allylic *C-H* partners suitable as radical precursors for the functionalization of 2-CF_3 pyridine **1b**, chosen for its excellent reactivity and regioselectivity profile (Figure 2.28.a). Cyclic alkenes of different ring sizes and substitution patterns afforded the desired products with complete *C4* selectivity (products **3ii-mm**). Tetramethylethylene (**3nn**) as well as heterocycles such as dihydropyran (**3oo**) and a protected piperidine (**3pp**) were also amenable to this transformation. Finally, benzylic precursors such as tetrahydronaphtalene (**3qq**) and acenaphthylene (**3rr**) successfully participated in the reaction. In certain cases (**3kk**, **3ll**, **3nn**, **3oo**), a mixture of regioisomers pertaining to the allylic substituent was obtained, stemming from the distinct mesomeric structures possible for allylic radicals, and, in case of **3kk** and **3ll**, from two distinct allylic *C-H* sites available for HAT in their respective allylic precursors (Figure 2.28.b).

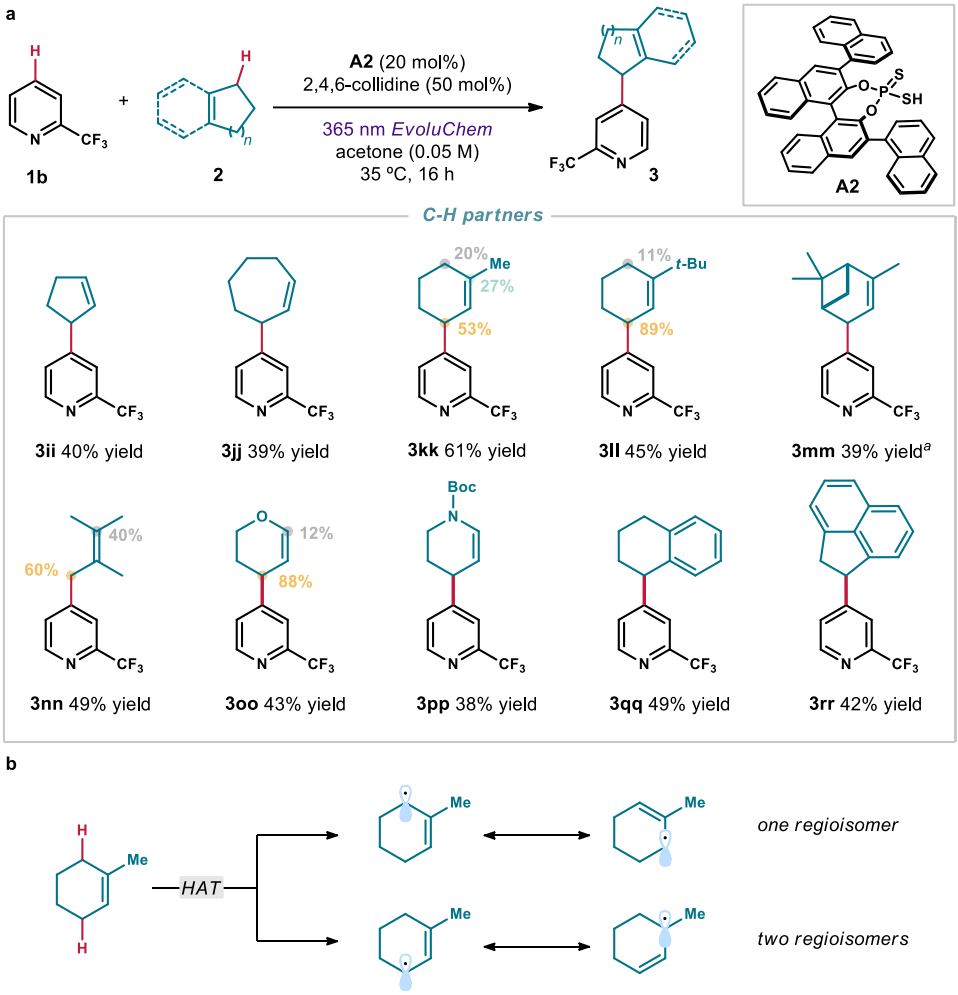

Figure 2.28. (**a**) Scope of C-H partners **2**. Reactions performed on a 0.2 mmol scale using 10 equiv. of **2**. Yields refer to isolated products **3** after purification. Products **3** were obtained as single regioisomers (> 20:1 r.r.). When applicable, *d.r.* was ~1:1. [a]Yield determined by ^{1}H NMR analysis. Boc: *tert*-butyloxycarbonyl. (**b**) Rationale for allylic regioisomer formation.

2.4.5 Reaction limitations

We also uncovered the limitations of this protocol with respect to the scope of pyridines and allylic *C-H* substrates (Figure 2.29). A general trend is that pyridines decorated with electron-donating substituents or with any substituents at the *C4* position are not amenable to this reaction. Pyridines bearing o*rtho*-halogen substituents were also unsuccessful, instead undergoing dehalogenation. Carbonyl groups such as ketone and aldehyde were incompatible with the protocol, forming complex mixtures of products.

The scope of allylic *C-H* partners was limited to cyclic allylic and benzylic substrates, with the exception of tetramethylethylene. Linear substrates (hexene-1, benzyl methyl ether) did not yield any product. Simple THF or benzaldehyde did not afford any product either.

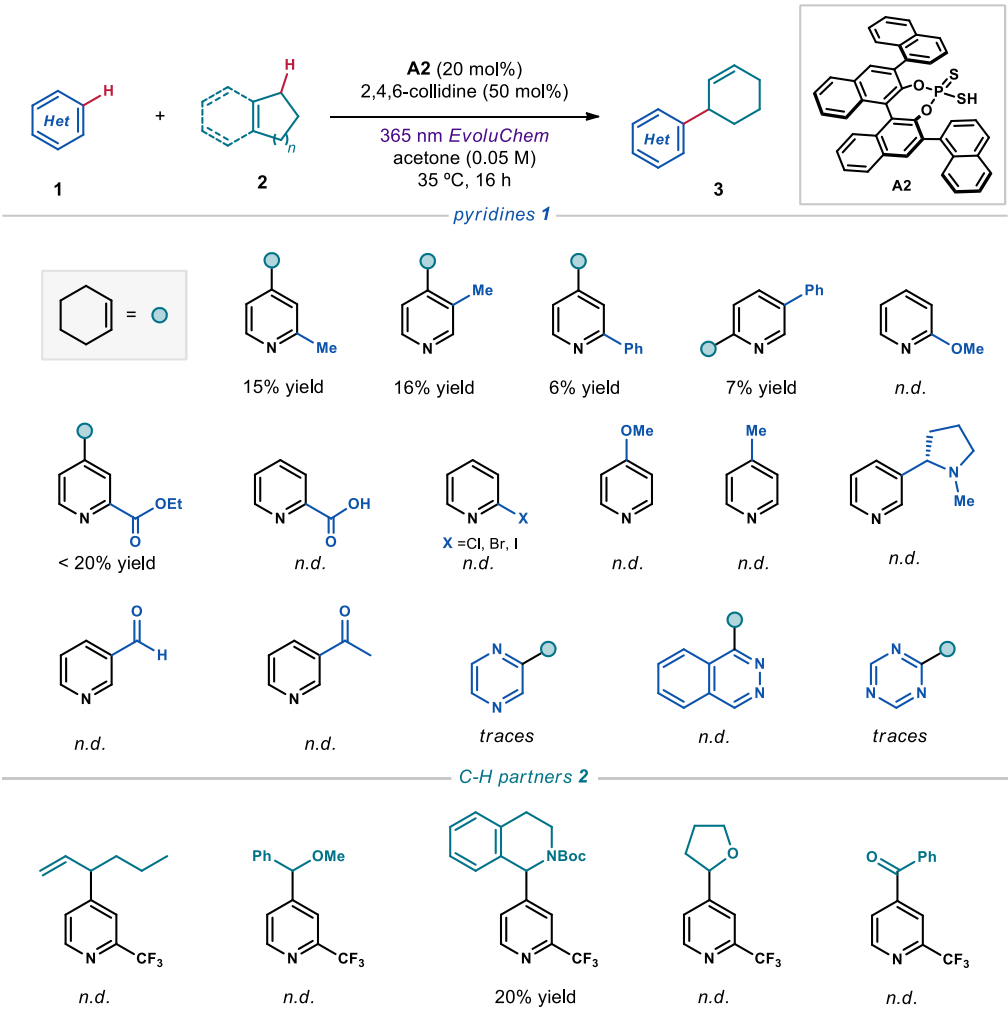

Figure 2.29. Moderately successful and unsuccessful substrates. Yields were determined by ^{1}H NMR analysis using trichloroethylene as the internal standard. *n.d.*: not detected.

Overall, the limitations imposed on the character of the *C-H* partners are consistent with the previously established reactivity of the dithiophosphoric acid catalysts **A** (Section 1.3).[49] The reasons for incompatibility of electron-donating substituents as well as substituents at the *C4* position remain unclear.

2.5 Mechanistic investigations

2.5.1 Regioselectivity of the reaction

To rationalize the regioselectivity of this protocol, several observations have been made. First, spin density distribution of the key pyridinyl radicals **III** has been evaluated with DFT calculations, performed using uB3LYP/6-31G+(d) level of theory. Greater spin density was found at *C4* compared to the *C2* position (Figure 2.30) for all radicals studied, which is in agreement with the literature data for EPR-derived spin densities of **III** (discussed in the Section 2.2.4).[46] Natural bond orbital (NBO) analysis revealed that the singly occupied molecular orbital (SOMO) is localized preferentially at the *C4* position. These results, along with the observed preference for *C4* positional selectivity, might indicate that the spin density distribution could affect the positional outcome of the transformation. For other azines (isoquinoline, pyridimidine and pyridazine), the spin density distribution is also consistent with the observed regioisomeric outcome.

The influence of the steric factors has been inferred from the series of the nicotinic acid derivatives, all of which selectively afforded the *C6*-functionalized products. In stark contrast, 3-cyanopyridine afforded *C4*-functionalized product with high regioselectivity (14:1). An obvious difference between these substrates is the size of the cyano group, which is much smaller than the methyl ester (A(CN) = 0.17 against A(CO_2Me) = 1.23 where A is A-value for the given substituent).[62] As such, we propose that, in the absence of steric effects, the positional outcome would correspond to the maximum of the spin density distribution. Otherwise, the steric effects would dominate and direct the functionalization to the unhindered position with the highest value of the spin density.

[62] Eliel, E.L.; Wilen, S.H.; Mander, L.N. "Stereochemistry of Organic Compounds" **1994** *New York: Wiley.*

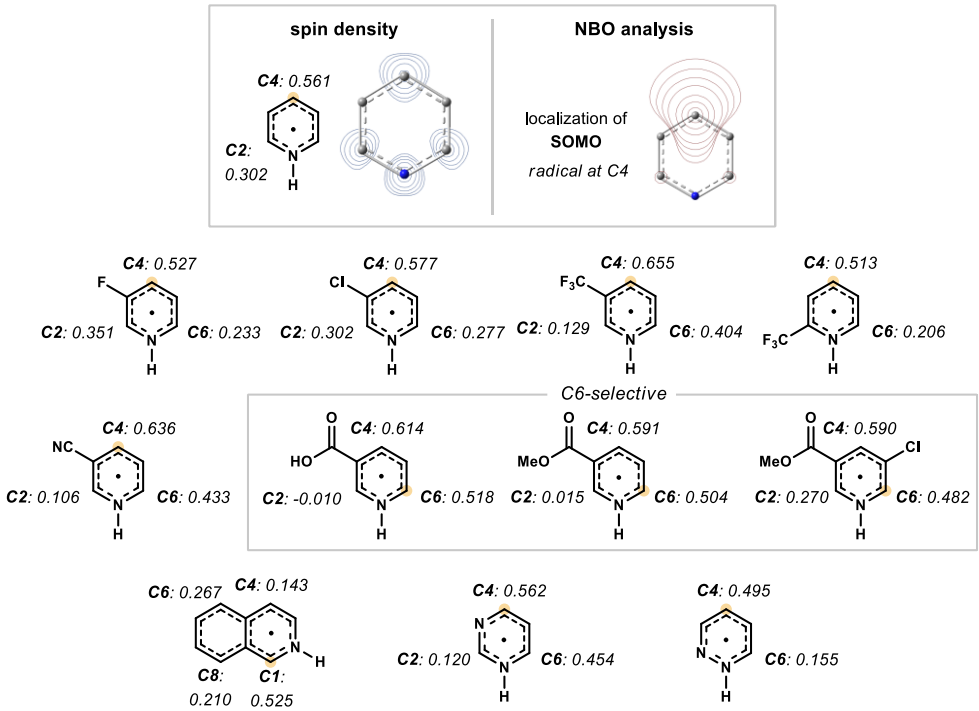

Figure 2.30. Calculated spin densities for representative examples from the scope. The sites corresponding to the major regioisomer are highlighted by a yellow circle.

2.5.2 Photophysical studies

To better understand the chemistry of our catalysts **A**, we characterized the excited state of **A2**$^{-}$ using photophysical methods. These experiments provided essential data to better understand the overall reaction mechanism.

Estimation of the excited-state potential of A2^{-}

The excited-state reduction potential $E(\mathbf{A2}^{\bullet}/[\mathbf{A2}^{-}]^{*})$ was estimated by applying the *Rehm-Weller formalism* (Figure 2.31, Equation 2.1, red box).[63] This value was calculated from the ground-state reduction potential $E(\mathbf{A2}^{\bullet}/\mathbf{A2}^{-})$ measured by cyclic voltammetry (CV, blue box) and the energy difference between zeroth vibrational levels of the excited and ground states $E_{00}([\mathbf{A2}^{-}]^{*}/\mathbf{A2}^{-})$, which was approximated by including the long wavelength tail of the absorption spectrum (λ_{tail}) into Equation 2.2 (Figure 2.31, purple box).[64]

[63] Buzzetti, L.; Crisenza, G. E. M.; Melchiorre, P. "Mechanistic Studies in Photocatalysis" *Angew. Chem. Int. Ed.* **2019**, *58*, 3730.

[64] Details about CV and UV-vis studies can be found in the experimental section.

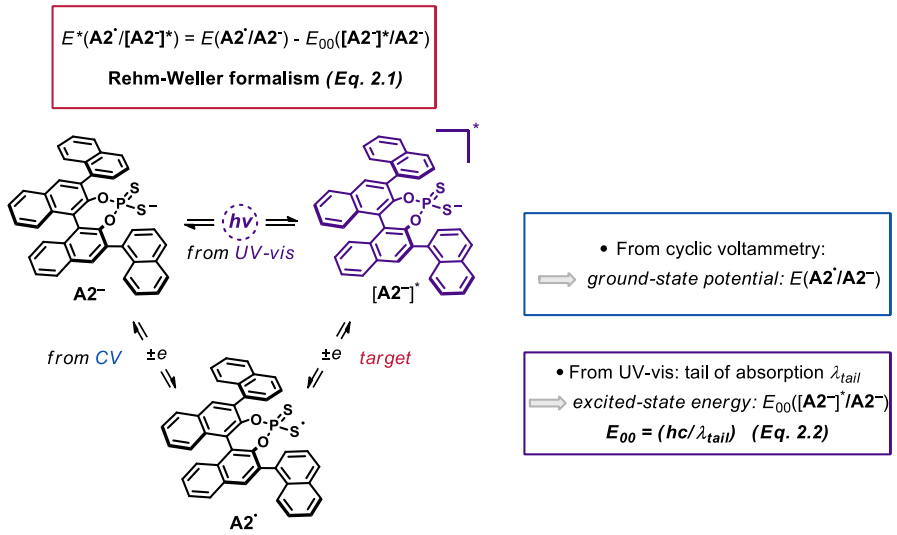

Figure 2.31. Determination of the excited-state potential of **A2**$^{-}$ using the Rehm-Weller equation. **A2**$^{-}$ was formed by mixing **A2** with 1 equiv. of Na_2HPO_4 followed by filtration. *h*: Planck's constant; c: speed of light in vacuum.

E(**A2•**/**A2**$^{-}$) = 1.12 V (vs Ag/AgCl) was measured by CV. From UV-vis spectroscopic data, λ_{tail} was found at 370 nm, which together equated to an excited-state energy E_{00}(**[A2**$^{-}$**]***/**A2**$^{-}$) = 3.350 V.

Using these data, the following potential was calculated using Equation 2.1:

$$E(\mathbf{A2^{\bullet}/[A2^{-}]^{*}}) = 1.12 - 3.35 = \mathbf{-2.23\ V}\ (\text{vs Ag/AgCl})$$

This value indicates that SET reduction of pyridinium **I** to the pyridinyl radical **III** by **[A2**$^{-}$**]*** is highly exergonic ($E_{1/2}$ (**I**/**III**) = -0.6 V vs Ag/AgCl).

Transient Absorption Spectroscopy (TAS)[65]

Excited electronic states could be reached upon light absorption and are transient in nature. The lifetime of an excited state (τ_0) is usually rather short (ps to ms range) and cannot be observed with classical, *steady-state* experimental methods that require comparatively long detection times. Knowledge of τ_0 is useful for interpreting photochemical reaction mechanisms, as it directly influences the probability of participation of an excited-state species in a bimolecular process such as SET or EnT. A *time-resolved* experimental technique that could be employed to measure τ_0 is called *transient absorption spectroscopy* (TAS), also known as *flash photolysis*. In this experiment a *pump-probe* approach is performed, where the analyte is excited with a laser flash of an appropriate wavelength (355 nm in our study), and

[65] Balzani, V., Ceroni, P., Juris, A. "Photochemistry and Photophysics: Concept, Research and Applications" Weinheim, Wiley-VCH, 2014.

then the light absorption is recorded as a function of time at a second wavelength (625 nm in our study), depending on the absorption characteristics of target excited state.

In a typical experiment, a solution of **A2**$^{-}$ in degassed acetone ([**A2**] = 0.01M) was studied. The variation of optical density (ΔOD) was measured as a function of time and plotted in Figure 2.32. The excited state of **A2**$^{-}$ displayed a first-order exponential decay with a half-life of approximately **½ τ_0 = 5 µs**.

This value indicates that **[A2^{-}]*** is sufficiently long-lived to engage in bimolecular photochemical processes.

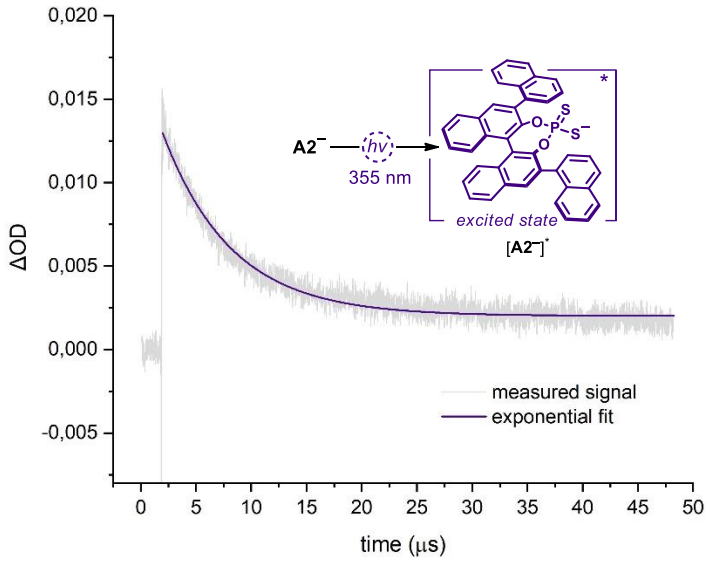

Figure 2.32. Absorption at 625 nm of the transient excited state of **A2**$^{-}$ generated upon excitation with a 355 nm laser. A first order exponential fit (purple line) was applied to the signal to facilitate the lifetime measurement. ΔOD: optical density variation.

In an additional TAS experiment, we attempted to measure the lifetime of the excited state of the unsubstituted catalyst **A1**. Absorption at wavelengths from 400 nm to 700 nm was inspected down to 10 ns scale, but no signal was detected. This result suggests that the 3,3'-substituents might significantly increase the excited state lifetime of the dithiophosphoric acid catalyst, facilitating productive SET with pyridinium ions **I**.

Stern-Volmer quenching studies

In order to detect and quantify interactions between the excited thiolate catalyst **[A2^{-}]*** and pyridinium **I**, we performed a Stern-Volmer quenching study. This technique is based on measurement of the effect of a compound (called quencher, Q) on the fluorescence of an excited-state species. This species can undergo relaxation in a few different ways: either by emitting a quant of light (fluorescence and phosphorescence) or through a so-called non-

radiative pathway. One such pathway is called dynamic quenching, and it is caused by a collision with a molecule of quencher Q. This collision triggers a subsequent relaxation either via a SET process, an energy transfer process, or via formation of an exciplex (excited-state complex). The fluorescence is easily detectable by a spectrofluorometer apparatus, and its decrease following the addition of quencher Q is the analytical signal in this experiment. The linear relationship between I_0/I (I_0 and I are the fluorescence intensities at a selected wavelength without and with the quencher respectively) and the concentration of quencher in solution is as follows (Equation 2.3).

$$I_0/I = 1 + k_q\tau_0[\mathrm{Q}] = 1 + K_{SV}[\mathrm{Q}] \qquad \textbf{(2.3)}$$

Here k_q is the kinetic constant of the dynamic quenching process and τ_0 is the lifetime of the excited state in the absence of quencher. The product $k_q\tau_0$ is usually referred to as the Stern-Volmer constant, K_{SV}.

The preformed salts **A2**·Et_3N and **1a**·HCl were used so that the species in solution were $\mathbf{A2}^-$ and **I**. The emission spectrum of $\mathbf{A2}^-$ was recorded first. For this, **A2**·Et_3N was dissolved in thoroughly degassed acetone ([**A2**·Et_3N] = 5 mM) in a 1x1cm quartz cuvette, and was irradiated with 350 nm light, yielding the emission spectrum (Figure 2.33).

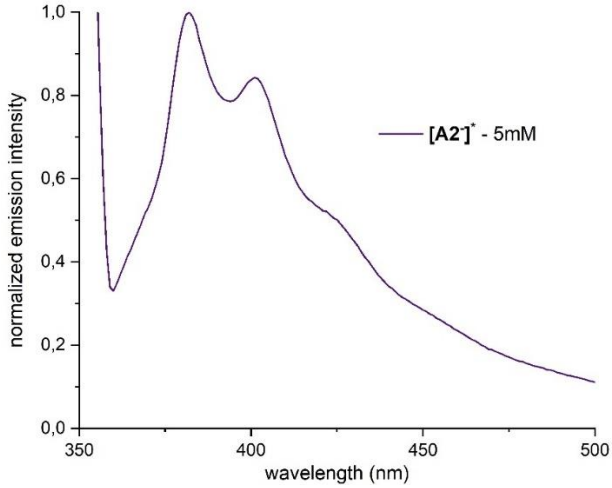

Figure 2.33. Normalized emission of **[A2⁻]*** upon irradiation at 350 nm of a 5 mM **A2**·Et_3N solution in acetone.

Then, emission quenching studies of the excited state of $\mathbf{A2}^-$ were performed using pyridinium salt **1a**·HCl as the quencher. Experimentally, a 5×10^{-3} M solution of **A2**·Et_3N in thoroughly degassed acetone was used. Sequential addition of a solution of **1a**·HCl resulted in decrease of emission intensity (Figure 2.34, left panel). The Stern-Volmer plot was constructed (Figure 2.34, right panel), conforming to a linear correlation between I_0/I and [**1a**·HCl]. From this data, a Stern-Volmer constant of $\boldsymbol{K_{SV}}$ **= 346 M^{-1}** was determined.

No change in the absorption spectrum of **A2**$^{-}$ was observed upon additions of **1a**·HCl, thus excluding a possible ground-state association between these two species which could lead to a decrease in emission intensity.

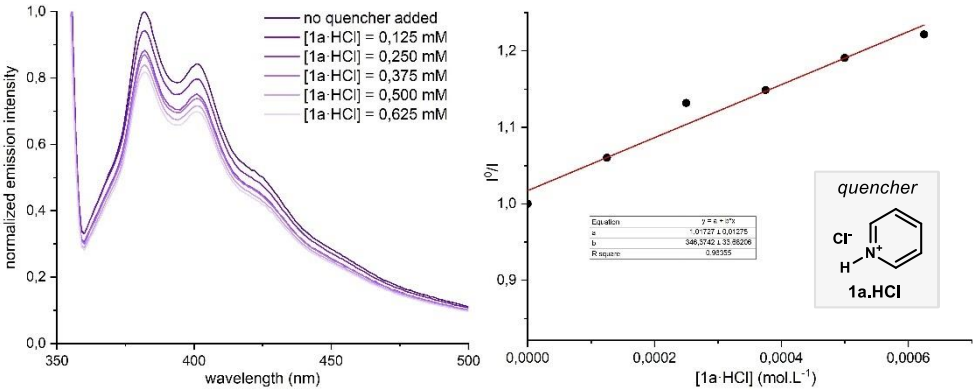

Figure 2.34. Quenching of **A2**$^{-}$emission (5×10^{-3} M in acetone) in the presence of increasing amounts of pyridinium **I**.

Under the same conditions, the effect of collidinium **XX** as a quencher was evaluated using 2,4,6-collidine hydrochloride. As shown in Figure 2.35, quenching was observed as well, with a Stern-Volmer constant K_{SV} = **283 M^{-1}**.

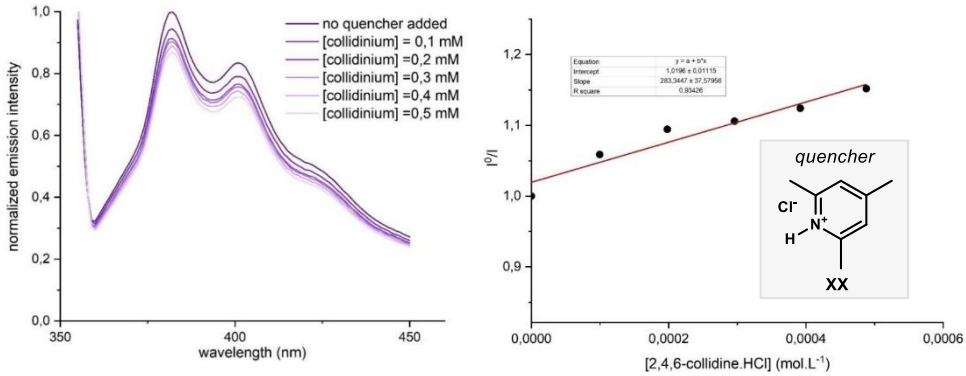

Figure 2.35. Quenching of **A2**$^{-}$emission (5×10^{-3} M in acetone) in the presence of increasing amounts of collidinium **XX**.

These results indicate that both pyridinium ion **I** and collidinium **XX** can quench the excited state of **A2**$^{-}$, therefore confirming the feasibility of an SET event taking place from **A2**$^{-}$ to both **I** and **XX**. The value of the Stern-Volmer constants suggests a faster quenching with **I**, although they are in the same order of magnitude. A possible role of collidine in the process will be discussed later (Section 2.5.4).

Since the reaction can also be performed under blue light irradiation with an external photoredox catalyst, quenching studies under these conditions were also performed. Upon irradiation of a 5×10^{-6} M solution of $[Ir(dtbbpy)(ppy)_2]PF_6$ in thoroughly degassed acetone with a 390 nm light, emission of the photocatalyst was detected with a maximum around 600 nm. Sequential addition of a solution of **1a**·HCl caused a decrease in emission intensity (Figure 2.36, left panel). The Stern-Volmer plot was constructed (Figure 2.36, right panel) conforming to a linear correlation between I_0/I and [**I**]. From this data, a Stern-Volmer constant of $\boldsymbol{K_{SV}}$ **= 90 M^{-1}** was determined. The quenching constant $\boldsymbol{k_q}$ **= 1.6 · 10^8 M^{-1}·s^{-1}** was calculated considering the lifetime of $[Ir(dtbbpy)(ppy)_2]PF_6$ in the excited state (0.557 μs).[66]

No change in the absorption spectrum of $[Ir(dtbbpy)(ppy)_2]PF_6$ was observed upon additions of **I**, thus excluding a possible ground-state association between these two species which could lead to a decrease in emission intensity.

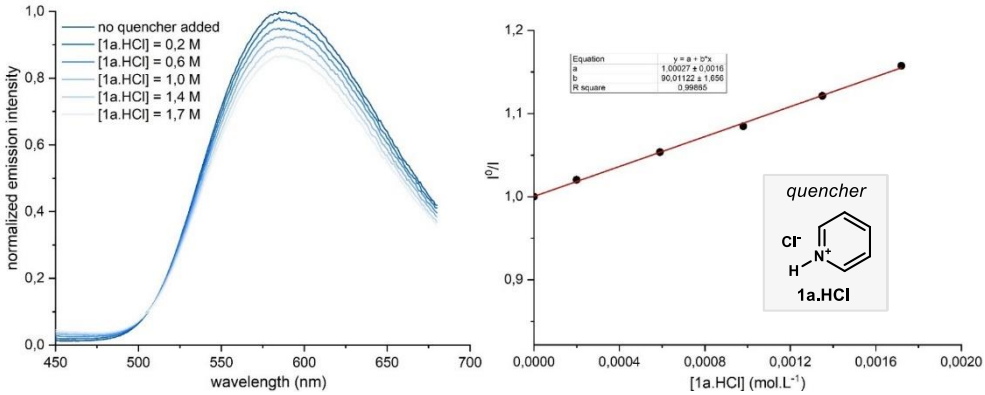

Figure 2.36. Quenching of $[Ir(dtbbpy)(ppy)_2]PF_6$ emission (5×10^{-6} M in acetone) in the presence of increasing amounts of pyridinium **I**.

[66] Wu, Y.; Kim, D.; Teets, T. S. "Photophysical Properties and Redox Potentials of Photosensitizers for Organic Photoredox Transformations" *Synlett* **2022**, *33*, 1154.

2.5.3 Pyridinyl radical formation

Additional spectroscopic and synthetic mechanistic experiments were undertaken to identify the key pyridinyl radical **III**.

Electron Paramagnetic Resonance (EPR)[67]

EPR spectroscopy, also known as electron spin resonance (ESR) spectroscopy, is a method useful for the detection of unpaired electrons in open-shell species. Similarly to NMR, upon subjecting the molecule to a magnetic field, a Zeeman splitting takes place and several energy levels of an electronic state could be detected via absorption or emission of photons. Instead of chemical shifts in ppm, the magnetic field strength expressed in Gauss (G) constitutes the *x*-axis. The Landé *g*-factor is a characteristic property of an electron in a weak magnetic field, and appears in the following Equation 2.4:

$$h\nu = g\mu_B B_0 \qquad \textbf{(2.4)}$$

where h is the Planck's constant, ν is the frequency of the absorbed/emitted photons (usually in the microwave region), μ_B the Bohr magneton constant, and B_0 the magnetic field.

The *g*-factor is characteristic of the chemical environment of the electron, *i.e.* the nucleus on which it is located. Since ν and B_0 are set by the operator, g can be deduced from Equation 4. For further elucidation, *hyperfine* coupling phenomenon is used. It is caused by the coupling of the electronic spin with nearby nuclear spins, producing multiplets reminiscent of NMR signals.

To probe the formation of pyridinyl radical **III** under irradiation with **A2**, we recorded the EPR spectrum of a 5:1 mixture of **1a**/**A2** before and after 15 min of irradiation at 77 K (Figure 2.37). After irradiation, a signal was detected with a calculated **g-value of 2.00324**, which is in range with the literature values for the pyridinyl radicals **III**.[46] Unfortunately, hyperfine coupling constants could not be calculated due to the poor resolution of the spectrum. Still, this result indicates that the proposed pyridinyl radical **III** can indeed be generated from pyridine **1a** via photoinduced SET process mastered by **A2**.

[67] McMillan, J. A. "Electron Paramagnetic Resonance of Free Radicals" *J. Chem. Educ.* **1961**, *38*, 438.

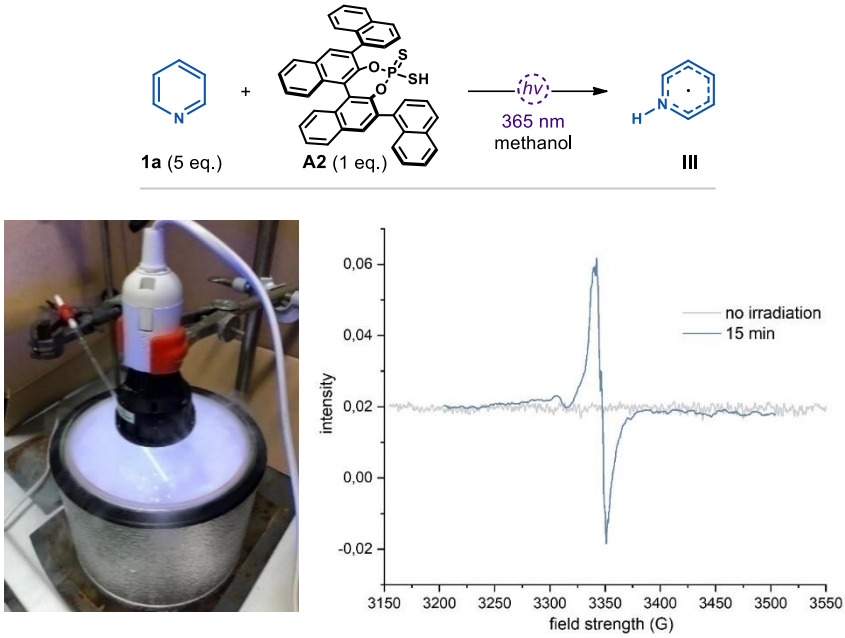

Figure 2.37. Experimental setup for the EPR experiment (*left*) and measured EPR spectra of a 5:1 mixture of **1a** and **A2** in methanol before and after 15 min of irradiation (*right*).

Radical clock experiments [68]

Altogether, the quenching and EPR experiments demonstrate the ability of $\mathbf{A2}^-$ to reduce pyridinium ion **I** to afford the pyridinyl radical **III** upon excitation. We wanted to have evidence that this process could happen also *under reaction conditions*. Therefore, we conducted the radical-clock experiments detailed in Figure 2.38. We used tailored pyridine substrates **21a** and **21b** containing a *gem*-diphenyl substituted cyclopropyl ring, primed for radical ring opening. Both substrates underwent ring opening under the standard conditions to give products **22a** and **22b** in 51% and 45% yield, respectively. The formation of these products is consistent with the intermediacy of pyridinyl radical **III**, which, upon ring opening to a highly stabilized benzylic radical **XXI**, can undergo radical coupling with the allylic radical **IV**.

[68] Griller, D.; Ingold, K. U. "Free-Radical Clocks" *Acc. Chem. Res*. **1980**, *13*, 317.

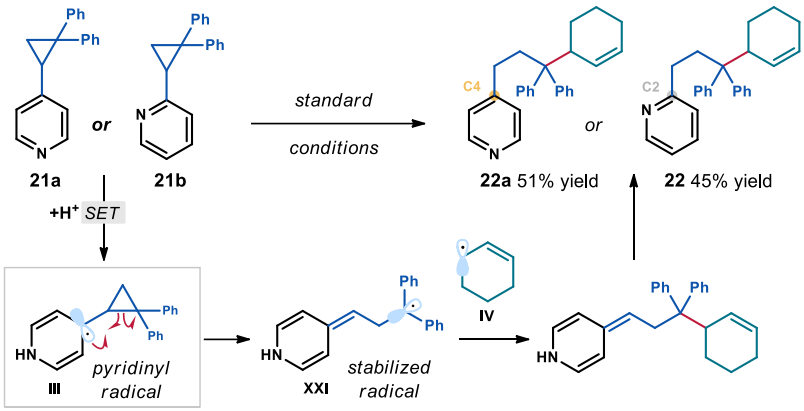

Figure 2.38. Probing the formation of pyridinyl radicals **III** under the reaction conditions.

2.5.4 Discussion on the role of collidine

The precise role of 2,4,6-collidine in the reaction has remained unclear, but some experimental observations allowed us to formulate a hypothesis. As collidine (pK_{aH} = 7.4) is more basic than pyridine (pK_{aH} = 5.3), a dynamic equilibrium between pyridinium and collidinium is expected. Similar to pyridine, collidine exhibited no reduction down to -2.5 V, while a reversible reduction wave was observed for the collidinium trifluoroacetate salt **XX** at -0.6 V (Figure 2.39).

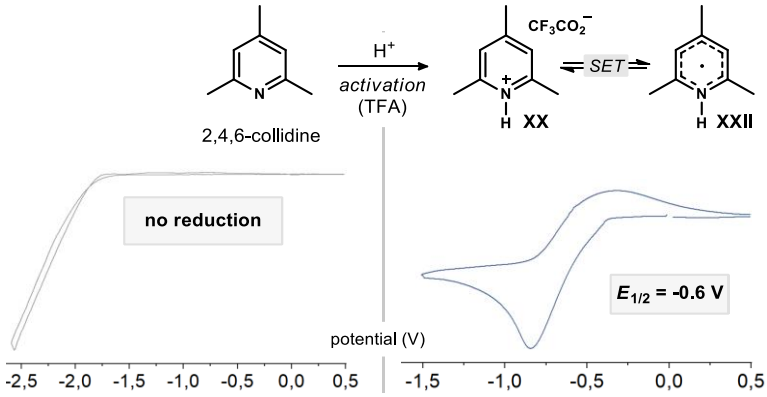

Figure 2.39. Electrochemical studies using collidine and pre-formed collidinium **XX**. Ag/AgCl (3.0M NaCl) reference electrode in CH_3CN.

Stern-Volmer studies have also confirmed that reduction of collidinium **XX** by the excited photocatalyst **A2**$^-$ is feasible with comparable K_{SV} to pyridinium **I**. However, radical coupling of **XXII** with an allylic radical **IV** is likely hampered by the steric influence of the methyl groups at *ortho* and *para* positions, thus avoiding by-product formation. Altogether, this allowed us to propose that collidine may act as an *electron shuttle* in the reaction (Figure

2.40). As such, when **XXII** is formed, it would not couple with an allylic radical **IV** due to steric hindrance, but instead it would deliver an electron to pyridinium ion **I** to generate the productive pyridinyl radical **III**. Similar electron shuttling from a Hantzsch pyridine has been proposed previously.[69]

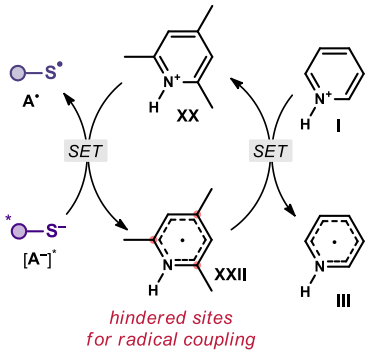

Figure 2.40. Possible role of collidine as an electron shuttle.

2.5.5 Oxidation of the dihydropyridine intermediate

As presented in Figure 2.41, the initial product of the radical coupling is dihydropyridine **XIX**. However, this species was never observed in the course of this study. This section details a series of experiments conducted to understand how the dihydropyridine **XIX** is oxidized to form the final product **3a**. During our studies, we observed stoichiometric formation of isopropanol during the reaction, presumably coming from the reduction of acetone (the solvent used in this process). As such, we concluded that acetone is likely to serve as the formal oxidant in the reaction, though the exact oxidation mechanism still needed clarification.

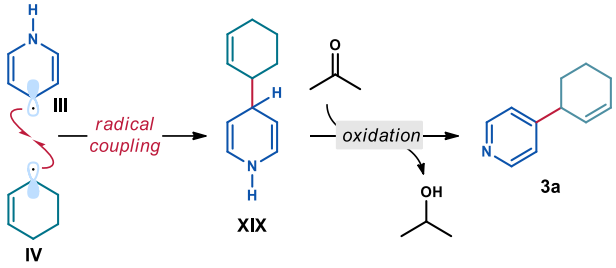

Figure 2.41. Formal oxidation of **XIX** by acetone and formation of isopropanol.

[69] Bieszczad, B.; Perego, L. A.; Melchiorre, P. "Photochemical C-H Hydroxyalkylation of Quinolines and Isoquinolines" *Angew. Chem. Int. Ed*. **2019**, *58*, 16878.

While the direct reduction of acetone by the excited state **[A2^{-}]*** is endergonic (for cyclohexanone E_{red} = -2.33 V vs SCE < E_{red}^{*}(**A2**$^{-}$) = -2.23 V),[70] formation of the ketyl radical **XXIV** via such SET process is feasible if the acetone is protonated to form **XXIII**.[71] As such, we propose an SET reduction of **XXIII**, forming a thiyl radical **A•** and a ketyl radical **XXIV.** The thyil radical **A•** is poised to abstract the *C4* hydrogen atom from the dihydropyridine intermediate **XIX** (BDE(*S-H*) = 83.3 kcal·mol^{-1} for **A1**, and for NADH analogues BDE(*C4-H*) ~ 69 kcal·mol^{-1}).[43b] The ketyl radical [**XXIV,** (BDE(*C-H*) = 91 kcal·mol^{-1})][72] can abstract a hydrogen atom from **A2** to form a thiyl radical **A•** to afford isopropanol. The substituted pyridinyl (**XXV**) would ultimately undergo SET oxidation forming the final product **3** (Figure 2.42).

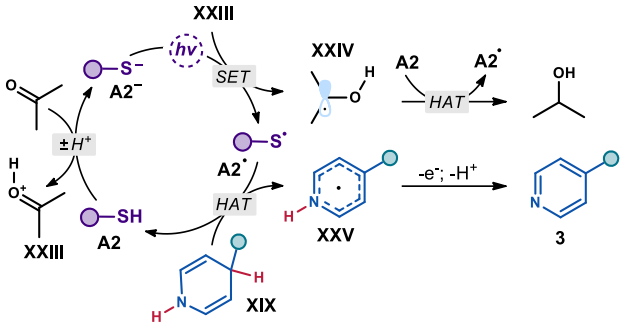

Figure 2.42. Possible explanation of the oxidation mechanism of **XIX**.

To test this hypothesis, we submitted a stable dihydropyridine derivative, 9,10-dihydroacridine **23**, to the reaction conditions (Figure 2.43.a). Full consumption of the starting material was observed, along with the formation of acridine **24** in 60% yield and isopropanol in 40% yield. In the absence of light or catalyst, no conversion of **23** was observed. This experiment suggests that **A2•** is indeed capable of abstracting the *C4-H* atom in **XIX**, thus initiating the oxidative rearomatization process.

To gauge the ability of the catalyst **A2** to reduce acetone, a similar experiment was conducted, excluding both 9,10-dihydroacridine and 2,4,6-collidine (Figure 2.43.b). 14% (0.07 mmol) of the dimer **25** and 17% (0.17 mmol) of isopropanol were formed during the reaction (using 0.02 mmol **A2**). The formation of isopropanol under these conditions supports the ability of

[70] Roth, H. G.; Romero, N. A.; Nicewicz, D. A. "Experimental and Calculated Electrochemical Potentials of Common Organic Molecules for Applications to Single-Electron Redox Chemistry" *Synlett* **2016**, *27*, 714.

[71] Tarantino, K. T.; Liu, P.; Knowles, R. R. "Catalytic Ketyl-Olefin Cyclizations Enabled by Proton-Coupled Electron Transfer" *J. Am. Chem. Soc*. **2013**, *135*, 10022.

[72] Capaldo, L.; Ravelli, D.; Fagnoni, M. "Direct Photocatalyzed Hydrogen Atom Transfer (HAT) for Aliphatic C–H Bonds Elaboration" *Chem. Rev*. **2022**, *122*, 1875

the excited state **[A2^{-}]*** to reduce acetone in a photocatalytic manifold. In control experiments in the absence of light or catalyst, no product formation was observed.

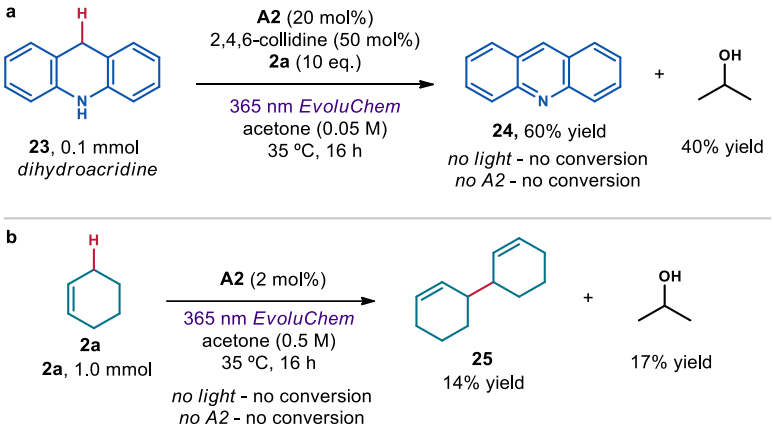

Figure 2.43. (**a**) Oxidation of 9,10-dihydroacridine and reduction of acetone under the reaction conditions. (**b**) Reduction of acetone to isopropanol by **[A2^{-}]*** accompanied by dimer **25** formation.

2.6 Conclusions

In this chapter, a new strategy for the radical functionalization of pyridines and related heteroarenes has been detailed, based on the unique reactivity of previously neglected pyridinyl radicals. These intermediates can undergo effective radical coupling with allylic radicals. This photochemical process is based on the exploitation of the LUMO-lowering effect of pyridine protonation that enables facile SET to the π-system of the resultant pyridinium ion. The process is mediated by a dithiophosphoric acid photocatalyst that serves three distinct roles during the reaction, sequentially acting as a Brønsted acid for pyridine protonation, an SET reductant for pyridinium ion reduction upon light excitation, and a HAT acceptor for the allylic *C-H* bonds upon formation of the thyl radical. This protocol offers good to excellent regioselectivity of functionalization, which has been linked both to the spin density distribution across the pyridine core, as well as the steric effects of the substituents. The key intermediates have been detected in a mechanistic investigation campaign including spectroscopic, electrochemical, and computational studies.

2.7 Experimental section

General information. The ^{1}H NMR, ^{19}F NMR, ^{13}C NMR spectra and UPC^2 traces are available in the published article[1] and are not reported in the present dissertation.

The NMR spectra were recorded at 300 MHz, 400 MHz, and 500 MHz for ^{1}H; 75 MHz, 101 MHz, and 126 MHz for ^{13}C; 376 MHz for ^{19}F; 162 MHz for ^{31}P. The chemical shifts (δ) for ^{1}H and $^{13}C\{^{1}H\}$ are given in ppm relative to residual signals of the solvents ($CHCl_3$ @ 7.26 ppm ^{1}H NMR, $CDCl_3$ @ 77.00 ppm ^{13}C NMR). Coupling constants are given in Hz. The following abbreviations are used to indicate the multiplicity: s, singlet; d, doublet; t, triplet; q, quartet; m, multiplet; br s, broad signal.

High-resolution mass spectra (HRMS) were obtained from the ICIQ High-Resolution Mass Spectrometry Unit on MicroTOF Focus and Maxis Impact (Bruker Daltonics) with electrospray ionization or atmospheric pressure chemical ionization. Cyclic voltammetry (CV) studies were carried out on a Princeton Applied Research PARSTAT 2273 potentiostat offering compliance voltage up to ± 100 V (available at the counter electrode), ± 10 V scan range and ± 2 A current range. UV-vis measurements were carried out on a Shimadzu UV-2401PC spectrophotometer equipped with photomultiplier detector, double beam optics and D2 and W light sources. The emission spectra were recorded using a Fluorolog Horiba Jobin Yvon spectrofluorimeter equipped with a photomultiplier detector, a double monochromator, and a 350W xenon light source.

Yield of isolated products refer to materials of >95% purity as determined by ^{1}H NMR analysis.

General Procedures. All reactions were set up under an argon atmosphere in oven-dried glassware using standard Schlenk techniques, unless otherwise stated. Synthesis grade solvents were used as purchased. Anhydrous solvents were taken from a commercial SPS solvent dispenser. Chromatographic purification of products was accomplished using flash column chromatography (FC) on silica gel (230-400 mesh). For thin layer chromatography (TLC) analysis throughout this work, Merck precoated TLC plates (silica gel 60 GF_{254}, 0.25 mm) were used, using UV light as the visualizing agent and either phosphomolybdic acid in EtOH, or basic aqueous potassium permanganate ($KMnO_4$), and heat as developing agents. Organic solutions were concentrated under reduced pressure on a Büchi rotary evaporator (*in vacuo* at 40 ºC, ~5 mbar).

Determination of Diastereomeric Ratio. The diastereomeric ratios were determined by ^{1}H NMR analysis of the isolated materials through integration of diagnostic signals, or by UPC^2 analysis on chiral stationary phase using a Waters Acquity instrument. The exact conditions for the analyses are specified within the characterization section.

Materials. Commercial grade reagents and solvents were purchased at the highest commercial quality from Sigma Aldrich, Fluka, Acros Organics, Fluorochem, or Alfa Aesar and used as received, unless otherwise stated. Thiophosphoric acid **A8** and imide **A9** were synthesized following reported procedures.[73]

2.7.1 Synthesis of photocatalysts

2.7.1.1 *Synthesis of BINOLs*

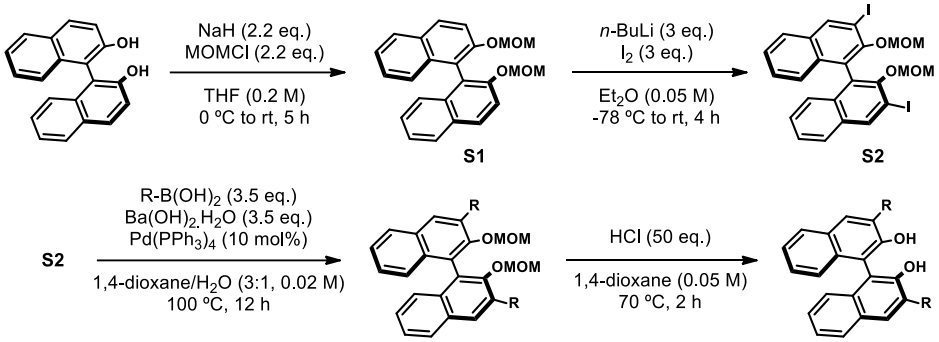

Figure 2.44. Synthetic route for the preparation of 3,3'-substiuted (*S*)-binol derivatives.

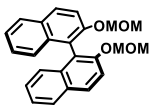

S1

(*S*)-2,2'-bis(methoxymethoxy)-1,1'-binaphthalene (S1) NaH (1.8 g, 2.2 equiv., 60% in mineral oil) was suspended in dry THF (90 mL) at 0 ºC under an atmosphere of argon. A solution of (*S*)-2,2'-dihydroxy- 1,1'-binaphthyl (5.73 g, 20.0 mmol) in THF (30 mL) was added dropwise and the mixture stirred at 0 ºC for 1 h and then at room temperature for 30 min. After the mixture was cooled-down to 0 ºC, chloromethyl methyl ether (3.33 mL, 2.2 equiv.) was slowly added and the reaction mixture was warmed-up to room temperature and stirred for 5 h. Saturated NH_4Cl (50 mL) was added to the flask, then the solvent was removed in vacuo. The residue was extracted with CH_2Cl_2 (50 mL × 3). The organic layers were combined, washed with brine (50 mL), dried over $MgSO_4$, filtered and concentrated. The crude product was triturated with cold hexanes, filtered and dried under high vacuum to afford **S1** as a white solid (6.82 g, 91% yield).

^{1}H NMR (400 MHz, $CDCl_3$) δ 7.97 (d, *J* = 8.7 Hz, 2H), 7.89 (d, *J* = 8.1 Hz, 2H), 7.60 (d, *J* = 9.0 Hz, 2H), 7.36 (ddd, *J* = 8.1, 6.6, 1.3 Hz, 2H), 7.24 (ddd, *J* = 8.1, 6.7, 1.3 Hz, 2H), 7.18 (d, *J* = 8.5 Hz, 2H), 5.10 (d, *J* = 6.8 Hz, 2H), 5.00 (d, *J* = 6.8 Hz, 2H), 3.17 (s, 6H).

[73] Kato, S.; Saga, Y.; Kojima, M.; Fuse, H.; Matsunaga, S.; Fukatsu, A.; Kondo, M.; Masaoka, S.; Kanai, M. "Hybrid Catalysis Enabling Room-Temperature Hydrogen Gas Release from N-Heterocycles and Tetrahydronaphthalenes" *J. Am. Chem. Soc*. **2017**, *139*, 2204.

^{13}C NMR (126 MHz, $CDCl_3$) δ 152.7, 134.0, 129.9, 129.4, 127.9, 126.3, 125.6, 124.1, 121.3, 117.3, 95.2, 55.8, 29.7.

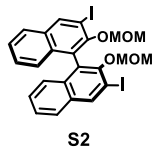

S2

(*S*)-3,3'-diiodo-2,2'-bis(methoxymethoxy)-1,1'-binaphthalene (S2) To a solution of MOM protected (*S*)-binol **S1** (6.82 g, 18.2 mmol) in dry Et_2O (350 mL, 0.05 M), was added *n*-BuLi (2.5 M in hexanes, 21.9 mL, 3 equiv.) at 0 ºC. The resulting mixture was warmed-up to room temperature and stirred for 3 h. It was then cooled down to -78 ºC and I_2 (13.9 g, 3 equiv.) was added portionwise. The reaction mixture was allowed to warm-up to room temperature overnight. Saturated NH_4Cl (100 mL) was then added and the biphasic mixture diluted with water (100 mL) and EtOAc (100 mL). The aqueous layer was extracted with EtOAc (100 mL x 2), and the combined organic layers washed with water (100 mL x 2), 10% $Na_2S_2O_3$ (100 mL x 2), brine, dried over $MgSO_4$, filtered and concentrated under reduced pressure. The crude product was purified by column chromatography (SiO_2, 5:95 EtOAc/hexanes) to afford **S2** as an off-white foamy solid (6.9 g, 60% yield).

^{1}H NMR (500 MHz, $CDCl_3$) δ 8.56 (s, 2H), 7.80 (d, *J* = 7.8 Hz, 2H), 7.45 (ddd, *J* = 8.1, 6.7, 1.2 Hz, 2H), 7.32 (ddd, *J* = 8.2, 6.8, 1.3 Hz, 2H), 7.19 (d, *J* = 8.5 Hz, 2H), 4.83 (d, *J* = 5.7 Hz, 2H), 4.71 (d, *J* = 5.7 Hz, 2H), 2.62 (s, 6H).

The remaining steps for the synthesis of substituted binols are illustrated with the preparation of the 1-naphthyl-subsituted binol.

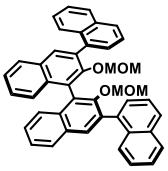

(*S*)-3,3'-bis(1-naphtyl)-2,2'-bis(methoxymethoxy)-1,1'-binaphthalene To **S2** (4.0 g, 6.39 mmol), $Ba(OH)_2{\cdot}8H_2O$ (7.1 g, 3.5 equiv.), and $Pd(PPh_3)_4$ (738 mg, 0.1 equiv.) was added 1,4-dioxane/H_2O (320 mL, 0.02 M, 3:1 mixture) at room temperature, under an atmosphere of argon. Naphthalene-1-boronic acid (3.85 g, 3.5 equiv.) was then added in one portion, and the mixture stirred at 100 ºC for 12 h. 1,4-dioxane was then removed under reduced pressure, and the residue extracted with CH_2Cl_2 (100 mL x 3), the combined organic layers washed with brine, dried over $MgSO_4$, filtered, and concentrated under reduced pressure. The crude product was purified by column chromatography (SiO_2, 5:95 EtOAc/hexanes) to afford the product as a white solid (3.85 g, 96% yield).

NMR analysis of this compound is complicated by the presence of multiple conformers due to slow rotation around the 3,3′-biaryl bonds and the unsymmetrical nature of the 1-naphthyl substituent.

^{1}H NMR (400 MHz, $CDCl_3$) δ 8.05 – 7.35 (m, 24H), 4.53 – 4.18 (m, 4H), 2.20 – 2.12 (m, 6H).

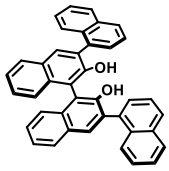

(*S*)-3,3'-bis(1-naphthyl)-2,2'-dihydroxy-1,1'-binaphtalene To (*S*)-3,3'-bis(1-naphtyl)-2,2'-bis(methoxymethoxy)-1,1'-binaphthalene (3.85 g, 6.2 mmol) dissolved in 1,4-dioxane (20 mL, 0.3M) was added concentrated HCl (10 mL). The resulting mixture was stirred at 70 ºC for 2h. The solvent was then removed under reduced pressure, the residue dissolved in CH_2Cl_2 (100 mL) and the organic layer washed with water (100 mL), saturated $NaHCO_3$ (100 mL), brine, dried over $MgSO_4$, filtered and concentrated under reduced pressure. After drying under high vacuum for several hours, the product was obtained as a light-yellow solid (3.4 g, quant. yield) that was used in the next step without further purification.

NMR analysis of this compound is complicated by the presence of multiple conformers due to slow rotation around the 3,3′-biaryl bonds and the unsymmetrical nature of the 1-naphthyl substituent.

^{1}H NMR (400 MHz, CDCl3) δ 8.07 – 8.02 (m, 2H), 8.02 – 7.91 (m, 6H), 7.89 – 7.83 (m, 1H), 7.78 – 7.59 (m, 5H), 7.59 – 7.35 (m, 10H), 5.30 – 5.16 (m, 2H).

2.7.1.2 *Synthesis of catalysts A1-A7*

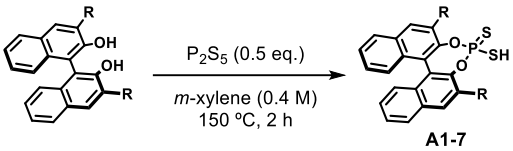

Figure 2.45. General procedure.

General procedure. A flame dried flask was charged with the appropriate (*S*)-binol derivative (1.0 equiv.), P_2S_5 (0.5 equiv.), and anhydrous *m*-xylene (0.2 M). The flask was equipped with a condenser and placed in an aluminum heating block preheated to 150 ºC. The progress of the reaction was monitored by disappearance of the phenolic protons, as inferred by ^{1}H NMR analysis of the crude mixture. After 2 h, the reaction mixture was cooled to ambient temperature. The solvent was removed in vacuo. The crude product was dissolved in a minimum amount of CH_2Cl_2 and treated with hexanes. The resulting fine precipitate was then collected by filtration and the operation repeated until no more precipitate was formed. The pure dithiophosphoric acids **A1-7** were obtained after washing the precipitates with cold hexanes.

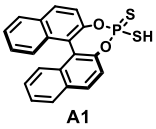

A1

(11bS)-4-mercaptodinaphtho[2,1-d:1',2'-f][1,3,2]dioxaphosphepine 4-sulfide (A1) Prepared according to general procedure using (S)-1,1'-bi-2-naphtol (2.23g, 5.86 mmol). **A1** (2.23g, 5.86 mmol, 73% yield) was obtained as a white powder which displayed spectroscopic data consistent with those reported previously.[49]

^{1}H NMR (400 MHz, $CDCl_3$) δ 8.13 – 8.07 (m, 2H), 8.00 (dd, *J* = 8.1, 1.2 Hz, 2H), 7.60 (dd, *J* = 8.8, 1.4 Hz, 2H), 7.54 (ddt, *J* = 8.0, 6.8, 1.1 Hz, 2H), 7.48 – 7.42 (m, 2H), 7.36 (ddd, *J* = 8.4, 6.7, 1.3 Hz, 2H).

^{13}C NMR (75 MHz, $CDCl_3$) δ 147.2, 132.4, 132.0, 131.1, 128.6, 127.2, 126.9, 126.1, 122.6, 121.1.

^{31}P NMR (162 MHz, $CDCl_3$) δ 100.2.

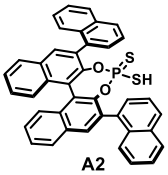

A2

(11bS)-4-mercapto-2,6-di(naphthalen-1-yl)dinaphtho[2,1-d:1',2'-f][1,3,2]dioxaphosphepine 4-sulfide (A2) Prepared according to general procedure using (1′S)-[1,3′:1′,1″:3″,1‴-Quaternaphthalene]-2′,2″-diol (1.25 g, 2.32 mmol). **A2** (1.17 g, 1.85 mmol, 80% yield) was obtained as a white powder which displayed spectroscopic data consistent with those reported previously.[74]

NMR analysis of this compound is complicated by the presence of multiple conformers due to slow rotation around the 3,3′-biaryl bonds and the unsymmetrical nature of the 1-naphthyl substituent.

^{1}H NMR (400 MHz, $CDCl_3$) δ 8.24 – 7.31 (m, 24H).

^{31}P NMR (162 MHz, $CDCl_3$) δ 96.3, 96.2, 96.1.

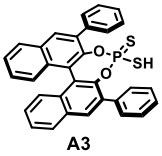

A3

(11bS)-4-mercapto-2,6-diphenyldinaphtho[2,1-d:1',2'-f][1,3,2]dioxaphosphepine 4-sulfide (A3) Prepared according to general procedure using (1S)-3,3′-Diphenyl[1,1′-binaphthalene]-2,2′-diol (317 mg, 0.72 mmol). **A3** (256 mg, 0.48 mmol, 67% yield) was obtained as a white powder which displayed spectroscopic data consistent with those reported previously.[49]

^{1}H NMR (500 MHz, CDCl3) δ 8.14 (s, 2H), 8.06 – 8.02 (m, 2H), 7.75 – 7.71 (m, 4H), 7.58 (dt, J = 7.0, 1.0 Hz, 2H), 7.52 – 7.42 (m, 8H), 7.38 (ddd, J = 8.5, 6.8, 1.3 Hz, 3H).

^{13}C NMR (101 MHz, CDCl3) δ 137.2, 131.4, 130.2, 129.6, 128.9, 128.6, 128.3, 127.8, 127.1, 126.7, 126.3.

[74] Shapiro, N. D.; Rauniyar, V.; Hamilton, G. L.; Wu, J.; Toste, F. D. "Asymmetric Additions to Dienes Catalyzed by a Dithiophosphoric Acid." *Nature* **2011**, *470*, 245

^{31}P NMR (202 MHz, CDCl3) δ 96.2.

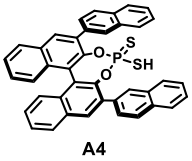

A4

(11bS)-4-mercapto-2,6-di(naphthalen-2-yl)dinaphtho[2,1-d:1',2'-f][1,3,2]dioxaphosphepine 4-sulfide (A4) Prepared according to general procedure using (1′S)-[2,3′:1′,1″:3″,2‴-Quaternaphthalene]-2′,2″-diol (590 mg, 1.1 mmol). **A4** (564 mg, 0.89 mmol, 81% yield) was obtained as a white powder.

^{1}H NMR (400 MHz, $CDCl_3$) δ 8.24 – 8.18 (m, 4H), 8.06 (d, *J* = 8.2 Hz, 2H), 7.97 – 7.82 (m, 8H), 7.61 – 7.55 (m, 2H), 7.54 – 7.48 (m, 6H), 7.44 – 7.35 (m, 2H).

^{13}C NMR (126 MHz, $CDCl_3$) δ 134.7, 133.3, 132.8, 132.0, 131.7, 129.3, 128.6, 128.4, 128.0, 127.8, 127.7, 127.1, 126.8, 126.4, 126.3, 126.2.

^{31}P NMR (162 MHz, $CDCl_3$) δ 96.3.

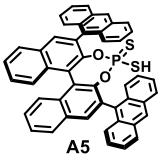

A5

(11bS)-2,6-di(anthracen-9-yl)-4-mercaptodinaphtho[2,1-d:1',2'-f][1,3,2]dioxaphosphepine 4-sulfide (A5) Prepared according to general procedure using (1S)-3,3′-Di-9-anthracenyl[1,1′-binaphthalene]-2,2′-diol (585 mg, 0.92 mmol). **A5** (543 mg, 0.74 mmol, 81% yield) was obtained as a white powder.

^{1}H NMR (400 MHz, $CDCl_3$) δ 8.54 – 8.49 (m, 2H), 8.17 (s, 2H), 8.08 – 7.95 (m, 8H), 7.74 – 7.61 (m, 6H), 7.57 – 7.50 (m, 2H), 7.46 – 7.37 (m, 4H), 7.36 – 7.26 (m, 4H).

^{13}C NMR (126 MHz, $CDCl_3$) δ 134.7, 131.6, 131.0, 131.0, 130.9, 130.3, 128.7, 128.6, 128.4, 128.1, 127.5, 127.2, 126.5, 126.3, 126.2, 125.1, 125.1, 125.0.

^{31}P NMR (122 MHz, $CDCl_3$) δ 93.2.

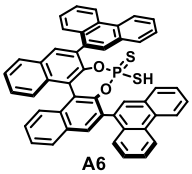

A6

(11bS)-4-mercapto-2,6-di(phenanthren-9-yl)dinaphtho[2,1-d:1',2'-f][1,3,2]dioxaphosphepine 4-sulfide (A6) Prepared according to general procedure using (1S)-3,3′-Di-9-phenanthrenyl[1,1′-binaphthalene]-2,2′-diol (540 mg, 0.85 mmol). **A6** (460 mg, 0.63 mmol, 74% yield) was obtained as a white powder.

^{1}H NMR (500 MHz, $CDCl_3$) δ 8.84 – 8.71 (m, 4H), 8.25 – 8.02 (m, 5H), 8.00 – 7.89 (m, 3H), 7.75 – 7.58 (m, 12H), 7.58 – 7.43 (m, 4H).

^{31}P NMR (202 MHz, $CDCl_3$) δ 96.5.

(11bS)-4-mercapto-2,6-bis(trifluoromethyl)dinaphtho[2,1-d:1',2'-f][1,3,2]dioxaphosphepine 4-sulfide (A7) Prepared according to general procedure using (1S)-3,3′-Bis(trifluoromethyl)[1,1′-binaphthalene]-2,2′-diol (470 mg, 1.1 mmol). **A7** (487 mg, 0.94 mmol, 85% yield) was obtained as a white powder.

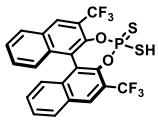

A7

^{1}H NMR (500 MHz, $CDCl_3$) δ 8.46 (s, 2H), 8.09 (d, *J* = 8.2 Hz, 2H), 7.63 (t, *J* = 7.6 Hz, 2H), 7.43 (t, *J* = 8.4 Hz, 1H), 7.16 (d, *J* = 8.6 Hz, 2H).

^{13}C NMR (126 MHz, $CDCl_3$) δ 143.1, 143.0, 133.9, 130.3, 130.3, 130.1, 129.5, 129.3, 127.4, 126.9, 123.6, 123.6, 121.8, 121.4.

^{19}F NMR (471 MHz, $CDCl_3$) δ -59.1.

^{31}P NMR (202 MHz, $CDCl_3$) δ 97.7.

2.7.2 Substrate synthesis

Most nicotinamides and nicotinic esters were synthesized from nicotinoyl chloride as depicted in Figure 2.46.

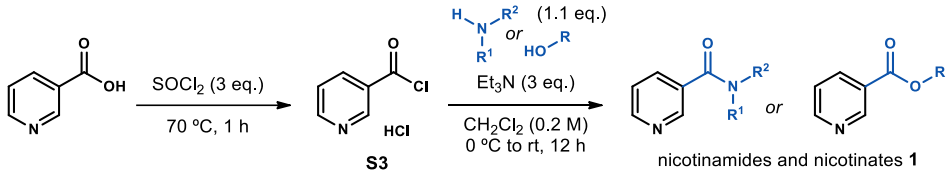

Figure 2.46. Synthesis of nicotinic acid derivatives from nicotinoyl chloride **S3**.

A suspension of nicotinic acid (1.0 equiv.) in thionyl chloride (3.0 equiv.) was stirred at 70 ºC for 1 h. The mixture was cooled down to room temperature and concentrated under reduced pressure to afford the crude nicotinoyl chloride hydrochloride **S3** as a white solid which was used in the next step without further purification.

To an ice-cold suspension of **S3** (1.0 equiv.) in dichloromethane (0.2 M) was added the amine or alcohol (1.1 equiv.) in portions, followed by dropwise addition of triethylamine (3.0 equiv.). The reaction was allowed to warm-up to room temperature over 12 h. The mixture was washed with water, brine, dried over magnesium sulfate, filtered, and concentrated under reduced pressure. Purification by column chromatography afforded the pure nicotinamides and nicotinates **1**.

The amino acid-derived nicotinamides were prepared using EDCI hydrochloride as a coupling agent (Figure 2.47).

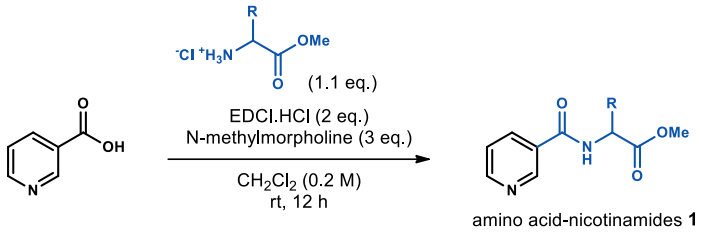

Figure 2.47. Synthesis of amino acid-derived nicotinamides.

To a suspension of nicotinic acid (1.0 equiv.) in dichloromethane (0.2 M) was added EDCI hydrochloride (2.0 equiv.), followed by *N*-methylmorpholine (3.0 equiv.) and the hydrochloride salt of the amino acid methyl ester (1.1 equiv.). The reaction mixture was stirred at room temperature overnight. The mixture was diluted with dichloromethane, washed with water, brine, dried over magnesium sulfate, filtered and concentrated under reduced pressure. Purification by column chromatography afforded the pure nicotinamides **1**.

The substrates for the radical clock experiments **21a** and **21b** were synthesized from the corresponding vinyl pyridines *via* cyclopropanation with diphenyldiazomethane (Figure 2.48).

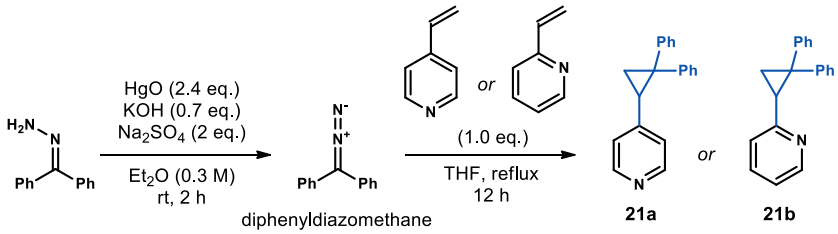

Figure 2.48. Synthesis of radical clock substrates **21a** and **21b**.

Diphenyldiazomethane. To benzophenone hydrazone (2.5 g, 12.7 mmol), anhydrous sodium sulfate (3.62 g, 2 equiv.), yellow mercuric oxide (II) (6.62 g, 2.4 equiv.), and potassium hydroxide (500 mg, 0.7 equiv., in 1 mL EtOH), was added 40 mL (0.3 M) of diethyl ether. The suspension was stirred at room temperature for 2 hours. The reaction mixture was filtered, and the filtrate concentrated under reduced pressure. The resulting dark red oil was dissolved in hexanes at 50 °C and filtered again. The solvent was evaporated under reduced pressure to obtain a dark red oil that was left to freeze overnight. Dark red crystals (2.47 g, quantitative yield) of diphenyldiazomethane formed when warmed-up to room temperature.

(2,2-diphenylcyclopropyl)pyridines) Diphenyldiazomethane (1.17 g, 6.0 mmol) and vinylpyridine (1.0 equiv.) were dissolved in THF (10 mL, 0.6 M). The solution was stirred under reflux overnight. After cooling down to room temperature, the dark solution was diluted with hexanes and filtered to remove the precipitate. The filtrate was concentrated under

reduced pressure and the crude mixture purified by column chromatography to afford the pure (2,2-diphenylcyclopropyl)pyridines.

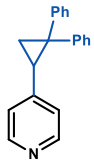

21a

4-(2,2-diphenylcyclopropyl)pyridine (21a) Prepared using 4-vinylpyridine (643 µL, 6.0 mmol). Purification by column chromatography (SiO_2, 1:40:59 Et_3N/EtOAc/hexanes) afforded **21a** as a light-yellow wax (1.1 g, 65% yield).

^{1}H NMR (400 MHz, $CDCl_3$) δ 8.29 (d, *J* = 6.2 Hz, 2H), 7.31 (d, *J* = 4.3 Hz, 4H), 7.25 – 7.10 (m, 6H), 6.74 (d, *J* = 6.2 Hz, 2H), 2.81 (dd, *J* = 8.8, 6.4 Hz, 1H), 2.05 (dd, *J* = 6.4, 5.5 Hz, 1H), 1.93 (dd, *J* = 8.8, 5.5 Hz, 1H).

^{13}C NMR (101 MHz, $CDCl_3$) δ 148.9, 148.5, 146.0, 139.2, 131.0, 128.5, 128.3, 127.3, 126.8, 126.3, 123.0, 40.8, 31.4, 21.5.

HRMS (ESI$^+$) Calculated for $C_{20}H_{18}N$ $[M+H]^+$: 272.1434 found: 272.1434.

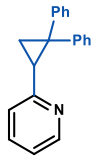

21b

2-(2,2-diphenylcyclopropyl)pyridine (21b) Prepared using 2-vinylpyridine (645 µL, 6.0 mmol). Purification by column chromatography (SiO_2, 1:40:59 Et_3N/EtOAc/hexanes) afforded **21b** as a light-yellow wax (1.0 g, 63% yield).

^{1}H NMR (400 MHz, $CDCl_3$) δ 8.35 (ddd, *J* = 4.9, 1.9, 0.9 Hz, 1H), 7.41 – 7.34 (m, 3H), 7.32 – 7.26 (m, 2H), 7.22 – 7.16 (m, 1H), 7.16 – 7.06 (m, 5H), 6.95 (ddd, *J* = 7.5, 4.9, 1.2 Hz, 1H), 6.80 (dt, *J* = 7.9, 1.1 Hz, 1H), 3.13 (dd, *J* = 8.7, 6.5 Hz, 1H), 2.34 (dd, *J* = 6.5, 5.1 Hz, 1H), 1.85 (dd, *J* = 8.7, 5.1 Hz, 1H).

^{13}C NMR (101 MHz, $CDCl_3$) δ 158.4, 148.6, 146.5, 140.2, 135.3, 131.0, 128.3, 127.9, 127.5, 126.2, 126.0, 122.3, 120.6, 40.2, 33.8, 20.3.

HRMS (ESI$^+$) Calculated for $C_{20}H_{18}N$ $[M+H]^+$: 272.1434 found: 272.1433.

2.7.3 Electrochemical studies

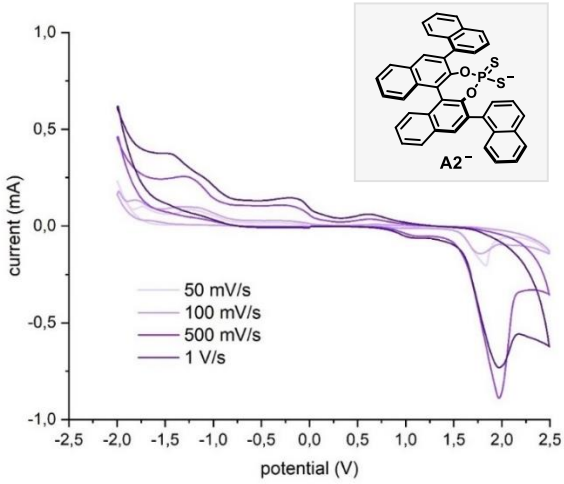

Figure 2.49. Cyclic voltammogram for the anion of catalyst **A2** [0.02M] in [0.1 M] $TBAPF_6$ in CH_3CN. Measurement started by oxidation from 0 to +2.0 V and finishing at 0 V. Platinum disk working electrode, AgCl/Ag (NaCl 3 M) reference electrode, Pt wire auxiliary electrode. One irreversible oxidation observed at **+1.12 V**.

2.7.4 Absorption spectroscopy analysis

No EDA complex between **A2** and pyridine **1a** or 2,4,6-collidine was observed using absorption spectroscopy (Figure 2.50). The tail of absorption of $\mathbf{A2}^-$ was located at approximately 370 nm (light blue, green, and orange lines).

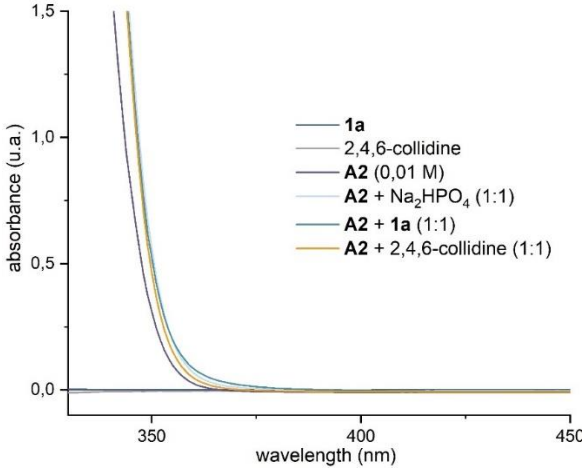

Figure 2.50. Absorption spectra of the reaction components under optimized conditions, recorded in acetone.

2.7.5 General procedures for the photochemical reactions

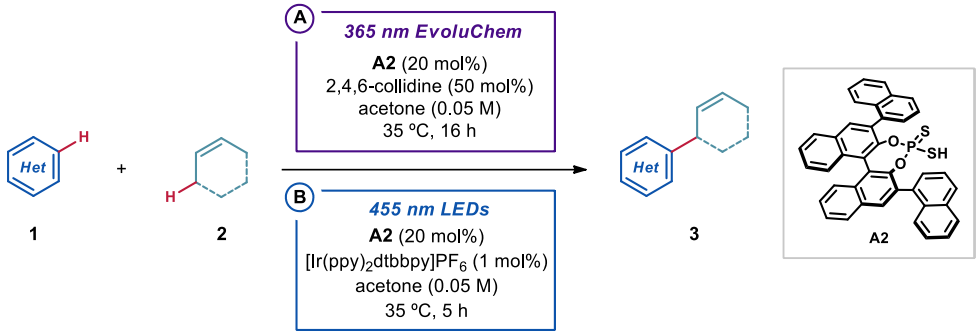

Figure 2.51. Schematic representation of general procedures.

General Procedure A. To an argon-purged glass vial, containing dithiophosphoric acid catalyst **A2** (25.3 mg, 0.04 mmol), and pyridine derivative **1** (0.2 mmol), was added 2,4,6-collidine (13.2 µL, 0.1 mmol), followed by the allylic precursor **2** (2.0 mmol) and argon-sparged HPLC grade acetone (0.05 M). The vial was sealed with Parafilm and placed in the 365 nm irradiation setup (Figure 2.52, left panel). The reaction was stirred for 16 h, then the solvent was evaporated and the crude mixture purified by flash column chromatography on silica gel to furnish the product **3**

General Procedure B. To an argon-purged glass vial, containing dithiophosphoric acid catalyst **A2** (25.3 mg, 0.04 mmol), $[Ir(ppy)_2(dtbbpy)]PF_6$ (1.8 mg, 2.0 µmol), and pyridine derivative **1** (0.2 mmol), was added the allylic precursor **2** (2.0 mmol) followed by argon-sparged HPLC grade acetone (0.05 M). The vial was sealed with Parafilm and placed in the 455 nm irradiation setup (Figure 2.52, right panel). The reaction was stirred for 5 h, then the solvent was evaporated and the crude mixture purified by flash column chromatography on silica gel to furnish the product **3**.

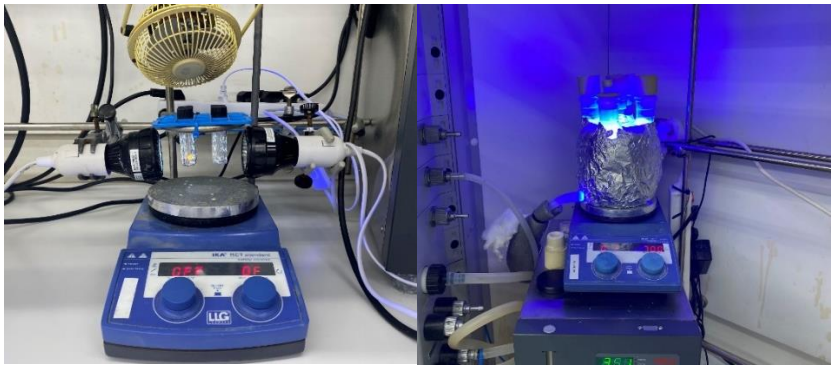

Figure 2.52. UV light (365 nm) setup using EvoluChem PF365 LED spotlights and a fan (*left*). Visible light (455 nm) setup using a 14 W LEDs strip and a minichiller to control the temperature (*right*).

2.7.6 Characterization of products 3

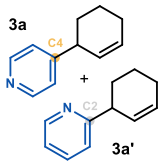

4-(cyclohex-2-en-1-yl)pyridine (3a) + 2-(cyclohex-2-en-1-yl)pyridine (3a')

Prepared according to General Procedure A using pyridine **1a** (16.2 µL, 0.2 mmol) and cyclohexene **2a** (203 µL, 2.0 mmol). The regioisomeric ratio **3a**/**3a'** (6:1) of the crude mixture was measured by ^{1}H NMR analysis. Purification by column chromatography (SiO_2, 1:10:89 Et_3N/EtOAc/hexanes) afforded product **3a** as a colorless oil (17.6 mg, 55% yield, > 20:1 *r.r.*). The minor regioisomer **3a'** was not isolated after column chromatography.

^{1}H NMR (400 MHz, $CDCl_3$) δ 8.53 – 8.49 (m, 2H), 7.17 – 7.14 (m, 2H), 5.97 (m, 1H), 5.70 – 5.65 (m, 1H), 3.40 (m, 1H), 2.16 – 2.09 (m, 2H), 2.08 – 1.98 (m, 1H), 1.80 – 1.71 (m, 1H), 1.69 – 1.61 (m, 1H), 1.61 – 1.51 (m, 1H).

^{13}C NMR (126 MHz, $CDCl_3$) δ 155.3, 149.7, 129.7, 128.2, 123.1, 41.1, 31.7, 24.9, 20.8.

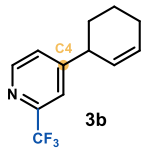

4-(cyclohex-2-en-1-yl)-2-(trifluoromethyl)pyridine (3b)

Prepared according to General Procedure A using 2-(trifluoromethyl)pyridine (23.0 µL, 0.2 mmol) and cyclohexene **2a** (203 µL, 2.0 mmol). No other regioisomer was detected in the crude mixture. Purification by column chromatography (SiO_2, 1:5:96 Et_3N/EtOAc/hexanes) afforded product **3b** as a colorless oil (29.3 mg, 65% yield, > 20:1 *r.r.*).

^{1}H NMR (500 MHz, $CDCl_3$) δ 8.64 (d, *J* = 5.0 Hz, 1H), 7.56 (d, *J* = 1.6 Hz, 1H), 7.36 (dd, *J* = 5.0, 1.6 Hz, 1H), 6.04 (m, 1H), 5.68 (m, 1H), 3.54 – 3.47 (m, 1H), 2.18 – 2.11 (m, 2H), 2.11 – 2.05 (m, 1H), 1.77 – 1.71 (m, 1H), 1.71 – 1.64 (m, 1H), 1.61 – 1.52 (m, 1H).

^{13}C NMR (126 MHz, $CDCl_3$) δ 157.5, 149.9, 148.3 (q, *J* = 34.0 Hz), 130.6, 127.1 (q, 274.1 Hz), 125.8, 119.8 (q, *J* = 2.9 Hz), 41.2, 31.8, 29.7, 24.8, 20.7.

^{19}F NMR (471 MHz, $CDCl_3$) δ -67.9.

HRMS (ESI$^+$) Calculated for $C_{12}H_{13}F_3N$ $[M+H]^+$: 228.0995 found: 228.0988.

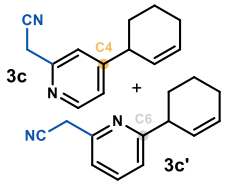

2-(4-(cyclohex-2-en-1-yl)pyridin-2-yl)acetonitrile (3c) + 2-(6-(cyclohex-2-en-1-yl)pyridin-2-yl)acetonitrile (3c')

Prepared according to General Procedure A using 2-pyridylacetonitrile (23.6 mg, 0.2 mmol) and cyclohexene **2a** (203 µL, 2.0 mmol). The regioisomeric ratio **3c**/**3c'** (8:1) of the crude mixture was measured by ^{1}H NMR analysis. Purification by column chromatography (SiO_2, 1:50:49

Et_3N/EtOAc/hexanes) afforded product **3c** as a colorless oil (17.4 mg, 44% yield, > 20:1 *r.r.*). The minor regioisomer **3c'** was not isolated after column chromatography.

^{1}H NMR (500 MHz, $CDCl_3$) δ 8.48 (d, *J* = 5.1 Hz, 1H), 7.30 (s, 1H), 7.14 (dd, *J* = 5.1, 1.6 Hz, 1H), 6.06 – 5.97 (m, 1H), 5.71 – 5.62 (m, 1H), 3.94 (s, 2H), 3.49 – 3.39 (m, 1H), 2.17 – 2.09 (m, 2H), 2.08 – 2.00 (m, 1H), 1.80 – 1.70 (m, 1H), 1.70 – 1.61 (m, 1H), 1.60 – 1.50 (m, 1H).

^{13}C NMR (126 MHz, $CDCl_3$) δ 157.3, 150.4, 149.8, 130.2, 127.6, 122.5, 121.6, 117.2, 41.2, 31.7, 26.6, 24.8, 20.8.

HRMS (ESI$^+$) Calculated for $C_{13}H_{15}N_2$ $[M+H]^+$: 199.1230 found: 199.1229.

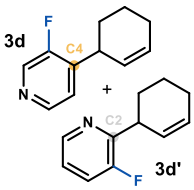

4-(cyclohex-2-en-1-yl)-3-fluoropyridine (3d) + 2-(cyclohex-2-en-1-yl)-3-fluoropyridine (3d')

Prepared according to General Procedure A using 3-fluoropyridine (17.2 µL, 0.2 mmol) and cyclohexene **2a** (203 µL, 2.0 mmol). The regioisomeric ratio **3d/3d'** (5:1) of the crude mixture was measured by ^{1}H NMR analysis. Purification by column chromatography (SiO_2, 1:4:95 Et_3N/EtOAc/hexanes) afforded a mixture of products **3d** and **3d'** as a colorless oil (16.5 mg, 47% yield, 6:1 *r.r.*). An analytically pure sample of **3d** was obtained by preparative TLC (SiO_2, 1:4:95 Et_3N/EtOAc/hexanes, >20:1 *r.r.*). Only the major product **3d** is described.

^{1}H NMR (400 MHz, $CDCl_3$) δ 8.39 (s, 1H), 8.35 (d, *J* = 4.9 Hz, 1H), 7.21 (dd, *J* = 6.5, 4.9 Hz, 1H), 6.06 – 5.98 (m, 1H), 5.68 – 5.57 (m, 1H), 3.85 – 3.74 (m, 1H), 2.18 – 2.10 (m, 2H), 2.09 – 2.03 (m, 1H), 1.76 – 1.66 (m, 2H), 1.63 – 1.53 (m, 1H).

^{13}C NMR (126 MHz, $CDCl_3$) δ 145.7 (d, *J* = 5.1 Hz), 141.7 (d, *J* = 12.4 Hz), 137.7, 137.5, 130.45, 126.9, 123.8, 33.8, 29.8, 24.8, 20.6.

^{19}F{^{1}H} NMR (471 MHz, $CDCl_3$) δ -59.03, -134.28 (d, *J* = 6.4 Hz).

HRMS (APCI$^+$) Calculated for $C_{11}H_{13}FN$ $[M+H]^+$: 178.1027 found: 178.1029.

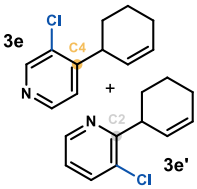

3-chloro-4-(cyclohex-2-en-1-yl)pyridine (3e) + 3-chloro-2-(cyclohex-2-en-1-yl)pyridine (3e')

Prepared according to General Procedure A using 3-chloro pyridine (22.7 mg, 0.2 mmol) and cyclohexene **2a** (203 µL, 2.0 mmol). Purification by column chromatography (SiO_2, 1:5:94 Et_3N/EtOAc/hexanes) afforded products **3e** + **3e'** (14.9 mg, 39% yield, 8:1 *r.r.*) as a colorless oil. Only the major product **3e** is described.

^{1}H NMR (400 MHz, $CDCl_3$) δ 8.54 (s, 1H), 8.41 (d, *J* = 5.0 Hz, 1H), 7.21 (d, *J* = 5.0 Hz, 1H), 6.09 – 6.02 (m, 1H), 5.67 – 5.58 (m, 1H), 3.91 – 3.83 (m, 1H), 2.17 – 2.06 (m, 3H), 1.73 – 1.65 (m, 2H), 1.58 – 1.44 (m, 1H).

^{13}C NMR (101 MHz, $CDCl_3$) δ 152.1, 149.3, 147.7, 131.7, 130.6, 127.2, 123.8, 37.6, 29.1, 24.9, 20.5.

HRMS (ESI$^+$) Calculated for $C_{11}H_{13}ClN$ $[M+H]^+$: 194.0731 found: 194.0732.

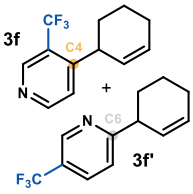

4-(cyclohex-2-en-1-yl)-3-(trifluoromethyl)pyridine (3f) + 6-(cyclohex-2-en-1-yl)-3-(trifluoromethyl)pyridine (3f')

Prepared according to General Procedure A using 3-(trifluoromethyl)pyridine (23.0 µL, 0.2 mmol) and cyclohexene **2a** (203 µL, 2.0 mmol). The regioisomeric ratio **3f/3f'** (9:1) of the crude mixture was measured by ^{1}H NMR analysis. Purification by column chromatography (SiO_2, 1:4:95 Et_3N/EtOAc/hexanes) afforded product **3f** as a colorless oil (20.1 mg, 44% yield, > 20:1 *r.r.*). The minor regioisomer **3f'** was not isolated after column chromatography.

^{1}H NMR (500 MHz, $CDCl_3$) δ 8.84 (s, 1H), 8.70 (d, *J* = 5.2 Hz, 1H), 7.38 (d, *J* = 5.2 Hz, 1H), 6.08 – 5.95 (m, 1H), 5.62 – 5.51 (m, 1H), 3.87 – 3.80 (m, 1H), 2.20 – 2.13 (m, 2H), 2.13 – 2.08 (m, 1H), 1.88 – 1.77 (m, 1H), 1.77 – 1.65 (m, 1H), 1.51 – 1.43 (m, 1H).

^{13}C NMR (126 MHz, $CDCl_3$) δ 155.0, 152.9, 146.8 (q, *J* = 6.5 Hz), 130.0, 127.9, 124.0, 37.6 (d, *J* = 1.8 Hz), 31.9, 24.7, 21.2.

^{19}F{^{1}H} NMR (376 MHz, $CDCl_3$) δ -59.1, -59.1.

HRMS (ESI$^+$) Calculated for $C_{12}H_{13}F_3N$ $[M+H]^+$: 228.0995 found: 228.0987.

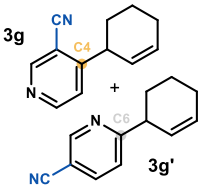

4-(cyclohex-2-en-1-yl)nicotinonitrile (3g) + 6-(cyclohex-2-en-1-yl)nicotinonitrile (3g')

Prepared according to General Procedure A using nicotinonitrile (20.8 mg, 0.2 mmol) and cyclohexene **2a** (203 µL, 2.0 mmol). The regioisomeric ratio **3g/3g'** (14:1) of the crude mixture was measured by ^{1}H NMR analysis. Purification by column chromatography (SiO_2, 1:4:95 Et_3N/EtOAc/hexanes) afforded product **3g** as a colorless oil (18.0 mg, 50% yield, > 20:1 *r.r.*). The minor regioisomer **3g'** was not isolated after column chromatography.

^{1}H NMR (400 MHz, $CDCl_3$) δ 8.81 (s, 1H), 8.69 (d, *J* = 5.3 Hz, 1H), 7.34 (d, *J* = 5.2 Hz, 1H), 6.10 – 6.05 (m, 1H), 5.63 – 5.58 (m, 1H), 3.86 – 3.80 (m, 1H), 2.20 – 2.11 (m, 3H), 1.76 – 1.67 (m, 2H), 1.58 – 1.49 (m, 1H).

^{13}C NMR (101 MHz, $CDCl_3$) δ 159.0, 153.2, 152.9, 131.6, 126.1, 123.0, 116.0, 110.1, 39.9, 30.9, 24.8, 20.7.

HRMS (APCI$^+$) Calculated for $C_{12}H_{13}N_2$ $[M+H]^+$: 185.1073 found: 185.1075.

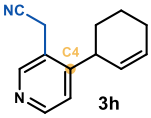

2-(4-(cyclohex-2-en-1-yl)pyridin-3-yl)acetonitrile (3h)

Prepared according to General Procedure A using 3-pyridylacetonitrile (21.3 µL, 0.2 mmol) and cyclohexene **2a** (203 µL, 2.0 mmol) prolonging the reaction time to 48 hours. No other regioisomer was detected in the crude mixture. Purification by column chromatography (SiO_2, 1:9:90 Et_3N/EtOAc/hexanes) afforded product **3h** as a colorless oil (13.0 mg, 33% yield, > 20:1 *r.r.*).

^{1}H NMR (400 MHz, $CDCl_3$) δ 8.50 (d, *J* = 2.4 Hz, 1H), 7.64 (dd, *J* = 8.1, 2.4 Hz, 1H), 7.25 (d, *J* = 8.1 Hz, 1H), 6.00 – 5.93 (m, 1H), 5.81 – 5.75 (m, 1H), 3.74 (s, 2H), 3.64 – 3.57 (m, 1H), 2.17 – 2.04 (m, 3H), 1.79 – 1.63 (m, 3H).

^{13}C NMR (101 MHz, $CDCl_3$) δ 153.6, 150.2, 150.1, 130.7, 127.5, 124.2, 123.5, 117.2, 37.8, 30.5, 24.8, 21.0, 18.8.

HRMS (ESI$^+$) Calculated for $C_{13}H_{15}N_2$ $[M+H]^+$: 199.1230 found: 199.1233.

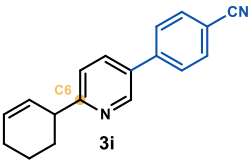

4-(6-(cyclohex-2-en-1-yl)pyridin-3-yl)benzonitrile (3i)

Prepared according to General Procedure A using 4-(pyridin-3-yl)benzonitrile **1i** (36.0 mg, 0.2 mmol) and cyclohexene **2a** (203 µL, 2.0 mmol).). No other regioisomer was detected in the crude mixture. Purification by column chromatography (SiO_2, 1:10:89 Et_3N/EtOAc/hexanes) afforded product **3i** as a white solid (16.1 mg, 31% yield, > 20:1 *r.r.*).

^{1}H NMR (400 MHz, $CDCl_3$) δ 8.81 (dd, *J* = 2.5, 0.9 Hz, 1H), 7.84 (dd, *J* = 8.1, 2.5 Hz, 1H), 7.80 – 7.76 (m, 2H), 7.72 – 7.68 (m, 2H), 7.35 (dd, *J* = 8.1, 0.8 Hz, 1H), 6.04 – 5.97 (m, 1H), 5.89 – 5.81 (m, 1H), 3.72 – 3.64 (m, 1H), 2.20 – 2.09 (m, 3H), 1.88 – 1.63 (m, 3H).

^{13}C NMR (101 MHz, $CDCl_3$) δ 165.9, 147.7, 142.5, 134.9, 132.8, 132.3, 129.4, 128.2, 127.6, 122.0, 118.7, 111.6, 43.8, 30.7, 25.0, 21.1.

HRMS (ESI$^+$) Calculated for $C_{18}H_{17}N_2$ $[M+H]^+$: 261.1386 found: 261.1398.

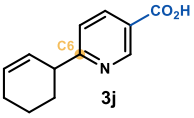

6-(cyclohex-2-en-1-yl)nicotinic acid (3j)

Prepared according to General Procedure A using nicotinic acid (24.6 mg, 0.2 mmol) and cyclohexene **2a** (203 µL, 2.0 mmol). No other regioisomer was detected in the crude mixture. The yield (65%, single regioisomer) of **3j** was inferred by ^{1}H NMR analysis of the crude reaction mixture using trichloroethylene as the internal standard. A 92% pure sample of **3j** (estimated by ^{1}H NMR integration) was obtained after purification by column chromatography (SiO_2, 1:4:95 AcOH/MeOH/CH_2Cl_2 as an off-white solid.

^{1}H NMR (400 MHz, MeOD) δ 9.10 (d, *J* = 1.4 Hz, 1H), 8.40 (dd, *J* = 8.2, 2.2 Hz, 1H), 7.51 (d, *J* = 8.2 Hz, 1H), 6.06 (dtd, *J* = 9.9, 3.7, 2.3 Hz, 1H), 5.88 – 5.79 (m, 1H), 3.73 (tq, *J* = 5.6, 2.8 Hz, 1H), 2.30 – 2.11 (m, 3H), 1.92 – 1.70 (m, 3H).

^{13}C NMR (101 MHz, MeOD) δ 169.3, 166.6, 149.6, 138.3, 129.4, 127.1, 125.0, 121.8, 43.7, 30.2, 24.5, 20.7.

HRMS (ESI^{+}) Calculated for $C_{12}H_{14}NO_2$ $[M+H]^{+}$: 204.1019 found: 204.1028.

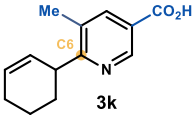

3k

6-(cyclohex-2-en-1-yl)-5-methylnicotinic acid (3k)

Prepared according to General Procedure A using 5-methylnicotinic acid (27.4 mg, 0.2 mmol) and cyclohexene **2a** (203 µL, 2.0 mmol). No other regioisomer was detected in the crude mixture. Purification by column chromatography (SiO_2, 1:49:50 AcOH/EtOAc/hexanes) afforded product **3k** as a white solid (21.0 mg, 48% yield, > 20:1 *r.r.*).

^{1}H NMR (400 MHz, MeOD) δ 8.86 (d, *J* = 2.1 Hz, 1H), 8.14 (dd, *J* = 2.1, 0.9 Hz, 1H), 5.97 – 5.90 (m, 1H), 5.70 – 5.63 (m, 1H), 3.95 – 3.88 (m, 1H), 2.45 (s, 3H), 2.17 (ddd, *J* = 12.7, 6.1, 3.0 Hz, 2H), 2.07 – 1.99 (m, 1H), 1.90 (ddd, *J* = 11.9, 5.4, 2.9 Hz, 1H), 1.80 – 1.62 (m, 2H).

^{13}C NMR (101 MHz, MeOD) δ 168.4, 148.4, 140.9, 133.0, 129.7, 129.1, 41.8, 30.0, 25.8, 22.9, 18.6.

HRMS (ESI^{-}) Calculated for $C_{13}H_{14}NO_2$ $[M-H]^{+}$: 216.1030 found: 216.1027.

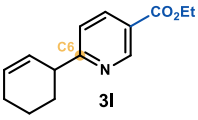

3l

ethyl 6-(cyclohex-2-en-1-yl)nicotinate (3l)

Prepared according to General Procedure A using ethyl nicotinate (27.3 µL, 0.2 mmol) and cyclohexene **2a** (203 µL, 2.0 mmol). No other regioisomer was detected in the crude mixture. Purification by column chromatography (SiO_2, 1:5:94 Et_3N/EtOAc/hexanes) afforded product **3l** as a yellowish oil (30.4 mg, 66% yield, > 20:1 *r.r.*).

^{1}H NMR (400 MHz, $CDCl_3$) δ 9.13 (dd, *J* = 2.2, 0.9 Hz, 1H), 8.19 (dd, *J* = 8.2, 2.2 Hz, 1H), 7.26 (dd, *J* = 8.2, 0.9 Hz, 1H), 5.95 (dtd, *J* = 9.8, 3.7, 2.2 Hz, 1H), 5.80 – 5.75 (m, 1H), 4.38 (q, *J* = 7.1 Hz, 2H), 3.67 – 3.61 (m, 1H), 2.17 – 2.02 (m, 3H), 1.79 – 1.60 (m, 3H), 1.38 (t, *J* = 7.1 Hz, 3H).

^{13}C NMR (101 MHz, $CDCl_3$) δ 169.9, 165.4, 150.6, 137.4, 129.5, 127.8, 123.9, 121.3, 61.1, 44.1, 30.5, 24.8, 21.0, 14.2.

HRMS: (ESI^{+}) calculated for $C_{14}H_{18}NO_2$ $[M+H^{+}]$: 232.1332, found 235.1326.

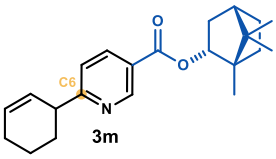

3m

1,7,7-trimethylbicyclo[2.2.1]heptan-2-yl 6-(cyclohex-2-en-1-yl)nicotinate (3m)

Prepared according to General Procedure A using 1,7,7-trimethylbicyclo[2.2.1]heptan-2-yl nicotinate **1m** (52.0 mg, 0.2 mmol) and cyclohexene **2a** (203 µL, 2.0 mmol). No other regioisomer was detected in the crude mixture. Purification by column chromatography (SiO_2, 2:98 EtOAc/hexanes) afforded product **3m** as a colorless oil (49.0 mg, 72% yield, > 20:1 *r.r.*).

^{1}H NMR (500 MHz, $CDCl_3$) δ 9.19 (dd, *J* = 2.2, 0.8 Hz, 1H), 8.22 (dd, *J* = 8.2, 2.2 Hz, 1H), 7.29 (dd, *J* = 8.2, 0.9 Hz, 1H), 5.99 – 5.95 (m, 1H), 5.80 – 5.77 (m, 1H), 5.13 – 5.10 (m, 1H), 3.68 – 3.65 (m, 1H), 2.47 (dddd, *J* = 13.5, 9.9, 4.7, 3.3 Hz, 1H), 2.15 – 2.04 (m, 4H), 1.84 – 1.63 (m, 5H), 1.44 – 1.36 (m, 1H), 1.32 – 1.24 (m, 1H), 1.10 (ddd, *J* = 13.8, 3.5, 1.3 Hz, 1H), 0.96 (s, 3H), 0.90 (d, *J* = 4.8 Hz, 6H).

^{13}C NMR (126 MHz, $CDCl_3$) δ 170.0, 165.8, 150.8, 137.6, 129.6, 128.0, 124.5, 121.6, 81.0, 49.3, 48.0, 45.1, 44.3, 37.0, 30.7, 28.2, 27.5, 25.0, 21.2, 19.8, 19.0, 13.7.

HRMS: (ESI$^+$) calculated for $C_{22}H_{30}NO_2$ [M+H$^+$]: 340.2271, found 340.2274.

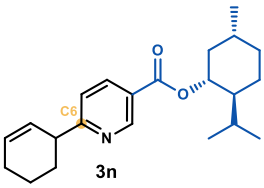

3n

(1R,2S,5R)-2-isopropyl-5-methylcyclohexyl 6-(cyclohex-2-en-1-yl)nicotinate (3n)

Prepared according to General Procedure A using (1R,2S,5R)-2-isopropyl-5-methylcyclohexyl nicotinate **1n** (52.3 mg, 0.2 mmol) and cyclohexene **2a** (203 µL, 2.0 mmol). No other regioisomer was detected in the crude mixture. Purification by column chromatography (SiO_2, 1:99 EtOAc/hexanes) afforded product **3n** as a colorless oil (34.0 mg, 50% yield, > 20:1 *r.r.*).

^{1}H NMR (400 MHz, $CDCl_3$) δ 9.14 (dd, *J* = 2.2, 0.9 Hz, 1H), 8.20 (dd, *J* = 8.2, 2.2 Hz, 1H), 7.28 (d, *J* = 0.8 Hz, 1H), 5.99 – 5.94 (m, 1H), 5.80 – 5.75 (m, 1H), 4.93 (td, *J* = 10.9, 4.4 Hz, 1H), 3.68 – 3.62 (m, 1H), 2.14 – 2.06 (m, 4H), 1.96 – 1.88 (m, 1H), 1.80 – 1.65 (m, 6H), 1.58 – 1.51 (m, 2H), 1.17 – 1.05 (m, 2H), 0.91 (dd, *J* = 8.7, 6.8 Hz, 6H), 0.78 (d, *J* = 6.9 Hz, 3H).

^{13}C NMR (101 MHz, $CDCl_3$) δ 170.0, 165.1, 150.7, 137.6 (d1,d2), 129.6 (d1,d2), 128.0, 124.4, 121.6 (d1,d2), 75.4, 47.4, 44.3, 41.1, 34.4, 31.6, 30.7 (d1,d2), 26.7 (d1,d2), 25.0, 23.8(d1,d2), 22.1, 21.2(d1,d2), 20.9, 16.7(d1,d2).

HRMS: (ESI$^+$) calculated for $C_{22}H_{32}NO_2$ [M+H$^+$]: 342.2428, found 342.2439.

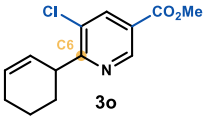

3o

Methyl 5-chloro-6-(cyclohex-2-en-1-yl)nicotinate (3o)

Prepared according to General Procedure A using methyl 5-chloronicotinate (34.3 mg, 0.2 mmol) and cyclohexene **2a** (203 µL, 2.0 mmol). No other regioisomer was detected in the crude mixture. Purification by column

chromatography (SiO_2, 1:2:97 Et_3N/EtOAc/hexanes) afforded product **3o** as a colorless oil (23.0 mg, 46% yield, > 20:1 *r.r.*).

^{1}H NMR (400 MHz, $CDCl_3$) δ 9.05 (d, *J* = 1.9 Hz, 1H), 8.23 (d, *J* = 1.9 Hz, 1H), 6.03 – 5.96 (m, 1H), 5.77 – 5.70 (m, 1H), 4.17 – 4.09 (m, 1H), 3.94 (s, 3H), 2.24 – 2.05 (m, 3H), 1.93 – 1.85 (m, 1H), 1.77 – 1.64 (m, 2H).

^{13}C NMR (101 MHz, $CDCl_3$) δ 166.5, 165.0, 148.6, 137.9, 130.9, 129.2, 127.5, 125.1, 52.7, 40.6, 28.6, 24.8, 21.8.

HRMS (ESI$^+$) Calculated for $C_{13}H_{15}ClNO_2$ $[M+H]^+$: 252.0786 found: 252.0785.

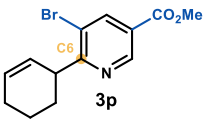

3p

Methyl 5-bromo-6-(cyclohex-2-en-1-yl)nicotinate (3p)

Prepared according to General Procedure A using methyl 5-bromonicotinate (43.2 mg, 0.2 mmol) and cyclohexene **2a** (203 µL, 2.0 mmol) prolonging the reaction time to 24 hours. No other regioisomer was detected in the crude mixture. Purification by column chromatography (SiO_2, 1:2:97 Et_3N/EtOAc/hexanes) afforded product **3p** as a colorless oil (18.5 mg, 31% yield, > 20:1 *r.r.*).

^{1}H NMR (400 MHz, $CDCl_3$) δ 9.09 (d, *J* = 1.9 Hz, 1H), 8.41 (d, *J* = 1.9 Hz, 1H), 6.03 – 5.95 (m, 1H), 5.77 – 5.71 (m, 1H), 4.18 – 4.10 (m, 1H), 3.94 (s, 3H), 2.24 – 2.09 (m, 3H), 1.93 – 1.87 (m, 1H), 1.75 – 1.60 (m, 2H).

^{13}C NMR (101 MHz, $CDCl_3$) δ 167.6, 164.8, 149.2, 141.3, 129.1, 127.7, 125.2, 120.9, 52., 42.7, 28.8, 24.8, 21.8.

HRMS (ESI$^+$) Calculated for C13H15BrNO2 $[M+H]^+$: 296.0281 found: 296.0283.

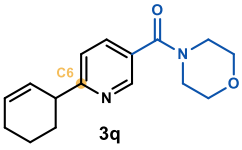

3q

(6-(cyclohex-2-en-1-yl)pyridin-3-yl)(morpholino)methanone (3q)

Prepared according to General Procedure A using morpholino(pyridin-3-yl)methanone **1q** (38.4 mg, 0.2 mmol) and cyclohexene **2a** (203 µL, 2.0 mmol). No other regioisomer was detected in the crude mixture. Purification by column chromatography (SiO_2, 1:99 Et_3N/EtOAc) afforded product **3q** as a colorless oil (21.6 mg, 40% yield, > 20:1 *r.r.*).

^{1}H NMR (500 MHz, $CDCl_3$) δ 8.62 (d, *J* = 2.4 Hz, 1H), 7.71 (dd, *J* = 8.0, 2.3 Hz, 1H), 7.29 (d, *J* = 8.0, 1H), 6.03 – 5.94 (m, 1H), 5.82 – 5.76 (m, 1H), 3.95 – 3.40 (m, 9H), 2.17 – 2.05 (m, 3H), 1.82 – 1.74 (m, 1H), 1.73 – 1.64 (m, 2H).

^{13}C NMR (126 MHz, $CDCl_3$) δ 168.2, 167.3, 147.6, 135.7, 129.5, 128.6, 128.0, 121.8, 66.8, 44.0, 30.6, 24.9, 21.0.

HRMS (ESI$^+$) Calculated for $C_{16}H_{21}N_2O_2$ $[M+H]^+$: 273.1598 found: 273.1595.

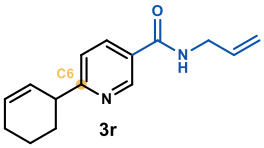

3r

N-allyl-6-(cyclohex-2-en-1-yl)nicotinamide (3r)

Prepared according to General Procedure A using *N*-allylnicotinamide **1r** (32.4 mg, 0.2 mmol) and cyclohexene **2a** (203 μL, 2.0 mmol). No other regioisomer was detected in the crude mixture. Purification by column chromatography (SiO_2, 1:9:90 Et_3N/EtOAc/hexanes to 1:24:75 Et_3N/EtOAc/hexanes) afforded product **3r** as a colorless oil (16.0 mg, 33% yield, > 20:1 *r.r.*).

^{1}H NMR (400 MHz, $CDCl_3$) δ 8.90 (dd, *J* = 2.4, 0.9 Hz, 1H), 8.05 (dd, *J* = 8.1, 2.4 Hz, 1H), 7.28 (dd, *J* = 8.1, 0.9 Hz, 1H), 6.24 (s, 1H), 5.99 – 5.88 (m, 2H), 5.80 – 5.74 (m, 1H), 5.27 (dq, *J* = 17.1, 1.6 Hz, 1H), 5.20 (dq, *J* = 10.2, 1.4 Hz, 1H), 4.10 (tt, *J* = 5.8, 1.6 Hz, 2H), 3.68 – 3.60 (m, 1H), 2.15 – 2.05 (m, 3H), 1.79 – 1.63 (m, 3H).

^{13}C NMR (101 MHz, $CDCl_3$) δ 169.0, 165.8, 147.5, 135.7, 134.0, 129.7, 128.1, 127.9, 121.9, 117.1, 44.2, 42.6, 30.7, 25.1, 21.2.

HRMS (ESI$^+$) Calculated for $C_{15}H_{19}N_2O$ $[M+H]^+$: 243.1492 found: 243.1501.

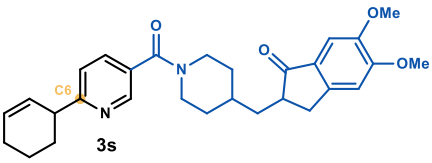

3s

2-((1-(6-(cyclohex-2-en-1-yl)nicotinoyl)piperidin-4-yl)methyl)-5,6-dimethoxy-2,3-dihydro-1H-inden-1-one (3s)

Prepared according to General Procedure A using donepezil nicotinate **1s** (78.9 mg, 0.2 mmol) and cyclohexene **2a** (203 μL, 2.0 mmol). No other regioisomer was detected in the crude mixture. Purification by column chromatography (SiO_2, 1:1:98 Et_3N/MeOH/CH_2Cl_2) afforded product **3s** (48.6 mg, 51% yield, > 20:1 *r.r.*) as a colorless oil.

^{1}H NMR (400 MHz, $CDCl_3$) δ 8.62 (dd, *J* = 2.3, 0.9 Hz, 1H), 7.71 (dd, *J* = 8.0, 2.3 Hz, 1H), 7.28 (d, *J* = 8.1 Hz, 1H), 7.18 (s, 1H), 6.88 (s, 1H), 6.02 – 5.95 (m, 1H), 5.86 – 5.76 (m, 1H), 4.74 (br s, 1H), 3.98 (s, 3H), 3.92 (s, 3H), 3.88 – 3.73 (m, 1H), 3.70 – 3.59 (m, 1H), 3.29 (dd, *J* = 17.4, 8.0 Hz, 1H), 3.10 (br s, 1H), 2.85 (br s, 1H), 2.77 – 2.68 (m, 2H), 2.17 – 2.06 (m, 3H), 2.02 – 1.82 (m, 3H), 1.82 – 1.64 (m, 2H), 1.48 – 1.37 (m, 2H).

^{13}C NMR (101 MHz, $CDCl_3$) δ 207.2, 168.0, 166.8, 155.6, 149.6, 148.6, 147.4, 135.5, 129.5, 129.4, 129.2, 128.1, 121.7, 107.3, 104.4, 56.3, 56.1, 44.0, 30.6, 24.9, 21.1.

HRMS: (ESI$^+$) calculated for $C_{29}H_{34}N_2NaO_4$ $[M+Na^+]$: 497.2411, found 497.2415.

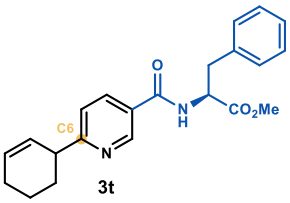

3t

Methyl (6-(cyclohex-2-en-1-yl)nicotinoyl)-L-phenylalaninate (3t)

Prepared according to General Procedure A using methyl nicotinoyl-L-phenylalaninate **1t** (26.0 mg, 0.2 mmol) and cyclohexene **2a** (203 µL, 2.0 mmol). No other regioisomer was detected in the crude mixture. Purification by column chromatography (SiO_2, 1:9:90 Et_3N/EtOAc/hexanes to 1:19:80 Et_3N/EtOAc/hexanes) afforded product **3t** as a white solid (30.0 mg, 41% yield, 1:1 *d.r.*, > 20:1 *r.r.*). The diastereomeric ratio was determined by UPC^2 analysis on a Daicel Chiralpak ID-3 column (gradient: 1 min 100% CO_2; 5 min from 100% CO_2 to 60% CO_2 - 40% MeOH; flow rate 2.0 mL/min; λ = 268 nm: τ_1 = 5.6 min, τ_2 = 5.9 min).

^{1}H NMR (400 MHz, $CDCl_3$) δ 8.83 (dt, *J* = 2.2, 1.0 Hz, 1H), 7.95 (dd, *J* = 8.2, 2.4 Hz, 1H), 7.31 – 7.22 (m, 4H), 7.13 – 7.11 (m, 2H), 6.57 (d, *J* = 7.6 Hz, 1H), 5.99 – 5.94 (m, 1H), 5.79 – 5.74 (m, 1H), 5.07 (dt, *J* = 7.6, 5.6 Hz, 1H), 3.77 (s, 3H), 3.65 – 3.60 (m, 1H), 3.24 (qd, *J* = 13.9, 5.6 Hz, 2H), 2.13 – 2.04 (m, 3H), 1.77 – 1.63 (m, 3H).

^{13}C NMR (101 MHz, $CDCl_3$) δ 172.0, 169.2, 165.4, 147.8, 147.8, 135.7, 135.6, 129.6, 129.4, 128.9, 128.0, 127.5, 127.3, 121.8, 53.6, 52.6, 44.2, 37.9, 30.7, 25.0, 21.1.

HRMS: (ESI$^+$) calculated for $C_{22}H_{25}N_2O_3$ [M+H$^+$]: 365.1860, found 365.1864.

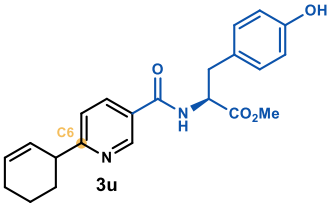

3u

Methyl (6-(cyclohex-2-en-1-yl)nicotinoyl)-L-tyrosinate (3u)

Prepared according to General Procedure A using methyl nicotinoyl-L-tyrosinate **1u** (60.0 mg, 0.2 mmol) and cyclohexene **2a** (203 µL, 2.0 mmol). No other regioisomer was detected in the crude mixture. Purification by column chromatography (SiO_2, 1:29:70 Et_3N/acetone/hexanes) afforded product **3u** as a white solid (31.8 mg, 42% yield, 1:1 d.r., > 20:1 *r.r.*). The diastereomeric ratio was determined by UPC^2 analysis on a Daicel Chiralpak ID-3 column (gradient: 1 min 100% CO_2; 5 min from 100% CO_2 to 60% CO_2 - 40% MeOH; flow rate 2.0 mL/min; λ = 268 nm: τ_1 = 10.8 min, τ_2 = 11.3 min).

^{1}H NMR (400 MHz, $CDCl_3$) δ 8.80 (d, *J* = 1.5 Hz, 1H), 8.03 (ddd, *J* = 8.1, 2.4, 1.5 Hz, 1H), 7.29 (d, *J* = 8.1 Hz, 1H), 6.98 – 6.94 (m, 2H), 6.76 – 6.71 (m, 2H), 6.65 (d, *J* = 7.8 Hz, 1H), 5.98 – 5.93 (m, 1H), 5.78 – 5.70 (m, 1H), 5.04 (dt, *J* = 7.7, 5.6 Hz, 1H), 3.78 (s, 3H), 3.69 – 3.60 (m, 1H), 3.16 (qd, *J* = 14.1, 5.7 Hz, 2H), 2.13 – 2.04 (m, 3H), 1.77 – 1.62 (m, 3H).

^{13}C NMR (101 MHz, $CDCl_3$) δ 172.2, 169.2, 165.4, 156.0, 147.3, 136.2, 130.5, 129.9, 127.7, 127.6, 126.9, 122.1, 115.9, 53.8, 52.7, 44.0, 37.1, 30.7, 25.0, 21.1.

HRMS: (ESI$^+$) calculated for $C_{22}H_{24}N_2NaO_4$ [M+Na$^+$]: 403.1628, found 403.1627.

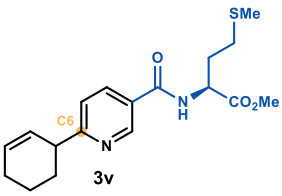

3v

Methyl (6-(cyclohex-2-en-1-yl)nicotinoyl)-L-methioninate (3v)

Prepared according to General Procedure A using methyl nicotinoyl-L-methioninate **1v** (53.7 mg, 0.2 mmol) and cyclohexene **2a** (203 µL, 2.0 mmol). No other regioisomer was detected in the crude mixture. Purification by column chromatography (SiO_2, 1:9:90 Et_3N/EtOAc/hexanes to 1:23:76 Et_3N/EtOAc/hexanes) afforded product **3v** as a white solid (31.0 mg, 44% yield, 1:1 *d.r.*, > 20:1 *r.r.*). The diastereomeric ratio was determined by UPC^2 analysis on a Daicel Chiralpak ID-3 column (gradient: 1 min 100% CO_2; 5 min from 100% CO_2 to 60% CO_2 - 40% EtOH; flow rate 2.0 mL/min; λ = 268 nm: τ_1 = 11.7 min, τ_2 = 12.0 min).

^{1}H NMR (400 MHz, $CDCl_3$) δ 8.96 (d, *J* = 2.4 Hz, 1H), 8.04 (dd, *J* = 8.1, 2.4 Hz, 1H), 7.27 (d, *J* = 8.2 Hz, 1H), 7.14 (d, *J* = 7.6 Hz, 1H), 5.98 – 5.93 (m, 1H), 5.78 – 5.74 (m, 1H), 4.91 (td, *J* = 7.3, 5.0 Hz, 1H), 3.78 (s, 3H), 3.65 – 3.60 (m, 1H), 2.58 (t, *J* = 7.2 Hz, 2H), 2.31 – 2.22 (m, 1H), 2.17-2.04 (m, 4H), 2.10 (s, 3H), 1.77 – 1.63 (m, 3H).

^{13}C NMR (101 MHz, $CDCl_3$) δ 172.5, 169.2, 165.6, 148.0, 135.7, 129.6, 128.0, 127.1, 121.8, 52.8, 52.3, 44.1, 31.3, 30.7, 30.3, 25.0, 21.1, 15.7.

HRMS: (ESI$^+$) calculated for $C_{18}H_{23}N_2O_3S$ [M+H$^+$]: 347.1435, found 347.1439.

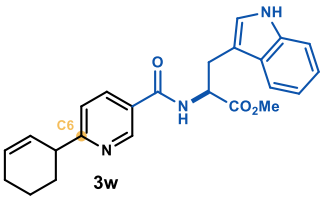

3w

Methyl (6-(cyclohex-2-en-1-yl)nicotinoyl)-L-tryptophanate (3w)

Prepared according to General Procedure A using methyl nicotinoyl-L-tryptophanate **1w** (64.7 mg, 0.2 mmol) and cyclohexene **2a** (203 µL, 2.0 mmol). No other regioisomer was detected in the crude mixture. Purification by column chromatography (SiO_2, 1:19:80 Et_3N/EtOAc/hexanes to 1:59:40 Et_3N/EtOAc/hexanes) afforded product **3w** as a white solid (32.5 mg, 40% yield, 1:1 *d.r.*, > 20:1 *r.r.*). The diastereomeric ratio was determined by UPC^2 analysis on a Daicel Chiralpak IA-3 column (gradient: 1 min 100% CO_2; 5 min from 100% CO_2 to 60% CO_2 - 40% EtOH; flow rate 2.0 mL/min; λ = 268 nm: τ_1 = 6.9 min, τ_2 = 7.2 min).

^{1}H NMR (400 MHz, $CDCl_3$) δ 8.81 (ddd, *J* = 3.3, 2.3, 0.8 Hz, 1H), 8.40 (br s, 1H), 7.90 (dt, *J* = 8.2, 1.9 Hz, 1H), 7.53 (d, *J* = 7.9 Hz, 1H), 7.33 (d, *J* = 8.1 Hz, 1H), 7.20 (d, *J* = 8.2 Hz, 1H), 7.19 – 7.15 (m, 1H), 7.08 (ddd, *J* = 8.0, 7.0, 1.0 Hz, 1H), 6.99 (d, *J* = 2.4 Hz, 1H), 6.69 (d, *J* = 7.7 Hz, 1H), 5.98 – 5.93 (m, 1H), 5.78 – 5.73 (m, 1H), 5.12 (dt, *J* = 7.6, 5.3 Hz, 1H), 3.72 (s, 3H), 3.64 – 3.59 (m, 1H), 3.45 – 3.43 (m, 2H), 2.12 – 2.03 (m, 3H), 1.77 – 1.61 (m, 3H).

^{13}C NMR (101 MHz, $CDCl_3$) δ 172.4, 169.1, 165.5, 147.9, 147.9, 136.3, 135.7, 135.7, 129.7, 129.6, 128.0, 127.7, 127.3, 123.0, 122.5, 121.7, 119.9, 118.6, 111.5, 109.9, 53.5, 52.7, 44.1, 30.7, 30.7, 27.7, 25.0, 21.1.

HRMS: (ESI$^+$) calculated for $C_{24}H_{26}N_3O_3$ [M+H$^+$]: 404.1969, found 404.1979.

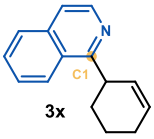

1-(cyclohex-2-en-1-yl)isoquinoline (3x)

Prepared according to General Procedure A using isoquinoline (23.5 µL, 0.2 mmol) and cyclohexene **2a** (203 µL, 2.0 mmol). No other regioisomer was detected in the crude mixture. Purification by column chromatography (SiO_2, 1:99 Et_3N/hexanes to 1:5:94 Et_3N/EtOAc/hexanes) afforded product **3x** as a colorless oil (16.6 mg, 40% yield, > 20:1 *r.r.*).

^{1}H NMR (500 MHz, $CDCl_3$) δ 8.51 (d, *J* = 5.7 Hz, 1H), 8.25 (d, *J* = 8.5 Hz, 1H), 7.82 (dt, *J* = 8.2, 1.0 Hz, 1H), 7.66 (ddd, *J* = 8.2, 6.9, 1.2 Hz, 1H), 7.58 (ddd, *J* = 8.3, 6.9, 1.4 Hz, 1H), 7.50 (dd, *J* = 5.7, 1.0 Hz, 1H), 6.04 – 5.99 (m, 1H), 5.95 (dtdd, *J* = 10.1, 2.5, 1.6, 1.1 Hz, 1H), 4.48 – 4.43 (m, 1H), 2.31 – 2.11 (m, 3H), 1.96 – 1.75 (m, 3H).

^{13}C NMR (126 MHz, $CDCl_3$) δ 164.6, 142.1, 136.5, 129.6, 129.1, 128.2, 127.6, 126.9, 126.5, 125.0, 119.2, 40.3, 30.2, 24.9, 22.1.

HRMS: (ESI$^+$) calculated for $C_{15}H_{16}N$ [M+H$^+$]: 210.1277, found 210.1271.

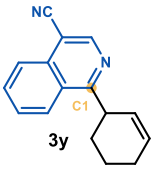

1-(cyclohex-2-en-1-yl)isoquinoline-4-carbonitrile (3y)

Prepared according to General Procedure A using isoquinoline-4-carbonitrile (30.8 mg, 0.2 mmol) and cyclohexene **2a** (203 µL, 2.0 mmol). No other regioisomer was detected in the crude mixture. Purification by column chromatography (SiO_2, 10:90 EtOAc/hexanes) afforded product **3y** as a white solid (14.6 mg, 31% yield, > 20:1 *r.r.*).

^{1}H NMR (400 MHz, $CDCl_3$) δ 8.87 (s, 1H), 8.35 (ddt, *J* = 8.5, 1.3, 0.7 Hz, 1H), 8.20 (ddd, *J* = 8.4, 1.3, 0.7 Hz, 1H), 7.89 (ddd, *J* = 8.3, 7.0, 1.3 Hz, 1H), 7.75 (dddd, *J* = 8.6, 7.0, 1.3, 0.3 Hz, 1H), 6.08 – 6.03 (m, 1H), 5.88 (dtdd, *J* = 10.1, 2.4, 1.8, 1.1 Hz, 1H), 4.54 – 4.46 (m, 1H), 2.30 – 2.12 (m, 3H), 1.97 – 1.74 (m, 3H).

^{13}C NMR (101 MHz, $CDCl_3$) δ 169.9, 147.7, 135.0, 132.2, 129.0, 128.8, 127.8, 125.7, 125.6, 125.1, 116.4, 104.3, 40.7, 30.2, 24.8, 21.8.

HRMS: (ESI$^+$) calculated for $C_{16}H_{15}N_2$ [M+H$^+$]: 235.1230, found 235.1234.

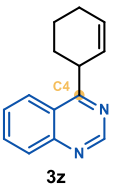

4-(cyclohex-2-en-1-yl)quinazoline (3z)

Prepared according to General Procedure A using quinazoline (26.0 mg, 0.2 mmol) and cyclohexene **2a** (203 µL, 2.0 mmol). No other regioisomer was detected in the crude mixture. Purification by column chromatography (SiO_2, 1:10:89 Et_3N/EtOAc/hexanes) afforded product **3z** (8.3 mg, 20% yield, > 20:1 *r.r.*) as a colorless oil.

^{1}H NMR (400 MHz, $CDCl_3$) δ 9.28 (s, 1H), 8.22 (d, *J* = 8.4 Hz, 1H), 8.06 (d, *J* = 8.5 Hz, 1H), 7.88 (ddd, *J* = 8.4, 6.9, 1.4 Hz, 1H), 7.64 (ddd, *J* = 8.3, 6.9, 1.3 Hz, 1H), 6.11 – 6.02 (m, 1H), 5.93 – 5.84 (m, 1H), 4.44 (ddp, *J* = 8.4, 5.6, 2.7 Hz, 1H), 2.31 – 2.11 (m, 3H), 2.02 – 1.71 (m, 3H).

^{13}C NMR (101 MHz, $CDCl_3$) δ 174.1, 154.9, 150.2, 133.4, 129.4, 129.3, 127.5, 127.4, 124.4, 123.5, 40.0, 29.9, 24.8, 21.8.

HRMS (ESI$^+$) Calculated for $C_{14}H_{15}N_2$ $[M+H]^+$: 211.1230 found: 211.1236.

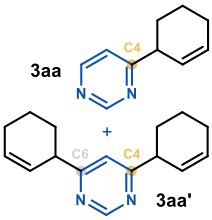

4-(cyclohex-2-en-1-yl)pyrimidine (3aa) + 4,6-di(cyclohex-2-en-1-yl)pyrimidine (3aa')

Prepared according to General Procedure B using pyrimidine (15.6 µL, 0.2 mmol) and cyclohexene **2a** (203 µL, 2.0 mmol). Purification by column chromatography (SiO_2, 1:5:94 Et_3N/EtOAc/hexanes) afforded product **3aa** (8.8 mg, 27% yield, > 20:1 *r.r.*) as a colorless oil.

^{1}H NMR (500 MHz, $CDCl_3$) δ 9.16 (d, *J* = 1.4 Hz, 1H), 8.65 (d, *J* = 5.2 Hz, 1H), 7.25 (dd, *J* = 5.2, 1.4 Hz, 1H), 6.08 – 5.97 (m, 1H), 5.86 – 5.75 (m, 1H), 3.59 – 3.52 (m, 1H), 2.21 – 2.07 (m, 3H), 1.81 – 1.65 (m, 3H).

^{13}C NMR (126 MHz, $CDCl_3$) δ 173.7, 158.8, 156.9, 130.2, 126.7, 119.5, 43.5, 29.9, 24.8, 20.8.

HRMS (ESI$^+$) Calculated for $C_{10}H_{13}N_2$ $[M+H]^+$: 161.1073 found: 161.1076.

Product **3aa'** (3.8 mg, 8% yield, > 20:1 *r.r.*) was also isolated as a colorless oil.

^{1}H NMR (500 MHz, $CDCl_3$) δ 9.09 (d, *J* = 1.3 Hz, 1H), 7.12 (d, *J* = 1.3 Hz, 1H), 6.07 – 5.99 (m, 2H), 5.82 – 5.74 (m, 2H), 3.59 – 3.47 (m, 2H), 2.22 – 2.04 (m, 6H), 1.86 – 1.63 (m, 6H).

^{13}C NMR (126 MHz, $CDCl_3$) δ 173.7, 158.5, 130.0, 127.1, 117.2, 43.5, 30.0, 24.9, 21.0.

HRMS (ESI$^+$) Calculated for $C_{16}H_{21}N_2$ $[M+H]^+$: 241.1699 found: 241.1699.

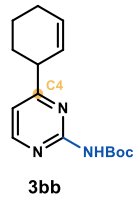

3bb

tert-butyl (4-(cyclohex-2-en-1-yl)pyrimidin-2-yl)carbamate (3bb)

Prepared according to General Procedure A using tert-butyl pyrimidin-2-ylcarbamate **1bb** (39.0 mg, 0.2 mmol) and cyclohexene **2a** (203 µL, 2.0 mmol). No other regioisomer was detected in the crude mixture. Purification by column chromatography (SiO_2, 1:10:89 Et_3N/EtOAc/hexanes) afforded product **3bb** (17.9 mg, 27% yield, > 20:1 *r.r.*) as a colorless oil.

^{1}H NMR (400 MHz, $CDCl_3$) δ 8.53 (d, *J* = 5.1 Hz, 1H), 7.54 (brs, 1H), 6.88 (d, *J* = 5.1 Hz, 1H), 6.04 – 5.93 (m, 1H), 5.80 – 5.72 (m, 1H), 3.54 – 3.40 (m, 1H), 2.17 – 2.04 (m, 3H), 1.82 – 1.63 (m, 3H), 1.55 (s, 9H).

^{13}C NMR (101 MHz, $CDCl_3$) δ 175.4, 158.2, 157.6, 150.6, 129.9, 126.9, 113.8, 81.2, 43.3, 29.6, 28.2, 24.8, 20.9.

HRMS (ESI$^+$) Calculated for $C_{15}H_{21}N_3NaO_2$ $[M+Na]^+$: 298.1526 found: 298.1522.

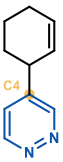

3cc

4-(cyclohex-2-en-1-yl)pyridazine (3cc)

Prepared according to General Procedure A using pyridazine (14.5 µL, 0.2 mmol) and cyclohexene **2a** (203 µL, 2.0 mmol). No other regioisomer was detected in the crude mixture. Purification by column chromatography (SiO_2, 1:40:59 Et_3N/EtOAc/hexanes) afforded product **3cc** (10.0 mg, 31% yield, > 20:1 *r.r.*) as a brown oil.

^{1}H NMR (400 MHz, $CDCl_3$) δ 9.10 (s, 1H), 9.08 (d, *J* = 5.5 Hz, 1H), 7.33 (dd, *J* = 5.3, 2.4 Hz, 1H), 6.05 (dq, *J* = 9.8, 3.4 Hz, 1H), 5.70 – 5.61 (m, 1H), 3.45 (m, 1H), 2.17 – 2.11 (m, 2H), 2.10 – 2.04 (m, 1H), 1.77 – 1.62 (m, 2H), 1.61 – 1.52 (m, 1H).

^{13}C NMR (101 MHz, $CDCl_3$) δ 152.3, 151.1, 145.6, 131.1, 126.3, 125.2, 38.8, 31.3, 24.7, 20.4.

HRMS (ESI$^+$) Calculated for $C_{10}H_{13}N_2$ $[M+H]^+$: 161.1073 found: 161.1073.

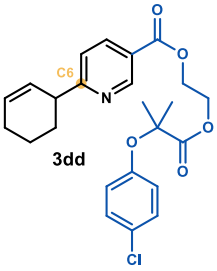

3dd

2-((2-(4-chlorophenoxy)-2-methylpropanoyl)oxy)ethyl 6-(cyclohex-2-en-1-yl)nicotinate (3dd)

Prepared according to General Procedure A using Etofibrate **1dd** (72.8 mg, 0.2 mmol) and cyclohexene **2a** (203 µL, 2.0 mmol). No other regioisomer was detected in the crude mixture. Purification by column chromatography (SiO_2, 1:10:89 Et_3N/EtOAc/hexanes) afforded product **3dd** as a colorless oil (47.8 mg, 54% yield, > 20:1 *r.r.*).

^{1}H NMR (400 MHz, $CDCl_3$) δ 9.10 (dd, *J* = 2.3, 0.9 Hz, 1H), 8.07 (dd, *J* = 8.2, 2.2 Hz, 1H), 7.28 (dd, *J* = 8.2, 0.9 Hz, 1H), 7.13 – 7.08 (m, 2H), 6.79 – 6.74 (m, 2H), 6.05 – 5.97 (m, 1H),

5.85 – 5.77 (m, 1H), 4.58 – 4.49 (m, 4H), 3.73 – 3.63 (m, 1H), 2.22 – 2.03 (m, 3H), 1.86 – 1.65 (m, 3H), 1.60 (s, 6H).

^{13}C NMR (101 MHz, $CDCl_3$) δ 173.9, 170.5, 165.1, 153.9, 150.7, 137.4, 129.6, 129.1, 127.8, 127.2, 123.1, 121.5, 120.2, 79.4, 63.0, 62.5, 44.2, 30.5, 25.3, 24.9, 21.0.

HRMS (ESI$^+$) Calculated for $C_{24}H_{27}ClNO_5$ $[M+H]^+$: 444.1572 found: 444.1565.

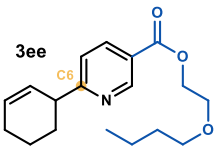

2-butoxyethyl 6-(cyclohex-2-en-1-yl)nicotinate (3ee)

Prepared according to General Procedure A using Nicoboxil **1ee** (44.7 mg, 0.2 mmol) and cyclohexene **2a** (203 µL, 2.0 mmol). No other regioisomer was detected in the crude mixture. Purification by column chromatography (SiO_2, 1:2:97 Et_3N/EtOAc/hexanes) afforded product **3ee** as a light-yellow oil (32.3 mg, 53% yield, > 20:1 *r.r.*).

^{1}H NMR (500 MHz, $CDCl_3$) δ 9.19 (d, *J* = 2.2 Hz, 1H), 8.25 (dd, *J* = 8.1, 2.2 Hz, 1H), 7.30 (d, *J* = 8.2 Hz, 1H), 6.05 – 5.96 (m, 1H), 5.88 – 5.79 (m, 1H), 4.53 – 4.45 (m, 2H), 3.81 – 3.75 (m, 2H), 3.72 – 3.65 (m, 1H), 3.53 (t, *J* = 6.6 Hz, 2H), 2.22 – 2.06 (m, 3H), 1.83 – 1.64 (m, 3H), 1.64 – 1.55 (m, 2H), 1.45 – 1.35 (m, 2H), 0.93 (t, *J* = 7.4 Hz, 3H).

^{13}C NMR (126 MHz, $CDCl_3$) δ 170.1, 165.5, 150.8, 137.6, 129.6, 127.9, 123.7, 121.4, 71.3, 68.5, 64.4, 44.2, 31.7, 30.6, 24.9, 21.0, 19.3, 13.9.

HRMS (ESI$^+$) Calculated for $C_{18}H_{26}NO_3$ $[M+H]^+$: 304.1907 found: 304.1904.

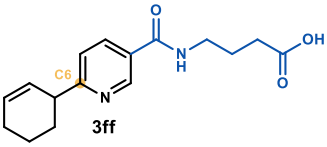

4-(6-(cyclohex-2-en-1-yl)nicotinamido)butanoic acid (3ff)

Prepared according to General Procedure A using Picamilon (41.6 mg, 0.2 mmol) and cyclohexene **2a** (203 µL, 2.0 mmol). No other regioisomer was detected in the crude mixture. Purification by column chromatography (SiO_2, 1:40:59 AcOH/EtOAc/hexanes to 1:99 AcOH/EtOAc) afforded product **3ff** as a white solid (43.4 mg, 75% yield, > 20:1 *r.r.*).

^{1}H NMR (400 MHz, Acetone) δ 9.05 (d, *J* = 2.7 Hz, 1H), 8.39 (s, 1H), 8.27 (dd, *J* = 8.2, 2.4 Hz, 1H), 7.37 (d, *J* = 8.2 Hz, 1H), 5.95 – 5.89 (m, 1H), 5.82 – 5.75 (m, 1H), 3.71 – 3.61 (m, 1H), 3.52 (q, *J* = 6.7 Hz, 2H), 2.43 (t, *J* = 7.0 Hz, 2H), 2.07 (p, *J* = 2.2 Hz, 4H), 1.93 (p, *J* = 7.1 Hz, 2H), 1.83 – 1.71 (m, 2H), 1.70 – 1.59 (m, 1H).

^{13}C NMR (101 MHz, Acetone) δ 147.8, 136.1, 128.8, 128.1, 121.3, 54.1, 43.5, 39.2, 24.6, 20.8.

HRMS (ESI$^+$) Calculated for $C_{16}H_{21}N_2O_3$ $[M+H]^+$: 289.1547 found: 289.1543.

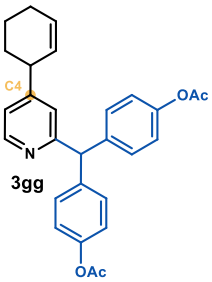

((4-(cyclohex-2-en-1-yl)pyridin-2-yl)methylene)bis(4,1-phenylene) diacetate (3gg)

Prepared according to General Procedure B using bisacodyl (72.3 mg, 0.2 mmol) and cyclohexene **2a** (203 µL, 2.0 mmol). No other regioisomer was detected in the crude mixture. Purification by column (SiO_2, 1:9:90 Et_3N/EtOAc/hexanes) afforded product **3gg** as a colorless oil (29.0 mg, 33% yield, > 20:1 *r.r.*).

^{1}H NMR (400 MHz, $CDCl_3$) δ 8.48 (d, *J* = 5.1 Hz, 1H), 7.21 – 7.17 (m, 4H), 7.03 – 6.98 (m, 6H), 5.94 – 5.89 (m, 1H), 5.63 – 5.59 (m, 2H), 3.35 – 3.30 (m, 1H), 2.27 (s, 6H), 2.09 – 2.04 (m, 2H), 2.00 – 1.94 (m, 1H), 1.73 – 1.63 (m, 2H), 1.62 – 1.59 (m, 1H), 1.52 – 1.42 (m, 1H).

^{13}C NMR (101 MHz, $CDCl_3$) δ 169.6, 162.5, 156.4, 149.6, 149.4, 140.4, 140.3, 130.4, 130.4, 129.8, 128.2, 123.5, 121.5, 121.2, 58.2, 41.3, 31.9, 25.0, 21.3, 21.0.

HRMS: (ESI$^+$) calculated for $C_{28}H_{28}NO_4$ [M+H$^+$]: 442.2013, found 442.2031.

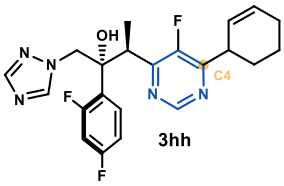

3-(6-(cyclohex-2-en-1-yl)-5-fluoropyrimidin-4-yl)-2-(2,4-difluorophenyl)-1-(1H-1,2,4-triazol-1-yl)butan-2-ol (3hh)

Prepared according to General Procedure A using voriconazole (69.9 mg, 0.2 mmol) and cyclohexene **2a** (203 µL, 2.0 mmol). No other regioisomer was detected in the crude mixture. Purification by column chromatography (SiO_2, 1:50:49 Et_3N/EtOAc/hexanes) afforded product **3hh** (37.6 mg, 44% yield, 1:1 *d.r.*, > 20:1 *r.r.*) as an off-white solid.

^{1}H NMR (400 MHz, $CDCl_3$) *1:1 mixture of diastereoisomers* δ 8.85 (dd, *J* = 7.4, 1.8 Hz, 1H), 7.99 (d, *J* = 4.3 Hz, 1H), 7.67 – 7.58 (m, 1H), 7.54 (d, *J* = 5.2 Hz, 1H), 6.90 – 6.79 (m, 2H), 6.73 (s, 0.5H), 6.68 (s, 0.5H), 6.10 – 6.02 (m, 1H), 5.77 – 5.67 (m, 1H), 4.72 (dd, *J* = 14.2, 3.5 Hz, 1H), 4.32 (dd, *J* = 17.3, 14.1 Hz, 1H), 4.19 – 4.10 (m, 1H), 4.04 – 3.92 (m, 1H), 2.27 – 2.14 (m, 2H), 2.14 – 2.05 (m, 1H), 1.99 – 1.89 (m, 1H), 1.86 – 1.71 (m, 2H), 1.12 – 1.08 (m, 3H).

^{13}C NMR (101 MHz, $CDCl_3$) *1:1 mixture of diastereoisomers* δ 164.1, 163.9, 162.1, 162.0, 162.0, 161.9, 161.6, 161.5, 159.8, 159.7, 158.1, 158.0, 157.4, 157.3, 155.1, 153.0, 152.9, 152.9, 152.8, 152.5, 152.5, 150.8, 144.0, 143.9, 130.7, 130.7, 130.7, 130.6, 130.3, 130.2, 125.4, 125.4, 123.6, 123.6, 111.7, 111.5, 104.3, 104.1, 103.8, 57.5, 57.5, 37.3, 37.1, 36.5, 28.2, 28.1, 24.5, 21.3, 21.2, 16.2.

^{19}F{^{1}H} NMR (376 MHz, $CDCl_3$) *1:1 mixture of diastereoisomers* δ -109.17 (d, *J* = 8.2 Hz), -109.19 (d, *J* = 8.0 Hz), -110.55 (d, *J* = 8.1 Hz), -138.87, -139.00.

HRMS (ESI$^+$) Calculated for $C_{22}H_{23}F_3N_5O$ [M+H]$^+$: 430.1849 found: 430.1854.

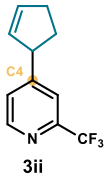

3ii

4-(cyclopent-2-en-1-yl)-2-(trifluoromethyl)pyridine (3ii)

Prepared according to General Procedure A using 2-(trifluoromethyl)pyridine (23.0 µL, 0.2 mmol) and cyclopentene (183 µL, 2.0 mmol). No other regioisomer was detected in the crude mixture. Purification by column chromatography (SiO_2, 5:95 EtOAc/hexanes) afforded product **3ii** as colorless oil (17.1 mg, 40% yield, > 20:1 *r.r.*).

^{1}H NMR (400 MHz, $CDCl_3$) δ 8.60 (d, *J* = 5.0 Hz, 1H), 7.49 (d, *J* = 1.7 Hz, 1H), 7.30 (dd, *J* = 5.0, 1.7 Hz, 1H), 6.09 – 6.05 (m, 1H), 5.76 – 5.72 (m, 1H), 4.00 – 3.93 (m, 1H), 2.60 – 2.40 (m, 3H), 1.77 – 1.67 (m, 1H).

^{13}C NMR (101 MHz, $CDCl_3$) δ 157.5, 150.0, 148.4 (q, *J* = 34.1 Hz), 134.4, 131.6, 125.2, 121.7 (q, *J* = 274.2 Hz), 119.3 (q, *J* = 2.8 Hz), 50.6, 33.1, 32.4.

^{19}F NMR (376 MHz, $CDCl_3$) δ -68.0.

HRMS: (ESI$^+$) calculated for $C_{11}H_{11}F_3N$ $[M+H]^+$: 214.0838, found 214.0829.

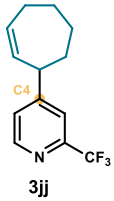

3jj

4-(cyclohept-2-en-1-yl)-2-(trifluoromethyl)pyridine (3jj)

Prepared according to General Procedure A using 2-(trifluoromethyl)pyridine (23.0 µL, 0.2 mmol) and cycloheptene (233 µL, 2.0 mmol) with a reaction time of 24 hours. No other regioisomer was detected in the crude mixture. Purification by column chromatography (SiO_2, 5:95 EtOAc/hexanes) afforded product **3jj** as colorless oil (21.2 mg, 44% yield, > 20:1 *r.r.*).

^{1}H NMR (400 MHz, $CDCl_3$) δ 8.62 (d, *J* = 5.0 Hz, 1H), 7.55 (d, *J* = 2.2 Hz, 1H), 7.35 (dd, *J* = 5.0, 1.9 Hz, 1H), 5.96 (dddd, *J* = 11.3, 6.9, 5.5, 2.3 Hz, 1H), 5.64 (dddt, *J* = 11.3, 4.2, 1.9, 0.8 Hz, 1H), 3.66 – 3.60 (m, 1H), 2.29 – 2.19 (m, 2H), 1.97 – 1.88 (m, 1H), 1.88 – 1.66 (m, 4H), 1.53 – 1.42 (m, 1H).

^{13}C NMR (101 MHz, $CDCl_3$) δ 158.2, 150.1, 148.4 (q, *J* = 34.1 Hz), 133.9, 133.6, 125.3, 121.7 (q, *J* = 274.5 Hz), 119.5 (q, *J* = 2.9 Hz), 46.3, 35.2, 29.7, 28.7, 26.6.

^{19}F NMR (376 MHz, $CDCl_3$) δ -68.03.

HRMS: (ESI$^+$) calculated for $C_{13}H_{15}F_3N$ $[M+H]^+$: 242.1151, found 242.1157.

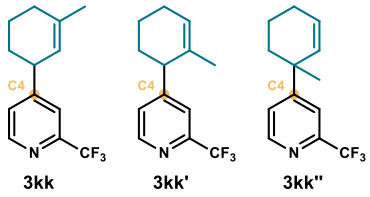

4-(3-methylcyclohex-2-en-1-yl)-2-(trifluoromethyl)pyridine (3kk) + 4-(2-methylcyclohex-2-en-1-yl)-2-(trifluoromethyl)pyridine (3kk') + 4-(1-methylcyclohex-2-en-1-yl)-2-(trifluoromethyl)pyridine (3kk'')

Prepared according to General Procedure A using 2-(trifluoromethyl)pyridine (23.0 µL, 0.2 mmol) and 1-methylcyclohex-1-ene (237 µL, 2.0 mmol). Purification by column chromatography (SiO_2, 1:99 Et_3N/hexanes) afforded a mixture of products **3kk, 3kk', and 3kk''** as a colorless oil (29.7 mg, 61% yield, 2:0.75:1 allylic *r.r.*). For NMR characterization, when possible, the signals are assigned to the corresponding isomer (COSY and HSQC spectra used for assignment).

^{1}H NMR (400 MHz, $CDCl_3$) δ 8.61 (dm, *J* = 5.0 Hz, 1H, **3kk'**), 8.61 (dm, *J* = 5.0 Hz, 1H, **3kk''**), 8.60 (dp, *J* = 5.0 Hz, 0.7 Hz, 1H, **3kk**), 7.65 (dd, *J* = 1.8, 0.8 Hz, 1H, **3kk''**), 7.52 – 7.51 (m, 1H, **3kk**), 7.51 – 7.50 (m, 1H, **3kk'**), 7.46 (ddq, *J* = 5.2, 1.8, 0.6 Hz, 1H, **3kk''**), 7.32 (ddt, *J* = 5.0, 1.7, 0.6 Hz, 1H, **3kk**), 7.30 (ddt, *J* = 5.0 Hz, 1.6, 0.5 Hz, 1H, **3kk'**), 5.96 (dtd, *J* = 10.1, 3.7, 0.6 Hz, 1H, **3kk''**), 5.79 (tp, *J* = 3.9, 1.4 Hz, 1H, **3kk'**), 5.64 (dtd, *J* = 10.1, 2.2, 1.1 Hz, 1H, **3kk''**), 5.36 (ddtd, *J* = 2.9, 2.2, 1.5, 0.7 Hz, 1H, **3kk**), 3.45 (ddp, *J* = 8.0, 5.5, 2.5 Hz, 1H, **3kk**), 3.32 (t, *J* = 5.9 Hz, 1H, **3kk'**), 2.15 – 1.26 (m, 6H, CH_2) 1.77 – 1.76 (m, 3H, **3kk**), 1.50 – 1.49 (m, 3H, **3kk'**), 1.40 (s, 3H, **3kk''**)

^{13}C NMR (101 MHz, $CDCl_3$) δ 161.0, 158.2, 156.7, 149.8, 149.8, 149.7, 148.2 (q, *J* = 34.0 Hz), 148.2 (q, *J* = 34.0 Hz, **3kk**), 148.1 (q, *J* = 33.6 Hz), 137.9, 132.5 (**3kk''**), 131.9, 128.9 (**3kk''**), 126.4 (**3kk'**), 125.8 (q, *J* = 1.0 Hz), 124.6 (q, *J* = 1.1 Hz, **3kk''**), 121.8 (q, *J* = 273.9 Hz, **3kk''**), 121.7 (q, *J* = 274.2 Hz, **3kk**), 121.7 (q, *J* = 274.1 Hz, **3kk'**), 121.4 (**3kk**), 120.4 (q, *J* = 2.5 Hz), 119.8 (q, *J* = 2.5 Hz), 118.6 (q, *J* = 2.8 Hz), 45.4 (**3kk'**), 41.6 (**3kk**), 39.7 (**3kk''**), 38.3, 31.9, 31.5 (**3kk**), 29.7, 28.5 (**3kk''**), 25.1, 24.8, 23.9 (**3kk**), 22.5 (**3kk'**), 21.1 (**3kk**), 18.8, 18.3 (**3kk'**).

^{19}F NMR (376 MHz, $CDCl_3$) δ 67.9 (**3kk''**), 68.0 (**3kk'**), 68.0 (**3kk**)

HRMS: (ESI$^+$) calculated for $C_{13}H_{15}F_3N$ $[M+H]^+$: 242.1151, found 242.1152.

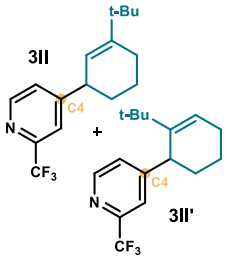

4-(3-(tert-butyl)cyclohex-2-en-1-yl)-2-(trifluoromethyl)pyridine (3ll) and 4-(2-(tert-butyl)cyclohex-2-en-1-yl)-2-(trifluoromethyl)pyridine (3ll')

Prepared according to General Procedure A using 2-(trifluoromethyl)pyridine (23.0 µL, 0.2 mmol) and 1-(tert-butyl)cyclohex-1-ene (330 µL, 2.0 mmol). Purification by column chromatography (SiO_2, 5:95 EtOAc/hexanes) afforded products **3ll** + **3ll'**

as colorless oil (25.8 mg, 46% yield, 8:1 allylic *r.r.*). Only characterization data for the major product **3ll** is described.

^{1}H NMR (400 MHz, $CDCl_3$) δ 8.61 (dt, *J* = 5.0, 0.7 Hz, 1H), 7.50 (dt, *J* = 1.5, 0.7 Hz, 1H), 7.31 (ddt, *J* = 5.0, 1.7, 0.7 Hz, 1H), 5.44 – 5.42 (m, 1H), 3.49 (ddq, *J* = 8.4, 5.5, 2.7 Hz, 1H), 2.16 – 2.09 (m, 2H), 2.00 (dtd, *J* = 13.1, 6.6, 2.8 Hz, 1H), 1.79 – 1.69 (m, 1H), 1.65 – 1.55 (m, 1H), 1.44 (dddd, *J* = 13.1, 10.6, 8.2, 3.0 Hz, 1H), 1.09 (s, 9H).

^{13}C NMR (101 MHz, $CDCl_3$) δ 158.5, 149.8, 149.5, 148.2 (q, *J* = 34.0 Hz), 125.7, 121.7 (q, *J* = 273.9 Hz), 119.9 (q, *J* = 2.8 Hz), 41.6, 35.6, 31.6, 30.0, 29.1, 24.3, 21.5.

^{19}F NMR (376 MHz, $CDCl_3$) δ -68.0.

HRMS: (ESI$^+$) calculated for $C_{16}H_{21}F_3N$ $[M+H]^+$: 284.1621, found 284.1623.

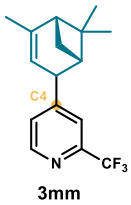

3mm

2-(trifluoromethyl)-4-(4,6,6-trimethylbicyclo[3.1.1]hept-3-en-2-yl)pyridine (3mm)

Prepared according to General Procedure A using 2-(trifluoromethyl)pyridine (23.0 µL, 0.2 mmol) and alpha-Pinene (318 µL, 2.0 mmol) with a reaction time of 60 hours. The yield (39%, single regioisomer) of **3mm** was inferred by ^{1}H NMR analysis of the crude reaction mixture using trichloroethylene as the internal standard. A 90% pure sample of **3mm** (estimated by ^{1}H NMR integration) was obtained after purification by column chromatography (SiO_2, 3:97 Et_2O/hexanes) as a colorless oil.

^{1}H NMR (400 MHz, $CDCl_3$) δ 8.60 (dt, *J* = 5.0, 0.7 Hz, 1H), 7.54 (dt, *J* = 1.6, 0.7 Hz, 1H), 7.35 (ddt, *J* = 5.1, 1.7, 0.7 Hz, 1H), 5.32 (td, *J* = 2.9, 1.6 Hz, 1H), 3.62 (h, *J* = 2.3 Hz, 1H), 2.17 – 2.13 (m, 1H), 1.81 (t, *J* = 1.9 Hz, 3H), 1.35 (s, 3H), 1.21 – 1.14 (m, 1H), 1.01 (s, 3H).

^{13}C NMR (101 MHz, $CDCl_3$) δ 156.3, 149.6, 148.6, 148.0 (q, *J* = 34.3 Hz), 126.4, 121.8 (q, *J* = 274.1 Hz), 120.5 (q, *J* = 2.6 Hz), 115.6, 47.6, 46.8, 45.1, 42.1, 26.3, 26.2, 23.2, 20.5.

^{19}F NMR (376 MHz, $CDCl_3$) δ -67.5.

HRMS: (ESI$^+$) calculated for $C_{16}H_{19}F_3N$ $[M+H]^+$: 282.1464, found 282.1473.

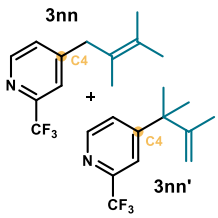

4-(2,3-dimethylbut-2-en-1-yl)-2-(trifluoromethyl)pyridine (3nn) and 4-(2,3-dimethylbut-3-en-2-yl)-2-(trifluoromethyl)pyridine (3nn')

Prepared according to General Procedure A using 2-(trifluoromethyl)pyridine (23.0 µL, 0.2 mmol) and tetramethylethylene (238 µL, 2.0 mmol) with a reaction time of 60 hours. Purification by column chromatography (SiO_2, 5:95 EtOAc) afforded the mixture of products **3nn** + **3nn'** as a colorless oil (22.4 mg, 43% yield, 3:2 allylic *r.r.*).

^{1}H NMR of **3nn** (400 MHz, $CDCl_3$) δ 8.58 (dt, *J* = 5.0, 0.7 Hz, 1H), 7.47 – 7.42 (m, 1H), 7.27 – 7.24 (m, 1H), 3.47 – 3.45 (m, 2H), 1.76 – 1.75 (m, 6H), 1.63 – 1.56 (m, 3H).

^{13}C NMR of **3nn** (101 MHz, $CDCl_3$) δ 152.4, 149.8, 148.2 (q, *J* = 34.2 Hz), 128.5, 126.3 (q, *J* = 1.1 Hz), 123.6, 121.7 (q, *J* = 274.5 Hz), 120.5 (q, *J* = 2.7 Hz), 39.6, 20.7, 20.6, 18.5.

^{19}F NMR of **3nn** (376 MHz, $CDCl_3$) δ -68.1.

^{1}H NMR of **3nn'** (400 MHz, $CDCl_3$) δ 8.62 (dp, *J* = 5.1, 0.6 Hz, 1H), 7.59 (dd, *J* = 1.8, 0.7 Hz, 1H), 7.41 (ddq, *J* = 5.1, 1.8, 0.6 Hz, 1H), 5.03 (dq, *J* = 1.4, 0.7 Hz, 1H), 5.00 (p, *J* = 1.4 Hz, 1H), 1.52 (dd, *J* = 1.4, 0.7 Hz, 3H), 1.44 (s, 6H).

^{13}C NMR of **3nn'** (101 MHz, $CDCl_3$) δ 159.9, 149.9, 149.8, 148.3 (q, *J* = 34.0 Hz), 124.1 (q, *J* = 1.1 Hz), 121.7 (q, *J* = 274.1 Hz), 118.2 (q, *J* = 2.7 Hz), 111.7, 44.2, 27.6, 20.0.

^{19}F NMR of **3nn'** (376 MHz, $CDCl_3$) δ -67.9.

HRMS of **3nn** + **3nn'**: (ESI^+) calculated for $C_{12}H_{15}F_3N$ $[M+H]^+$: 230.1151, found 230.1161.

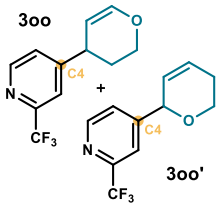

4-(3,4-dihydro-2H-pyran-4-yl)-2-(trifluoromethyl)pyridine (3oo) + 4-(5,6-dihydro-2H-pyran-2-yl)-2-(trifluoromethyl)pyridine (3oo')

Prepared according to General Procedure A using 2-(trifluoromethyl)pyridine (23.0 µL, 0.2 mmol) and 3,4-dihydropyran (182 µL, 2.0 mmol). Purification by column chromatography (SiO_2, 10:90 EtOAc/hexanes) afforded products **3oo** + **3oo'** as a colorless oil (19.8 mg, 43% yield, 7:1 allylic *r.r.*). Only the major product **3oo** is described.

^{1}H NMR (400 MHz, $CDCl_3$) δ 8.65 – 8.63 (m, 1H), 7.60 – 7.58 (m, 1H), 7.40 (m, 1H), 6.64 (dd, *J* = 6.3, 1.9 Hz, 1H), 4.72 (dddd, *J* = 6.3, 3.3, 1.0, 0.7 Hz, 1H), 4.03 (dddt, *J* = 11.0, 8.0, 3.0, 0.4 Hz, 1H), 3.96 (ddd, *J* = 11.1, 6.9, 3.2 Hz, 1H), 2.25 (dddddd, *J* = 13.8, 6.9, 6.3, 3.0, 1.1, 0.5 Hz, 1H), 1.84 (m, 1H).

^{13}C NMR (101 MHz, $CDCl_3$) δ 156.6, 150.0, 148.4 (q, *J* = 34.3 Hz), 146.3, 125.6, 121.6 (q, *J* = 274.2 Hz), 119.7 (q, *J* = 2.7 Hz), 100.7, 63.4, 35.8, 31.1.

^{19}F NMR (376 MHz, $CDCl_3$) δ -68.0.

HRMS: (ESI^+) calculated for $C_{11}H_{11}F_3NO$ $[M+H]^+$: 230.0787, found 230.0788.

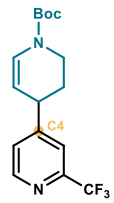

3pp

tert-butyl 2'-(trifluoromethyl)-3,4-dihydro-[4,4'-bipyridine]-1(2H)-carboxylate (3pp)

Prepared according to General Procedure A using 2-(trifluoromethyl)pyridine 23.0 µL, 0.2 mmol) and tert-butyl 3,4-dihydropyridine-1(2H)-carboxylate (367 mg, 2.0 mmol). Purification by column chromatography (SiO_2, 5:95 to 12:88 EtOAc/hexanes) afforded product **3pp** as colorless oil (24.8 mg, 38% yield, 20:1 allylic *r.r.*) and recovered olefin (311 mg, 1.7 mmol). Due to presence of N-Boc rotamers the ^{1}H NMR and ^{13}C NMR spectra were recorded at 328K which produced singular broad singlets for these signals.

^{1}H NMR (500 MHz, $CDCl_3$, 328K) δ 8.63 (d, *J* = 5.0 Hz, 1H), 7.55 (d, *J* = 2.0 Hz, 1H), 7.36 (dd, *J* = 5.0, 1.9 Hz, 1H), 7.08 (br. s, 1H), 4.82 (br. s, 1H), 3.67 – 3.51 (m, 3H), 2.19 (dtd, *J* = 13.4, 6.2, 3.6 Hz, 1H), 1.82 (dtd, *J* = 13.5, 7.4, 4.0 Hz, 1H), 1.52 (s, 9H).

^{13}C NMR (126 MHz, $CDCl_3$, 328K) δ 156.3, 152.2, 150.1, 148.8 (q, *J* = 34.5 Hz), 128.1, 125.5, 121.7 (q, *J* = 274.3 Hz), 119.7 (q, *J* = 2.7 Hz), 104.5, 81.3, 39.7, 37.8, 30.4, 28.3.

^{19}F NMR (376 MHz, $CDCl_3$) δ -68.0.

HRMS: (ESI$^+$) calculated for $C_{16}H_{20}F_3N_2O_2$ $[M+H]^+$: 329.1471, found 329.1471.

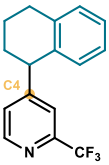

3qq

4-(1,2,3,4-tetrahydronaphthalen-1-yl)-2-(trifluoromethyl)pyridine (3qq)

Prepared according to General Procedure A using 2-(trifluoromethyl)pyridine (23.0 µL, 0.2 mmol) and 1,2,3,4-tetrahydronaphthalene (273 µL, 2.0 mmol). No other regioisomer was detected in the crude mixture. Purification by column chromatography (SiO_2, 1:100 Et_3N/hexanes to 1:3:96 Et_3N/EtOAc/hexanes) afforded product **3qq** as pale-yellow oil (27.3 mg, 49% yield, > 20:1 *r.r.*).

^{1}H NMR (400 MHz, $CDCl_3$) δ 8.60 (d, *J* = 5.0 Hz, 1H), 7.46 (d, *J* = 1.7 Hz, 1H), 7.21 – 7.17 (m, 3H), 7.12 – 7.05 (dt, *J* = 7.7, 4.2 Hz, 1H), 6.75 (dd, *J* = 7.6, 1.0 Hz, 1H), 4.23 (t, *J* = 6.4 Hz, 1H), 3.00 – 2.82 (m, 2H), 2.27 – 2.17 (m, 1H), 1.90 – 1.77 (m, 3H).

^{13}C NMR (101 MHz, $CDCl_3$) δ 158.5, 149.9, 148.3 (q, *J* = 34.1 Hz), 137.6, 136.2, 129.8, 129.5, 126.9, 126.7, 126.1, 121.6 (q, *J* = 274.3 Hz), 120.6 (q, *J* = 2.7 Hz), 45.1, 32.6, 29.4, 20.4.

^{19}F NMR (376 MHz, $CDCl_3$) δ -68.0.

HRMS: (ESI$^+$) calculated for $C_{16}H_{15}F_3N$ $[M+H]^+$: 278.1151, found 278.1152.

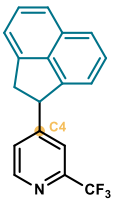

3rr

4-(1,2-dihydroacenaphthylen-1-yl)-2-(trifluoromethyl)pyridine (3rr)

Prepared according to General Procedure A using 2-(trifluoromethyl)pyridine (23.0 μL, 0.2 mmol) and 1,2-dihydroacenaphthylene (308 mg, 2.0 mmol). No other regioisomer was detected in the crude mixture. Purification by column chromatography (SiO_2, 5:95 EtOAc/hexanes) afforded product **3rr** as colorless oil (25.4 mg, 42% yield, > 20:1 *r.r.*).

^{1}H NMR (400 MHz, $CDCl_3$) δ 8.66 – 8.62 (m, 1H), 7.75 (t, *J* = 7.2 Hz, 2H), 7.60 – 7.54 (m, 2H), 7.51 (t, *J* = 7.6 Hz, 1H), 7.37 (d, *J* = 7.1 Hz, 1H), 7.31 – 7.27 (m, 1H), 7.12 (d, *J* = 7.1 Hz, 1H), 5.00 – 4.94 (m, 1H), 4.04 (dd, *J* = 17.6, 8.8 Hz, 1H), 3.39 (d, *J* = 17.3 Hz, 1H).

^{13}C NMR (101 MHz, $CDCl_3$) δ 156.5, 150.3, 148.6 (q, *J* = 34.3 Hz), 145.8, 142.5, 138.6, 131.6, 128.4, 128.1, 125.5, 123.9, 123.0, 121.5 (q, *J* = 274.3 Hz), 120.2, 119.8, 119.7 (q, *J* = 2.8 Hz), 48.7, 41.0.

^{19}F NMR (376 MHz, $CDCl_3$) δ -67.6.

HRMS: (ESI$^+$) calculated for $C_{18}H_{13}F_3N$ $[M+H]^+$: 300.0995, found 300.0997.

2.7.7 Procedure for the 1 mmol reaction

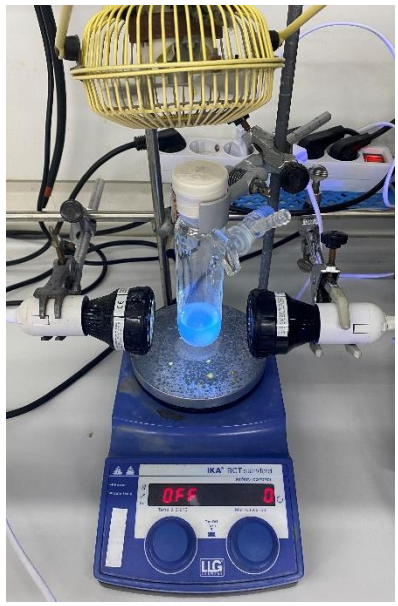

Figure 2.53. Setup for reaction scale-up using 2xEvoluChem PF365 LED spotlights and a fan.

To an argon-purged 100 ml Schlenk tube, containing dithiophosphoric acid catalyst **A2** (127 mg, 0.2 mmol), argon-sparged HPLC grade acetone was added (20 mL, 0.05 M), followed by pyridine **1a** (81 µL, 1 mmol), 2,4,6-collidine (66 µL, 0.5 mmol), and finally cyclohexene **2a** (1 mL, 10 mmol). The vial was sealed with Parafilm and placed in the 365 nm irradiation setup (Figure 2.53). The reaction was stirred for 16 h, then the solvent was evaporated. The regioisomeric ratio **3a**/**3a'** (2.6:1) of the crude mixture was measured by ^{1}H NMR analysis. Purification by column chromatography (SiO_2, 1:10:89 Et_3N/EtOAc/hexanes) afforded product **3a** as a light-yellow oil (81.2 mg, 51% yield, > 20:1 *r.r.*). The minor regioisomer **3a'** was not isolated after column chromatography.

Chapter III

Reductive Cross-Coupling of Olefins via a Radical Pathway

Target

To develop a protocol for reductive cross-coupling of olefins utilizing radicals catalytically generated from electron-poor olefins via a single electron reduction – protonation sequence.

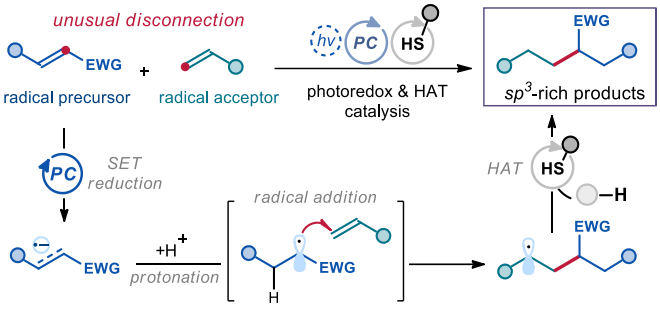

Tool

A dual catalytic system based on a photoredox catalyst to promote single electron transfer (SET) processes and a simple thiol catalyst to promote hydrogen atom transfer (HAT) processes, in conjunction with a commercially available hydrogen atom donor to furnish the reductive cross-coupling products.[1]

3.1 Introduction

Olefins are ubiquitous motifs in petroleum-derived feedstocks, natural products, pharmaceuticals, and materials.[2] Due to this abundance, numerous methods of olefin functionalization have been developed (Figure 3.1).

[1] The project discussed in this chapter has been conducted in collaboration with Dr. Wei Zhou. I was involved in the optimization of the reaction conditions, investigation of the scope of the reaction, mechanistic elucidation and drafting of the article. This study has been published: Zhou, W.[§]; Dmitriev, I. A.[§]; Melchiorre, P. "Reductive Cross-Coupling of Olefins via a Radical Pathway" *J. Am. Chem. Soc.* **2023**, *145*, 25098–25102.

[2] Zabicky, J., Ed. "Patai's Chemistry of Functional Groups"; *The Alkenes, Vol. 2*; Wiley: London, **1970**.

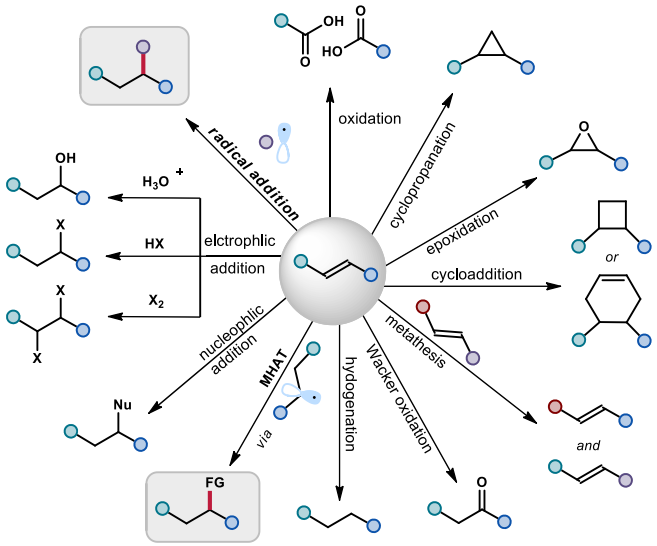

Figure 3.1. Reaction map of olefins.

One way to rapidly increase the molecular structural complexity is the intermolecular cross-coupling of two olefins, as it enables the formation of new *C–C* bonds directly from these abundant feedstocks.[3] One such procedure was reported by Baran in 2014 (Figure 3.2),[4] based on MHAT (metal-hydride hydrogen atom transfer) mechanism.[5] In this protocol, electron-poor olefins **1** (substituted with an electron-withdrawing group, EWG) and electron-neutral olefins **2** underwent reductive cross-coupling, furnishing valuable sp^3-dense products **3**.[6] The catalytic cycle started with the formation of iron hydride species Fe^{III}-H, which underwent MHAT process with the olefin **2**, forming a nucleophilic radical **I**. This radical subsequently attacked the electron-poor olefin **1** in a Giese-type addition path, furnishing radical **II**. This radical is easy to reduce due to the presence of an electron-withdrawing group. As such, radical **II** underwent a sequence of single electron transfer (SET) reduction and protonation to form product **3**.

[3] (a) RajanBabu, T. V. "Asymmetric Hydrovinylation Reaction." *Chem. Rev.* **2003**, *103*, 2845; (b) Hirano, M. "Recent Advances in the Catalytic Linear Cross-Dimerizations." *ACS Catal.* **2019**, *9*, 1408.

[4] (a) Lo, J. C.; Yabe, Y.; Baran, P. S. "A Practical and Catalytic Reductive Olefin Coupling." *J. Am. Chem. Soc.* **2014**, *136*, 1304; (b) Lo, J. C.; Gui, J.; Yabe, Y.; Pan, C.-M.; Baran, P. S., "Functionalized olefin cross-coupling to construct carbon–carbon bonds." *Nature* **2014**, *516*, 343-348.

[5] Shevick, S. L.; Wilson, C. V.; Kotesova, S.; Kim, D.; Holland, P. L.; Shenvi, R. A. "Catalytic Hydrogen Atom Transfer to Alkenes: a Roadmap for Metal Hydrides and Radicals." *Chem. Sci.* **2020**, *11*, 12401

[6] Lovering, F.; Bikker, J.; Humblet, C. "Escape from Flatland: Increasing Saturation as an Approach to Improving Clinical Success." *J. Med. Chem.* **2009**, *52*, 6752.

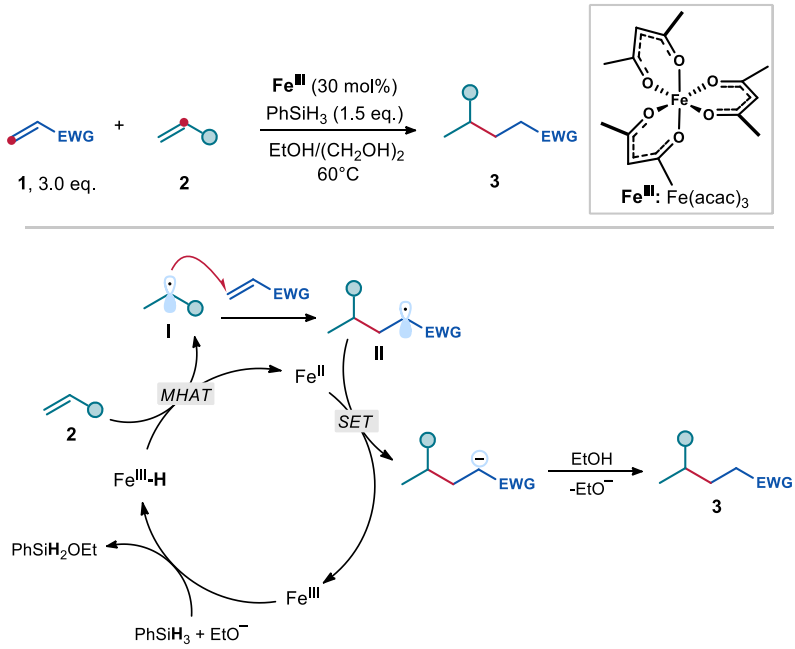

Figure 3.2. Reductive cross-coupling of olefins reported by Baran. EWG: electron-withdrawing group.

Inspired by this protocol, we wondered whether it would be possible to use the same olefin starting materials but form a product **4** with a distinct connectivity. To achieve this, a distinct mechanistic scenario has to be realized. Specifically, we surmised that **1** could be reduced via SET to form a radical anion **III**, which upon protonation would deliver a carbon radical **IV** adjacent to an electron-withdrawing group (α-EWG). This electrophilic radical **IV** would be favorably poised to react with an electron-rich or neutral olefin **2** via radical addition.[7] Eventually, the ensuing radical **V** would be reduced via a hydrogen atom transfer (HAT) path to afford the desired olefin cross-coupling product **4**.

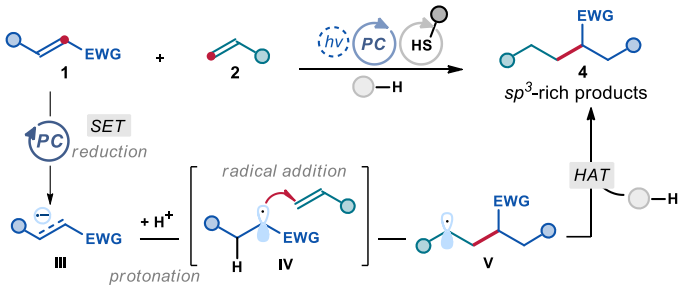

Figure 3.3. Reductive cross-coupling of olefins via SET reduction of electron-poor olefins **1**

[7] Parsaee, F.; Senarathna, M.C.; Kannangara, P.B.; Alexander, N.S.; Arche P.D.E.; Welin E.R. "Radical philicity and its role in selective organic transformations." *Nat. Rev. Chem.* **2021**, *5*, 486.

This transformation would offer a complementary strategy to the olefin cross-coupling protocol developed by Baran, as sp^3-rich products with different connectivity, arising from opposite disconnections, become available. This is due to the use of entirely different strategies to generate radicals.

This chapter details the realization of this idea. In the following sections, the important literature precedents on the radical transformations of olefins are discussed, as well as literature data that served as inspiration for this project.

3.2 Background

3.2.1 Addition of electrophilic radicals to olefins

In radical transformations, olefins are particularly suitable substrates due to the ability of either their HOMO (*highest occupied molecular orbital*) or LUMO (*lowest unoccupied molecular orbital*) to interact with the SOMO (*singly occupied molecular orbital*) of the radicals. Moreover, due to tunability of their HOMO and LUMO energy levels via substitution, the efficacy of interaction could be enhanced both for high SOMO energy radicals (such radicals are called *nucleophilic*), or for low SOMO energy radicals (called *electrophilic*).[8] The *polarity matching* (or *philicity matching*) concept states that if the energy levels of frontier orbitals of attacking radical and acceptor olefin are closely matching, this results in the stabilization of the early transition state, resulting in a higher rate of addition. For example, the high SOMO of a nucleophilic radical would match well with the low LUMO of an electron-deficient olefin (Figure 3.4.a) but would not match well with either HOMO or LUMO of an electron-rich olefin (Figure 3.4.b). The principle applies the same to the low SOMO of an electrophilic radical that is a good match for high HOMO of the electron-rich olefin (Figure 3.4.c).[7,8]

[8](a) De Vleeschouwer, F.; Van Speybroeck, V.; Waroquier, M.; Geerlings, P.; De Proft, F. "Electrophilicity and Nucleophilicity Index for Radicals" *Org. Lett.* **2007**, *9*, 2721; (b) Fischer, H.; Random, L. "Factors Controlling the Addition of Carbon-Centered Radicals to Alkenes–An Experimental and Theoretical Perspective" *Angew. Chem. Int. Ed.* **2001**, *40*, 1340; (c) Héberger, K.; Lopata, A. "Assessment of nucleophilicity and electrophilicity of radicals, and of polar and enthalpy effects on radical addition reactions." *J. Org. Chem.* **1998**, *63*, 8646; (d) Giese, B. "Formation of C-C Bonds by Addition of Free Radicals to Alkenes." *Angew. Chem., Int. Ed.* **1983**, *22*, 753; (e) J. M. Tedder, "Which Factors Determine the Reactivity and Regioselectivity of Free Radical Substitution and Addition Reactions?" *Angew. Chem. Int. Ed. Engl.* **1982**, *21*, 401.

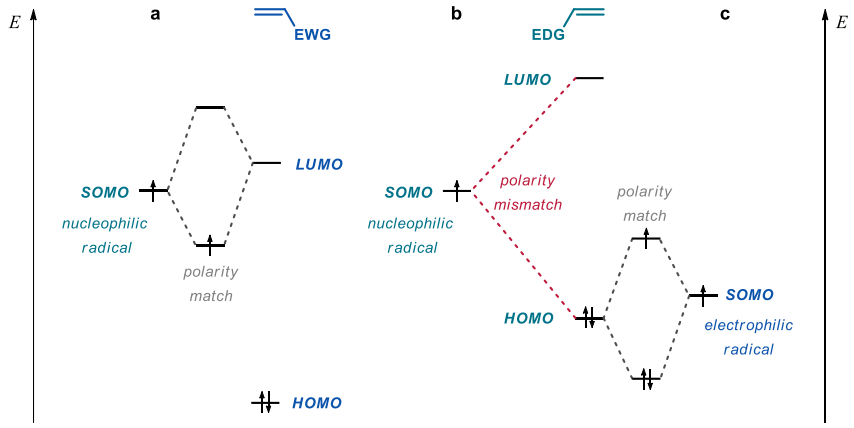

Figure 3.4. (a) Polarity-matched interaction between the SOMO of a nucleophilic radical and an electron-deficient olefin. (b) Polarity-mismatched interaction between the SOMO of a nucleophilic radical and an electron-rich olefin. (c) Polarity-matched interaction between the SOMO of an electrophilic radical and an electron-rich olefin. EWG: electron-withdrawing group. EDG: electron-donating group.

This concept is demonstrated by the *Kharash reaction*, reported in 1940s (Figure 3.5.a).[9] Here, a methyl radical is generated from diacetyl peroxide, furnishing an electrophilic *α*-EWG radical **IV** upon bromine atom abstraction from substrate **7**. The radical **IV** is then involved in an addition to an electron-rich or electron neutral olefin **2**, forming radical **V** which then starts a chain propagation event via bromine atom abstraction from substrate **7**.

Hydroalkylation protocols based on the same principle of attack by electrophilic radical on electron-rich olefins have also been reported (Figure 3.5.b).[10] For example, in a protocol published in 2014 by the group of Ryo, a radical **IV** and a bromine radical were produced via photolysis of *C-Br* bond in substrate **7**. Attack by electrophilic radical **IV** on an electron-rich olefin **2** formed intermediate **V**, while the bromine radical participated in hydrogen atom transfer (HAT, discussed in sections 1.1 and 1.2) with the allylic *C-H* bond of substrate **2**, forming an HBr molecule and an intermediate **VI**. The intermediate was reduced by HAT by HBr molecule, forming product **8**, while two molecules of **VI** coupled to furnish the dimer **9**.

[9] (a) Kharasch, M. S.; Jensen, E. V.; Urry, W. H., "Addition of carbon tetrachloride and chloroform to olefins" *Science* **1945**, *102*, 128; (b) Kharasch, M. S.; Skell, P. S.; Fisher, P., "Reactions of Atoms and Free Radicals in Solution. XII. The Addition of Bromo Esters to Olefins" *J. Am. Chem. Soc.* **1948**, *70*, 1055.

[10] (a) Giese, B.; Horler, H.; Leising, M. "Umpolungsreaktionen mit dem Malonyl-Radikal." *Chem. Ber.* **1986**, *119*, 444; (b) Sumino, S.; Fusano, A.; Ryu, I. "Reductive Bromine Atom-Transfer Reaction." *Org. Lett.* **2013**, *15*, 2826; (c) Huang, Q.; Suravarapu, S. R.; Renaud, P. A "Giese reaction for electron-rich alkenes." *Chemical Science* **2021**, *12*, 2225.

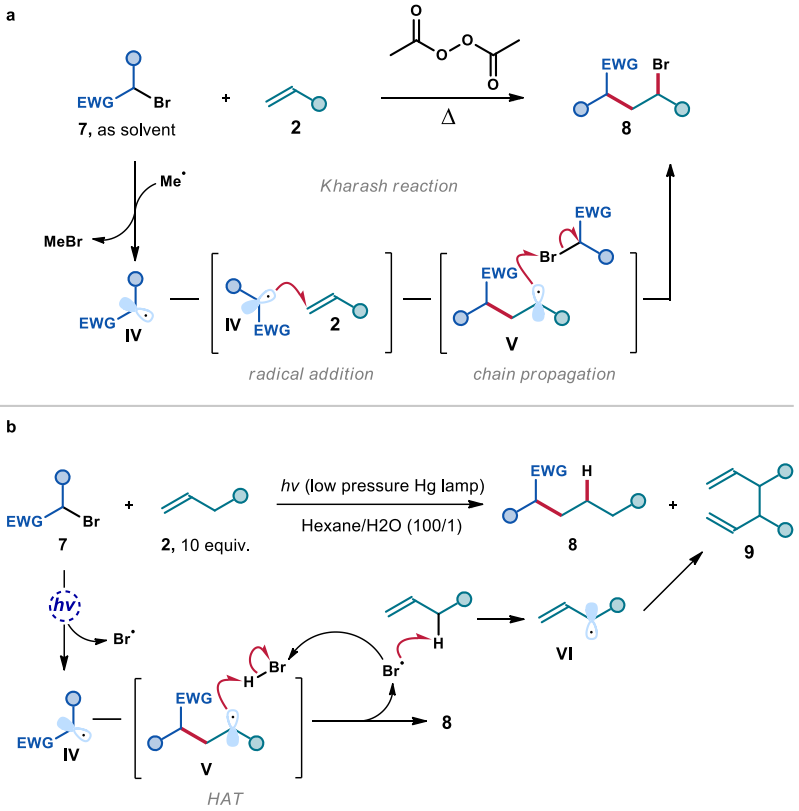

Figure 3.5. (a) Kharash reaction. (b) Hydroalkylation of electron-rich olefins via formation of electrophilic radicals.

While these processes have recently been implemented in photoredox-catalyzed manifolds, the radical sources of choice are still α-EWG haloalkanes.[11] Exploiting the abundant electron-poor olefins as radical sources of electron-deficient radicals for olefin hydroalkylation reactions would enable the rapid molecular complexity increase via formation of sp^3-rich products.

3.2.2 Olefins as sources of electrophilic radicals

A possible strategy to obtain electrophilic carbon-centered radical starting from an olefin is a radical attack by a nucleophilic radical on an electron-poor olefin. Upon this, an electrophilic

[11] (a) Arceo, E.; Montroni, E.; Melchiorre, P. "Photo-Organocatalysis of Atom-Transfer Radical Additions to Alkenes" *Angew. Chem. Int. Ed.* **2014**, *53*, 1; (b) Nakajima, M.; Lefebvre, Q.; Rueping, M. "Visible light photoredox-catalysed intermolecular radical addition of α-halo amides to olefins." *Chem. Commun.* **2014**, *50*, 3619; (c) Spinnato, D.; Schweitzer-Chaput, B.; Goti, G.; Ošeka, M. A; Melchiorre, P. "Photochemical Organocatalytic Strategy for the α-Alkylation of Ketones using Radicals." *Angew. Chem., Int. Ed*. **2020**, *59*, 9485.

radical **IV** is formed, which could either be reduced, or it could attack another olefin to furnish a product of a multicomponent cascade. Such strategy has been reported by Mizuno in 1988 in form of a carboallylation protocol (Figure 3.6.a).[12] In this transformation, a nucleophilic radical **VII** was generated from a corresponding iodide **10** via halogen atom abstraction by a tributyl tin radical. This nucleophilic radical **VII** then attacked an electron-poor olefin **1** in a polarity-match step. The ensuing electrophilic radical **IV** was finally trapped by an electron-rich olefin **11** possessing a tributyltin group in the allylic position. This group was subsequently released upon radical fragmentation, sustaining a radical chain reaction.

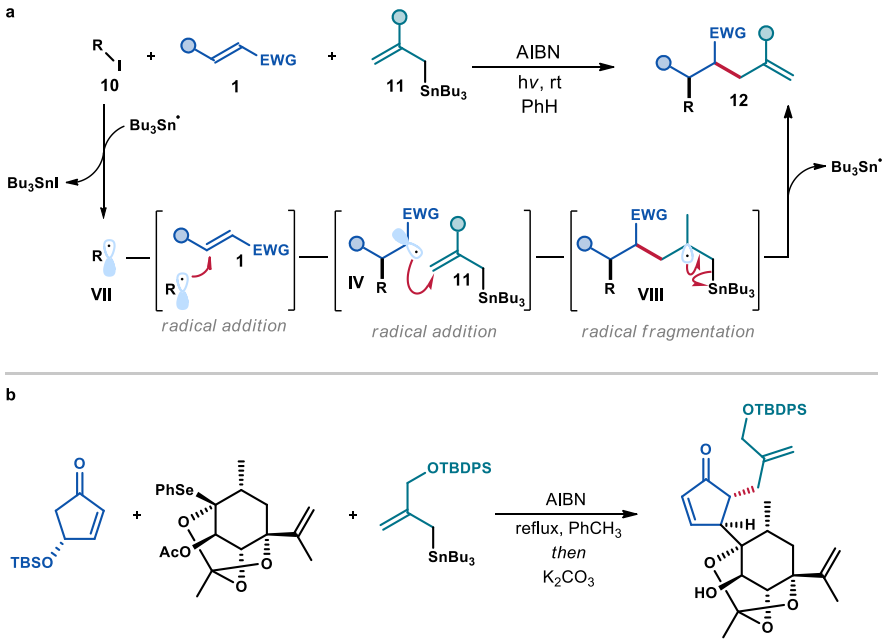

Figure 3.6. (a) Three component reaction in which an electrophilic radical **IV** participates in a radical addition step. (b) Utilization of this strategy in total synthesis of *Resiniferatoxin*.

This strategy has been used in total synthesis of complex natural products, as it simultaneously forges two *C*-*C* bonds with high degree of chemo- and regioselectivity (Figure 3.6.b),[13] highlighting the synthetic potential of electron-poor olefins as sources of electrophilic radicals. However, this particular protocol only works for a very precise set of reagents and is inherently limited to three component reactions. A more direct way of generating

[12] Mizuno, K.; Ikeda, M.; Toda, S.; Otsuji, Y. "Regioselective double vicinal carbon-carbon bond forming reactions of electron-deficient alkenes by use of allylic stannanes and organoiodo compounds." *J. Am. Chem. Soc*. **1988**, *110*, 1288.

[13] Murai, K.; Katoh, S.-I.; Urabe, D.; Inoue, M. "A radical-based approach for the construction of the tetracyclic structure of resiniferatoxin." *Chemical Science* **2018**, *4*, 2364.

electrophilic radicals from electron-poor olefins would provide new avenues for the development of useful synthetic methodologies.

3.2.3 Single-electron reduction of electron-poor olefins

Another method for generating open-shell intermediates from electron-poor olefins **1** is through their SET reduction. Historically, this radical generating strategy has been accomplished via electrochemical means or by action of stoichiometric reducing agents, including SmI_2 or polyaromatic radical anions.[14] For example, one of the most successful commercialized organic electrochemical processes is the "Monsanto process" for adiponitrile synthesis, developed by Baizer at Monsanto company in 1964 (Figure 3.7).[15] The precise mechanism of this transformation has been long debated. Contemporary understanding suggests that acrylonitrile **13** is reduced forming the radical anion **III**. Two of these radical anions **III** then undergo radical dimerization, forming a dianionic intermediate **IX** which furnishes the product after protonation.[16] From the mesomeric structures of **III** (Figure 3.7), it could be deduced that this species should theoretically be capable of reacting as either radical or anion at the *β*-position, and correspondingly as either anion or radical at the *α*-position. The acrylonitrile coupling is an example of reactivity as a radical at the *β*-position and anion at the *α*-position.

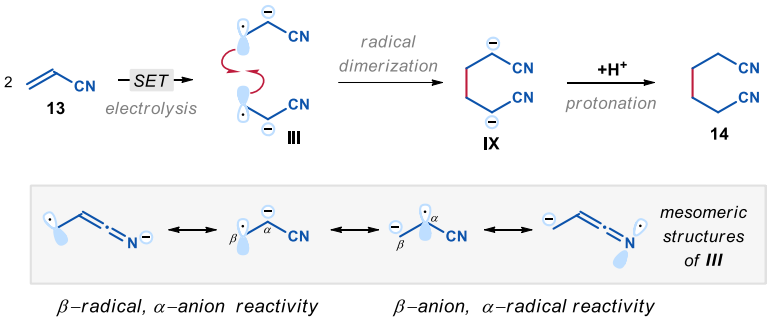

Figure 3.7. Mechanism of adiponitrile synthesis and the mesomeric forms of intermediate **III**

[14] (a) Kise, N.; Mashiba, S.-I.; Ueda, N. "Stereoselective Hydrocoupling of Optically Active 3-trans-Cinnamoyloxazolidinones by Electroreduction" *J. Org. Chem.* **1998**, *63*, 7931; (b) Hutton, T. K.; Muir, K. W.; Procter, D. J. "Switching between Novel Samarium(II)-Mediated Cyclizations by a Simple Change in Alcohol Cosolvent" *Org. Lett.* **2003**, *5*, 4811; (c) Yang, J.; Felton, G. A.; Bauld, N. L.; Krische, M. J. "Chemically induced anion radical cycloadditions: intramolecular cyclobutanation of bis(enones) via homogeneous electron transfer." *J. Am. Chem. Soc*. **2004**. 126, 1634-1635; (d) A. Baba, M. Yasuda, Y. Nishimoto, "Partial Reduction of Enones, Styrenes, and Related Systems." *Comprehensive Organic Synthesis II*, **2014**, 673.

[15] (a) Baizer, M. M. "Electrolytic Reductive Coupling: I. Acrylonitrile" *J. Electrochem. Soc*. **1964**, *111*, 215 (b) Botte, G. G. "Electrochemical Manufacturing in the Chemical Industry." *The Electrochemical Society Interface* **2014**, *23*, 49.

[16] Costentin, C.; Saveant, J.-M. "Dimerization of electrochemically generated ion radicals: mechanisms and reactivity factors" *J. Electroanal. Chem.* **2004**, *564*, 99.

An example of *β*-anion, *α*-radical reactivity of intermediate **III** was reported in 2003 by the group of Procter.[14b] The authors demonstrated that adjusting the rate of protonation of the radical anion **III** via solvent choice could influence the reactivity profile of this intermediate (Figure 3.8). When methanol was used (path *i*), the protonation of the acrylate radical anion **III** proceeded efficiently furnishing the *α*-EWG radical **IV**, which was further reduced by another equivalent of samarium iodide to undergo an intramolecular nucleophilic cyclization, forming a cyclopentanol ring. Alternatively, the choice of *tert*-butyl alcohol inhibited the protonation (Figure 3.8, path *ii*), enabling radical anion **III** to cyclize with the ketone moiety straight away, forming a cyclobutanol ring. This process resulted in the formation of α-EWG radical **IV'** that once again was further reduced to furnish the product after an aqueous workup.

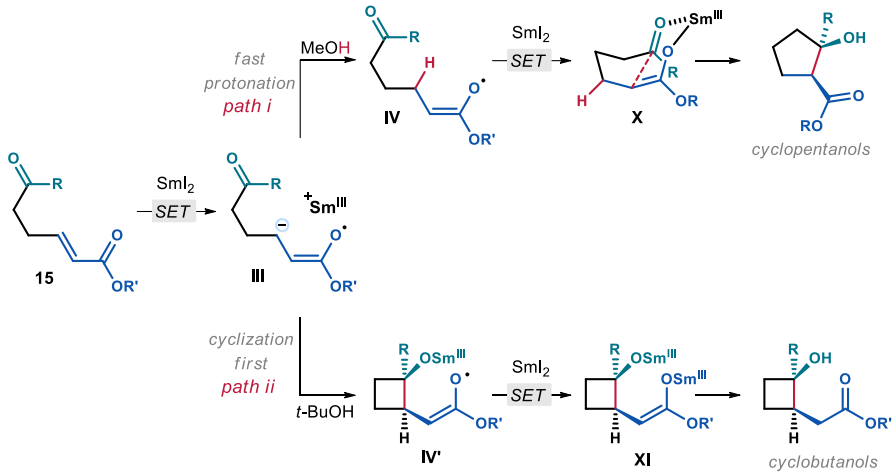

Figure 3.8. Effect of protonation on the reaction profile of radical-anion **III**

This protocol demonstrated that it is possible to generate an electrophilic radical **IV** from electron-poor olefins via a SET reduction/protonation sequence, though the radical reactivity was not fully exploited as the radical was simply reduced to the anion and protonated to form the product. Moreover, superstoichiometric quantities of SmI_2 were required, limiting the synthetic viability of the protocol.

With the advent of photoredox catalysis, radical generation has become possible under much milder and more efficient conditions. Photoredox catalysis also served to reduce electron-poor olefins to form the corresponding radical anions **III**.[17] Generally, the radical anion **III**

[17] Selected examples: (a) N. J. Venditto, Y. S. Liang, R. K. El Mokadem, D. A. Nicewicz, "Ketone-Olefin Coupling of Aliphatic and Aromatic Carbonyls Catalyzed by Excited-State Acridine Radicals." *J. Am. Chem. Soc*. **2022**. 144, 11888-11896; (b) T. Ju et al., "Dicarboxylation of alkenes, allenes and (hetero)arenes with CO2 via visible-light photoredox catalysis." *Nat. Catal*. **2021**, *4*, 304-311; (c) Kang, W.-J.; Li, B.; Duan, M.;

participated in the reactions at the nucleophilic anionic carbon, with the resulting radical **IV** being subsequently reduced via a SET or HAT process (Figure 3.9).

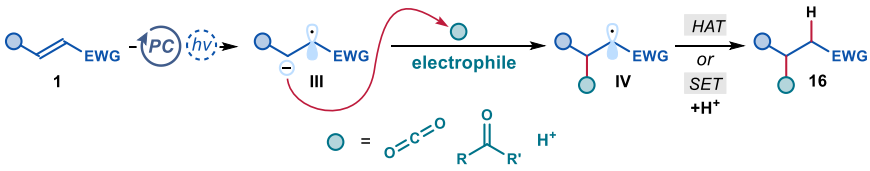

Figure 3.9. Photocatalytic generation of radical anion **III** via SET reduction of electron-poor olefins

For example, reactivity similar to that described by Procter was implemented in a photoredox manifold by Nicewicz in 2022 (Figure 3.10).[17a] This process was mediated by an acridinium photocatalyst Mes-Acr^{+} that upon photoexcitation underwent reduction by *N*,*N*-diisopropylethylamine (DIPEA). The reduced form of the photocatalyst (Mes-Acr$^{\bullet}$) was than excited by a second photon, forming a highly reductive excited state (*Mes-Acr$^{\bullet}$; E_{red}* = −3.36 V vs SCE in MeCN). This species reduced substrate **17**, furnishing the radical anion **III**. This radical anion then underwent a reversible cyclization to form the five-membered ring of the radical **IV'** that was further transformed to product **18** following protonation and HAT with 1,4-cyclohexadiene. Alternatively, the radical anion **III** could be protonated to radical **IV**, forming byproduct **19** after subsequent HAT reduction.

Pan, G.; Sun, W.; Ding, A.; Zhang, Y.; Houk, K. N.; Guo, H., "Discovery of a Thioxanthone–TfOH Complex as a Photoredox Catalyst for Hydrogenation of Alkenes Using p-Xylene as both Electron and Hydrogen Sources." *Angew. Chem. Int. Ed.* **2022**, *61*, e202211562.

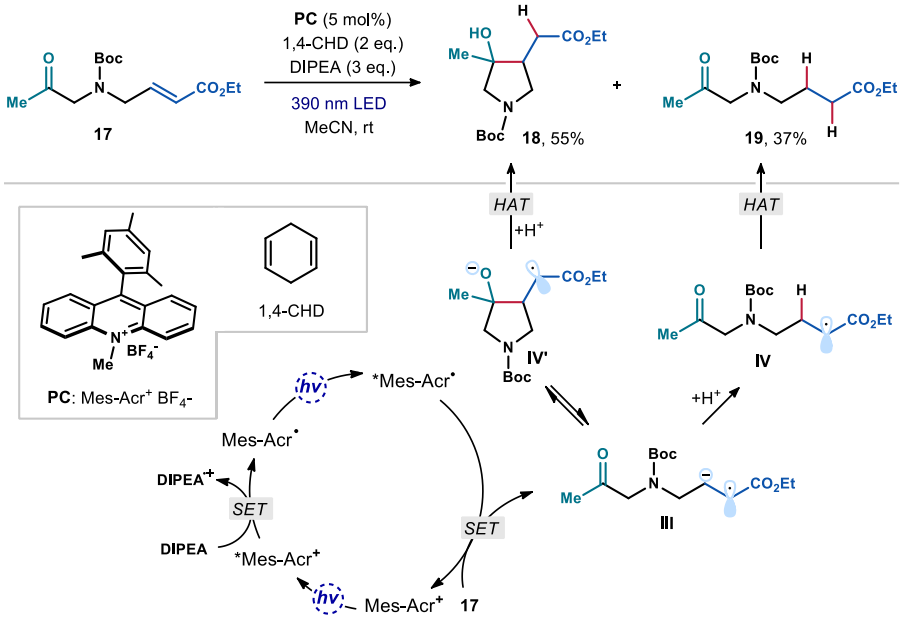

Figure 3.10. Photocatalytic intramolecular nucleophilic cyclization via SET reduction of electron-poor olefins

As is the case with other mentioned studies, the radical reactivity of intermediate **IV** has not been fully exploited in this protocol. The first example of a strategy that took advantage of radical **IV** was reported by the group of Huang in 2021 (Figure 3.11).[18] In this protocol, *N*-arylacrylamides **20** were protonated with triflic acid, enabling their SET reduction by the reduced form of iridium photocatalyst, leading to the electrophilic radical **IV**. This radical then underwent intramolecular radical addition to the electron-rich aromatic ring, forming radical **V** which was subsequently oxidized by the excited photocatalyst and deprotonated to form product **21**. Addition of lithium bromide drastically increased the yield and rate of the reaction, suggesting that bromide anion was the initial quencher of the excited state of the photocatalyst, forming bromine radical that could participate in a reversible bromination reaction with the radical **IV**.

[18] Liu, Z.; Zhong, S.; Ji, X.; Deng, G.-J.; Huang, H. Hydroarylation of Activated Alkenes Enabled by Proton-Coupled Electron Transfer. *ACS Catal.* **2021**, *11*, 4422.

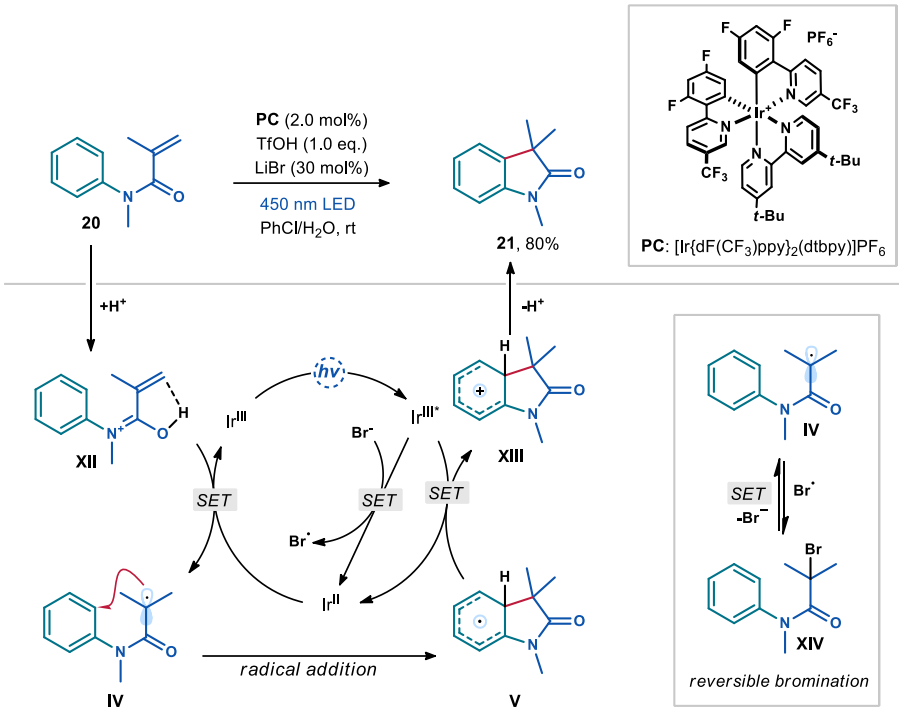

Figure 3.11. Photocatalytic intramolecular radical cyclization via single electron reduction of electron-poor olefins

When we started our studies on exploiting the radical reactivity of intermediate **IV** for olefin cross-coupling, the studies mentioned represented the full extent of existing knowledge in this field. However, during our research, the group of Gevorgyan reported a Pd-catalyzed MHAT-based strategy for olefin hydroalkenylation (Figure 3.12), furnishing the products with the same unusual connectivity targeted in our research.[19] In this protocol, a Pd^{II}-hydride complex was formed after oxidative addition of a Pd^{0} complex with a Brønsted acid (HX). The authors proposed that photoexcitation of the palladium hydride complex would enhance its hydricity, enabling regioselective hydropalladation of electron-deficient olefins **1** with subsequent *Pd-C* bond cleavage to yield Pd^{I} hybrid radical species **XV**, bearing the radical at the *α*-position to the EWG.[20] Following a radical attack by this electrophilic species to polarity-matched electron-rich styrenes **22**, a new Pd^{I} hybrid radical species **XVI** was formed, furnishing the unsaturated product **23** while regenerating the Pd^{II}-hydride complex upon *β*-H elimination.

[19] Sarkar, S.; Ghosh, S.; Kurandina, D.; Noffel, Y.; Gevorgyan, V., "Enhanced Excited-State Hydricity of Pd–H Allows for Unusual Head-to-Tail Hydroalkenylation of Alkenes." *J. Am. Chem. Soc.* **2023**, *145*, 12224.

[20] Jardim, G. A. M.; Dantas J. A.; Barboza A. A.; Paixão M. W.; Ferreira M. A. B., "Light-Driven Palladium-Radical Hybrid Species: Mechanistic Aspects and Recent Examples" *Synthesis* **2022**, *54*, 4629.

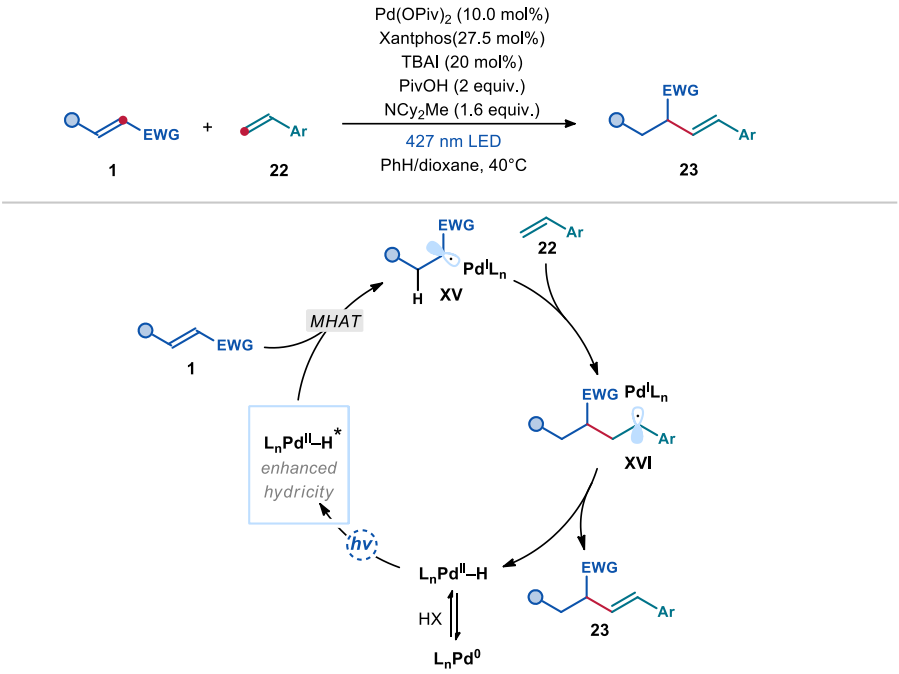

Figure 3.12. Photocatalytic reduction of electron-poor olefins and subsequent transformations with electrophiles **15**.

While this protocol demonstrated the synthetic viability of α-EWG radicals **IV** in an olefin cross-coupling reaction, the scope of the reaction partners was rather limited. For electron-poor olefins, only acrylates and acrylamides were reactive, while only styrenes were broadly amenable to this transformation serving as radical acceptors.

Overall, the reported methodologies demonstrated the viability of radical generation from electron-poor olefins through SET or MHAT strategies, including photocatalyzed protocols. However, the scope of these transformations has remained limited, providing opportunities to design novel synthetic protocols.

3.3 Design and target of the project

Our research group is interested in the discovery of new radical reactions triggered by visible light. This particular study was motivated by the lack of a general strategy to perform an olefin cross-coupling utilizing electron-poor olefins as a radical source – a process that would yield sp^3-rich products with unusual connectivity starting from olefins, which are abundant feedstock chemicals. Specifically, we aimed to exploit the electronic differences of two olefins, one being electron-poor and another electron-rich or electron-neutral. We surmised that the electron-poor substrate **1** would be susceptible to SET reduction mediated by a photocatalyst **PC**, forming the radical anion **III** which, upon protonation, would deliver a α-EWG carbon radical **IV**. This electrophilic radical **IV** would be favorably poised to react with the second electron-rich or neutral olefin **2** via radical addition. The resultant nucleophilic radical **V** would eventually undergo a polarity-matched HAT with the thiol catalyst **5** (HAT catalysis discussed in Sections 1.1 and 1.2), furnishing the reductive olefin cross-coupling products **4**. The thiyl radical formed in this process would undergo a subsequent polarity-matched HAT from a H atom donor, thus closing the HAT catalytic cycle. Overall, sp^3-rich products **4** with a distinct connectivity would be formed from two simple olefins.

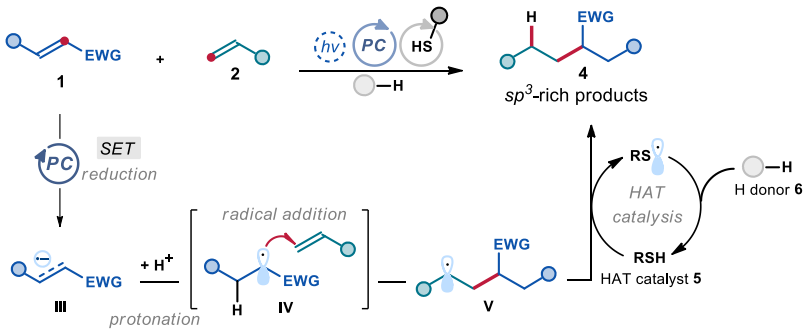

Figure 3.13. Design plan for the reductive olefin coupling using the combination of photoredox and HAT catalysis.

3.4 Results and discussion

3.4.1 Optimization

We started our investigations by using dimethyl fumarate **1a** as the radical precursor and styrene **2a** as the radical acceptor (Table 3.1). The experiments were performed in 1,2-dichloroethane (DCE) as the solvent in the presence of γ-terpinene **6a** as H atom donor[21] (2.0 equiv.) and thiophenol **5a** (20 mol. %) as the HAT catalyst under irradiation by a blue *EvoluChem* LED lamp (λ_{max} = 450 nm). We initially tested the highly reducing iridium-based photoredox catalysts **A** (E^*[(Ir(IV)/Ir(III)*] = -1.88 V vs SCE),[22] as it had the required redox power to activate **1a** [E (**1a**/**1a**$^{\cdot-}$) = -1.47 V vs SCE].[23] The cross-coupling reaction of **1a** and **2a** proceeded smoothly affording the target product **4a** in good yield (entry 1). The use of organic photocatalyst **B** [E^*(PC$^{\bullet+}$/PC*) = -1.60 V vs SCE][24] led to a drastically reduced reactivity (entry 2). The screening of other HAT catalysts **5** (entries 3-4) and H donors **6** (entry 5) confirmed that γ-terpinene **6a** and thiophenol **5a** offered the best results. We also used a stoichiometric amount of thiophenol **5a** to avoid the need of any additional H donor (entry 6), but product **4a** was obtained in low yield because of competitive thiol-ene and sulfa-Michael processes. Control experiments established that the presence of the H donor (γ-terpinene **6a**, entry 6), the HAT catalyst (thiophenol **5a**, entry 7), photocatalyst **A** (entry 8), and light (entry 9) was essential for reactivity. When adding the radical scavenger TEMPO under the optimal conditions, the reactivity was completely inhibited (entry 10), which was congruent with a radical path being operative.

---

[21] Bhunia, A.; Studer, A. Recent advances in radical chemistry proceeding through pro-aromatic radicals. *Chem* **2021**, *7*, 2060.

[22] Wu, Y.; Kim, D.; Teets, T. S. "Photophysical Properties and Redox Potentials of Photosensitizers for Organic Photoredox Transformations." *Synlett* **2022**, *33*, 1154.

[23] Montanaro, S.; Ravelli, D.; Merli, D.; Fagnoni, M.; Albini, A. "Decatungstate as Photoredox Catalyst: Benzylation of Electron-Poor Olefins." *Org. Lett.* **2012**, *14*, 4218.

[24] Speckmeier, E.; Fischer, T. G.; Zeitler, K. A "Toolbox Approach to Construct Broadly Applicable Metal-Free Catalysts for Photoredox Chemistry: Deliberate Tuning of Redox Potentials and Importance of Halogens in Donor-Acceptor Cyanoarenes." *J. Am. Chem. Soc.* **2018**, *140*, 15353.

Table 3.1. Optimization studies.

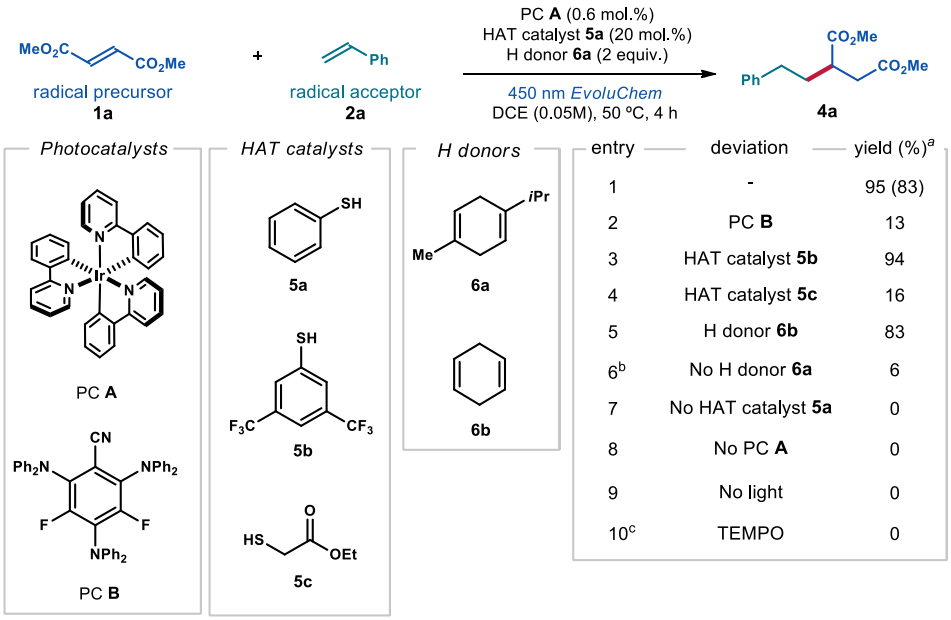

Reactions performed on a 0.1 mmol scale using 1 equiv. of styrene **2a** and 1.5 equiv. of dimethyl fumarate **1a** under illumination by a blue LED (*EvoluChem*) at 450 nm. [a]Yield of **4a** determined by GC-FID analysis of the crude reaction mixture using 1,3,5-trimethoxybenzene as the internal standard. Yields of isolated **4a** are reported in parentheses (0.2 mmol scale). [b] Performed using 2.0 equiv. of thiophenol **5a**. [c] Using 1.5 equiv. of TEMPO.

3.4.2 Mechanistic proposal

From the control experiments described in Table 3.1, entries 7-9, we knew that light, photocatalyst **A**, and HAT catalyst **5** were each required for the reaction to proceed. To gain insight into the reaction mechanism, we conducted Stern−Volmer quenching studies (experimental details in section 3.7.6.1; theoretical basis for this experiment discussed in Section 2.5.2). Irradiating a DCE solution of photoredox catalyst **A** at 440 nm revealed emission with a maximum at 513 nm. Measurements in the presence of increasing amounts of quenchers showed that dimethyl fumarate **1a** is an effective quencher, much more so than styrene **2a** (Figure 3.14.a). This observation aligns with our mechanistic proposal in which the excited photocatalyst can effectively reduce the electron-poor olefin **1** via SET, leading to the reactive radical anion of type **III** (Figure 3.14.b). The ensuing radical anion **III** would then undergo protonation to give radical **IV**, which can be intercepted by olefin **2**. The resulting radical **V** could then abstract a hydrogen atom from thiol **5**, leading to the reductive olefin coupling product **4** and thiyl radical **RS•**. Meanwhile, thiolate **RS**$^-$ [E (**PhS•**/**PhS**$^-$) =

+0.07 V vs SCE][25] could be oxidized by the oxidized photocatalyst (E[Ir(IV)/Ir(III)] = 0.77 V vs SCE)[22] to turn over the photocatalyst and generate the thiyl radical **RS•**. This latter radical can abstract a hydrogen atom from γ-terpinene **6a** to regenerate the thiol catalyst **5**.

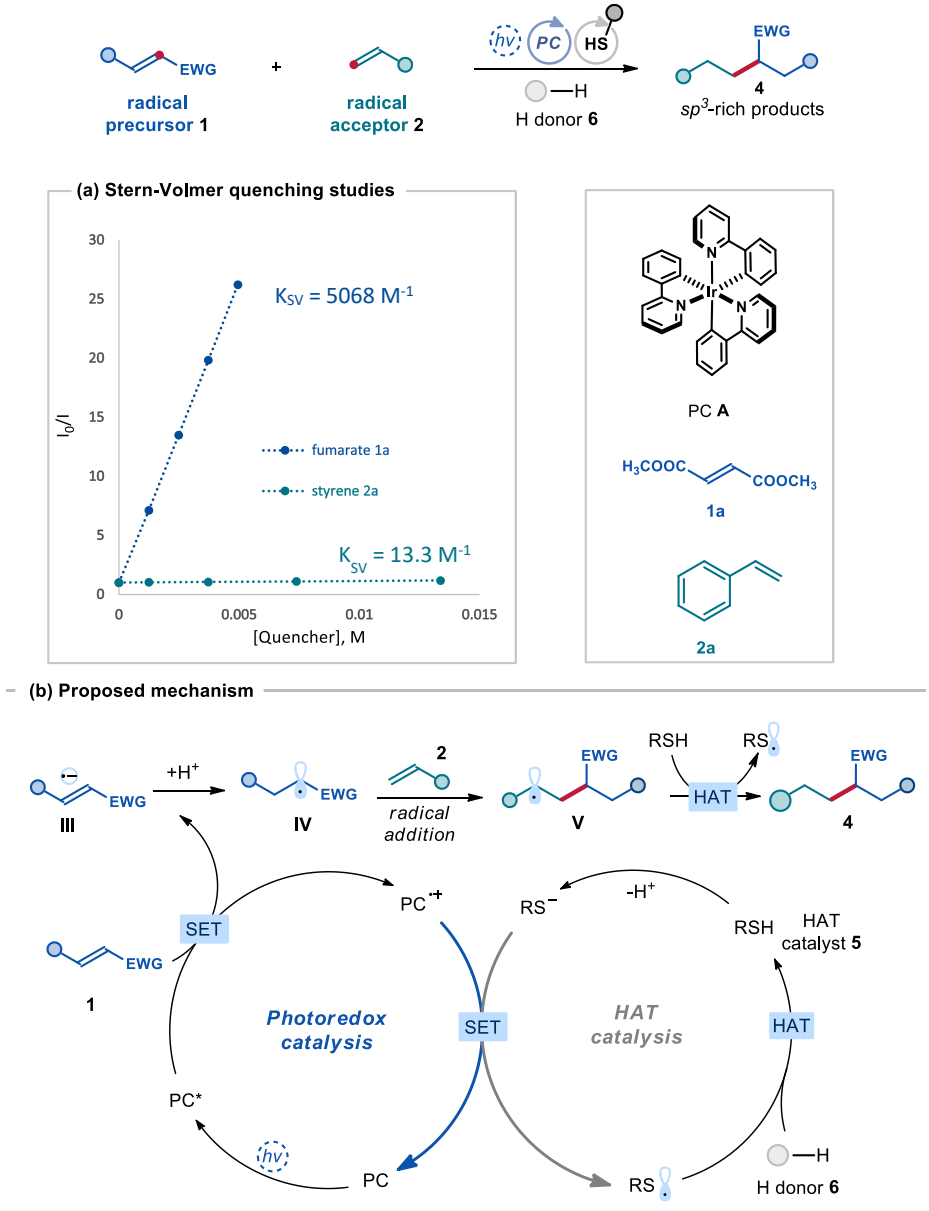

Figure 3.14. (a) Stern-Volmer quenching plot. (b) Mechanistic proposal

[25] Bordwell, F. G.; Zhang, X.-M.; Satish, A. V.; Cheng, J. P. "Assessment of the Importance of Changes in Ground-State Energies on the Bond Dissociation Enthalpies of the O-H Bonds in Phenols and the S-H Bonds in Thiophenols." *J. Am. Chem. Soc.* **1994,** *116*, 6605.

3.4.3 Generality of the system

With the optimized conditions in hand (entry 1 in Table 3.1), we investigated the scope of radical acceptors using fumarate **1a** as the radical precursor (Figure 3.15). First, we demonstrated that the process was equally efficient on a 5 mmol scale, yielding 1.0 gram of product **4a** (80% yield). Styrenes with different substitution at the *ortho*-, *meta*-, and *para*-position afforded the olefin cross-coupling products **4b-h** with good to excellent yields. Non-activated terminal olefins bearing aliphatic substituents were suitable for this process, affording the corresponding products **4i**-**n** in good yields. A variety of functional groups were tolerated well, including a free alcohol (products **4j** and **4m**), a halogen atom (**4l**), and an aldehyde (**4n**). Electron-rich and heteroatom-functionalized olefins were also reactive, affording products **4o-q**. While terminal disubstituted olefins offered good yields (adduct **4m-n**, **4s-w**), internal olefins exhibited reduced reactivity. For example, *trans*-*β*-methyl styrene afforded product **4r** in 44% yield (see Section 3.4.5 for an overview of substrates that proved unreactive or poorly reactive). The higher reactivity of terminal olefins allowed us to chemoselectively functionalize a derivative of *Gibberellic* acid (adduct **4t**), leaving the internal double bond unaffected. Our methodology was also suitable for the late-stage functionalization of natural products and their derivatives bearing an olefin moiety. For example, *Biotin* and *Bezafibrate* derivatives reacted smoothly to provide adducts **4s** and **4u**, respectively. When *β*-pinene or *caryophyllene oxide* were reacted, the ring-opening products **4v** and **4w**, respectively, were obtained in good yields. This observation supports the involvement of a radical of type **V** (Figure 3.14) as an intermediate in the process.

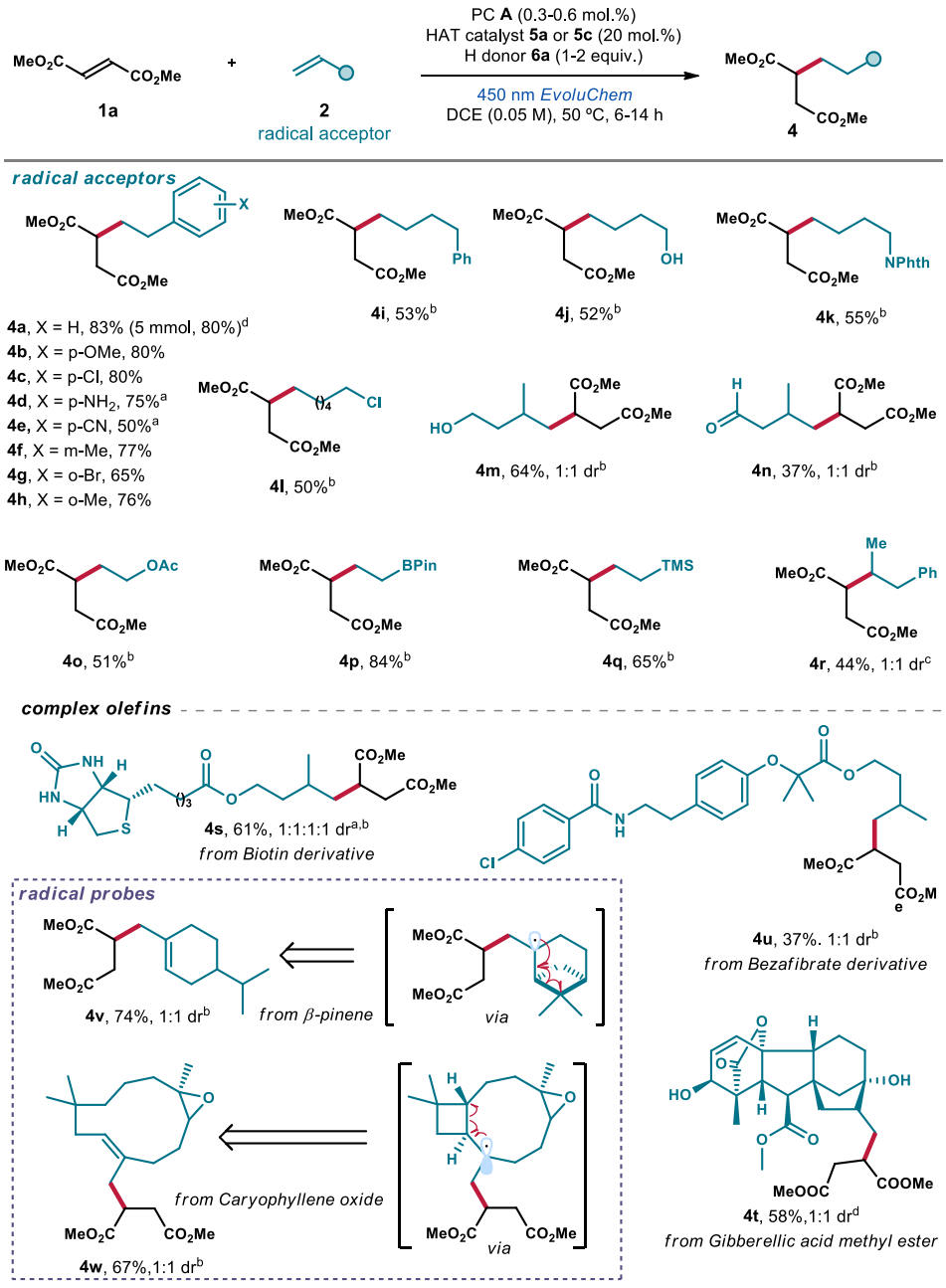

Figure 3.15. Substrate scope of the radical acceptors. Reactions performed on a 0.2 mmol scale at 50°C using **1a** (1.5 equiv.), PC **A** (0.6 mol%), thiophenol **5a** (20 mol%) and γ-terpinene **6a** (2.0 equiv.). Yields refer to isolated products **4**. [a]Yield determined by ^{1}H NMR analysis of the crude mixture using dibromomethane as the internal standard. [b]Performed using PC **A** (0.3 mol.%), ethyl thyoglycolate **5c** (20 mol.%), γ-terpinene **6a** (1 equiv.) and an excess of **2** (3 equiv). [c]Performed using PC **A** (0.3 mol.%), thiophenol **5a** (20 mol.%), γ-terpinene **6a** (1 equiv.) and an excess of **2** (3 equiv). [d]Performed using PC **A** (0.3 mol.%), ethyl thyoglycolate **5c** (20 mol.%), γ-terpinene **6a** (1 equiv.) and an excess of **2** (3 equiv), with the addition of 1.0 ml of acetone. *N*-Phth: phthalimide; Ac: acetyl; Bpin: bis(pinacolato)boron; TMS: trimethylsilyl.

Next, we assessed the electron-poor olefins capable of reacting with styrene **2a** in our olefin cross-coupling protocol (Figure 3.16).

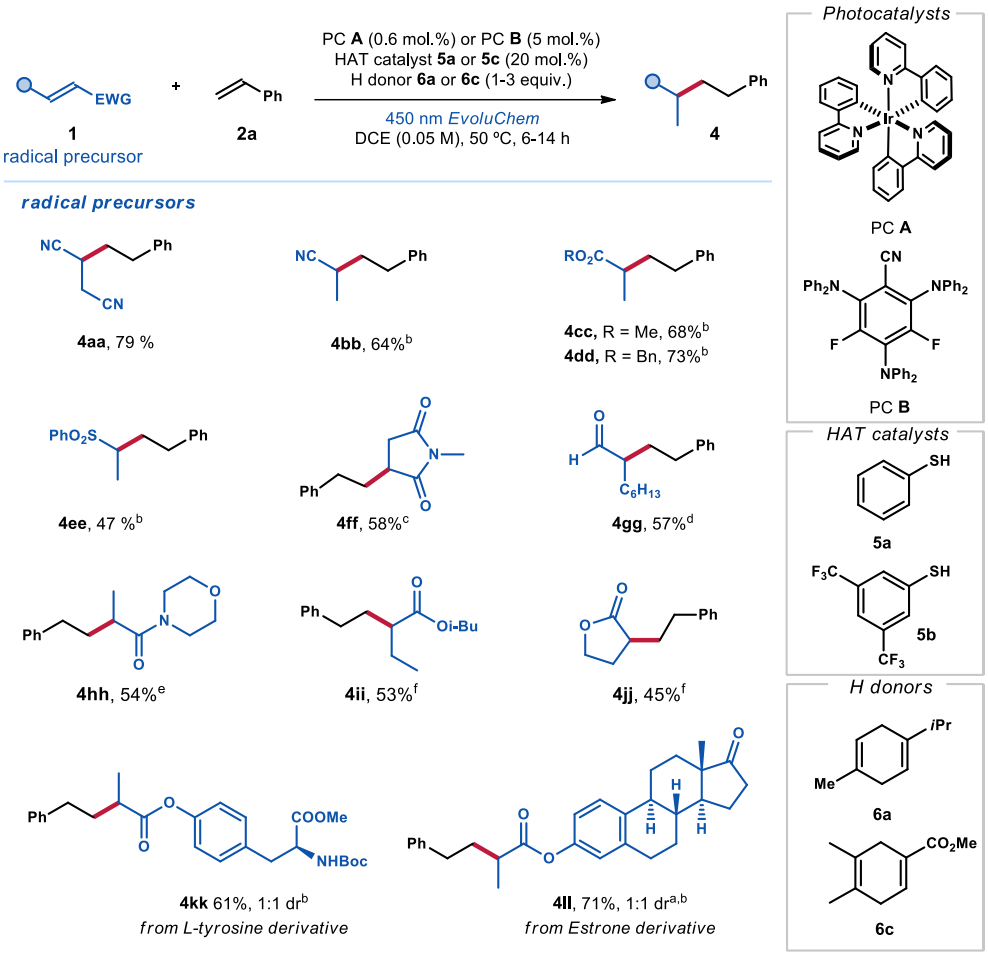

Figure 3.16. Substrate scope of the electron-poor olefins as the radical precursors. Reactions performed on a 0.2 mmol scale using PC **A** (0.6 mol.%), thiophenol **5a** (20 mol. %) and γ-terpinene **6a** (3.0 equiv.); yields refer to isolated products **4.** [a]Yield determined by ^{1}H NMR analysis of the crude mixture using dibromomethane as the internal standard. [b]Performed using PC **B** (5.0 mol.%), thiophenol **5a** (20 mol. %) and 2,4,6-collidine (100 mol.%); [c]Performed using PC **A** (0.6 mol.%), HAT catalyst **5b** (20 mol.%) and H donor **6c** (2 equiv.); [d]Performed using PC **B** (5.0 mol.%), HAT catalyst **5b** (20 mol.%) and H donor **6c** (3 equiv.); [e]Performed using PC **A** (1.5 mol.%), HAT catalyst **5b** (20 mol.%) and H donor **6c** (3 equiv.); [f]Performed using PC **A** (1.5 mol. %), Cs_2CO_3 (1 equiv.), thiophenol **5a** (20 mol.%), H donor **6a** (3 equiv.) in MeCN (0.05 M). Bn: benzyl; *i*-Bu: isobutyl.

We found that fumaronitrile could serve as a radical precursor, yielding product **4aa** in high yield. By using photocatalyst **B** in combination with a weak base (2,4,6-collidine, 1 equiv.), we achieved enhanced reactivity with less activated electron-poor olefins (a possible rationale for this phenomenon is provided in section 3.5.3). Under these slightly modified conditions,

acrylonitrile, acrylates, and vinyl sulfone underwent smooth reactions, yielding the corresponding products **4bb-ee** in moderate to good yields. Other electron-poor olefins, such as *N*-methyl maleimide, an enal, and an acrylamide, suffered from excessive formation of the corresponding reduced products (the mechanism of byproduct formation is discussed in Section 3.4.4). This issue was resolved by using a more electrophilic HAT catalyst **5b** and the H atom donor **6c**, which furnished products **4ff–hh** in decent yields. The protocol was also effective for internal and cyclic acrylates, affording adducts **4ii-jj**. Furthermore, acrylates derived from bio-relevant molecules successfully participated in our coupling method (products **4kk-ll**).

To demonstrate the versatility of the methodology, we investigated cross-coupling reactions between less activated benzyl acrylate **1d** and substrates other than styrene **2a**, leading to the formation of adducts **4mm** and **4nn** in moderate yield (Figure 3.17).

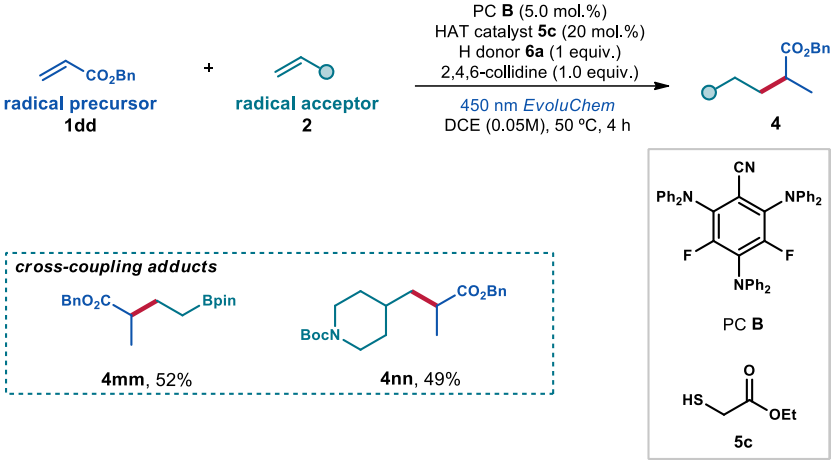

Figure 3.17. Expanding the substrate scope. Reactions performed on a 0.2 mmol scale; yields refer to isolated products **4**.

3.4.4 Byproducts of the reaction

In this reaction, the only major byproduct we observed is the reduced product **24** (Figure 3.18). This product is the result of hydrogen atom transfer between the electrophilic radical **IV**, generated upon SET reduction and protonation, and the polarity-matched H donor **6**.

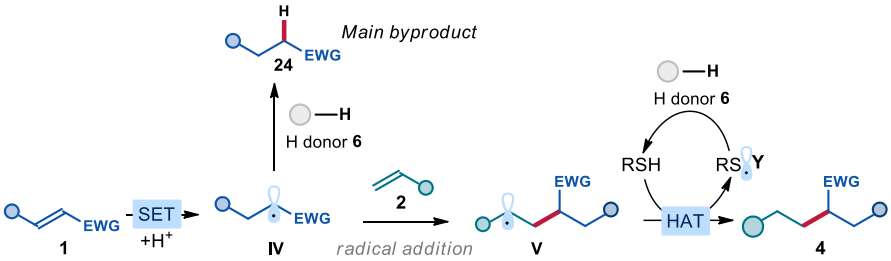

Figure 3.18. Mechanistic proposal for the formation of byproduct **24**.

3.4.5 Reaction limitations

We have encountered several substrate classes that are not compatible with our olefin cross-coupling protocol (Figure 3.19). For the radical acceptors, only one internal olefin was operative (product **4r**, Figure 3.15), with the rest exhibiting drastically reduced reactivity and yields, including acyclic, cyclic, and heteroatom substituted electron-rich internal olefins (Figure 3.19.a). In these reactions, complete conversion of the radical precursor was observed, with the formation of the reduced byproduct (Figure 3.18). We attribute this to steric effects, as internal olefins are significantly more hindered than terminal ones, thus inhibiting the rate of radical addition of radical **IV**. Therefore, byproduct **24** formation via competitive HAT process with the H donor **5** becomes the dominant reaction pathway (Figure 3.18).

As for the radical precursors (Figure 3.19.b), *β*-phenyl substituted electron-poor olefins delivered the cross-coupling products only in low yield, mainly because of the formation of [2+2] photocycloaddition byproducts. Acyclic and cyclic enones also proved to be incompatible with the protocol, forming complex mixtures of products.

Our attempts to engage less activated olefins (Figure 3.19.c), namely methyl acrylate and 4-phenylbutene, with each other only resulted in low yields of the product, once again due to formation of the reduced byproduct **24**.

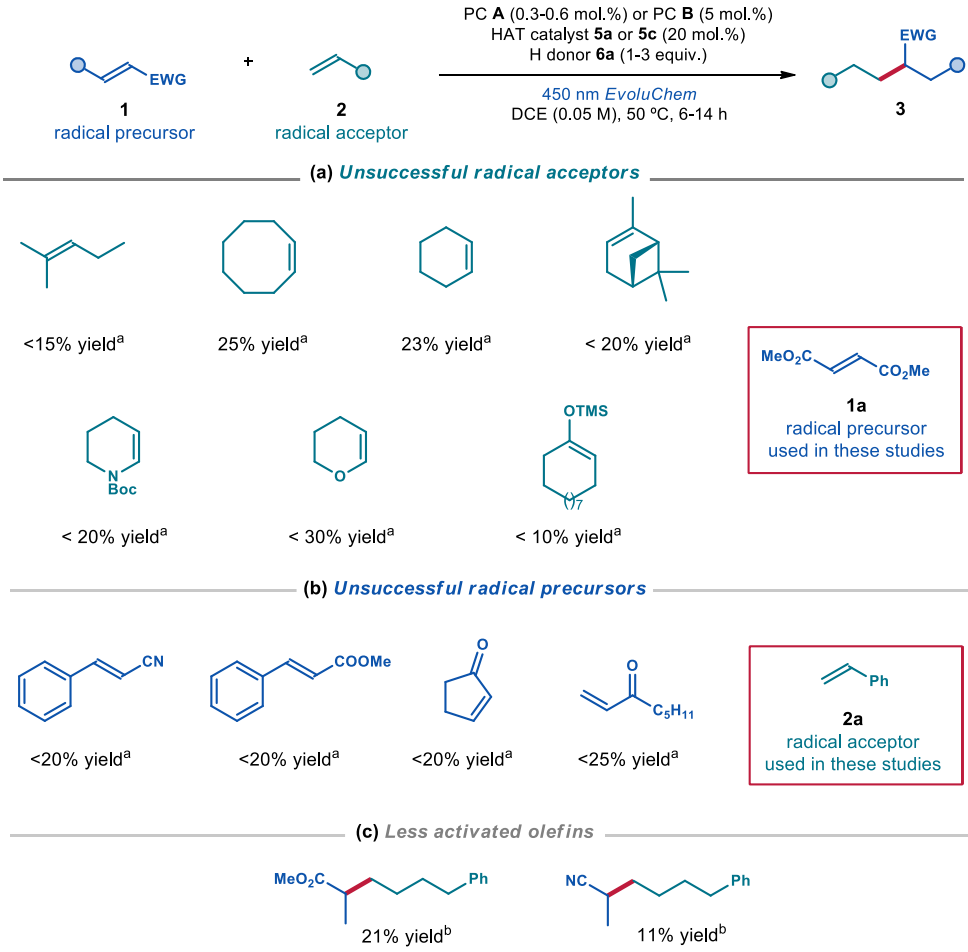

Figure 3.19. Moderately successful and unsuccessful substrates. Reactions performed on a 0.2 mmol scale. [a]Yield determined by ^{1}H NMR analysis of the crude mixture using dibromomethane as the internal standard. [b]Yield determined by GC-FID analysis of the crude reaction mixture using 1,3,5-trimethoxybenzene as the internal standard

3.5 Mechanistic investigations

3.5.1 Radical clock experiment

To gain an indication of intermediacy of the radical **IV** under the reaction conditions, we performed a radical clock experiment. A cyclopropyl-containing olefin **25** was used, which provided the ring-opening product **26** in good yield (Figure 3.20). This product formation is congruent with the addition of radical **IV** to substrate **25** to form radical **V**, which subsequently undergoes cyclopropane ring opening to radical **V'**, which finally is reduced via HAT to form product **26**.

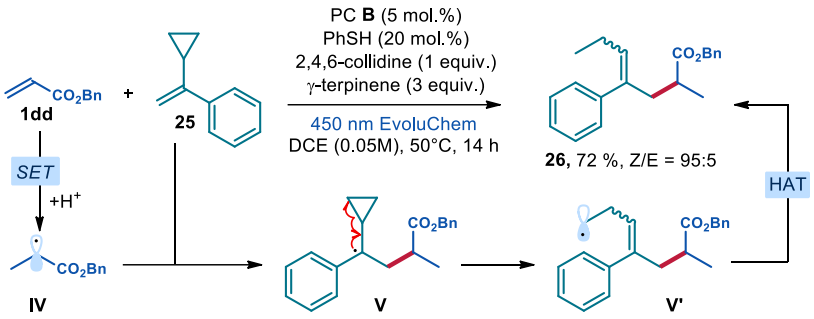

Figure 3.20. Radical clock experiment

3.5.2 Deuterium labeling experiment

To gain further insight into the reaction mechanism, we performed a deuterium labeling study (Figure 3.21). For this, we added D_2O into the standard reaction involving benzyl acrylate **1dd** and styrene **2a**. A partially deuterated product **4dd-D** was formed in 52% yield, with 70% deuterium incorporation at the *β*-position of the acrylate moiety, and 30% deuterium incorporation at the benzylic position. These results are consistent with the formation of the radical anion **III**, its subsequent deuteration by the D_2O forming radical **IV**, followed by radical addition to styrene **2a** to form radical **V**. This nucleophilic radical can undergo a hydrogen atom transfer with a polarity matched PhSH or PhS**D**, which could form *in situ* via deuterium exchange with D_2O, furnishing the deuterated product **4dd-D**.

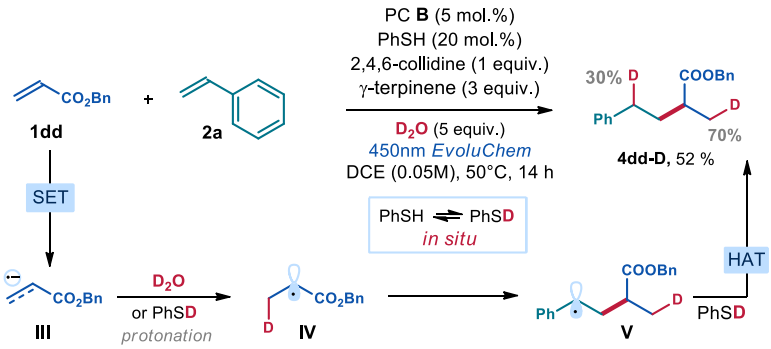

Figure 3.21. Deuterium labeling experiment

3.5.3 Mechanistic rationale for less activated substrates

As demonstrated by the Stern-Volmer quenching experiments (Sections 3.4.2 and 3.7.6.1), PC **A** (E*[(Ir(IV)/Ir(III)*] = -1.88 V vs SCE)[22] in the model conditions was capable of reducing the more activated substrates (i.e. dimethyl fumarate **1a**, E(**1a**/**1a**$^{\bullet-}$) = -1.47 V vs SCE).[23]

Mechanistic experiments (Sections 3.5.1 and 3.5.2) suggested that the reaction with less activated substrates, such as benzyl acrylate **1dd** [E(**1dd**/**1dd**$^{\bullet-}$) = -2.2 V vs SCE],[26] proceeded through the same intermediary radical anion **III**, which was protonated to the radical **IV**. However, the reaction with these substrates did not proceed under model conditions (Table 3.1, entry 1), requiring significant modifications (use of PC **B** and addition of 1 equivalent of 2,4,6-collidine). We propose that, due to the mild basicity of 2,4,6-collidine (pK_{aH} = 7.5), a dynamic equilibrium between thiophenol (pK_a = 6.6) and thiophenolate was established in solution (Figure 3.22). PC **B** [$E_{1/2}$(PC*/PC$^{\bullet-}$) = +0.92 V vs SCE][24] is capable of oxidizing thiophenolate (E_{ox} = +0.07 V vs SCE)[25], furnishing the highly reductive radical anion PC **B**$^{\bullet-}$ [$E_{1/2}$(PC **B**/PC **B**$^{\bullet-}$) = -1.92 V].[24] This species is more poised to reduce the less activated electron-poor substrates, furnishing the intermediate **III** which would then be involved in the reaction as described before to finally form product **4**.

[26] Matsunami, M.; Sakai, N.; Morimoto, T.; Maekawa, H.; Nishiguchi, I., "Magnesium-Promoted One-Pot Double C-Acylation and Cycloaddition of Anthracene and Double C-Acylation of Benzyl Acrylates." *Synlett* **2007**, *5*, 769.

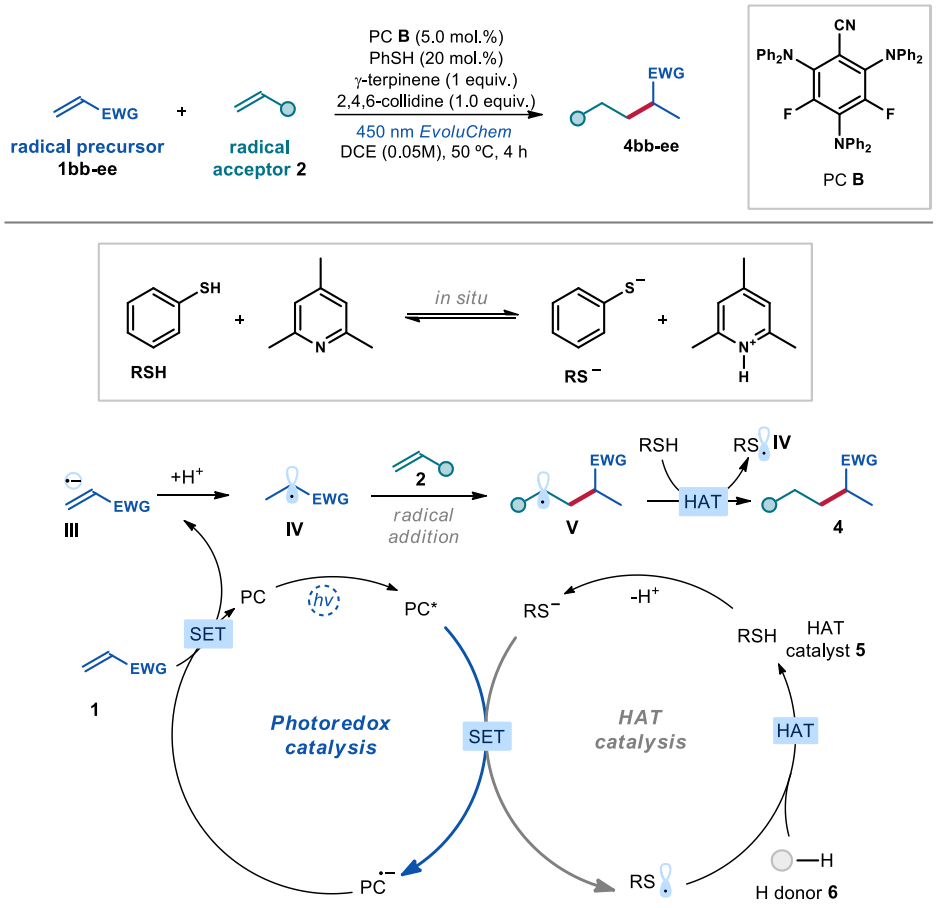

Figure 3.22. Mechanistic proposal for reactions with less activated substrates **1**.

3.6 Conclusions

In this chapter, a new light-driven strategy for the reductive olefin cross-coupling has been detailed, providing sp^3-rich products with a distinct connectivity. Central to this strategy is the exploitation of electronic differences between the two olefin partners, enabling selective radical generation via photoredox-mediated SET reduction of the electron-deficient olefins. Overall, the electron-poor substrates were readily coupled with various styrenes and other readily available neutral olefins. A notable feature of this method is its high functional group tolerance, which was leveraged for the late-stage modification of biorelevant compounds. The mechanistic proposal was supported by a mechanistic campaign, including Stern-Volmer quenching study.

3.7 Experimental section

General Information. The ^{1}H NMR, ^{19}F NMR, ^{13}C NMR spectra and UPC^{2} traces are available in the published article[1] and are not reported in the present dissertation.

The NMR spectra were recorded at 400 MHz and 500 MHz for ^{1}H, 101 or 126 MHz for ^{13}C. The chemical shift (δ) for ^{1}H and ^{13}C are given in ppm relative to residual signals of the solvents ($CHCl_3$ @ 7.26 ppm ^{1}H NMR, $CDCl_3$ @ 77.16 ppm ^{13}C NMR, and tetramethylsilane @ 0 ppm). Coupling constants are given in Hertz. The following abbreviations are used to indicate the multiplicity: s, singlet; d, doublet; t, triplet; q, quartet; m, multiplet; br. s., broad singlet; app, apparent.

High-resolution mass spectra (HRMS) were obtained from the ICIQ High-Resolution Mass Spectrometry Unit on MicroTOF Focus and Maxis Impact (Bruker Daltonics) with electrospray ionization or atmospheric pressure chemical ionization. Cyclic voltammetry (CV) studies were carried out on a Princeton Applied Research PARSTAT 2273 potentiostat offering compliance voltage up to ± 100 V (available at the counter electrode), ± 10 V scan range and ± 2 A current range.

UV-vis measurements were carried out on a Shimadzu UV-2401PC spectrophotometer equipped with photomultiplier detector, double beam optics and D_2 and W light sources or an Agilent Cary60 spectrophotometer. Spectrofluorimetry experiments were performed on a Fluorolog Horiba Jobin Yvon spectrofluorimeter equipped with a photomultiplier detector, a double monochromator, and a 350W xenon light source. Yields refer to isolated materials of >95% purity as determined by ^{1}H NMR analysis.

General Procedures. All reactions were set up under an argon atmosphere in oven-dried glassware. Synthesis grade solvents were used as purchased; anhydrous solvents were taken from a commercial SPS solvent dispenser. Chromatographic purification of products was accomplished using forced-flow chromatography (FC) on silica gel (230-400 mesh). For thin layer chromatography (TLC) analysis throughout this work, Merck pre-coated TLC plates (silica gel 60 GF_{254}, 0.25 mm) were employed, using UV light as the visualizing agent and an acidic mixture of vanillin, basic aqueous potassium permanganate ($KMnO_4$) or phosphomolybdic acid (PMA, ethanol solution) as stain solutions, and heat as developing agents. Organic solutions were concentrated under reduced pressure on a Büchi rotatory evaporator at 40°C.

Materials. Most of the starting materials used in this study are commercial and were purchased at the highest purity available from Sigma-Aldrich, Fluka, Alfa Aesar, Fluorochem, TCI, and used as received, without further purifications, unless otherwise stated.

Determination of Diastereomeric Ratio. The diastereomeric ratios were determined by ^{1}H NMR analysis of the crude reaction mixture through integration of diagnostic signals.

Materials. Most of the starting materials used in this study are commercial and were purchased at the highest purity available from Sigma-Aldrich, Fluka, Alfa Aesar, Fluorochem, TCI, and used as received, without further purifications, unless otherwise stated.

3.7.1 Substrate synthesis

Photocatalyst **B** (3DPA2FBN),[27] 4,5-dimethylcyclohexa-1,4-diene-1-carboxylate,[28] 3-methyl-3-butenal,[29] and acrylates **1k**[30] and **1l**[31] were synthesized according to reported procedures. Below, the procedures for the substrates that we have synthesized are detailed.

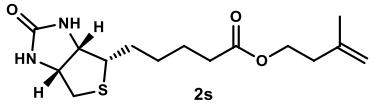

2s

3-methylbut-3-en-1-yl 5-((3aS,4S,6aR)-2-oxohexahydro-1H-thieno[3,4-d]imidazol-4-yl)pentanoate (2s): Synthesized according to a modified procedure.[32] To an oven-dred 100 mL round-bottom flask containing a magnetic stir-bar, Biotin (1.05 g, 4.3 mmol), DMAP (269 mg, 2.2 mmol) and 1-ethyl-3-(3-dimethylaminopropyl)carbodiimide hydrochloride (1.26 g, 6.6 mmol) were added. The flask was sealed with a septum and filled with argon. Dry DMF (50 ml) and 3-methylbut-3-en-1-ol (0.53 ml, 5.2 mmol) were added subsequently and the stirring was switched on. The flask was placed onto a 40 °C bath and kept overnight. The solvent was evaporated, the material dried on high vacuum and then purified via silica gel column chromatography (DCM:MeOH = 30/1) to afford the product as a white solid (1.05 g, 78% yield).

^{1}H NMR (500 MHz, $CDCl_3$) δ 5.92 (s, 1H), 5.50 (s, 1H), 4.80 – 4.78 (m, 1H), 4.73 – 4.71 (m, 1H), 4.49 (ddt, *J* = 7.8, 5.0, 1.2 Hz, 1H), 4.30 (ddd, *J* = 7.8, 4.4, 1.5 Hz, 1H), 4.18 (t, *J* = 6.9 Hz, 2H), 3.14 (ddd, *J* = 8.5, 6.5, 4.6 Hz, 1H), 2.90 (dd, *J* = 12.8, 5.0 Hz, 1H), 2.73 (d, *J* = 12.8

[27] Askey, H. E.; Grayson, J. D.; Tibbetts, J. D.; Turner-Dore, J. C.; Holmes, J. M.; Kociok-Kohn, G.; Wrigley, G. L.; Cresswell, A. J., Photocatalytic Hydroaminoalkylation of Styrenes with Unprotected Primary Alkylamines. *J. Am. Chem. Soc.* **2021**, *143*, 15936

[28] Agudo, R.; Roiban, G.-D.; Reetz, M. T. Achieving Regio- and Enantioselectivity of P450-Catalyzed Oxidative CH Activation of Small Functionalized Molecules by Structure-Guided Directed Evolution. *ChemBioChem* **2012**, *13*, 1465

[29] Henßen B., Kasparyan E., Marten G., and Pietruszka J. Synthesis of Psymberic Acid. *Heterocycles* **2007**, *74*, 245

[30] Choudhary, S.; Cannas, D. M.; Wheatley, M.; Larrosa, I. A manganese(i)tricarbonyl-catalyst for near room temperature alkene and alkyne hydroarylation. *Chem. Sci.* **2022**, *13*, 13225

[31] Hell, S. M.; Meyer, C. F.; Laudadio, G.; Misale, A.; Willis, M. C.; Noël, T.; Trabanco, A. A.; Gouverneur, V., Silyl Radical-Mediated Activation of Sulfamoyl Chlorides Enables Direct Access to Aliphatic Sulfonamides from Alkenes. *J. Am. Chem. Soc.* **2020**, *142*, 720

[32] Huang J., Zhao R., Qin S., Yang S., Li W., Mo J., Du Y., Weng X., Zhou X., 4-Thiouridine-Enhanced Peroxidase-Generated Biotinylation of RNA. *ChemBioChem* **2020**, *22*, 212

Hz, 1H), 2.35 – 2.28 (m, 4H), 1.74 (ddt, *J* = 1.4, 0.9, 0.5 Hz, 3H), 1.73 – 1.59 (m, 4H), 1.51 – 1.36 (m, 2H).

^{13}C NMR (126 MHz, $CDCl_3$) δ 173.8, 163.8, 141.8, 112.4, 62.6, 62.1, 60.2, 55.6, 40.7, 36.8, 34.0, 28.5, 28.4, 24.9, 22.6.

HRMS: (ESI$^+$) calculated for $C_{15}H_{24}N_2NaO_3S^+$ [M+Na$^+$]: 335.1400, found 335.1401.

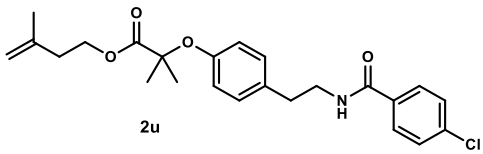

2u

3-Methylbut-3-en-1-yl 5-((3aS,4S,6aR)-2-oxohexahydro-1H-thieno[3,4-d]imidazol-4-yl)pentanoate (2u): Synthesized according to a modified procedure. To an oven-dred 100 mL round-bottom flask containing a magnetic stir-bar, Bezafibrate (778 mg, 2.15 mmol), DMAP (135 mg, 1.1 mmol) and EDCI hydrochloride (633 mg, 3.3 mmol) were added. The flask was sealed with a septum and filled with argon. Dry DMF (25 ml) and 3-methylbut-3-en-1-ol (263 μL, 2.6 mmol) were added subsequently and the stirring was switched on. The flask was placed onto a 40°C bath and kept for 5 hours. The solvent was evaporated, the material dried on high vacuum and then purified via silica gel column chromatography (DCM:MeOH = 30/1) to afford the product as a white solid (352 mg, 38% yield).

^{1}H NMR (500 MHz, $CDCl_3$) δ 7.63 – 7.58 (m, 2H), 7.40 – 7.35 (m, 2H), 7.10 – 7.05 (m, 2H), 6.83 – 6.78 (m, 2H), 6.07 (t, *J* = 5.8 Hz, 1H), 4.79 – 4.75 (m, 1H), 4.71 – 4.67 (m, 1H), 4.28 (t, *J* = 6.8 Hz, 2H), 3.66 (td, *J* = 7.0, 5.8 Hz, 2H), 2.85 (t, *J* = 7.0 Hz, 2H), 2.34 (t, *J* = 6.8 Hz, 2H), 1.73 – 1.71 (m, 3H), 1.57 (s, 6H).

^{13}C NMR (126 MHz, $CDCl_3$) δ 174.3, 166.5, 154.3, 141.4, 137.8, 133.1, 132.5, 129.6, 129.0, 128.4, 119.8, 112.7, 79.3, 63.6, 41.4, 36.7, 34.9, 25.6, 22.5.

HRMS: (ESI$^+$) calculated for $C_{24}H_{28}ClNNaO_4^+$ [M+Na$^+$]: 452.1599, found 452.1610.

3.7.2 Experimental setup

All reactions were performed using an *EvoluChem*™ P303-30-1 LEDs (18 W, λ_{max} = 450 nm, 1 cm away, Figure 3.23), a fan was used to cool down the reactor (ambient temperature 20-25°C). The temperature within the reaction vessel was measured to be between 45-55 ºC under the reaction conditions, thus 50°C is reported as the reaction temperature. This rise in temperature is attributed to heat generation from light absorption.

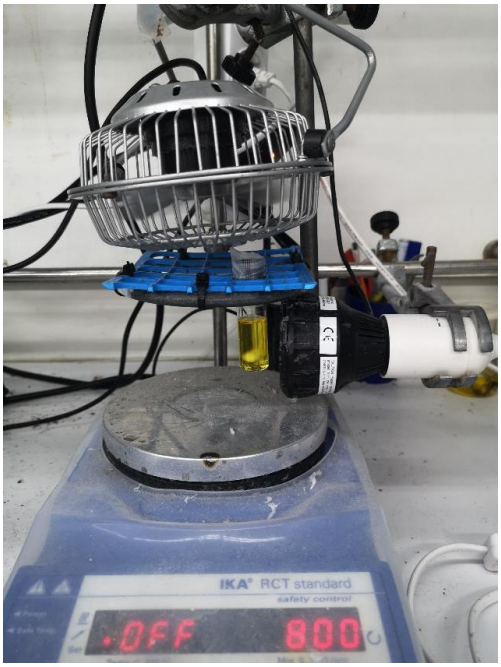

Figure 3.23. Photoreactor setup. The distance between the light source and the reaction vessel was maintained at 10 mm.

3.7.3 General procedure

Stock solution preparation of fac-Ir(ppy)$_3$: To an oven-dried 8 mL vial, 4.0 mg of *fac*-Ir(ppy)$_3$ were added. The vial was sealed with a septum, evacuated and backfilled with argon three times, and 4.0 mL of degassed DCE were added. The resulting suspension was sonicated for 10-15 minutes until complete dissolution and *used the same day as prepared*.

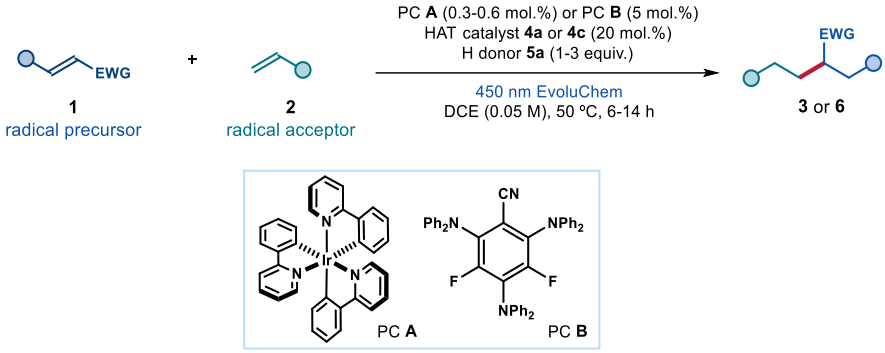

Figure 3.24. General procedure.

Procedure. To an oven dried 8 mL vial containing a dry Teflon stir bar, the photocatalyst (if 3DPA2FBN), the olefin substrates **1** and **2** (if solid) and bases (if solid and needed) were added. The vial was sealed with a Teflon septum screw cap, evacuated and backfilled with argon three times, and the solvent was added. Then the photocatalyst stock solution (if *fac*-Ir(ppy)$_3$), olefin substrates **1** and **2** (if liquid), H donor, HAT catalyst, and bases (if liquid and needed) were added sequentially. The amount of added solvent was such that the total amount of solvent (added + stock solution, if used) was 4.0 mL. The solvent used was DCE sparged with nitrogen for 15 minutes, unless otherwise stated. The vial was then placed in the photoreactor (Figure 3.23) and irradiated under stirring for 6 hours (if radical acceptors are styrenes) or 14 hours, unless otherwise specified. Then the solvent was evaporated, and the crude mixture purified by flash column chromatography on silica gel to furnish the target product **3** or **6**.

3.7.4 Characterization of products

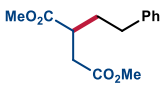

Dimethyl 2-phenethylsuccinate (4a): Synthesized according to the General Procedure using *fac*-Ir(ppy)$_3$ (800 µL stock solution, 0.6 mol%), PhSH (4.0 µL, 0.04 mmol, 20 mol%), γ-terpinene (64.0 µL, 0.4 mmol, 2 equiv.), dimethyl fumarate **1a** (43.0 mg, 0.3 mmol, 1.5 equiv.) and styrene **2a** (23.0 µL, 0.2 mmol, 1 equiv.). Upon 6 hours stirring, the crude mixture was purified by flash column

chromatography on silica gel (10% EtOAc in hexanes as eluent) to afford **4a** (41.5 mg, 83% yield) as a light-yellow oil.

^{1}H NMR (500 MHz, $CDCl_3$) δ 7.30 – 7.26 (m, 2H), 7.21 – 7.17 (m, 2H), 7.17 – 7.16 (m, 1H), 3.71 (s, 3H), 3.67 (s, 3H), 2.94 – 2.87 (m, 1H), 2.77 (dd, *J* = 16.5, 9.1 Hz, 1H), 2.69 – 2.58 (m, 2H), 2.49 (dd, *J* = 16.5, 5.3 Hz, 1H), 2.00 (dddd, *J* = 13.7, 9.4, 7.8, 6.5 Hz, 1H), 1.83 (dddd, *J* = 13.7, 9.4, 6.8, 6.0 Hz, 1H). ^{13}C NMR (126 MHz, $CDCl_3$) δ 175.3, 172.3, 141.2, 128.6, 128.5, 126.2, 52.0, 51.9, 40.9, 36.0, 33.7, 33.3.

Matching reported literature data.[33]

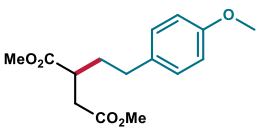

Dimethyl 2-(4-methoxyphenethyl)succinate (4b): Synthesized according to the General Procedure using *fac*-Ir(ppy)$_3$ (800 µL stock solution, 0.6 mol%), PhSH (4.1 µL, 0.04 mmol, 20 mol%), γ-terpinene (64.0 µL, 0.4 mmol, 2 equiv.), dimethyl fumarate **1a** (43.0 mg, 0.3 mmol, 1.5 equiv.) and 4-methoxystyrene **2b** (26.5 µL, 0.2 mmol, 1 equiv.). Upon 6 hours stirring, the crude mixture was purified by flash column chromatography on silica gel (10% EtOAc in hexanes as eluent) to afford **4b** (45.0 mg, 80% yield) as a light-yellow oil.

^{1}H NMR (500 MHz, $CDCl_3$) δ 7.10 – 7.06 (m, 2H), 6.84 – 6.80 (m, 2H), 3.78 (s, 3H), 3.70 (s, 3H), 3.66 (s, 3H), 2.87 (dddd, *J* = 9.2, 7.7, 6.0, 5.2 Hz, 1H), 2.75 (dd, *J* = 16.5, 9.2 Hz, 1H), 2.62 – 2.52 (m, 2H), 2.47 (dd, *J* = 16.5, 5.2 Hz, 1H), 1.95 (dddd, *J* = 13.7, 9.2, 7.8, 6.7 Hz, 1H), 1.78 (dddd, *J* = 13.7, 9.2, 6.9, 6.0 Hz, 1H).

^{13}C NMR (126 MHz, $CDCl_3$) δ 175.3, 172.4, 158.1, 133.2, 129.4, 114.0, 55.4, 52.0, 51.9, 40.8, 36.0, 33.9, 32.4.

HRMS: (ESI$^+$) calculated for $C_{15}H_{20}NaO_5^+$ [M+Na$^+$]: 303.1203, found 303.1210.

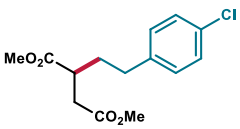

Dimethyl 2-(4-chlorophenethyl)succinate (4c): Synthesized according to General Procedure using *fac*-Ir(ppy)$_3$ (800 µL stock solution, 0.6 mol%), PhSH (4.1 µL, 0.04 mmol, 20 mol%), γ-terpinene (64.0 µL, 0.4 mmol, 2 equiv.), dimethyl fumarate **1a** (43.0 mg, 0.3 mmol, 1.5 equiv.) and 4-chlorostyrene **2c** (25.5 µL, 0.2 mmol, 1 equiv.). Upon 6 hours stirring, the crude mixture was purified by flash column chromatography on silica gel (9% to 11% EtOAc in hexanes as eluent) to afford **4c** (45.5 mg, 80% yield) as a colorless oil.

[33] Fini, F.; Beltrani, M.; Mancuso, R.; Gabriele, B.; Carfagna, C., Selective Aryl α-Diimine/Palladium-Catalyzed Bis-Alkoxy- carbonylation of Olefins for the Synthesis of Substituted Succinic Diesters. *Adv. Synth. Catal.* **2015**, *357*, 177

^{1}H NMR (500 MHz, $CDCl_3$) δ 7.26 – 7.22 (m, 2H), 7.11 – 7.08 (m, 2H), 3.70 (s, 3H), 3.66 (s, 3H), 2.86 (ddt, *J* = 8.9, 7.9, 5.6 Hz, 1H), 2.75 (dd, *J* = 16.5, 8.9 Hz, 1H), 2.66 – 2.53 (m, 2H), 2.47 (dd, *J* = 16.5, 5.4 Hz, 1H), 1.96 (dddd, *J* = 13.7, 9.4, 8.0, 6.3 Hz, 1H), 1.79 (dddd, *J* = 13.7, 9.5, 6.8, 5.8 Hz, 1H).

^{13}C NMR (126 MHz, $CDCl_3$) δ 175.1, 172.2, 139.6, 132.0, 129.9, 128.7, 52.1, 52.0, 40.8, 36.0, 33.5, 32.7. HRMS: (ESI^+) calculated for $C_{14}H_{17}ClNaO_4^+$ [M+Na^+]: 307.0708, found 307.0711.

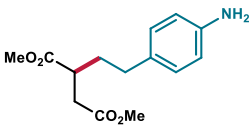

Dimethyl 2-(4-aminophenethyl)succinate (4d): Synthesized according to General Procedure using *fac*-Ir(ppy)$_3$ (800 µL stock solution, 0.6 mol%), PhSH (4.1 µL, 0.04 mmol, 20 mol%), γ-terpinene (64.0 µL, 0.4 mmol, 2 equiv.), dimethyl fumarate **1a** (43.0 mg, 0.3 mmol, 1.5 equiv.) and 4-aminostyrene **2d (**23.5 µL, 0.2 mmol, 1 equiv.). Upon 6 hours stirring, ^{1}H NMR (CH_2Br_2 as internal standard) revealed 75% NMR yield of **4d**. The crude mixture was purified by flash column chromatography on silica gel (25% to 33% EtOAc in hexanes as eluent) to afford **4d** (35.5 mg, 67%, ~90% purity) as an orange oil. An analytical sample was obtained via preparative HPLC (column: ChiralPak IC 250x4.6 mm, 5µm; mobile phase: Hex/EtOH 85:15; flow: 1 ml/min; wavelength: 254 nm).

^{1}H NMR (500 MHz, $CDCl_3$) δ 6.98 – 6.93 (m, 2H), 6.64 – 6.60 (m, 2H), 3.70 (s, 3H), 3.66 (s, 3H), 3.56 (br. s, 2H), 2.87 (dddd, *J* = 9.2, 7.6, 6.1, 5.1 Hz, 1H), 2.74 (dd, *J* = 16.5, 9.2 Hz, 1H), 2.51 (ddd, *J* = 9.3, 6.7, 2.9 Hz, 2H), 2.47 (dd, *J* = 16.5, 5.1 Hz, 1H), 1.93 (dddd, *J* = 13.6, 9.1, 7.6, 6.7 Hz, 1H), 1.81 – 1.71 (m, 1H).

^{13}C NMR (126 MHz, $CDCl_3$) δ 175.4, 172.5, 144.6, 131.2, 129.3, 115.4, 52.0, 51.9, 40.9, 36.0, 34.0, 32.5. HRMS: (ESI^+) calculated for $C_{14}H_{19}NNaO_4^+$ [M+Na^+]: 288.1206, found 288.1211.

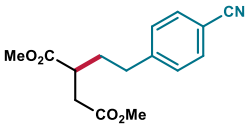

Dimethyl-2-(4-cyanophenethyl)succinate (4e): Synthesized according to the General Procedure using *fac*-Ir(ppy)$_3$ (800 µL stock solution, 0.6 mol%), PhSH (4.1 µL, 0.04 mmol, 20 mol%), γ-terpinene (64.0 µL, 0.4 mmol, 2 equiv.), dimethyl fumarate **1a** (43.0 mg, 0.3 mmol, 1.5 equiv.) and 4-cyanostyrene **2e** (25.1 µL, 0.2 mmol, 1 equiv.). Upon 6 hours stirring, ^{1}H NMR (CH_2Br_2 as internal standard) revealed 50% NMR yield of **4e**. The crude mixture was purified by flash column chromatography on silica gel (12% EtOAc in hexanes as eluent) to afford **4e** (26.7 mg, 48% yield, ~90% purity) as a light-yellow oil. An analytical sample was obtained via preparative HPLC (column: XSelect CSH Fluoro-Phenyl 150x4.6 mm, 3.5µm; mobile phase: H2O/MeOH 50:50; flow: 1 ml/min; wavelength: 254 nm).

^{1}H NMR (500 MHz, $CDCl_3$) δ 7.60 – 7.56 (m, 2H), 7.31 – 7.27 (m, 2H), 3.72 (s, 3H), 3.68 (s, 3H), 2.87 (tt, *J* = 8.3, 5.6 Hz, 1H), 2.76 (dd, *J* = 16.5, 8.6 Hz, 1H), 2.73 – 2.64 (m, 2H),

2.48 (dd, *J* = 16.5, 5.7 Hz, 1H), 1.99 (dddd, *J* = 14.1, 9.7, 8.2, 6.1 Hz, 1H), 1.83 (dddd, *J* = 13.7, 9.8, 6.6, 5.5 Hz, 1H).

^{13}C NMR (126 MHz, $CDCl_3$) δ 174.9, 172.1, 146.8, 132.5, 129.4, 119.1, 110.3, 52.2, 52.1, 40.8, 36.1, 33.5, 33.0.

HRMS: (ESI$^+$) calculated for $C_{15}H_{17}NNaO_4^+$ [M+Na$^+$]: 298.1050, found 298.1059.

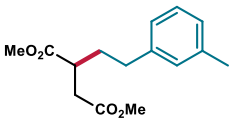

Dimethyl 2-(3-methylphenethyl)succinate (4f): Synthesized according to General Procedure using *fac*-Ir(ppy)$_3$ (800 µL stock solution, 0.6 mol%), PhSH (4.1 µL, 0.04 mmol, 20 mol%), γ-terpinene (64.0 µL, 0.4 mmol, 2 equiv.), dimethyl fumarate **1a** (43.0 mg, 0.3 mmol, 1.5 equiv.) and 3-methylstyrene **2f** (26.5 µL, 0.2 mmol, 1 equiv.). Upon 6 hours stirring, the crude mixture was purified by flash column chromatography on silica gel (6% to 9% EtOAc in hexanes as eluent) to afford **4f** (40.5 mg, 77% yield) as a yellowish oil.

^{1}H NMR (500 MHz, $CDCl_3$) δ 7.19 – 7.15 (m, 1H), 7.03 – 6.95 (m, 3H), 3.72 (s, 3H), 3.67 (s, 3H), 2.93 – 2.87 (m, 1H), 2.77 (dd, *J* = 16.5, 9.2 Hz, 1H), 2.65 – 2.54 (m, 2H), 2.49 (dd, *J* = 16.5, 5.2 Hz, 1H), 2.33 (s, 3H), 1.98 (dddd, *J* = 13.7, 9.5, 7.7, 6.6 Hz, 1H), 1.82 (dddd, *J* = 13.7, 9.5, 6.8, 6.0 Hz, 1H).

^{13}C NMR (126 MHz, $CDCl_3$) δ 175.3, 172.4, 141.1, 138.1, 129.3, 128.5, 127.0, 125.5, 52.0, 51.9, 41.0, 36.0, 33.8, 33.3, 21.5.

HRMS: (ESI$^+$) calculated for $C_{15}H_{20}NaO_4^+$ [M+Na$^+$]: 287.1254, found 287.1264.

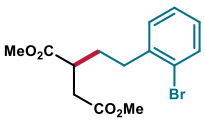

Dimethyl 2-(2-bromophenethyl)succinate (4g): Synthesized according to General Procedure using *fac*-Ir(ppy)$_3$ (800 µL stock solution, 0.6 mol%), PhSH (4.1 µL, 0.04 mmol, 20 mol%), γ-terpinene (64.0 µL, 0.4 mmol, 2 equiv.), dimethyl fumarate **1a** (43.0 mg, 0.3 mmol, 1.5 equiv.) and 2-bromostyrene **2g** (25.0 µL, 0.2 mmol, 1 equiv.). Upon 6 hours stirring, the crude mixture was purified by flash column chromatography on silica gel (8% EtOAc in hexanes as eluent) to afford **4g** (43.0 mg, 65% yield) as a yellowish oil.

^{1}H NMR (500 MHz, $CDCl_3$) δ 7.52 – 7.50 (m, 1H), 7.25 – 7.19 (m, 2H), 7.08 – 7.03 (m, 1H), 3.73 (s, 3H), 3.68 (s, 3H), 2.97 – 2.91 (m, 1H), 2.80 (dd, *J* = 16.6, 9.2 Hz, 1H), 2.79 – 2.69 (m, 2H), 2.53 (dd, *J* = 16.6, 5.3 Hz, 1H), 1.95 (dddd, *J* = 13.6, 10.3, 7.5, 6.1 Hz, 1H), 1.88 – 1.80 (m, 1H).

^{13}C NMR (126 MHz, $CDCl_3$) δ 175.1, 172.4, 140.5, 133.0, 130.5, 128.0, 127.7, 124.4, 52.1, 52.0, 41.0, 35.9, 33.7, 32.1.

HRMS: (ESI$^+$) calculated for $C_{14}H_{17}BrNaO_4^+$ [M+Na$^+$]: 351.0202, found 351.0214.

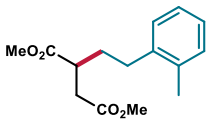

Dimethyl 2-(2-methylphenethyl)succinate (4h): Synthesized according to General Procedure using *fac*-Ir(ppy)$_3$ (800 µL stock solution, 0.6 mol%), PhSH (4.1 µL, 0.04 mmol, 20 mol%), γ-terpinene (64.0 µL, 0.4 mmol, 2 equiv.), dimethyl fumarate **1a** (43.0 mg, 0.3 mmol, 1.5 equiv.) and 2-methylstyrene **2h** (26.0 µL, 0.2 mmol, 1 equiv.). Upon 6 hours stirring, the crude mixture was purified by flash column chromatography on silica gel (6% to 9% EtOAc in hexanes as eluent) to afford **4h** (40.0 mg, 76% yield) as a colorless oil.

^{1}H NMR (500 MHz, $CDCl_3$) δ 7.15 – 7.09 (m, 4H), 3.73 (s, 3H), 3.68 (s, 3H), 2.95 (ddt, *J* = 8.9, 7.7, 5.6 Hz, 1H), 2.80 (dd, *J* = 16.5, 8.9 Hz, 1H), 2.68 – 2.54 (m, 2H), 2.51 (dd, *J* = 16.6, 5.5 Hz, 1H), 2.29 (s, 3H), 1.92 (dddd, *J* = 13.6, 10.6, 7.7, 6.1 Hz, 1H), 1.84 – 1.73 (m, 1H).

^{13}C NMR (126 MHz, $CDCl_3$) δ 175.2, 172.4, 139.4, 135.9, 130.4, 128.9, 126.4, 126.2, 52.0, 51.9, 41.3, 36.0, 32.5, 30.8, 19.2.

HRMS: (ESI$^+$) calculated for $C_{15}H_{20}NaO_4^+$ [M+Na$^+$]: 287.1254, found 287.1256.

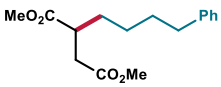

Dimethyl-2-(4-phenylbutyl)succinate (4i): Synthesized according to General Procedure using *fac*-Ir(ppy)$_3$ (400 µL stock solution, 0.3 mol%), HAT catalyst **5c** (Ethyl thioglycolate, 4.4 µL, 0.04 mmol, 20 mol%), γ-terpinene (32.0 µL, 0.2 mmol, 1 equiv.), dimethyl fumarate **1a** (28.8 mg, 0.2 mmol, 1 equiv.) and 4-Phenyl-1-butene **2i** (90.0 µL, 0.6 mmol, 3 equiv.). Upon 14 hours stirring, the crude mixture was purified by flash column chromatography on silica gel (3% EtOAc in hexanes as eluent) to afford **4i** (29.5 mg, 53 % yield) as a colorless oil.

^{1}H NMR (400 MHz, $CDCl_3$) δ 7.33 – 7.26 (m, 2H), 7.22 – 7.15 (m, 3H), 3.72 (s, 3H), 3.69 (s, 3H)2.91 – 2.81 (m, 1H), 2.73 (dd, *J* = 16.5, 9.3 Hz, 1H), 2.66 – 2.58 (m, 2H), 2.44 (dd, *J* = 16.5, 5.1 Hz, 1H), 1.73 – 1.56 (m, 4H), 1.43 – 1.30 (m, 2H).

^{13}C NMR (101 MHz, $CDCl_3$) δ 175.6, 172.6, 142.4, 128.5, 128.4, 125.9, 51.9, 51.9, 41.2, 35.9, 35.7, 31.8, 31.2, 26.6.

HRMS: (ESI$^+$) calculated for $C_{16}H_{22}NaO_4^+$ [M+Na$^+$]: 301.1410, found 301.1423.

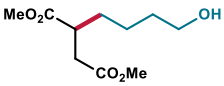

Dimethyl-2-(4-hydroxybutyl)succinate (4j): Synthesized according to General Procedure using *fac*-Ir(ppy)$_3$ (400 µL stock solution, 0.3 mol%), HAT catalyst **5c** (Ethyl thioglycolate, 4.4 µL, 0.04 mmol, 20 mol%), γ-terpinene (32.0 µL, 0.2 mmol, 1 equiv.), dimethyl fumarate **1a** (28.8 mg, 0.2 mmol, 1 equiv.) and 3-Buten-1-ol **2j** (51.5 µL, 0.6 mmol, 3 equiv.). Upon 14 hours stirring, the crude mixture was purified by flash column chromatography on silica gel (50% EtOAc in hexanes as eluent) to afford **4j** (22.5 mg, 52 % yield) as a colorless oil.

^{1}H NMR (400 MHz, $CDCl_3$) δ 3.72 (s, 3H), 3.69 (s, 3H), 3.65 (t, *J* = 6.4 Hz, 2H), 2.93 – 2.84 (m, 1H), 2.74 (dd, *J* = 16.5, 9.1 Hz, 1H), 2.49 (d, *J* = 5.3 Hz, 1H), 1.78 – 1.65 (m, 2H), 1.58 (dtdd, *J* = 14.7, 6.0, 4.7, 2.1 Hz, 3H), 1.46 – 1.41 (m, 1H).

^{13}C NMR (101 MHz, $CDCl_3$) δ 175.4, 172.5, 62.6, 52.0, 51.9, 41.2, 35.9, 32.5, 31.7, 23.3.

HRMS: (ESI$^+$) calculated for $C_{10}H_{18}NaO_5^+$ [M+Na$^+$]: 241.1046, found 241.1043.

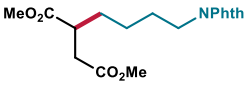

Dimethyl-2-(4-(1,3-dioxoisoindolin-2-yl)butyl)succinate (4k): Synthesized according to General Procedure using *fac*-Ir(ppy)$_3$ (400 µL stock solution, 0.3 mol%), HAT catalyst **5c** (Ethyl thioglycolate, 4.4 µL, 0.04 mmol, 20 mol%), γ-terpinene (32.0 µL, 0.2 mmol, 1 equiv.), dimethyl fumarate **1a** (28.8 mg, 0.2 mmol, 1 equiv.) and 2-(but-3-en-1-yl)isoindoline-1,3-dione **2k** (120.5 mg, 0.6 mmol, 3 equiv.). Upon 14 hours stirring, the crude mixture was purified by flash column chromatography on silica gel (40% EtOAc in hexanes as eluent) to afford **4k** (38.0 mg, 55 % yield) as a white solid.

^{1}H NMR (500 MHz, $CDCl_3$) δ 7.83 (dd, *J* = 5.4, 3.0 Hz, 2H), 7.71 (dd, *J* = 5.5, 3.0 Hz, 2H), 3.68 – 3.65 (m, 8H), 2.83 (dddd, *J* = 9.2, 7.5, 6.2, 5.2 Hz, 1H), 2.71 (dd, *J* = 16.6, 9.1 Hz, 1H), 2.42 (dd, *J* = 16.6, 5.2 Hz, 1H), 1.73 – 1.65 (m, 3H), 1.60 – 1.51 (m, 1H), 1.35 (p, *J* = 8.5 Hz, 2H).

^{13}C NMR (101 MHz, $CDCl_3$) δ 175.3, 172.4, 168.5, 134.0, 132.2, 123.3, 51.9, 51.9, 41.1, 37.7, 35.9, 31.4, 28.4, 24.3.

HRMS: (ESI$^+$) calculated for $C_{18}H_{21}NNaO_6^+$ [M+Na$^+$]: 370.1261, found 370.1265.

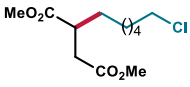

Dimethyl 2-(6-chlorohexyl)succinate (4l): Synthesized according to General Procedure using *fac*-Ir(ppy)$_3$ (400 µL stock solution, 0.3 mol%), HAT **4c** (Ethyl thioglycolate, 4.4 µL, 0.04 mmol, 20 mol%), γ-terpinene (32.0 µL, 0.2 mmol, 1 equiv.), dimethyl fumarate **1a** (28.8 mg, 0.2 mmol, 1 equiv.) 6-Chloro-1-hexene **2l** (79.5 µL, 0.6 mmol, 3 equiv.). Upon 36 hours stirring, the crude mixture was purified by flash column chromatography on silica gel (20% EtOAc in hexanes as eluent) to afford **4l** (26.5 mg, 50 % yield) as a colorless oil.

^{1}H NMR (400 MHz, $CDCl_3$) δ 3.72 (s, 3H), 3.69 (s, 3H), 3.54 (t, *J* = 6.7 Hz, 2H), 2.86 (dddd, *J* = 9.2, 7.4, 6.2, 5.2 Hz, 1H), 2.73 (dd, *J* = 16.5, 9.2 Hz, 1H), 2.45 (dd, *J* = 16.5, 5.2 Hz, 1H), 1.77 (dq, *J* = 8.8, 6.8 Hz, 2H), 1.70 – 1.61 (m, 1H), 1.58 – 1.49 (m, 1H), 1.48 – 1.40 (m, 2H), 1.38 – 1.26 (m, 4H).

^{13}C NMR (101 MHz, $CDCl_3$) δ 175.51, 172.53, 51.96, 51.90, 45.13, 41.23, 35.97, 32.59, 31.92, 28.75, 26.89, 26.75.

HRMS: (ESI$^+$) calculated for $C_{12}H_{21}ClNaO_4^+$ [M+Na$^+$]: 287.1021, found 287.1029.

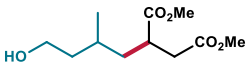

Dimethyl 2-(4-hydroxy-2-methylbutyl)succinate (4m): Synthesized according to General Procedure using *fac*-Ir(ppy)$_3$ (400 µL stock solution, 0.3 mol%), HAT catalyst **5c** (Ethyl thioglycolate, 4.4 µL, 0.04 mmol, 20 mol%), γ-terpinene (32.0 µL, 0.2 mmol, 1 equiv.), dimethyl fumarate **1a** (28.8 mg, 0.2 mmol, 1 equiv.) and 3-methyl-3-buten-1-ol **2m** (60.5 µL, 0.6 mmol, 3 equiv.). Upon 14 hours stirring, the crude mixture was purified by flash column chromatography on silica gel (17% to 50% EtOAc in hexanes as eluent) to afford **4m** (30.0 mg, 64% yield, 1:1 dr) as a colorless oil.

^{1}H NMR (500 MHz, $CDCl_3$, mixture of diastereomers) δ 3.68 (s, 6H), 3.72 – 3.59 (m, 4H), 3.65 (s, 3H), 3.65 (s, 3H), 2.96 – 2.87 (m, 2H), 2.69 (dd, *J* = 16.5, 8.7 Hz, 1H), 2.66 (dd, *J* = 16.7, 9.3 Hz, 1H), 2.44 (dd, *J* = 16.6, 5.0 Hz, 1H), 2.42 (dd, *J* = 16.5, 5.7 Hz, 1H), 1.71 (ddd, *J* = 13.9, 9.4, 4.8 Hz, 1H), 1.66 – 1.49 (m, 5H), 1.47 – 1.34 (m, 3H), 1.21 (ddd, *J* = 13.5, 8.8, 5.4 Hz, 1H), 0.93 (d, *J* = 6.5 Hz, 3H), 0.90 (d, *J* = 6.5 Hz, 3H).

^{13}C NMR (126 MHz, $CDCl_3$, mixture of diastereomers) δ 175.8, 175.8, 172.5, 172.4, 60.7, 60.6, 52.0, 52.0, 51.9, 51.9, 39.8, 39.4, 39.4, 39.3, 39.2, 39.2, 36.8, 35.9, 27.6, 27.4, 19.6, 19.6.

HRMS: (ESI$^+$) calculated for $C_{11}H_{20}NaO_5^+$ [M+Na$^+$]: 255.1203, found 255.1205.

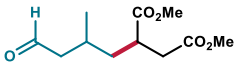

Dimethyl 2-(2-methyl-4-oxobutyl)succinate (4n): Synthesized according to General Procedure using *fac*-Ir(ppy)$_3$ (400 µL stock solution, 0.3 mol%), HAT catalyst **5c** (Ethyl thioglycolate, 4.4 µL, 0.04 mmol, 20 mol%), γ-terpinene (32.0 µL, 0.2 mmol, 1 equiv.), dimethyl fumarate **1a** (28.8 mg, 0.2 mmol, 1 equiv.) and 3-methylbut-3-enal **2n** as a solution in DCM (50.5 mg, 0.6 mmol, 3 equiv.). Upon 14 hours stirring, the crude mixture was purified by flash column chromatography on silica gel (5% to 20% EtOAc in hexanes as eluent) to afford **4n** (17.1 mg, 37% yield, 1:1 dr) as a colorless oil.

^{1}H NMR (500 MHz, $CDCl_3$, mixture of diastereomers) δ 9.73 (dd, *J* = 2.3, 1.4 Hz, 1H), 9.71 (dd, *J* = 2.3, 1.8 Hz, 1H), 3.70 (s, 3H), 3.69 (s, 3H), 3.66 (s, 3H), 3.66 (s, 3H), 2.94 – 2.84 (m, 2H), 2.74 – 2.67 (m, 2H), 2.50 (ddd, *J* = 16.6, 5.1, 1.5 Hz, 1H), 2.46 (dd, *J* = 16.7, 5.2 Hz, 1H), 2.42 (dd, *J* = 16.7, 5.8 Hz, 1H), 2.38 (ddd, *J* = 16.5, 5.7, 2.2 Hz, 1H), 2.30 – 2.23 (m, 2H), 2.13 – 2.01 (m, 2H), 1.70 (ddd, *J* = 13.7, 9.5, 5.1 Hz, 1H), 1.62 (dt, *J* = 13.8, 7.5 Hz, 1H), 1.45 (dt, *J* = 13.9, 7.0 Hz, 1H), 1.32 (ddd, *J* = 13.7, 9.2, 5.2 Hz, 1H), 1.00 (d, *J* = 6.6 Hz, 3H), 0.96 (d, *J* = 6.6 Hz, 3H).

^{13}C NMR (126 MHz, $CDCl_3$, mixture of diastereomers) δ 202.0, 202.0, 175.4, 175.2, 172.3, 172.2, 52.1, 52.1, 52.0 (2C), 51.1, 50.5, 39.3, 39.1, 39.1, 38.8, 36.7, 35.9, 26.1, 26.0, 20.0, 19.6.

HRMS: (ESI$^+$) calculated for $C_{11}H_{18}NaO_5^+$ [M+Na$^+$]: 253.1046, found 255.1044.

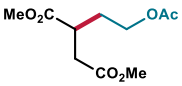

Dimethyl -2-(2-acetoxyethyl)succinate (4o): Synthesized according to General Procedure using *fac*-Ir(ppy)$_3$ (400 µL stock solution, 0.3 mol%), HAT catalyst **5c** (Ethyl thioglycolate, 4.4 µL, 0.04 mmol, 20 mol%), γ-terpinene (32.0 µL, 0.2 mmol, 1 equiv.), dimethyl fumarate **1a** (28.8 mg, 0.2 mmol, 1 equiv.) and vinyl acetate **2o** (55.0 µL, 0.6 mmol, 3 equiv.). Upon 14 hours stirring, the crude mixture was purified by flash column chromatography on silica gel (10% EtOAc in hexanes as eluent) to afford **4o** (23.5 mg, 51 % yield) as a colorless oil.

^{1}H NMR (400 MHz, $CDCl_3$) δ 4.11 (t, *J* = 6.3 Hz, 2H), 3.71 (s, 3H), 3.68 (s, 3H), 3.02 – 2.93 (m, 1H), 2.76 (dd, *J* = 16.6, 8.7 Hz, 1H), 2.51 (dd, *J* = 16.7, 5.6 Hz, 1H), 2.07 – 1.98(m, 4H), 1.90 – 1.8 (m, 1H).

^{13}C NMR (101 MHz, $CDCl_3$) δ 174.7, 172.1, 171.0, 62.0, 52.2, 52.0, 38.4, 35.7, 30.6, 21.0.

HRMS: (ESI$^+$) calculated for $C_{10}H_{16}NaO_6^+$ [M+Na$^+$]: 255.0839, found 255.0838.

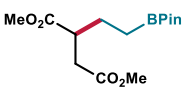

Dimethyl-2-(2-(4,4,5,5-tetramethyl-1,3,2-dioxaborolan-2-yl)ethyl)succinate (4p) : Synthesized according to General Procedure using *fac*-Ir(ppy)$_3$ (400 µL stock solution, 0.3 mol%), HAT catalyst **5c** (Ethyl thioglycolate, 4.4 µL, 0.04 mmol, 20 mol%), γ-terpinene (32.0 µL, 0.2 mmol, 1 equiv.), dimethyl fumarate **1a** (28.8 mg, 0.2 mmol, 1 equiv.) and vinylboronic acid pinacol ester **2p** (102.0 µL, 0.6 mmol, 3 equiv.). Upon 14 hours stirring, the crude mixture was purified by flash column chromatography on silica gel (20% EtOAc in hexanes as eluent) to afford **4p** (50.5 mg, 84 % yield) as a colorless oil.

^{1}H NMR (500 MHz, $CDCl_3$) δ 3.69 (s, 3H), δ 3.67 (s, 3H), 2.83 (dddd, *J* = 9.6, 7.5, 6.5, 4.7 Hz, 1H), 2.71 (dd, *J* = 16.6, 9.7 Hz, 1H), 2.44 (dd, *J* = 16.6, 4.8 Hz, 1H), 1.79 – 1.69 (m, 1H), 1.69 – 1.62 (m, 1H), 1.24 (s, 12H), 0.77 (d, *J* = 8.0 Hz, 2H).

^{13}C NMR (126 MHz, $CDCl_3$) δ 175.5, 172.6, 83.3, 51.8, 43.1, 35.7, 29.8, 26.6, 24.9.

HRMS: (ESI$^+$) calculated for $C_{14}H_{25}NaO_6B^+$ [M+Na$^+$]: 322.1673, found 322.1664.

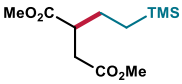

Dimethyl-2-(2-(trimethylsilyl)ethyl)succinate (4q): Synthesized according to General Procedure using *fac*-Ir(ppy)$_3$ (400 µL stock solution, 0.3 mol%), HAT catalyst **5c** (Ethyl thioglycolate, 4.4 µL, 0.04 mmol, 20 mol%), γ-terpinene (32.0 µL, 0.2 mmol, 1 equiv.), dimethyl fumarate **1a** (28.8 mg, 0.2 mmol, 1 equiv.) and vinyltrimethylsilane **2q** (88.0 µL, 0.6 mmol, 3 equiv.). Upon 14 hours stirring, the crude mixture was purified by flash column chromatography on silica gel (2% EtOAc in hexanes as eluent) to afford **4q** (32.0 mg, 65 % yield) as a colorless oil.

^{1}H NMR (400 MHz, $CDCl_3$) δ 3.70 (s, 3H), 3.67 (s, 3H), 2.87 – 2.78 (m, 1H), 2.71 (dd, *J* = 16.3, 9.3 Hz, 1H), 2.45 (dd, *J* = 16.3, 5.0 Hz, 1H), 1.68 – 1.58 (m, 1H), 1.56 – 1.48 (m, 1H), 0.51 – 0.41 (m, 2H), -0.02 (s, 9H).

^{13}C NMR (126 MHz, $CDCl_3$) δ 175.5, 172.7, 51.9, 51.8, 44.0, 35.4, 26.6, 13.7, -1.7.

HRMS: (ESI$^+$) calculated for $C_{11}H_{22}NaO_4Si^+$ [M+Na$^+$]: 269.1180, found 269.1177.

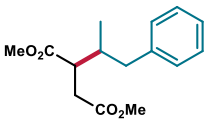

Dimethyl 2-(1-phenylpropan-2-yl)succinate (4r): Synthesized according to General Procedure using *fac*-Ir(ppy)$_3$ (400 µL stock solution, 0.3 mol%), PhSH (4.1 µL, 0.04 mmol, 20 mol%), γ-terpinene (32.0 µL, 0.2 mmol, 1 equiv.), dimethyl fumarate **1a** (28.8 mg, 0.2 mmol, 1.0 equiv.) and trans-beta-Methylstyrene **23** (78.0 µL, 0.6 mmol, 3 equiv.). Upon 14 hours stirring, the crude mixture was purified by flash column chromatography on silica gel (3% to 9% EtOAc in hexanes as eluent) to afford **4r** (23.2 mg, 44% yield, 1:1 dr) as a colorless oil.

^{1}H NMR (500 MHz, $CDCl_3$) δ 7.31 – 7.25 (m, 4H), 7.22 – 7.17 (m, 2H), 7.17 – 7.13 (m, 4H), 3.72 (s, 3H), 3.70 (s, 3H), 3.68 (s, 3H), 3.66 (s, 3H), 2.96 – 2.74 (m, 5H), 2.69 (dd, *J* = 13.5, 5.8 Hz, 1H), 2.50 – 2.35 (m, 4H), 2.29 – 2.20 (m, 1H), 2.14 – 2.05 (m, 1H), 0.88 (d, *J* = 6.8 Hz, 3H), 0.84 (d, *J* = 6.8 Hz, 3H).

^{13}C NMR (126 MHz, $CDCl_3$, mixture of diastereomers) δ 175.0, 174.4, 173.0, 172.8, 140.3, 140.1, 129.3, 129.1, 128.5, 128.4, 126.3, 126.2, 52.0, 52.0, 51.9, 51.8, 45.7, 45.6, 40.9, 40.7, 37.5, 36.8, 33.7, 31.9, 16.6, 16.1.

HRMS: (ESI$^+$) calculated for $C_{15}H_{20}NaO_4^+$ [M+Na$^+$]: 287.1254, found 287.1261.

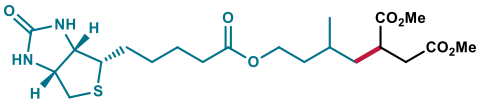

dimethyl 2-(2-methyl-4-((5-((3aS,4S,6aR)-2-oxohexahydro-1H-thieno[3,4-d]imidazol-4-yl)pentanoyl)oxy)butyl)succinate (4s): Synthesized according to General Procedure using *fac*-Ir(ppy)$_3$ (400 µL stock solution, 0.3 mol%), HAT catalyst **5c** (Ethyl thioglycolate, 4.4 µL, 0.04 mmol, 20 mol%), γ-terpinene (32.0 µL, 0.2 mmol, 1 equiv.), dimethyl fumarate **1a** (28.8 mg, 0.2 mmol, 1 equiv.) and 3-methylbut-3-en-1-yl 5-((3aS,4S,6aR)-2-oxohexahydro-1H-thieno[3,4-d]imidazol-4-yl)pentanoate **2s** (187.4 mg, 0.6 mmol, 3 equiv.). Upon 14 hours stirring, ^{1}H NMR (CH_2Br_2 as internal standard) revealed 62% NMR yield of **4s**. The crude mixture was purified by flash column chromatography on silica gel (3% MeOH in DCM as eluent) to afford a mixture of **4s** (54.2 mg, 59% yield, 1:1:1:1 dr) and **2s** (148.8 mg, 0.47 mmol) as colorless turbid oil. To obtain an analytically pure sample, preparative HPLC has been performed (column: XBridge

C18 150x4.6 mm, 5µm; mobile phase: H2O:MeOH 55.45; flow: 1ml/min; wavelength: 200 nm).

^{1}H NMR (500 MHz, $CDCl_3$, mixture of diastereomers) δ 5.23 (br. s, 2H), 4.88 (br. s, 2H), 4.54 – 4.49 (m, 2H), 4.35 – 4.30 (m, 2H), 4.15 – 4.04 (m, 4H), 3.70 (s, 3H), 3.70 (s, 3H), 3.68 (s, 6H), 3.21 – 3.13 (m, 2H), 2.96 – 2.87 (m, 4H), 2.76 – 2.63 (m, 4H), 2.43 (dd, *J* = 16.6, 7.5 Hz, 1H), 2.42 (dd, *J* = 16.6, 8.1 Hz, 1H), 2.35 – 2.29 (m, 4H), 1.77 – 1.39 (m, 20H), 1.30 – 1.22 (m, 2H), 0.96 (d, *J* = 6.5 Hz, 3H), 0.92 (d, *J* = 6.3 Hz, 3H).

^{13}C NMR (126 MHz, $CDCl_3$, mixture of diastereomers, peak overlapping observed) δ 175.7, 175.6, 175.6, 173.7, 172.5, 172.4, 163.1, 62.6, 62.6 (2C), 62.5, 62.0 (2C), 62.0, 62.0, 60.2, 55.4, 55.4, 52.1, 52.0, 52.0, 52.0, 40.7, 39.5, 39.5, 39.3, 39.2, 39.2, 36.8, 36.1, 35.7, 35.7, 35.2, 34.0, 34.0, 28.5, 28.5, 28.5, 28.4, 28.4 (2C), 28.4, 28.4, 28.1, 28.0, 27.9, 27.9, 24.9, 24.9, 19.5, 19.5, 19.3.

HRMS: (ESI$^+$) calculated for $C_{21}H_{34}N_2NaO_7S^+$ [M+Na$^+$]: 481.1979, found 481.1979.

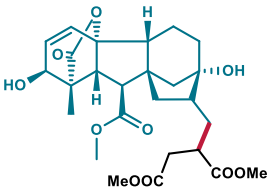

Dimethyl 2-(((1S,2S,4aR,4bR,7S,8R,9aS,10S,10aR)-2,7-dihydroxy-10-(methoxycarbonyl)-1-methyl-13-oxo-1,2,4b,5,6,7,8,9,10,10a-decahydro-4a,1-(epoxymethano)-7,9a-methanobenzo[a]azulen-8-yl)methyl)succinate (4t): Synthesized according to General Procedure using *fac*-Ir(ppy)$_3$ (400 µL stock solution, 0.3 mol%), HAT catalyst **5c** (Ethyl thioglycolate, 4.4 µL, 0.04 mmol, 20 mol%), γ-terpinene (32.0 µL, 0.2 mmol, 1 equiv.), dimethyl fumarate **1a** (28.8 mg, 0.2 mmol, 1 equiv.) and Gibberellic acid methyl ester **2t** (216.0 mg, 0.6 mmol, 3 equiv.) in DCE (4 ml) and acetone (1 ml). Upon 14 hours stirring, the crude mixture was purified by flash column chromatography on silica gel (67 % EtOAc in hexanes as eluent) to afford **4t** (58.5 mg, 58% yield, 1:1 dr) as a light-yellow oil.

^{1}H NMR (400 MHz, $CDCl_3$, mixture of diastereomers) δ 6.29 (d, *J* = 9.2 Hz, 1H), 5.89 (dd, *J* = 9.3, 3.7 Hz, 1H), 4.11 (d, *J* = 3.6 Hz, 1H), 3.73 (d, *J* = 3.1 Hz, 3H), 3.68 (s, 3H), 3.66 (s, 3H), 3.14 (dd, *J* = 10.6, 3.8 Hz, 1H), 2.85 – 2.82 (m, 1H), 2.75 – 2.64 (m, 2H), 2.48 (ddd, *J* = 21.7, 16.7, 5.4 Hz, 1H), 2.16 (s, 1H), 2.14 – 1.22 (m, 12H), 1.20 (d, *J* = 1.5 Hz, 3H).

^{13}C NMR (101 MHz, $CDCl_3$, mixture of diastereomers, peak overlapping observed) δ 178.7, 178.7, 175.6, 175.3, 173.0, 173.0, 172.4, 172.3, 132.8, 132.7, 132.7, 132.7, 90.7, 90.7, 78.5, 78.4, 69.9, 69.9, 53.8, 53.7, 53.6, 52.8, 52.8, 52.4, 52.3, 52.2, 52.1, 52.0, 52.0, 52.0, 51.9, 51.9, 46.3, 45.0, 44.6, 42.3, 42.2, 40.4, 40.1, 36.3, 36.1, 33.7, 33.4, 31.0, 30.3, 30.3, 16.6, 16.6, 14.5.

HRMS: (ESI$^+$) calculated for $C_{26}H_{34}NaO_{10}^+$ [M+Na$^+$]: 529.2044, found 529.2050.

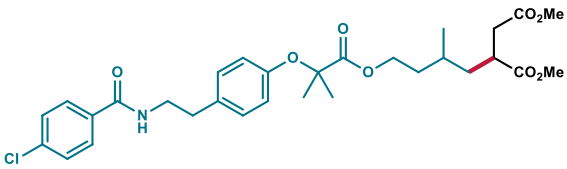

Dimethyl 2-(4-((2-(4-(2-(4-chlorobenzamido)ethyl)phenoxy)-2-methylpropanoyl)oxy)-2-methylbutyl)succinate (4u): Synthesized according to General Procedure using *fac*-Ir(ppy)$_3$ (400 µL stock solution, 0.3 mol%), HAT catalyst **5c** (Ethyl thioglycolate, 4.4 µL, 0.04 mmol, 20 mol%), γ-terpinene (32.0 µL, 0.2 mmol, 1 equiv.), dimethyl fumarate **1a** (28.8 mg, 0.2 mmol, 1 equiv.) and 3-methylbut-3-en-1-yl 2-(4-(2-(4-chlorobenzamido)ethyl)phenoxy)-2-methylpropanoate **2u** (257.9 mg, 0.6 mmol, 3 equiv.). Upon 14 hours stirring, the crude mixture was purified by flash column chromatography on silica gel (15% to 30% EtOAc in hexanes as eluent) to afford **4u** (41.6 mg, 37% yield, 1:1 dr) as a colorless oil and **2u** (196.7 mg, 0.46 mmol) as a white solid.

^{1}H NMR (500 MHz, $CDCl_3$, mixture of diastereomers) δ 7.65 – 7.60 (m, 4H), 7.38 – 7.34 (m, 4H), 7.09 – 7.06 (m, 4H), 6.79 – 6.75 (m, 4H), 6.28 (t, *J* = 5.2 Hz, 2H), 4.22 – 4.15 (m, 4H), 3.67 – 3.62 (m, 16H), 2.91 – 2.79 (m, 6H), 2.65 (dd, *J* = 16.5, 9.1 Hz, 1H), 2.57 (dd, *J* = 16.6, 9.5 Hz, 1H), 2.35 (dd, *J* = 16.5, 5.5 Hz, 1H), 2.33 (dd, *J* = 16.7, 4.9 Hz, 1H), 1.77 – 1.32 (m, 9H), 1.57 (s, 6H), 1.56 (s, 3H), 1.56 (s, 3H), 1.21 (ddd, *J* = 14.3, 9.0, 5.4 Hz, 1H), 0.90 (d, *J* = 6.4 Hz, 3H), 0.84 (d, *J* = 6.2 Hz, 3H). ^{13}C NMR (126 MHz, $CDCl_3$, mixture of diastereomers, peak overlapping observed) δ 175.6, 175.4, 174.4, 174.4, 172.4, 172.3, 166.5, 166.5, 154.3, 154.2, 137.7, 133.2, 133.2, 132.6, 132.5, 129.6, 128.9, 128.4, 119.5, 119.3, 79.2, 79.2, 63.5, 63.4, 52.0, 52.0, 51.9, 51.9, 41.4, 41.4, 39.4, 39.2, 39.1, 39.1, 36.7, 35.8, 35.6, 35.0, 34.8, 34.8, 27.9, 27.7, 25.6, 25.6, 25.3, 25.3, 19.2, 19.0.

HRMS: (ESI$^+$) calculated for $C_{30}H_{38}ClNNaO_8^+$ [M+Na$^+$]: 598.2178, found 598.2184.

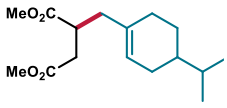

Dimethyl 2-((4-isopropylcyclohex-1-en-1-yl)methyl)succinate (4v): Synthesized according to General Procedure using *fac*-Ir(ppy)$_3$ (400 µL stock solution, 0.3 mol%), HAT catalyst **5c** (Ethyl thioglycolate, 4.4 µL, 0.04 mmol, 20 mol%), γ-terpinene (32.0 µL, 0.2 mmol, 1 equiv.), dimethyl fumarate **1a** (28.8 mg, 0.2 mmol, 1 equiv.) and (-)-beta-pinene **2v** (93.5 µL, 0.6 mmol, 3 equiv.). Upon 14 hours stirring, the crude mixture was purified by flash column chromatography on silica gel (6% EtOAc in hexanes as eluent) to afford **4v** (42.0 mg, 74% yield, 1:1 dr) as a colorless oil.

^{1}H NMR (500 MHz, $CDCl_3$, mixture of diastereomers) δ 5.43 – 5.39 (m, 2H), 3.67 (s, 3H), 3.66 (s, 3H), 3.65 (s, 6H), 3.02 – 2.95 (m, 2H), 2.64 (dd, *J* = 16.9, 9.5 Hz, 1H), 2.61 (dd, *J* = 16.9, 9.8 Hz, 1H), 2.41 (dd, *J* = 16.9, 4.8 Hz, 1H), 2.40 (dd, *J* = 16.9, 5.0 Hz, 1H), 2.36 – 2.28 (m, 2H), 2.11 – 2.03 (m, 2H), 2.03 – 1.88 (m, 6H), 1.79 – 1.64 (m, 4H), 1.48 – 1.39 (m, 2H), 1.23 – 1.12 (m, 4H), 0.88 – 0.84 (m, 12H).

^{13}C NMR (126 MHz, $CDCl_3$, mixture of diastereomers) δ 175.6, 175.5, 172.8, 172.7, 134.0, 133.9, 124.8, 124.7, 51.9, 51.9, 51.8, 51.8, 40.5, 40.2, 40.1, 40.0, 39.8, 39.6, 35.4, 35.1, 32.3, 32.3, 29.1, 29.1, 28.6, 28.5, 26.5, 26.4, 20.1, 20.0, 19.8, 19.8.

HRMS: (ESI^+) calculated for $C_{16}H_{26}NaO_4^+$ [M+Na^+]: 305.1723, found 305.1728.

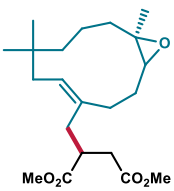

Dimethyl 2-(((11R,Z)-7,7,11-trimethyl-12-oxabicyclo[9.1.0]dodec-4-en-4-yl)methyl)succinate (4w): Synthesized according to General Procedure using *fac*-Ir(ppy)$_3$ (400 µL stock solution, 0.3 mol%), HAT catalyst **5c** (Ethyl thioglycolate, 4.4 µL, 0.04 mmol, 20 mol%), γ-terpinene (32.0 µL, 0.2 mmol, 1 equiv.), dimethyl fumarate **1a** (28.8 mg, 0.2 mmol, 1 equiv.) and (−)-Caryophyllene oxide **2w** (132.0 mg, 0.6 mmol, 3 equiv.). Upon 14 hours stirring, the crude mixture was purified by flash column chromatography on silica gel (6% to 20% EtOAc in hexanes as eluent) to afford **4w** (48.5 mg, 67% yield, 1:1 dr) as a colorless oil and (−)-Caryophyllene oxide **2w** (88.5 mg, 0.4 mmol) as white solid.

^{1}H NMR (500 MHz, $CDCl_3$, mixture of diastereomers) δ 5.35 (dd, *J* = 11.3, 2.4 Hz, 1H), 5.30 (dd, *J* = 11.3, 2.5 Hz, 1H), 3.70 (s, 3H), 3.65 (s, 3H), 3.64 (s, 3H), 3.64 (s, 3H), 2.93 (dddd, *J* = 8.9, 8.2, 6.6, 5.7 Hz, 1H), 2.89 – 2.83 (m, 1H), 2.74 (dd, *J* = 6.8, 1.8 Hz, 1H), 2.72 (dd, *J* = 6.8, 2.1 Hz, 1H), 2.70 (dd, *J* = 16.8, 8.9 Hz, 1H), 2.59 (dd, *J* = 16.8, 9.5 Hz, 1H), 2.56 (dd, *J* = 13.8, 8.5 Hz, 1H), 2.43 (dd, *J* = 16.7, 5.7 Hz, 1H), 2.43 (dd, *J* = 16.9, 4.6 Hz, 1H), 2.37 – 2.27 (m, 3H), 2.23– 2.14 (m, 3H), 2.13 – 2.07 (m, 2H), 2.05 – 1.91 (m, 5H), 1.67 – 1.57 (m, 2H), 1.51 – 1.34 (m, 4H), 1.23 – 1.12 (m, 4H), 1.15 (s, 6H), 0.92 (d, *J* = 0.6 Hz, 3H), 0.91 (d, *J* = 0.6 Hz, 3H), 0.84 (s, 3H), 0.83 (s, 3H), 0.80 – 0.73 (m, 4H).

^{13}C NMR (126 MHz, $CDCl_3$, mixture of diastereomers, peak overlapping observed) δ 175.3, 174.8, 172.5, 172.3, 134.1, 134.0, 127.9, 127.4, 62.8, 62.8, 62.7, 62.7, 52.2, 52.0, 51.9, 51.8, 40.8, 40.8, 40.3 (2C), 38.5, 38.5, 37.4, 37.2, 35.8, 35.5, 34.8, 34.7, 33.2, 33.2, 31.0, 30.6, 29.6, 29.6, 28.3 (2C), 24.6, 24.5, 18.5, 18.4, 18.0 (2C).

HRMS: (ESI^+) calculated for $C_{21}H_{34}NaO_5^+$ [M+Na^+]: 389.2298, found 389.2308.

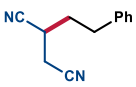

2-phenethylsuccinonitrile (4aa): Synthesized according to the General Procedure using *fac*-Ir(ppy)$_3$ (800 µL stock solution, 0.6 mol%), PhSH (4.1µL, 0.04 mmol, 20 mol%), γ-terpinene (64.1µL, 0.4 mmol, 2 equiv.), fumaronitrile (23.5 mg, 0.3 mmol, 1.5 equiv.) and styrene **2a** (23.0 µL, 0.2 mmol, 1 equiv.). Upon 14 hours stirring, the crude mixture was purified by flash column chromatography on silica gel (10% EtOAc in hexanes as eluent) to afford **4aa** (29.0 mg, 79% yield) as a light-yellow oil.

^{1}H NMR (500 MHz, $CDCl_3$) δ 7.36 – 7.31 (m, 2H), 7.28 – 7.24 (m, 1H), 7.24 – 7.19 (m, 2H), 2.97 (ddd, *J* = 13.7, 8.2, 5.2 Hz, 1H), 2.87 – 2.76 (m, 2H), 2.75 – 2.65 (m, 2H), 2.20 – 2.10 (m, 1H), 2.06 (dtd, *J* = 13.5, 8.2, 5.2 Hz, 1H).

^{13}C NMR (126 MHz, $CDCl_3$) δ 138.8, 129.0, 128.5, 127.0, 118.7, 115.4, 33.2, 32.8, 27.7, 21.2.

Matching reported literature data.[34]

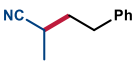

2-methyl-4-phenylbutanenitrile (4bb): Synthesized according to the General Procedure using 3DPA2FBN (6.4 mg, 5.0 mol%), PhSH (4.1 µL, 0.04 mmol, 20 mol%), 2,4,6-collidine (26.5µL, 0.2 mmol, 1 equiv.), γ-terpinene (96.0 µL, 0.6 mmol, 3 equiv.), acrylonitrile (13.0µL, 0.2 mmol, 1 equiv.) and styrene **2a** (68.5 µL, 0.6 mmol, 3 equiv.). Upon 14 hours stirring, the crude mixture was purified by flash column chromatography on silica gel (2% EtOAc in hexanes as eluent) to afford **4bb** (20.5 mg, 64% yield) as a colorless oil.

^{1}H NMR (500 MHz, $CDCl_3$) δ 7.33 – 7.28 (m, 2H), 7.24 – 7.18 (m, 3H), 2.88 (ddd, *J* = 14.3, 9.1, 5.4 Hz, 1H), 2.80 – 2.71 (m, 1H), 2.64 – 2.53 (m, 1H), 1.99 – 1.92 (m, 1H), 1.84 (dddd, *J* = 13.6, 9.1, 7.5, 5.5 Hz, 1H), 1.34 (d, *J* = 7.1 Hz, 3H).

^{13}C NMR (126 MHz, $CDCl_3$) δ 140.2, 128.7, 128.5, 126.5, 122.1, 35.8, 33.3, 24.9, 18.1.

Matching reported literature data.[35]

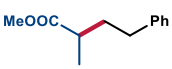

methyl-2-methyl-4-phenylbutanoate (4cc): Synthesized according to the General Procedure using 3DPA2FBN (6.4 mg, 5.0 mol%), PhSH (4.1 µL, 0.04 mmol, 20 mol%), 2,4,6-collidine (26.5µL, 0.2 mmol, 1 equiv.), γ-terpinene (96.0 µL, 0.6 mmol, 3 equiv.), methyl acrylate (18.0µL, 0.2 mmol, 1 equiv.) and styrene **2a** (68.5 µL, 0.6 mmol, 3 equiv.). Upon 14 hours stirring, the crude mixture was purified by flash column chromatography on silica gel (2% EtOAc in hexanes as eluent) to afford **4cc** (26.0 mg, 68% yield) as a colorless oil.

^{1}H NMR (400 MHz, $CDCl_3$) δ 7.31 – 7.27 (m, 2H), 7.22 – 7.16 (m, 3H), 3.68 (s, 3H), 2.62 (t, *J* = 8.0 Hz, 2H), 2.54 – 2.44 (m, 1H), 2.09 – 1.96 (m, 1H), 1.79 – 1.68 (m, 1H), 1.20 (d, *J* = 7.0 Hz, 3H).

^{13}C NMR (101 MHz, $CDCl_3$) δ 177.1, 141.7, 128.5, 128.5, 126.0, 51.6, 39.0, 35.5, 33.6, 17.2.

Matching reported literature data.[29]

---

[34] Zhang, Y.; Han, Y.; Zhu, S.; Qing, F.-L.; Xue, X.-S.; Chu, L., Light-Induced Divergent Cyanation of Alkynes Enabled by Phosphorus Radicals. *Angew. Chem., Int. Ed.* **2022**, *61*, e202210838

[35] Gaspar, B.; Carreira, E. M., Mild Cobalt-Catalyzed Hydrocyanation of Olefins with Tosyl Cyanide. *Angew. Chem., Int. Ed.* **2007**, *46*, 4519

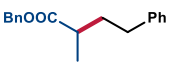

benzyl-2-methyl-4-phenylbutanoate (4dd): Synthesized according to the General Procedure using 3DPA2FBN (6.4 mg, 5.0 mol%), PhSH (4.1 µL, 0.04 mmol, 20 mol%), 2,4,6-collidine (26.5µL, 0.2 mmol, 1 equiv.), γ-terpinene (96.0 µL, 0.6 mmol, 3 equiv.), benzyl acrylate (30.5µL, 0.2 mmol, 1 equiv.) and styrene **2a** (68.5 µL, 0.6 mmol, 3 equiv.). Upon 14 hours stirring, the crude mixture was purified by flash column chromatography on silica gel (2% EtOAc in hexanes as eluent) to afford **4dd** (39.5 mg, 73% yield) as a colorless oil.

^{1}H NMR (500 MHz, $CDCl_3$) δ 7.38 – 7.35 (m, 4H), 7.35 – 7.31 (m, 1H), 7.28 – 7.25 (m, 2H), 7.20 – 7.16 (m, 1H), 7.15 – 7.11 (m, 2H), 5.13 (s, 2H), 2.60 (t, *J* = 8.0 Hz, 2H), 2.56 – 2.52 (m, 1H), 2.08 – 1.99 (m, 1H), 1.78 – 1.71 (m, 1H), 1.22 (d, *J* = 7.0 Hz, 3H).

^{13}C NMR (126 MHz, $CDCl_3$) δ 176.4, 141.7, 136.3, 128.7, 128.5, 128.5, 128.3, 128.2, 126.0, 66.2, 39.2, 35.5, 33.5, 17.2.

Matching reported literature data.[36]

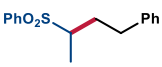

((4-phenylbutan-2-yl)sulfonyl)benzene (4ee): Synthesized according to the General Procedure using 3DPA2FBN (6.4 mg, 5.0 mol%), PhSH (4.1 µL, 0.04 mmol, 20 mol%), 2,4,6-collidine (26.5µL, 0.2 mmol, 1 equiv.), γ-terpinene (96.0 µL, 0.6 mmol, 3 equiv.), phenyl vinyl sulfone (33.5 mg, 0.2 mmol, 1 equiv.) and styrene **2a** (68.5 µL, 0.6 mmol, 3 equiv.). Upon 14 hours stirring, the crude mixture was purified by flash column chromatography on silica gel (5% EtOAc in hexanes as eluent) to afford **4ee** (26.0 mg, 47% yield) as a white solid.

^{1}H NMR (400 MHz, $CDCl_3$) δ 7.90 – 7.84 (m, 2H), 7.69 – 7.63 (m, 1H), 7.59 – 7.53 (m, 2H), 7.32 – 7.26 (m, 2H), 7.25 – 7.19 (m, 1H), 7.15 – 7.10 (m, 2H), 3.05 (dtd, *J* = 13.7, 6.8, 3.8 Hz, 1H), 2.84 (ddd, *J* = 14.3, 9.4, 5.3 Hz, 1H), 2.62 (ddd, *J* = 13.9, 9.0, 7.4 Hz, 1H), 2.34 (dddd, *J* = 13.4, 9.4, 7.4, 3.8 Hz, 1H), 1.82 – 1.68 (m, 1H), 1.34 (d, *J* = 6.9 Hz, 3H).

^{13}C NMR (101 MHz, $CDCl_3$) δ 140.1, 137.2, 133.6, 129.1, 128.9, 128.5, 128.3, 126.3, 59.1, 32.4, 30.7, 13.2. Matching reported literature data.[37]

[36] Ren, W.; Wang, M.; Guo, J.; Zhou, J.; Chu, J.; Shi, Y.; Shi, Y., Pd-Catalyzed Regioselective Branched Hydrocarboxylation of Terminal Olefins with Formic Acid. *Org. Lett.* **2022**, *24*, 886

[37] Schoenebeck, F.; Murphy, J. A.; Zhou, S.-z.; Uenoyama, Y.; Miclo, Y.; Tuttle, T., Reductive Cleavage of Sulfones and Sulfonamides by a Neutral Organic Super-Electron-Donor (S.E.D.) Reagent. *J. Am. Chem. Soc.* **2007**, *129*, 13368

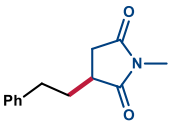

1-methyl-3-phenethylpyrrolidine-2,5-dione (4ff): Synthesized according to General Procedure using *fac*-Ir(ppy)$_3$ (800 µL stock solution, 0.6 mol%), HAT catalsyt **5b** (3,5-bis(trifluoromethyl)benzenethiol, 6.7 µL, 0.04 mmol, 20 mol%), methyl 4,5-dimethylcyclohexa-1,4-diene-1-carboxylate as H donor (64.0 µL, 0.4 mmol, 2 equiv.), *N*-Methylmaleimide (22.0 mg, 0.2 mmol, 1 equiv.) and styrene **2a** (68.5 µL, 0.6 mmol, 3 equiv.). Upon 14 hours stirring, the crude mixture was purified by flash column chromatography on silica gel (20% EtOAc in hexanes as eluent) to afford **4ff** (25.0 mg, 58% yield) as a white solid.

^{1}H NMR (300 MHz, $CDCl_3$) δ 7.32 – 7.26 (m, 2H), 7.24 – 7.15 (m, 3H), 2.97 (s, 3H), 2.88 – 2.65 (m, 4H), 2.44 – 2.35 (m, 1H), 2.27 (dtt, *J* = 11.8, 7.0, 2.3 Hz, 1H), 1.82 (dtd, *J* = 13.6, 8.7, 6.3 Hz, 1H).

^{13}C NMR (101 MHz, $CDCl_3$) δ 180.0, 176.7, 140.4, 128.7, 128.6, 126.5, 39.3, 34.6, 33.2, 33.1, 24.9.

Matching reported literature data.[38]

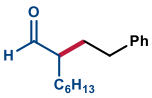

2-phenethyloctanal (4gg): Synthesized according to General Procedure using 3DPA2FBN (6.4 mg, 5.0 mol%), HAT catalsyt **5b** (3,5-bis(trifluoromethyl)benzenethiol, 6.7 µL, 0.04 mmol, 20 mol%), methyl 4,5-dimethylcyclohexa-1,4-diene-1-carboxylate as H donor (96.0 µL, 0.6 mmol, 3 equiv.), trans-2-Octenal (89.5 µL, 0.6 mmol, 3 equiv.) and styrene **2a** (23.0 µL, 0.2 mmol, 1 equiv.). Upon 14 hours stirring, the crude mixture was purified by flash column chromatography on silica gel (25% DCM in hexanes as eluent) to afford **4gg** (26.5 mg, 57% yield) as a colorless oil.

^{1}H NMR (500 MHz, $CDCl_3$) δ 9.60 (d, *J* = 2.9 Hz, 1H), 7.31 – 7.27 (m, 2H), 7.22 – 7.15 (m, 3H), 2.68 – 2.55 (m, 2H), 2.29 (ttd, *J* = 8.1, 5.4, 2.8 Hz, 1H), 2.01 – 1.93 (m, 1H), 1.79 – 1.71 (m, 1H), 1.69 – 1.63 (m, 1H), 1.53 – 1.45 (m, 1H), 1.31 – 1.25 (m, 9H), 0.89 – 0.86 (m, 3H).

^{13}C NMR (126 MHz, $CDCl_3$) δ 205.3, 141.6, 128.6, 128.5, 126.2, 51.4, 33.4, 31.7, 30.6, 29.4, 29.0, 27.0, 22.7, 14.1.

Matching reported literature data.[39]

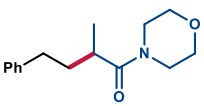

2-methyl-1-morpholino-4-phenylbutan-1-one (4hh): Synthesized according to General Procedure using *fac*-Ir(ppy)$_3$ (2.0 ml stock solution, 1.5 mol%), HAT catalsyt **5b** (3,5-

[38] Sharma, S.; Han, S. H.; Jo, H.; Han, S.; Mishra, N. K.; Choi, M.; Jeong, T.; Park, J.; Kim, I. S., Rhodium-Catalyzed Vinylic C–H Functionalization of Enol Carbamates with Maleimides. *Eur. J. Org. Chem.* **2016**, 3611

[39] Capacci, A. G.; Malinowski, J. T.; McAlpine, N. J.; Kuhne, J.; MacMillan, D. W. C., Direct, enantioselective α-alkylation of aldehydes using simple olefins. *Nat. Chem.* **2017**, *9*, 1073

bis(trifluoromethyl)benzenethiol, 6.7 µL, 0.04 mmol, 20 mol%), 2,4,6-collidine (26.5 µL, 0.2 mmol, 1 equiv.), methyl 4,5-dimethylcyclohexa-1,4-diene-1-carboxylate **6c** as H donor (96.0 µL, 0.6 mmol, 3 equiv.), 4-Acryloylmorpholine (25.0 µL, 0.2 mmol, 1 equiv.) and styrene **2a** (68.5 µL, 0.6 mmol, 3 equiv.). Upon 14 hours stirring, the crude mixture was purified by flash column chromatography on silica gel (25% EtOAc in hexanes as eluent) to afford **4hh** (26.5 mg, 58% yield) as a colorless oil.

^{1}H NMR (500 MHz, $CDCl_3$) δ 7.30 – 7.26 (m, 2H), 7.20 – 7.14 (m, 3H), 3.69 – 3.61 (m, 4H), 3.58 (t, *J* = 4.8 Hz, 2H), 3.37 – 3.28 (m, 2H), 2.69 – 2.56 (m, 3H), 2.09 – 2.01 (m, 1H), 1.74 – 1.67 (m, 1H), 1.14 (d, *J* = 6.8 Hz, 3H).

^{13}C NMR (126 MHz, $CDCl_3$) δ 174.9, 141.8, 128.6, 128.5, 126.1, 67.2, 66.8, 45.9, 42.1, 35.5, 34.1, 33.5, 17.6.

Matching reported literature data.[40]

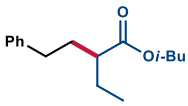

Isobutyl-2-ethyl-4-phenylbutanoate (4ii): Synthesized according to General Procedure using 3DPA2FBN (6.4 mg, 5.0 mol%), PhSH (4.1 µL, 0.04 mmol, 20 mol%), Cs_2CO_3 (32.5 mg, 0.2 mmol, 1 equiv.), γ-terpinene (96.0 µL, 0.6 mmol, 3 equiv), isobutyl trans-2-butenoate (32.0 µL, 0.2 mmol, 1 equiv.), styrene **2a** (68.5 µL, 0.6 mmol, 3 equiv.) and acetonitrile (4 ml) as solvent. Upon 14 hours stirring, the crude mixture was purified by flash column chromatography on silica gel (1% EtOAc in hexanes as eluent) to afford **4ii** (26.5 mg, 53% yield) as a light-yellow oil.

^{1}H NMR (400 MHz, $CDCl_3$) δ 7.31 – 7.26 (m, 2H), 7.20 – 7.16 (m, 3H), 3.89 (dd, *J* = 6.6, 0.9 Hz, 2H), 2.68 – 2.51 (m, 2H), 2.34 (ddd, *J* = 10.5, 9.0, 5.2 Hz, 1H), 2.05 – 1.89 (m, 2H), 1.77 (ddd, *J* = 6.7, 5.0, 2.5 Hz, 1H), 1.68 – 1.55 (m, 2H), 0.96 (d, *J* = 6.7 Hz, 6H), 0.91 (d, *J* = 7.4 Hz, 3H).

^{13}C NMR (101 MHz, $CDCl_3$) δ 176.2, 141.9, 128.5, 128.5, 126.0, 70.5, 47.1, 33.9, 33.9, 27.9, 25.6, 19.3, 11.8. HRMS: (ESI^+) calculated for $C_{16}H_{24}NaO_2^+$ [M+Na^+]: 271.1669, found 271.1667.

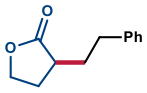

3-phenethyldihydrofuran-2(3H)-one (4jj): Synthesized according to General Procedure using 3DPA2FBN (6.4 mg, 5.0 mol%), PhSH (4.1 µL, 0.04 mmol, 20 mol%), Cs_2CO_3 (32.5 mg, 0.2 mmol, 1 equiv.), γ-terpinene (96.0 µL, 0.6 mmol, 3 equiv), 2-Furanone (14.5 µL, 0.2 mmol, 1 equiv.), styrene **2a** (68.5 µL, 0.6 mmol, 3 equiv.) and acetonitrile (4ml) as solvent. Upon 14 hours stirring, the crude

[40] Ling, J.; Bruneau-Voisine, A.; Journot, G.; Evano, G., Copper-Catalyzed Carbonylative Cross-Coupling of Alkyl Iodides and Amines. *Chem. Eur. J.* **2022**, *28*, e202201356

mixture was purified by flash column chromatography on silica gel (1% EtOAc in hexanes as eluent) to afford **4jj** (17.0 mg, 45% yield) as a light-yellow oil.

^{1}H NMR (500 MHz, $CDCl_3$) δ 7.32 – 7.28 (m, 2H), 7.24 – 7.19 (m, 3H), 4.35 (td, *J* = 8.8, 2.8 Hz, 1H), 4.17 (ddd, *J* = 9.8, 9.1, 6.7 Hz, 1H), 2.81 (ddd, *J* = 14.7, 9.1, 6.0 Hz, 1H), 2.72 (ddd, *J* = 13.8, 8.8, 7.1 Hz, 1H), 2.49 (ddt, *J* = 10.2, 8.9, 4.4 Hz, 1H), 2.38 (dddd, *J* = 12.5, 8.7, 6.7, 2.8 Hz, 1H), 2.28 – 2.20 (m, 1H), 1.96 (dtd, *J* = 12.5, 10.0, 8.5 Hz, 1H), 1.77 (dtd, *J* = 13.9, 8.9, 5.9 Hz, 1H).

^{13}C NMR (126 MHz, $CDCl_3$) δ 179.4, 140.8, 128.6, 128.5, 126.3, 66.5, 38.5, 33.4, 32.1, 28.9.

Matching reported literature data.[41]

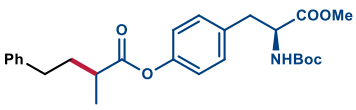

4-((S)-2-((tert-butoxycarbonyl)amino)-3-methoxy-3-oxopropyl)phenyl (S)-2-methyl-4-phenylbutanoate (4kk): Synthesized according to General Procedure using 3DPA2FBN (6.4 mg, 5.0 mol%), PhSH (4.1 µL, 0.04 mmol, 20 mol%), 2,4,6-collidine (26.5µL, 0.2 mmol, 1 equiv.), γ-terpinene (96.0 µL, 0.6 mmol, 3 equiv.), (S)-4-(2-((tert-butoxycarbonyl)amino)-3-methoxy-3-oxopropyl)phenyl acrylate **1k** (30.5mg, 0.2 mmol, 1 equiv.) and styrene **2a** (68.5 µL, 0.6 mmol, 3 equiv.). Upon 14 hours stirring, the crude mixture was purified by flash column chromatography on silica gel (5% to 10% EtOAc in hexanes as eluent) to afford **4kk** (55.5 mg, 61% yield, 1:1 dr) as a colorless oil.

^{1}H NMR (500 MHz, $CDCl_3$) δ 7.33 – 7.28 (m, 2H), 7.24 – 7.19 (m, 3H), 7.17 – 7.12 (m, 2H), 7.02 – 6.99 (m, 2H), 4.99 (d, *J* = 8.3 Hz, 1H), 4.62 – 4.54 (m, 1H), 3.71 (s, 3H), 3.15 – 3.02 (m, 2H), 2.77 – 2.67 (m, 3H), 2.19 – 2.11 (m, 1H), 1.89 – 1.82 (m, 1H), 1.43 (s, 9H), 1.34 (d, *J* = 7.0 Hz, 3H).

^{13}C NMR (126 MHz, $CDCl_3$) δ 175.1, 172.3, 155.2, 150.0, 141.6, 133.7, 130.4, 128.6, 128.6, 126.2, 121.7, 80.2, 54.5, 52.4, 39.3, 37.8, 35.5, 33.6, 28.4, 17.2.

HRMS: (ESI$^+$) calculated for $C_{26}H_{33}NNaO_6^+$ [M+Na$^+$]: 478.2200, found 478.2214.

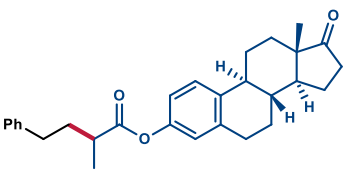

(8R,9S,13S,14S)-13-methyl-17-oxo-7,8,9,11,12,13,14,15,16,17-decahydro-6H-cyclopenta[a]phenanthren-3-yl 2-methyl-4-phenylbutanoate (4ll): Synthesized according to General Procedure using 3DPA2FBN (6.4 mg, 5.0 mol%), PhSH (4.1 µL, 0.04 mmol, 20 mol%), 2,4,6-collidine (26.5µL, 0.2 mmol, 1 equiv.), γ-terpinene (96.0 µL, 0.6 mmol, 3 equiv.), (8R,9S,13S,14S)-13-methyl-17-oxo-7,8,9,11,12,13,14,15,16,17-

[41] Miao, P.; Li, R.; Lin, X.; Rao, L.; Sun, Z., Visible-light induced metal-free cascade Wittig/hydroalkylation reactions. *Green Chemistry* **2021**, *23*, 1638

decahydro-6H-cyclopenta[a]phenanthren-3-yl acrylate **3l** (65.0 mg, 0.2 mmol, 1 equiv.) and styrene **2a** (68.5 µL, 0.6 mmol, 3 equiv.). Upon 14 hours stirring, ^{1}H NMR (CH_2Br_2 as internal standard) revealed 71% NMR yield of **4ll**. The crude mixture was purified by flash column chromatography on silica gel (9% EtOAc in hexanes as eluent) to afford **4ll** (54.5 mg, 90% purity, 57% adjusted yield, 1:1 dr) as a colorless oil (the impurity was the reduced acrylate, purity calculated from ^{1}H NMR data). To obtain an analytically pure sample, preparative HPLC has been performed (column: ChiralPak IC 250x4.6 mm, 5µm; mobile phase: Hex/EtOH 80:20; flow: 1ml/min; wavelength: 254 nm).

^{1}H NMR (500 MHz, $CDCl_3$) δ 7.32 – 7.27 (m, 3H), 7.24 – 7.19 (m, 3H), 6.85 (dd, *J* = 8.4, 2.6 Hz, 1H), 6.81 – 6.78 (m, 1H), 2.94 – 2.89 (m, 2H), 2.78 – 2.67 (m, 3H), 2.51 (ddd, *J* = 18.9, 8.8, 0.9 Hz, 1H), 2.45 – 2.38 (m, 1H), 2.29 (td, *J* = 10.6, 3.8 Hz, 1H), 2.20 – 2.11 (m, 2H), 2.09 – 1.95 (m, 3H), 1.86 (dddd, *J* = 13.7, 8.6, 7.3, 6.1 Hz, 1H), 1.69 – 1.39 (m, 6H), 1.34 (d, *J* = 7.0 Hz, 3H), 0.92 (s, 3H).

^{13}C NMR (126 MHz, $CDCl_3$) δ 220.9, 175.4, 148.8, 141.6, 138.1, 137.4, 128.6, 126.5, 126.1, 121.6, 118.8, 50.5, 48.0, 44.3, 39.2, 38.1, 36.0, 35.6, 33.6, 31.6, 29.5, 26.4, 25.9, 21.7, 17.2, 13.9.

HRMS: (ESI$^+$) calculated for $C_{29}H_{34}NaO_3^+$ [M+Na$^+$]: 453.2400, found 453.2411.

Benzyl-2-methyl-4-(4,4,5,5-tetramethyl-1,3,2-dioxaborolan-2-yl)butanoate (4mm): Synthesized according to General Procedure using 3DPA2FBN (6.4 mg, 5.0 mol%), HAT catalsyt **5c** (Ethyl thioglycolate, 4.4 µL, 0.04 mmol, 20 mol%), 2,4,6-collidine (26.5µL, 0.2 mmol, 1 equiv.), γ-terpinene (32.0 µL, 0.2 mmol, 1 equiv.), benzyl acrylate (30.5µL, 0.2 mmol, 1 equiv.) and vinylboronic acid pinacol ester (102.0 µL, 0.6 mmol, 3 equiv.). Upon 14 hours stirring, the crude mixture was purified by flash column chromatography on silica gel (2% acetone in hexanes as eluent) to afford **4mm** (33.0 mg, 52% yield) as a yellow oil.

^{1}H NMR (400 MHz, $CDCl_3$) δ 7.39 – 7.27 (m, 5H), 5.10 (s, 2H), 2.51 – 2.43 (m, 1H), 1.79 (dq, *J* = 13.6, 7.8 Hz, 1H), 1.58 – 1.52 (m, 1H), 1.23 (s, 12H), 1.16 (d, *J* = 7.0 Hz, 3H), 0.78 (t, *J* = 8.3 Hz, 2H).

^{13}C NMR (101 MHz, $CDCl_3$) δ 176.7, 136.4, 128.6, 128.1, 128.1, 83.2, 66.0, 41.6, 28.2, 24.9, 24.9, 16.8.

HRMS: (ESI$^+$) calculated for $C_{18}H_{27}NaO_4B^+$ [M+Na$^+$]: 340.1931, found 340.1931.

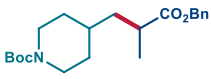

Tert-butyl-4-(3-(benzyloxy)-2-methyl-3-oxopropyl)piperidine-1-carboxylate (4nn): Synthesized according to General Procedure using 3DPA2FBN (6.4 mg, 5.0 mol%), HAT catalsyt **5c** (Ethyl thioglycolate, 4.4 µL, 0.04 mmol, 20 mol%), 2,4,6-collidine (26.5 µL, 0.2 mmol, 1 equiv.), γ-

terpinene (32.0 µL, 0.2 mmol, 1 equiv.), benzyl acrylate (30.5µL, 0.2 mmol, 1 equiv.) and tert-butyl 4-methylenepiperidine-1-carboxylate (118.5 µL, 0.6 mmol, 3 equiv.). Upon 14 hours stirring, the crude mixture was purified by flash column chromatography on silica gel (10% EtOAc in hexanes as eluent) to afford **4nn** (35.5 mg, 49% yield) as a colorless oil.

^{1}H NMR (500 MHz, $CDCl_3$) δ 7.40 – 7.30 (m, 5H), 5.18 – 5.06 (m, 2H), 4.02 (s, 2H), 2.66 – 2.38 (m, 3H), 1.69 – 1.52 (m, 3H), 1.44 (s, 9H), 1.35 – 1.28 (m, 2H), 1.16 (d, *J* = 6.9 Hz, 3H), 1.06 – 0.99 (m, 2H).

^{13}C NMR (126 MHz, $CDCl_3$) δ 176.7, 154.9, 136.2, 128.7, 128.3, 79.4, 66.2, 40.8, 36.9, 33.9, 32.0, 29.8, 28.6, 17.8.

HRMS: (ESI^+) calculated for $C_{21}H_{31}NNaO_4^+$ [$M+Na^+$]: 384.2145, found 384.2140.

3.7.5 Reaction Scale-Up

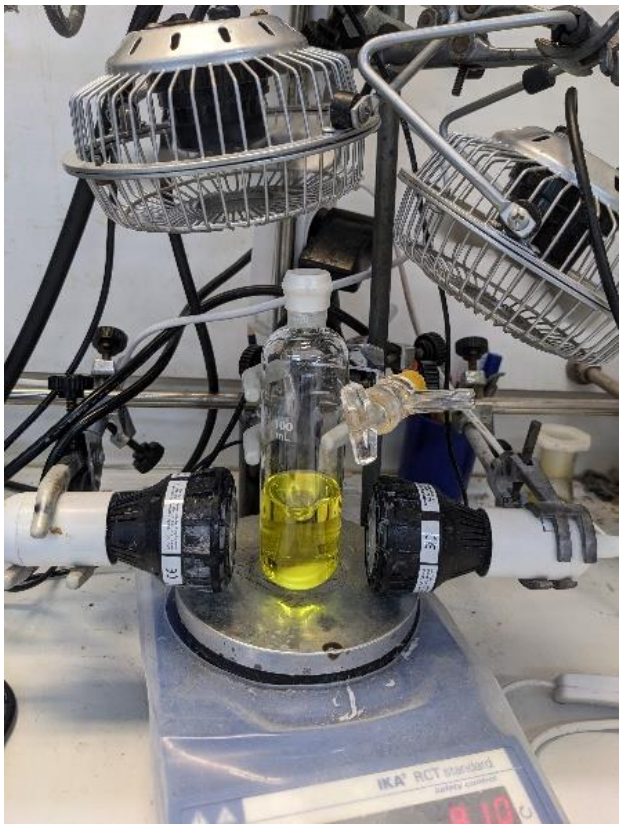

Figure 3.25. 5 mmol scale reaction between **1a** and **2a** using 2 *EvoluChem* 450 nm lamps.

An oven-dried 100 mL Schlenk flask containing a Teflon stir bar and dimethyl fumarate **1a** (1.08 g, 7.5 mmol, 1.5 equiv.) was sealed with a rubber septum and purged with argon. 1,2-Dichloroethane (45 ml, HPLC grade) was added followed by 5 ml of *fac*-Ir(ppy)$_3$ stock solution (prepared according to the General Procedure; 1.0 mg/mL in DCE, 5 mg, 0.15 mol%), styrene (572 µL, 5.0 mmol, 1 equiv.), γ-terpinene (1.60 ml, 10 mmol, 2 equiv.), and thiophenol (102 µL, 1.0 mmol, 20 mol%). Reaction vessel was placed into a photoreactor setup as depicted on Figure 3.25 with both lamps and fans running. In these conditions, internal temperature of the reaction was measured at 55-60°C due to the amount of heat from light absorption (ambient temperature 22°C). The consumption of dimethyl fumarate was monitored by taking an aliquot (50 µL) with a syringe and performing GC-MS analysis. After 84 hours, upon full consumption of dimethyl fumarate **1a**, the reaction mixture was allowed to cool down, washed with 2x20 mL saturated Na_2CO_3 solution and 20 mL of saturated NaCl solution and dried over Na_2SO_4. This solution was filtered through a silica plug washing with DCM (ca. 300 mL). The filtrate was evaporated and purified by silica gel chromatography

(10% EtOAc in Hexane). Fractions were evaporated and the material dried in a high vacuum (pressure 2.5*10^-1 mbar) at 40°C to remove dimethyl succinate impurity yielding 1005 mg of **4a** (80% yield) as a colorless oil.

3.7.6 Mechanistic experiments

3.7.6.1 Stern-Volmer Quenching Studies

The absorption spectra of *fac*-Ir(ppy)$_3$ (PC **A**) was recorded (Figure 3.26) in order to establish appropriate concentration and excitation wavelength. The spectra was recorded using a Shimadzu 2401PC UV−vis spectrophotometer and 10 mm path quartz cuvette. The concentration of 1.5 μM in DCE, and excitation wavelength of 440 nm were chosen for Stern-Volmer studies based on these results (absorbance value of 0.1 at 440 nm in these conditions).

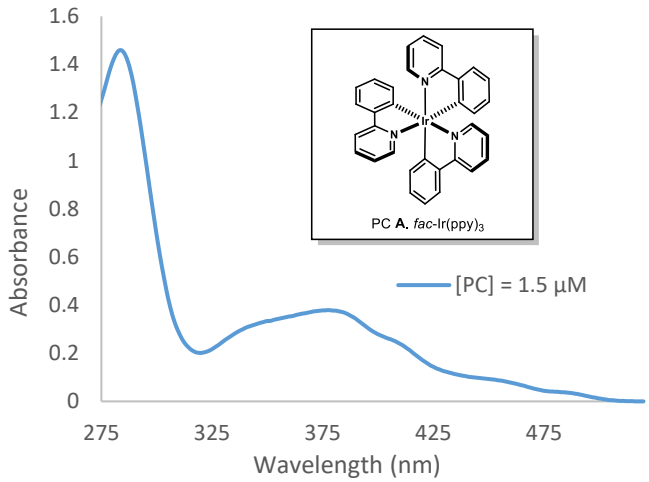

Figure 3.26. Absorption spectrum of PC **A** (1.5 μM in DCE, 10 mm light path).

The emission spectra was recorded in a Fluorolog Horiba Jobin Yvon spectrofluorimeter equipped with a photomultiplier detector, a double monochromator, and a 350W xenon light source. 2 mL of a 1.5 μM solution of PC **A** in thoroughly degassed DCE was placed in a 10x10 mm light path quartz fluorescence cuvette equipped with Silicone/PTFE 3.2 mm septum under an argon atmosphere. The excitation wavelength was fixed at 440 nm (incident light slit regulated to 1.5 nm), while the emission signal was acquired from 455 nm to 650 nm (emission light slit regulated to 1.5 nm).

A 0.5 M solution of dimethyl fumarate **1a** in DCE was prepared, and 5 μL of this stock solution were added to the solution of the catalyst. The addition of this solution was repeated four consecutive times. After each addition, an absorption spectrum and an emission spectrum

of the solution were recorded. The results shown in Figure 3.27 indicate that dimethyl fumarate **1a** quenches the excited state of the catalyst **PC**. No change in the absorption spectra of the solution was observed during the addition of **1a**.

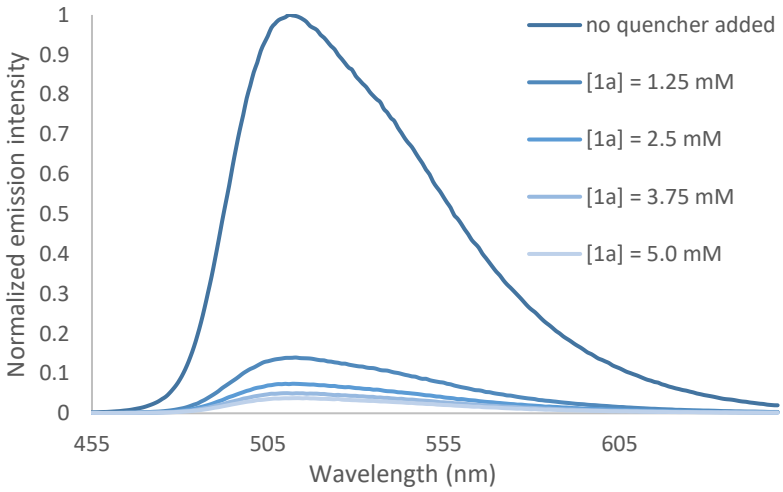

Figure 3.27. Quenching of the emission of **PC** (1.5 μM in DCE) in the presence of increasing amounts of **1a**.

The Stern-Volmer plot, reported in Figure 3.28, shows a linear correlation between the concentration of **1a** and the ratio I_0/I. On the basis of the Stern-Volmer equation $I_0/I = 1 + K_{SV}[Q]$, we calculated a Stern-Volmer quenching constant $\mathbf{K_{SV} = 5068\ M^{-1}}$. A 0.5 M solution of styrene **2a** in DCE was prepared, and portions of this stock solution were added to the solution of the catalyst. The addition of this solution was repeated five consecutive times. After each addition, an absorption spectrum and an emission spectrum of the solution were recorded.

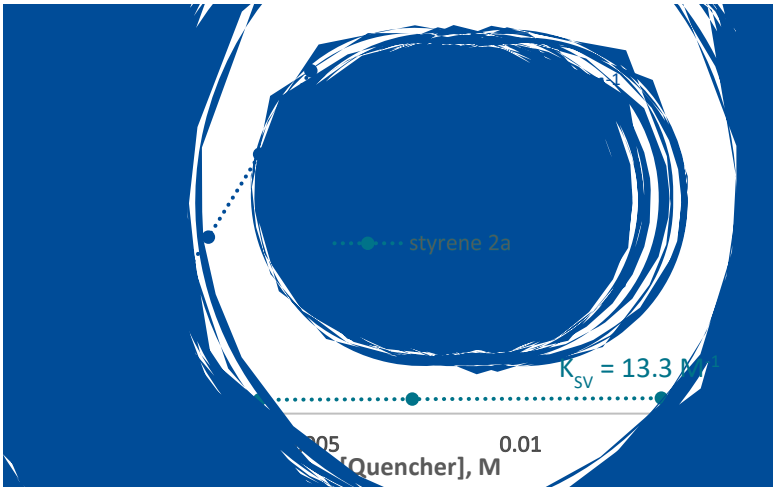

Figure 3.28. Stern-Volmer quenching plot using **1a** and **2a** as a quencher.

No change in the absorption spectra of the solution was observed during the addition of **2a**. The Stern-Volmer plot is reported in Figure 3.28. A much smaller Stern-Volmer constant was calculated in this case (**K_{SV} = 13.3 M^{-1}**).

3.7.6.2 Radical clock experiment

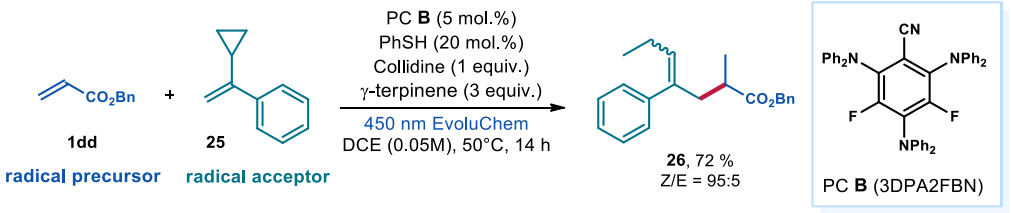

Figure 3.29. Radical clock experiment.

The radical clock experiment was performed according to the General Procedure using 3DPA2FBN (6.4 mg, 5.0 mol%), PhSH (4.1 µL, 0.04 mmol, 20 mol%), 2,4,6-collidine (26.4 µL, 0.2 mmol, 1 equiv.), γ-terpinene (96 µL, 0.6 mmol, 3 equiv.), benzyl acrylate (30.6 µL, 0.2 mmol, 1 equiv.) and α-cyclopropylstyrene (90.0 µL, 0.6 mmol, 3 equiv.). Upon 14 hours stirring, the crude mixture was purified by flash column chromatography on silica gel (2% EtOAc in hexanes as eluent) to afford **26** (44.5 mg, 72% yield, 95:5 Z/E) as a colorless oil.

^{1}H NMR (500 MHz, $CDCl_3$, major) δ 7.39 – 7.28 (m, 7H), 7.25 – 7.21 (m, 1H), 7.14 – 7.10 (m, 2H), 5.46 (t, *J* = 7.4, 1H), 5.04 (s, 2H), 2.81 (ddq, *J* = 13.4, 6.9, 1.1 Hz, 1H), 2.49 – 2.40

(m, 1H), 2.39 (ddq, *J* = 13.4, 7.4, 0.8 Hz, 1H), 1.97 – 1.84 (m, 2H), 1.13 (d, *J* = 6.9 Hz, 3H), 0.90 (t, *J* = 7.5 Hz, 3H).

^{13}C NMR (126 MHz, $CDCl_3$, major) δ 176.3, 140.3, 137.4, 136.3, 131.9, 128.7, 128.6, 128.2, 128.2, 128.2, 126.8, 66.1, 43.4, 38.2, 22.4, 16.8, 14.7.

HRMS: (ESI^+) calculated for $C_{21}H_{24}NaO_2^+$ [$M+Na^+$]: 331.1669, found 331.1670.

3.7.6.3 Deuterium labeling experiment

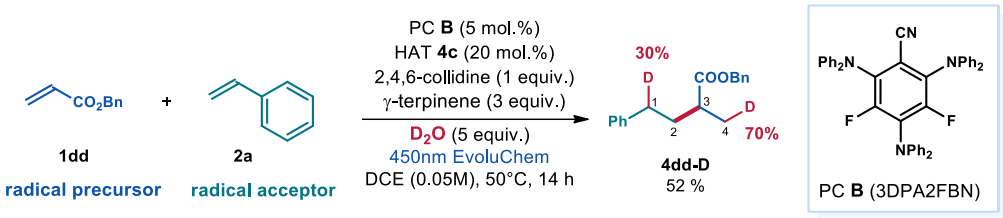

Figure 3.30. Deuterium labeling experiment.

To an 8 mL oven dried vial with a Teflon septum screw cap containing a dry Teflon stir bar, 3DPA2FBN (6.4 mg, 5.0 mol%) was added. The vial was sealed, evacuated and backfilled with argon three times, and the solvent was added. Then PhSH (4.1 µL, 0.04 mmol, 20 mol%), 2,4,6-collidine (26.4 µL, 0.2 mmol, 1 equiv.), γ-terpinene (96 µL, 0.6 mmol, 3 equiv.), benzyl acrylate **1dd (**30.6µL, 0.2 mmol, 1 equiv.), styrene **2a** (68.7 µL, 0.6 mmol, 3 equiv.) and **D_2O** (18.1 µL, 1.0 mmol, 5 equiv.) were added sequentially. The vial was sonicated for 1 minute and was then placed in the photoreactor (Figure 3.25) and irradiated with vigorous stirring for 14 hours. The solvent was evaporated, and the crude mixture purified by flash column chromatography on silica gel (2% EtOAc in hexanes as eluent) to furnish the target product **4dd-D (**27.9 mg, 52% yield) as a colorless oil. Deuteration ratio was reported based on integration of peaks in ^{13}C IGD (inverse-gated-decoupling) experiment. ^{13}C signals were assigned by analyzing HSQC (heteronuclear single quantum coherence) spectrum.

^{1}H NMR (500 MHz, $CDCl_3$) δ 7.41 – 7.33 (m, 5H), 7.30 – 7.25 (m, 2H), 7.22 – 7.17 (m, 1H), 7.15 (ddt, *J* = 7.7, 1.4, 0.7 Hz, 2H), 5.15 (s, 2H), 2.62 – 2.60 (m, 1.6H), 2.58 – 2.50 (m, 1H), 2.09 – 2.00 (m, 1H), 1.79 – 1.72 (m, 6.1 Hz, 1H), 1.25 – 1.19 (m, 2.3H).

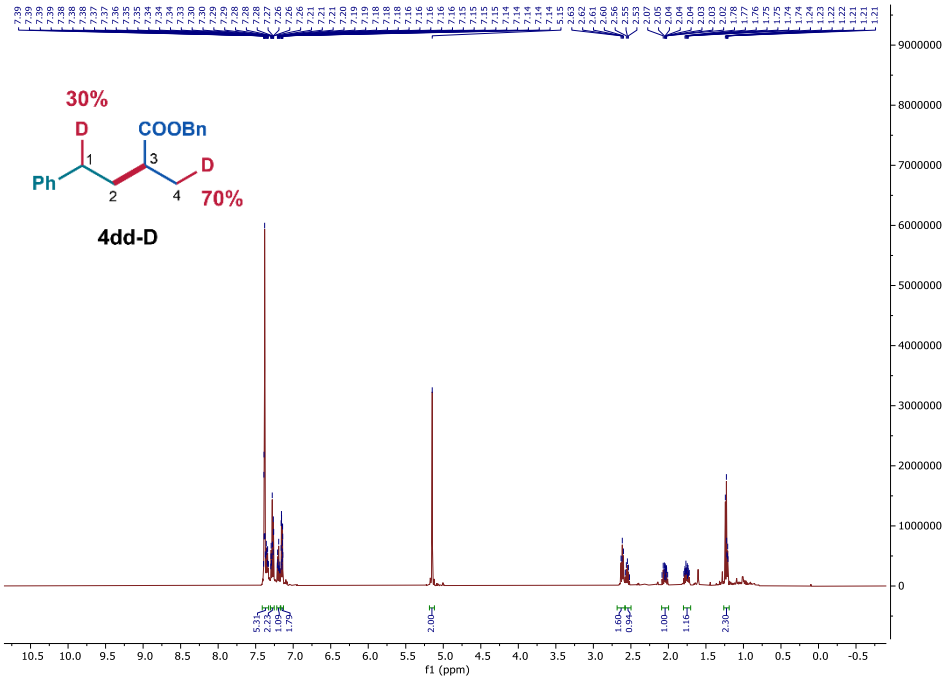

^{13}C NMR (126 MHz, $CDCl_3$) δ 176.43, 141.75, 136.31, 128.68, 128.54, 128.48, 128.30, 128.28, 126.02, 66.21, (39.20; 39.18; 39.13; 39.11: 1C), (35.57; 35.54; 35.49; 35.46: 1C), (33.55; 33.19 (t, *J* = 19.5 Hz): 1C), (17.27; 16.99 (t, *J* = 19.5 Hz): 1C).

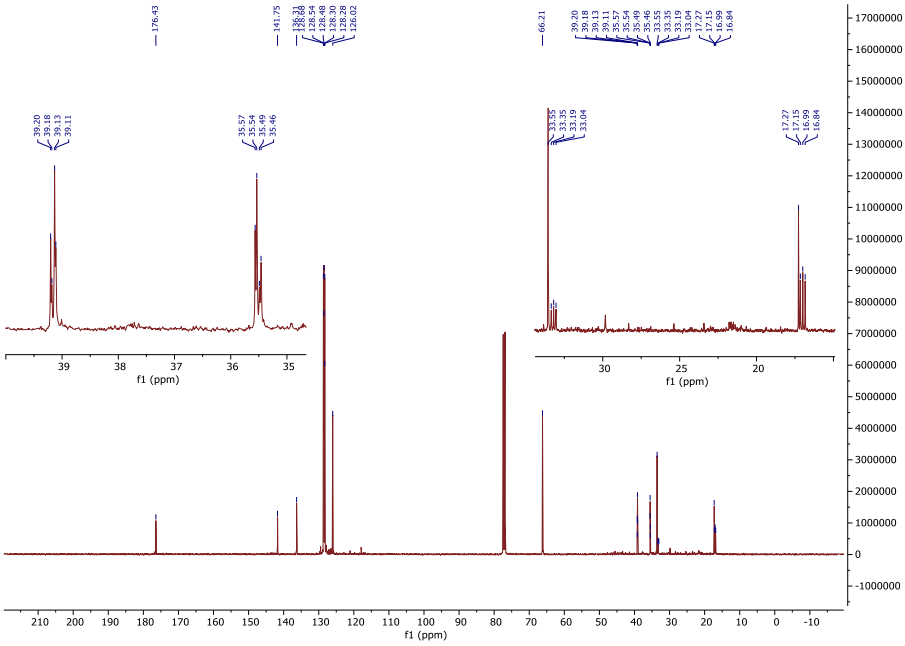

^{13}C NMR (126 MHz, $CDCl_3$, IGD, 10s delay) δ 33.55 (0.7C); 33.19 (t, *J* = 19.5 Hz, 0.3C), 17.27 (0.3C); 16.99 (t, *J* = 19.5 Hz, 0.7C).

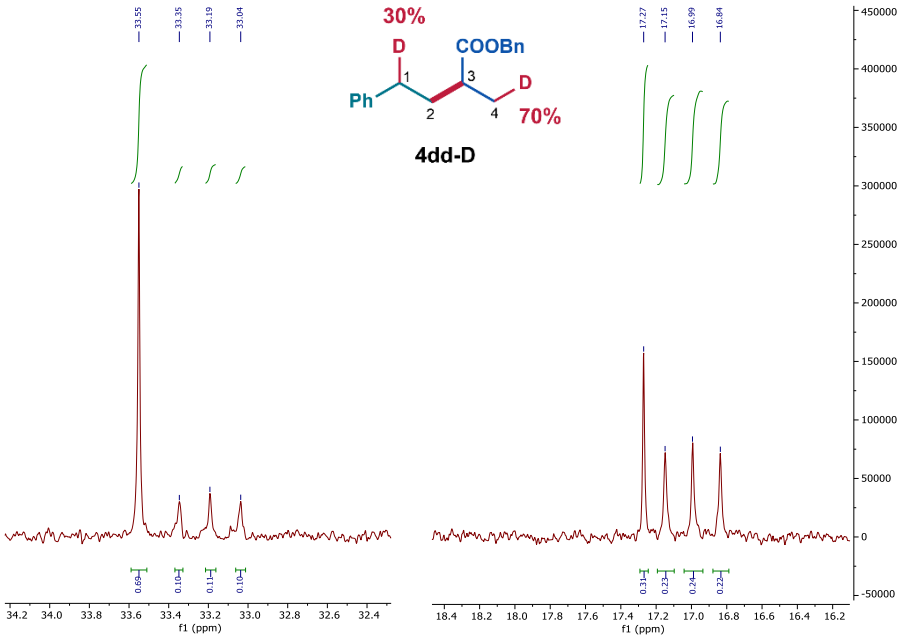

^{2}H NMR (77 MHz, $CHCl_3$; $CDCl_3$ added as internal reference) δ 2.61 (s, 1D), 1.24 (s, 2.47D).

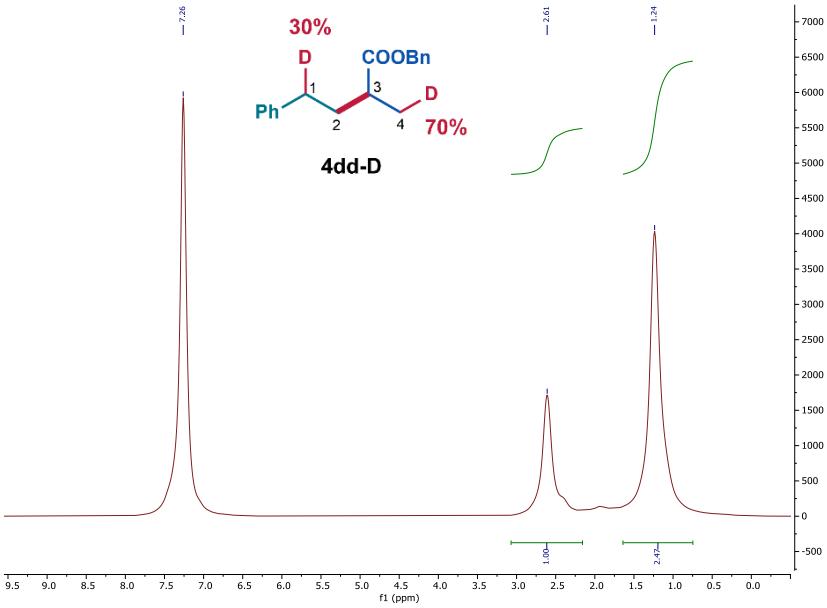

HSQC

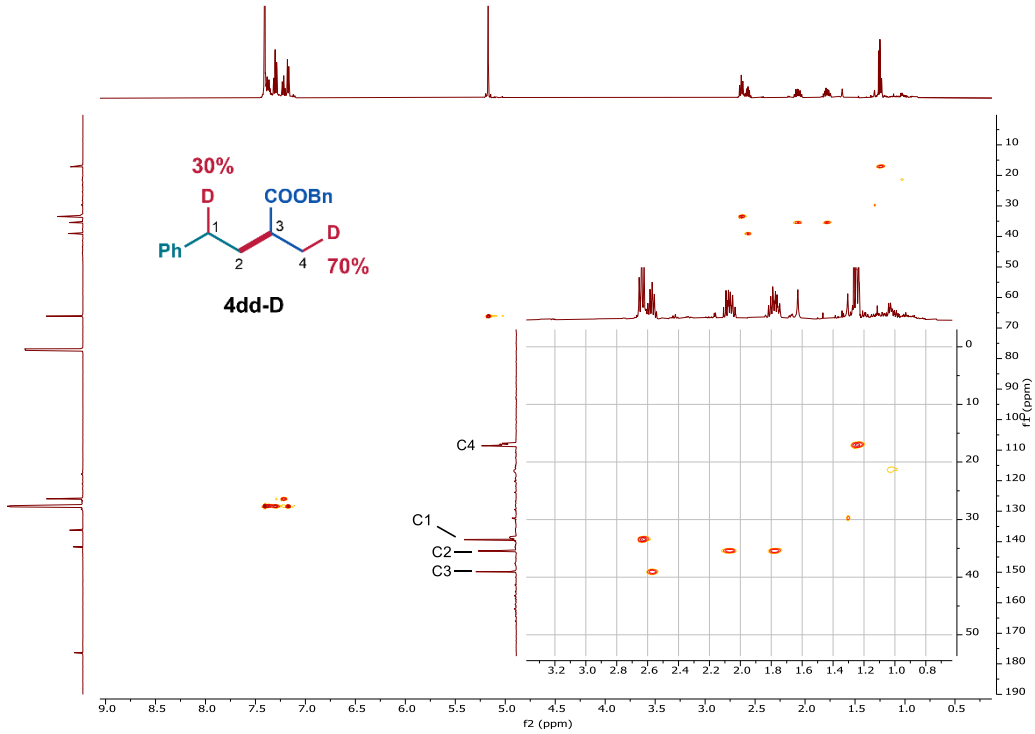

Chapter IV

General Conclusions

In this thesis, I have harnessed the synthetic potential of photocatalytic strategies to selectively forge new C(sp^2)-C(sp^3) and C(sp^3)-C(sp^3) bonds. Specifically, single-electron reduction of electron-deficient π-systems was exploited as a means of achieving unconventional reactivity.

Chapter II described a new strategy for the regioselective radical functionalization of pyridines and related heteroarenes, enriching the radical-based chemistry of pyridines. This strategy is enabled by the formation of previously neglected pyridinyl radicals, obtained in a catalytic manner via *single electron transfer* (SET) reduction of pyridinium ions. This reduction was facilitated by the lowering of the *lowest unoccupied molecular orbital* (LUMO) of the pyridine, achieved by protonation. The pyridinyl radical intermediates underwent effective and regioselective radical coupling with allylic radicals formed via *hydrogen atom transfer* (HAT) from allylic *C-H* bonds of readily available olefins. Key to the design of this protocol was the use of the dithiophosphoric acid catalyst, which served three distinct roles during the reaction, sequentially acting as a Brønsted acid for pyridine protonation, an SET reductant of pyridinium ions upon light excitation, and a HAT acceptor for the allylic *C-H* bonds upon formation of the thiyl radical. The key intermediates of this process have been identified, and the regioselectivity has been rationalized through a mechanistic investigation campaign that includes spectroscopic, electrochemical, and computational studies.

In chapter III, a new light-driven strategy for the reductive olefin cross-coupling has been detailed, providing sp^3-rich products with a distinct connectivity starting from broadly available olefin substrates. Central to this strategy was the exploitation of the electronic differences between the two olefin partners, enabling selective radical generation via photoredox-mediated SET reduction of the electron-deficient olefins. Overall, the electron-poor substrates were readily coupled with various styrenes and other electron-neutral olefins, finally undergoing reduction via HAT process mediated by a thiol catalyst. A notable feature of this method is its high functional group tolerance, which was leveraged for the late-stage modification of biorelevant compounds. The mechanistic proposal was supported by a mechanistic campaign, including Stern-Volmer quenching studies.

In conclusion, SET reduction in combination with thiol-mediated HAT processes have enabled the selective construction of new *C-C* bonds in an efficient photocatalytic manifold. The developed catalytic strategies provide new tools for synthetic organic chemistry.